Novel compartment-specific biosensors reveal a complementary subcellular distribution of bioactive Furin and PC7

PAR

Pierpaolo GINEFRA

EPFL

ÉCOLE POLYTECHNIQUE
FÉDÉRALE DE LAUSANNE

Suisse
2018

"Success is not final, failure is not fatal,

it is the courage to continue that counts"

Winston Churchill

For my mother

Acknowledgements

The accomplishment of this thesis would not have been possible without the great help and contribution of many people, to whom I would like to express my deepest and sincere gratitude.

I sincerely thank Prof. Daniel Constam for giving me the opportunity to work in his lab, for all the meetings and discussion that we had about this "Cluedo" project. He helped me to think critically about my data and taught me how to discuss and interpret the results. His passion and enthusiasm for science were truly inspiring, in particular during the bad moments of this amazing journey. Thank you Daniel.

In addition, I would like to thank my committee members Prof. Cathrin Brisken, Prof. Brian McCabe, Prof. Stefan Kunz, and Prof. Rainer Pepperkok for taking the time to evaluate my work and survey my thesis.

I would like to thank the BIOP team for training me and helping me with the image processing and data analysis.

A great special thank goes to the current and the former Constam lab members: Prudence, Sylvain, Séverine, Nancy, Stéphane, Florian, Nathalie, Simon, Mariella, Oliver, Katarina, Benjamin, Manuela and Lucia. Thanks guys for all the time spent together, the advices, the jokes. It has been an honour and a privilege to work with you. I would like in particular to thank Prudence, Sylvain and Benjamin for being such great mentors and teachers, I would have not reached my goal without your advices, critics and help. Thanks!

A proverb says: Friends are the family that you chose. I have to say that I choose wisely.

A special thank goes to the Pita's people. You are my family at EPFL! I love you guys!

I will be eternally grateful to all my friends here in Lausanne, you guys are my family here. Each of you has contributed in making my time here priceless. Thank you Andrea, Sophie, Alex, Marta, Valentina, Pino, Ribal, Elena, Enrico, Lucia.

I'm grateful as well to all my friends in Bari and Helsinki. Thank you Annarita, Valerio, Nicola, Flavia, Ester, Giacomo, Manuel, Annamaria, Dario and Maria for your support and for being my friends for almost 20 years of my life!

I want to thank Ivana, Stefania, Carmine and the beautiful Emma, for have being always supportive and to be my family just behind the Alps.

I would like to thank my incredible mother Isabella and amazing sister Claudia. I would not have made it without your support and your advices. You allow me to find my way and to go for what I want and wish. Thank to my angel, who is always with me.

Last but not least, I want to thank the person that I love and with whom I'm sharing my life, to be always by my side and just to be as you are. I love you Eli.

Summary

Proprotein Convertases (PCs) constitute a family of serine proteases that activate various hormones, growth factors and cell adhesion molecules by mediating endoproteolytic cleavage of their secreted inactive precursors during their transit in the secretory pathway. Their physiological roles in most tissues, in cancer and other diseases have remained nowadays poorly defined, partly because of technical hurdles in clearly distinguishing functionally overlapping PC activities from each other. Related to this, a major unsolved question is where, among the different subcellular compartments of the secretory pathway, substrate cleavage takes place. To address these questions, we mapped intracellular PC activities of two unrelated cell lines (HEK293T and B16F1 melanoma) by ratiometric and Förster Resonance Energy Transfer (FRET)-based imaging of the PC-specific biosensors, called cell-linked indicator of proteolysis (CLIP)v3 and CLIPv4 respectively, which are sorted to different subcellular compartments by specific trafficking signals. Until now, PCs have been thought to cleave the majority of the substrates in the *trans*-Golgi network (TGN). By contrast, our analysis of compartment-specific CLIPv3 and CLIPv4 variants in cultured cells suggested that PC activities are much higher in post-exocytic compartments. Furthermore, imaging in B16F1 Clustered Regularly Interspaced Short Palindromic Repeats (CRISPR)-edited clones for endogenously expressed Furin or PC7, revealed an enrichment of Furin activity in endosomes compared to TGN, whereas PC7 activity was confined to a distinct compartment resistant to the pan-PC inhibitor CMK, demonstrating that endogenous Furin and PC7 are biologically active in distinct compartments. In addition, we also demonstrated that substrate and protease localization are rate-limiting of how efficiently a given substrate is processed.

PC inhibition represses human primary melanoma cells motility and migration *in vitro* and proliferation in other skin cancer cells both *in vitro* and *in vivo*. To elucidate the roles of PC activities in melanoma progression and differentiation, we evaluated relative contribution of Furin and PC7 in B16F1 tumor grafts. Both proteins were required for tumor pigmentation, whereas Furin deletion reduced tumor growth, but its loss may be rescued by PC7 deletion. Altogether, these findings will be important to inform future therapeutic approaches and strategies for targeting PCs to preferentially block oncogenic activities.

Keywords: Proprotein Convertase, Furin, PC7, Trafficking, FRET, melanoma

Sommario

Le proproteine convertasi (PC) costituiscono una famiglia di serin proteasi che attivano diversi ormoni, fattori di crescita e molecole di adesione mediante taglio endoproteolitico dei loro precursori inattivi durante il transito nel pathway secretorio. I ruoli delle PC in diversi tessuti, tumori e in altre patologie sono stati sino ad ora poco studiati, in parte per via delle difficoltà tecniche nel distinguere chiaramente le attività delle singole PC in quanto esse combaciano tra di loro. In aggiunta, non è stato ancora definito in quale compartimento subcellulare avviene il taglio proteolitico di un determinato substrato. Per investigare dove esso avviene, abbiamo generato una mappa delle attività delle PC in due distinte linee cellulari (HEK293T e linea cellulare di melanoma B16F1), attraverso l'uso di biosensori basati su tecniche di imaging molecolare come il rapporto tra segnali di fluorescenza o trasferimento di energia per risonanza (FRET), chiamati rispettivamente cell-linked indicator of proteolysis (CLIP)v3 e CLIPv4, i quali sono smistati nei diversi compartimenti subcellulari attraverso sequenze segnale specifiche. Fino ad ora si è pensato che le PC tagliassero la maggior parte dei loro substrati nell'apparato del Golgi. Tuttavia, l'analisi di CLIPv3 e CLIPv4 smistati nei diversi compartimenti subcellulari in cellule in coltura, ha suggerito che le PC sono più attive nei compartimenti post-esocitici. Inoltre l'analisi da noi effettuata in cloni cellulari knockout per le PC endogene Furina e PC7, ottenuti tramite la tecnica di Clustered Regularly Interspaced Short Palindromic Repeats (CRISPR), ha mostrato un incremento della attività della Furina negli endosomi, e che PC7 è attiva in un compartimento ed è resistente all'inibitore generale delle PC CMK, dimostrando che Furina e PC7 sono attive in compartimenti separati. In aggiunta, noi abbiamo dimostrato anche che la localizzazione della proteasi e del substrato è rilevante ai fini di come il substrato viene processato.

L'inibizione delle proteasi in colture primarie umane di melanoma reprime la capacità delle cellule di muoversi e migrare *in vitro*, e la proliferazione di cellule di altri tumori della pelle sia *in vitro* che *in vivo*. Per elucidare i ruoli delle PC nel processo di progressione tumorale e di differenziazione nel melanoma, abbiamo valutato il contributo della Furina e della PC7 nella crescita dei tumori originati da cellule B16F1. Entrambe le proteine sono importanti per la tipica pigmentazione del tumore, in particolare la rimozione della Furina riduce la crescita tumorale, ma questo viene vanificato se anche PC7 è contemporaneamente rimossa. Questi risultati possono contribuire allo sviluppo di nuove strategie terapeutiche mirate a colpire selettivamente le attività oncogeniche delle PC.

Parole chiave: Proproteina convertasi, Furina, PC7, smistamento vescicolare, FRET, melanoma

Table of contents

Abbreviations

ADAM	A disintegrin and metalloproteinases domain-containing
BACE-1	β-site amyloid precursor protein-cleaving enzyme-1
BDNF	Brain-derived neurotrophic factor
BMP	Bone morphogenetic protein
CHRD	Cysteine-histidine rich domain
CLIP	Cell-linked indicator of proteolysis
CMK	Decanoyl-Arg-Val-Lys-Arg-CMK
CRD	Cysteine-rich domain
CRISPR	Clustered Regularly Interspaced Short Palindromic Repeats
ECM	Extracellular matrix
EGF	Epidermal growth factor
EMT	Epithelial-mesenchymal transition
ER	Endoplasmic reticulum
FRET	Förster Resonance Energy Transfer
GPI	Glycosylphospatidyl-inositol
HSPG	Heparin sulfate proteoglycans
hTfR1	Human transferrin receptor 1
IGF	Isulin growth factor
IGFR1	Insulin-like growth factor 1 receptor
M6PR	Mannose-6-phosphate receptor
MITF	Microphtalmia-associated transcription factor
MMP	Matrix metalloproteinase
MT-MMP	Membrane-bound matrix metalloproteinase
PACS-1	Phosphofurin acidic cluster sorting protein-1
PC	Proprotein convertase
PDGF	Platelet-derived growth factor
PMEL17	Pigment cell-specific-pre-melanosomal protein
PTM	Post-translational modification
TGFβ	Transforming growth factor-β
TGN	*Trans*-Golgi network
VEGF	Vascular endothelial growth factor

List of Figures

List of Tables

1 Introduction

1.1 Proprotein Convertases

Proteins such as hormones, enzymes and receptors become active through post-translational modifications (PTMs) of their inactive precursors. Different PTMs are introduced to the target protein via specific enzymatic steps. Some PTMs are reversible, such as serine/threonine/tyrosine-phosphorylation, others instead, are irreversible like N-terminal acetylation, C-terminal amidation, asparagine- and serine/theronine-glycosylation, protein lipidation, tyrosine-sulfation, cholesterol attachments, serine-octanoylation and disulfide bridge formation (Bürkle, 2001).

One of most common irreversible PTM is the proteolysis of specific proteins at selected sites mediated by specific enzyme called proteases. Almost 500 genes in human genome encode proteolytic enzymes (López-Otín and Overall, 2002) which vary in substrate specificity, subcellular localization and cleavage mechanism. Based on their enzymatic active site, proteases can be classified in six groups, *i.e.* serine, metallo, cysteinyl, aspartyl, threonine, and glutamyl. The ubiquitous serine proteases are the most abundant proteases and they are classified into two major families: those related to trypsin/chymotrypsin fold and those closer to bacterial subtilisin, generally called subtilases (Long and Cravatt, 2011; Siezen and Leunissen, 1997). The subtilases are further classified in different sub-families including the proprotein convertase family (Rawlings and Barrett, 1999; Seidah, 2011).

1.1.1 Discovery

Proprotein convertases (PCs) functions and activities have been thoroughly investigated since their discovery almost 30 years ago. The complete genomic sequence of the proprotein convertases prototype Furin was reported in the 1988 (Fuller et al., 1988), few years later the identification of the yeast convertase kexin (Julius et al., 1984) which shares with Furin high degree of sequence homology (van de Ven et al., 1990). Furin discovery led soon to the characterization of the two neuroendocrine PCs named PC1 and PC2 (Seidah et al., 1990; Smeekens et al., 1991). Inspired by this wave of discoveries, the identification of the other family members PC4, PC5, PACE, and PC7 soon followed (Kiefer et al., 1991; Lusson et al., 1993; Seidah et al., 1992, 1996)(and reviewd in Seidah, 2011). The eight member

subtilisin/kexin isozyme-1 (SKI-1) and the ninth member PCSK9 were characterized in 1999 and in 2003 respectively (Seidah et al., 1999a, 2003).

1.1.2 Structure and activity

Proprotein convertases are involved in the activation or inactivation of several proteins by cleaving their precursor in the secretory pathway. The first seven members, PC1, PC2, Furin, PC4, PC5, PACE4, and PC7, are called basic PCs and cleave precursor proteins at specific single or paired basic amino acids within the general consensus motif [R/K-(X)$_n$-R/K-R↓], where the arrow indicates the cleavage site, n represents the number 0,2,4,or 6 and X is any amino acid except cysteine (Seidah and Chretien, 1999; Turpeinen et al., 2011). In contrast to the seven basic PCs, SKI-1 cleaves at non-basic amino acid of the consensus motif [RX(L/V/I)X↓], where X is any amino acid except for cysteine and proline (Marschner et al., 2011; Pasquato et al., 2006). The last member of the family, PCSK9, cleaves only itself at the sequence (V/I/L)FAQ↓ within its prosegment. After this cleavage event, PCSK9 loses its proteolytic activity and regulates cholesterol and lipid homeostasis by enhancing degradation of the low-density lipoprotein receptor (LDLR) (Benjannet et al., 2004; Maxwell and Breslow, 2004; Nassoury et al., 2007; Park et al., 2004).

The seven basic PCs slightly differ in size but they share similar structures (Fig. 1). PCs are multi-domains proteins, with some domains conserved among the family members, whereas other are member-specific. The PC N-terminal domain consists of a signal peptide, which translocates the protein into the the endoplasmic reticulum (ER), and the prosegment, which plays a dual role of intramolecular chaperone and PC inhibitor. Indeed, the prosegment assists the correct folding of the protein inhibiting at the same time its proteolytic activity to avoid ectopic PC proteolytic cleavage. The prosegment is followed by a subtilisn/kexin-related catalytic domain containing the conserved amino acid aspartate (Asp), histidine (His) and serine (Ser), which form the catalytic triad (Nakayama, 1997). This domain exhibits the highest sequence similarity among PCs, since the catalytic domain of other PCs are 50 to 70% identical to the Furin sequence (Henrich et al., 2005). Besides the catalytic domain, all the PCs hare a P domain, which is conserved in eukaryoties but absent in bacteria. The P domain is essential for enzymatic activity since it might stabilize the acidic prodomain and the catalytic domain (Artenstein and Opal, 2011; Hatsuzawa et al., 1992; Takahashi et al., 1995a; Zhong et al., 1996; Zhou et al., 1998). In addition, recent mutagenesis experiments in the P domain have suggested that PC efficiency depends also on its integrity (Dahms et al., 2016a). Although similar in the N-terminal domains, PCs differ from in each other in their C-terminal domains, which determine PC trafficking and localization. Downstream the P domain, only

three of the seven basic PCs, Furin, PC5 and PACE4 possess a cysteine-rich domain (CRD) (Nakagawa et al., 1993; Seidah et al., 1994).
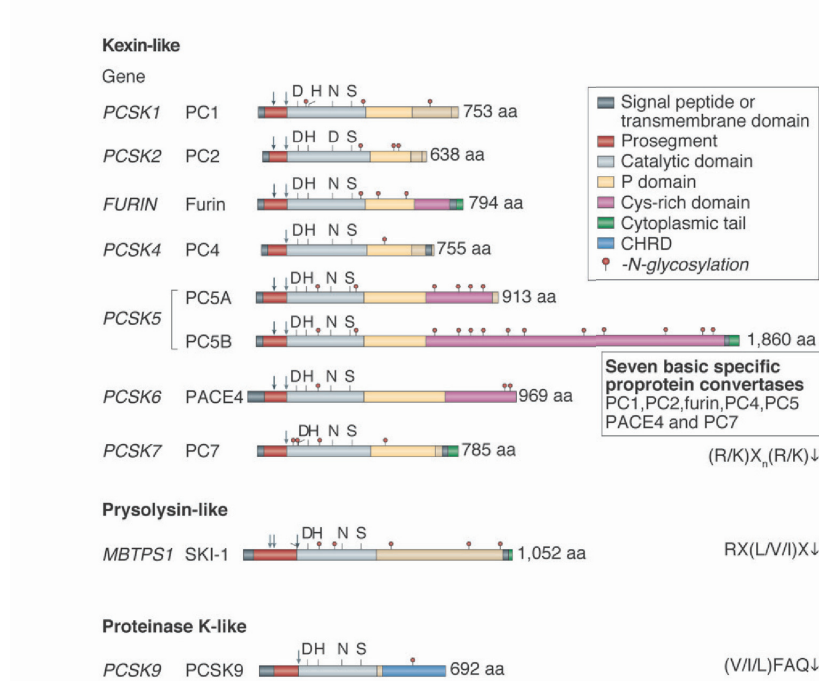
Figure 1. Schematic representation of the primary structures of the proprotein convertases

The kexin‑like basic amino acid (aa)‑specific proprotein convertases, pyrolysin‑like subtilisin kexin isozyme 1 (SKI‑1; encoded by the MBTPS1 gene) and proteinase K‑like proprotein convertase subtilisin kexin 9 (PCSK9) are individually grouped to emphasize their distinct subclasses. The various domains and N‑glycosylation positions are emphasized, along with the primary (depicted using light grey arrows, and a light grey double arrow for SKI‑1) as well as the secondary autocatalytic processing sites (depicted using dark grey arrows). Note that proprotein convertase 4 (PC4), PC7 and PCSK9 have only a primary site and that only PC5 exhibits two validated alternatively spliced forms, namely PC5A and PC5B. The membrane‑bound human proprotein convertases include furin, PC4, PC5B, PC7 and SKI‑1. The presence of a signal peptide, a prosegment and catalytic domain is common to all convertases that exhibit the typical catalytic triad residues Asp, His and Ser, as well as the Asn residue comprising the oxyanion hole (Asp for PC2). Downstream of the catalytic domain, all the basic amino acid‑specific convertases, except for SKI‑1 and PCSK9, exhibit a β‑barrel P domain that apparently stabilizes the catalytic pocket. The carboxy‑terminal domain of each convertase contains unique sequences regulating their cellular localization and trafficking. PC5 and paired basic amino acid cleaving enzyme 4 (PACE4) contain a specific Cys‑rich domain, which binds to heparan sulphate proteoglycans at the cell surface and the extracellular matrix. By contrast, PCSK9 exhibits a Cys‑His‑rich domain (CHRD) that is required for the trafficking of the PCSK9–LDLR (low‑density lipoprotein receptor) complex to endosomes and lysosomes (adapted from Seidah and Prat, 2012).

The widely expressed proprotein convertase PC5 is encoded by two mRNAs. The two isoforms give rise to the soluble PC5A (Lusson et al., 1993) and the type-I membrane protein PC5B which possesses an extended CRD domain (Nakagawa et al., 1993). Furin, PC5B and PC7

also possess a transmembrane domain and a cytosolic tail, which direct PCs proper sorting and trafficking in the different compartments of the secretory pathway. SKI-1 is also a type-I membrane-bound protease but does not have the CRD (Seidah et al., 1999a). Both PC1 and PC2 lack the CRD, the transmembrane domain and cytosolic tail and are sorted in dense core granules of neural and endocrine cells (Day et al., 1992; Seidah and Chretien, 1999), while PC4, PACE4 and PC5A are constitutively secreted (Seidah et al., 2006). However, since the CRD domain of both PACE4 and PC5 binds, through association with their CRD, to the tissue inhibitors of metalloprotease (TIMPs) or to heparin sulfate proteoglycans (HSPG), both PACE4 and PC5 can be retained at the cell surface (Nour et al., 2005; Tsuji et al., 2003). Finally, the C-terminal domain of PCSK9 consist in a cysteine-histidine rich domain (CHRD) which is require for proper PCSK9 cell surface localization (Nassoury et al., 2007).

1.1.3 Activation

Like other proteins trafficking in the secretory pathway, PCs undergo different and specific post-translational modifications before reaching their bioactive form and being able to cleave their substrates or to bind their targets. Like for other proteases, PCs are synthesized as inactive zymogens. Multiple proteolytic events are required to activate PCs precursor. The signal peptide guides the inactive precursor in the ER, where it is removed by a signal peptidase. With the exception of PC2, which maturates in the dense immature secretory granules (Hwang and Lindberg, 2001; Zhu et al., 1996), in the ER all PCs undergo the first intramolecular autocatalytic cleavage generating a non-covalently associated heterodimeric prosegment:PC complex (Seidah et al., 2008). The cleaved prosegment remains bound to the protease inhibiting its activity. The prosegment:PC complex exits the ER and is sorted to specific compartments where the second autocatalytic compartment-specific cleavage occurs. The cleavage occurs within the prosegment to release the active protease (Feliciangeli et al., 2006; Seidah et al., 2008). The compartment where the second autocatalytic cleavage occurs differs between PCs. PC1 and PC2 are activated in the immature secretory granules (Benjannet et al., 1993). The second autocatalytic cleavage is not required for PC4 and PC7 activation (Basak et al., 1999; Rousselet et al., 2011a). Furin appears to be activated in the trans-Golgi network (TGN) (Feliciangeli et al., 2006), PACE4 and PC5 resulted activated in the TGN or at the plasma membrane (Mayer et al., 2008; Nour et al., 2005), while SKI-1 is activated in the cis- and medial-Golgi (Espenshade et al., 1999; Pullikotil et al., 2007). Finally, PCSK9 is secreted as inactive prosegment:PC complex and binds its targets without inducing direct cleavage (Benjannet et al., 2004; McNutt et al., 2007). Thus, the compartment-specific

auto-activation process represent an exquisite mechanism to regulate PC activities, assuring substrates PC cleavage only at the proper intracellular or extracellular site(s).

1.1.4 Tissue and subcellular localization

Both tissue expression and subcellular distribution contribute to determine substrates specificity of each PC family member (Fig. 2). PC1 and PC2 localized to immature dense core granules of neural cells in the brain or endocrine cells of the pancreas (Day et al., 1992; Malide et al., 1995). This localization is consistent with their role in processing hormones within the secretory regulated pathway such as pro-insulin or propromelanocortin (POMC) (Seidah et al., 1999b; Smeekens et al., 1992). PC4 is expressed in ovaries and in the placenta in females (Gyamera-Acheampong and Mbikay, 2009) , and in specific testicular germ cells in males (Gyamera-Acheampong, 2006; Seidah et al., 1992). Both PC5 and PACE4 are widely expressed (Dong et al., 1995; Lusson et al., 1993). However, while PC5A is expressed in most of the tissues, PC5B is the major isoform in the small intestine and in the kidneys (Essalmani et al., 2006). Furthermore, while the trafficking of type-I membrane bound PC5B is controlled by a sorting signal in its cytosolic tail (De Bie et al., 1996; Xiang et al., 2000), both PC5A and PACE4 are either secreted, or they can bind TIMPs or HSPG at the cell surface or in the extracellular matrix (ECM) (Mayer et al., 2008; Nour et al., 2005; Tsuji et al., 2003). SKI-1 is expressed in many tissues and it localizes in *cis/medial*-Golgi, in endosomes or lysosomes (Pullikotil et al., 2007). Contrary to other membrane bound PCs, SKI-1 doesn't localize the cell surface and is shed to the medium (Elagoz et al., 2002). PCSK9 is mainly expressed in small intestine, liver and kidney (Seidah et al., 2003; Zaid et al., 2008) and is secreted as a soluble inactive prosegment:PC complex (Cunningham et al., 2007). Upon biding to its target, e.g. LDLR, PCSK9 can be internalized in endosomes and lysosomes for degradation (Maxwell et al., 2005; Nassoury et al., 2007).

Since most of this work is focused on Furin and PC7, their trafficking, localization and activities of these will be discussed in more details in the next two sections.

1.1.5 Furin: the Proprotein Convertase prototype

Among PCs, Furin is the best characterized family member and its role and function have been investigated in both physiological and in pathological conditions. Its gene, was identified in the upstream region of the c-fes/fps proto-oncogene (FES), and named FUR (FES upstream region) (Roebroek et al., 1986). The protein is ubiquitously expressed in many mammalian tissues and is conserved in both vertebrates and invertebrates (Seidah et al., 1998; Thacker and Rose, 2000). Multi-step and compartments-specific cleavages are required for proper

Furin activation. This finely regulated process leads to the removal of the inhibitory prosegment, which appears to occur in the TGN/endosomal system (Anderson et al., 2002; Feliciangeli et al., 2006).

Furin is known to cleave and activate a wide range of substrates like growth factors, receptors, adhesion molecules and other proteases mostly in the TGN (reviewed in Jaaks and Bernasconi, 2017; reviewed in Thomas, 2002). The ability to cleave diverse substrates *in vivo* is explained by its trafficking and sorting to many sites of the secretory pathway (Fig. 2). Many reports indicate that Furin localizes to the TGN and transit from the TGN to post-exocytic vesicles (Molloy et al., 1994; Takahashi et al., 1995b; Wan et al., 1998). Furthermore, Furin trafficking is also regulated by phosphorylation events at specific motif of the cytosolic domain, and by the interaction with sorting adaptor or cytoskeleton proteins (reviewed in Thomas, 2002). For example, in polarized cells basolateral sorting of Furin is dependent on the interaction with the ubiquitously expressed adaptor protein-4 (AP4) (Simmen et al., 2002).

Although budding from TGN to post-exocytic compartments is essential for proper Furin activity, the cytoplasmic machinery involved in Furin exocytic trafficking is not well understood. On the other hand, Furin endocytosis and retrieval from endosomes to TGN is well studied. Furin recruitment from the cell surface is dynamin/clathrin-dependent and is regulated by the interaction with the adaptor protein-2 (AP-2) (Teuchert et al., 1999a). It also involves other proteins such as filamin or sorting nexin-15 (SNX-15) (Barr et al., 2000; Stossel et al., 2001). From the endocytic compartments Furin is either able to recycle to the TGN or to the plasma membrane. The sorting is regulated by casein kinase 2 (CK2) phosphorylation of an acidic cluster in the cytolosic tail. Phosphorylation by CK2 leads to recycling to the cell surface, while dephosphorylation by the protein phosphatase 2A (PPA2) directs Furin back to the TGN (Mallet and Maxfield, 1999; Molloy et al., 1998). Moreover ,Furin recycling is regulated by the its interaction with the phosphofurin acidic cluster sorting protein-1(PACS-1), which connects Furin to the adaptor protein-1 (AP1) (Crump et al., 2001; Wan et al., 1998). Besides its role in substrate cleavage and activation in the constitutive secretory pathway, Furin contribution to substrate maturation has also been investigated in the regulated secretory pathway of neuroendocrine and endocrine cells. In these cells Furin has been found into the immature secretory granules (ISGs), which are also enriched with hormones and other proteases (reviewed in Thomas, 2002). These compartments undergo a series of membrane remodelling

during the transport to the cell surface (Tooze, 1998) and when they are closed to the cell periphery, Furin is removed from the ISGs and is recycled to the TGN (Dittié et al., 1997).

Many studies have uncovered role of Furin in embryogenesis and in several diseases. Mice lacking functional Furin die at the embryonic day 11 (E11) and exhibit multiple tissue abnormalities like abnormal yolk sac vasculature, failure of axial rotation and severe cardiac defects (Roebroek et al., 1998). This phenotype is likely due to the impaired Furin-activation of the transforming growth factor-β (TGF-β) family members Lefty, Nodal or bone morphogenetic protein-10 (BMP10) (Constam et al., 2000; Susan-Resiga et al., 2011). Similarly, Furin can cleave other TGF-β family members including bone morphogenetic protein-4 (BMP-4) and TGF-β-1 (Cui et al., 1998; Dubois et al., 2001). The embryonic lethality of Furin-null mice supports the idea of lack of redundancy between Furin and other family members, although PCs redundancy has been shown *in vivo* for some substrates (Bessonnard et al., 2015; Roebroek et al., 2004). However, few unique Furin substrates have been identified, such as PCSK9 in hepatocytes (Essalmani et al., 2011) and the Ac45 subunit of the vacuolar H^+-ATPase in pancreatic β cells (Louagie et al., 2008).

Although Furin is essential for embryogenesis, in certain conditions its activity might contribute the occurrence or the progression of several diseases. Furin and other family members are known to activate the precursor of the β-site amyloid precursor protein-cleaving enzyme-1 (BACE-1) (Bennett et al., 2000). The secreted enzyme BACE-1 is involved in the formation of the senile plaques in Alzheimer's disease (Vassar, 1999). However, Furin is also involved in activation of other proteases such as α-secretase (Hwang et al., 2006), whose activity leads to reduction senile plaques formation (Postina et al., 2004). In addition, Furin can activate several bacterial or viral pathogens. Indeed, Furin-dependent cleavage is a mandatory step in bacterial toxin activation. Many evidence indicate the role of Furin in activation of anthrax toxin or *Clostridium septicum* α-toxin at the cell surface of the host cells (Abrami et al., 1998; Gordon et al., 1997; Klimpel et al., 1992). Furthermore, other bacterial toxins, like *Pseudomonas* esotoxin A (PEA), diphtheria toxin, shiga-toxin and shiga-like toxin 1, can be processed and activated by Furin in endosomal compartments (reviewed in Thomas, 2002). Finally, many pathogenic viruses, including measles virus, human immunodeficiency virus-1 (HIV-1), avian

influenza virus, require Furin-dependent cleavage of their immature envelope glycoproteins for their activation (Molloy et al., 1999; reviewed in Thomas, 2002; Volchkov et al., 1998).
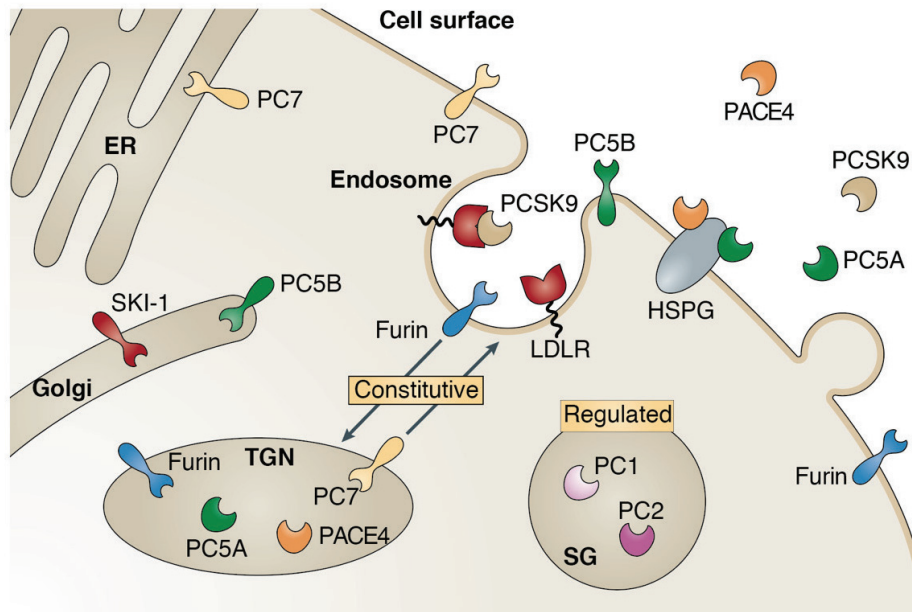
Figure 2. Subcellular localization of proprotein convertases

Upon exiting the endoplasmic reticulum (ER), most of the basic amino acid‑specific proprotein convertases traverse the Golgi apparatus towards the trans‑Golgi network (TGN). At this branching point the convertases proprotein convertase 1 (PC1) and PC2 are sorted to immature secretory granules where they are activated, cleave polypeptide hormones and are stored in dense‑core secretory granules (SGs) awaiting signals for regulated secretion. Conversely, the constitutively secreted furin, PC5 and paired basic amino acid cleaving enzyme 4 (PACE4) reach the cell surface from the TGN. PC7 is able to reach the same destination from both the TGN and by an unconventional secretion pathway directly from the ER. Upon binding to heparan sulphate proteoglycans (HSPGs) and tissue inhibitors of metalloproteinases, PC5A and PACE4 are retained at the cell surface and/or extracellular matrix. The membrane‑bound furin, PC5B and PC7 are recycled through endosomes back to the TGN. The activated membrane‑bound subtilisin kexin isozyme 1 (SKI‑1) is mostly concentrated in the cis- and medial‑Golgi, from where it is then sent to lysosomes for degradation, and does not normally reach the cell surface. Proprotein convertase subtilisin kexin 9 (PCSK9) is secreted from the TGN directly into the medium as an enzymatically inactive non‑covalent complex of the protease and its prosegment. Upon binding to the low‑density lipoprotein receptor (LDLR) at the cell surface, the PCSK9–LDLR complex is internalized into endosomes and then sent to lysosomes for degradation (adapted from Seidah and Prat, 2012).

1.1.6 PC7: The most ancestral and conserved PC

Identified in 1996 in the chromosome breakpoint region of human lymphoma cells carrying a t(11;14)(q23; q32) translocation (Meerabux et al., 1996), PC7, also called lymphoma PC (LPC), is the most ancient and conserved proprotein convertase family member (Bruzzaniti et al., 1996; Seidah et al., 1996). Although PC7 is ubiquitously expressed in embryo, adult tissues

and many cell lines (Constam et al., 1996; Meerabux et al., 1996; Rousselet et al., 2011a; Seidah et al., 1996), its localization, trafficking and function are barely investigated. PC7 is synthesized as an inactive zymogen in the ER, where it binds the molecular chaperone BiP to prevent aggregation (Creemers et al., 2000). Like other PCs, PC7 undergoes autocatalytic cleavage at KRAKR^{140}↓ (rat) (Seidah et al., 1996) or RRAKR^{141}↓ (human) sites (Meerabux et al., 1996). Cleavage of the PC prosegment is a slow process that has been shown to take hours (Creemers et al., 2000; Van De Loo et al., 1997). After exit of the ER, PC7 undergoes several PTMs (Van De Loo et al., 1997) such as N-glycosylation (Seidah et al., 1996), sulfation (Rousselet et al., 2011a) and reversible palmitoylation of 2 cysteines in the cytosolic tail (Van De Loo et al., 1997).

Contrary to other PCs, PC7 localization and trafficking are poorly investigated. Endogenous PC7 has been described to enrich in vesicles that localize beneath the plasma membrane and can be distinguished from those containing Furin (Leonhardt et al., 2010; Wouters et al., 1998), suggesting a spatial segregation of the two PCs. Moreover, several reports have demonstrated that overexpressed PC7 mainly localized in the TGN and a small fraction can be found at the cell surface (Declercq et al., 2012, 2016; Van De Loo et al., 1997). However, how PC7 trafficking is regulated remains a matter of controversy. In another report, overexpressed PC7 was not detected in TGN, early endosomes and lysosomes of HEK293T cells, whereas it co-localizes with the ER marker calreticulin and with flotillin-1 a known marker for clathrin-idependent endocytosis, suggesting that PC7 internalization is mediated by clathrin-independent endocytosis (Rousselet et al., 2011a). In the same report PC7 has been shown to traffic through both the conventional secretory pathway and the brefeldin-A and COPII-independent unconventional route. Intriguingly, while overexpression of Furin, PC5 and PC7 prosegments resulted in inhibition of PCs activity (Nour et al., 2003; Zhong et al., 1999), only PC7 prosegment is secreted (Munzer et al., 1997; Zhong et al., 1999) and traffics only through the conventional route (Rousselet et al., 2011a). In another report, PC7 internalizes via clathrin-mediated endocytosis in CHO-K1 cells (Declercq et al., 2012). A short motif of three amino acids, Pro^{724} Leu^{725} and Cys^{726} (PLC motif), and a cluster of basic amino acids in the cytosolic tail are essential for proper PC7 retrograde transport from the plasma membrane to the TGN (Declercq et al., 2012, 2016). The relevance of the C-terminus for directing PC7 trafficking and activity was confirmed in experiments where PC7 trans-membrane domains and cytosolic tail are swapped with Furin counterparts (Guillemot et al., 2013; Rousselet et al., 2011a).

A number of investigations aimed to define PC7 biological function. In sharp contrast to other PCs (Scamuffa et al., 2006), the PC7 knock-out mice are viable (Villeneuve et al., 2002),

although they manifest defects in memory and anxiolytic behaviour, probably due to impaired brain-derived neurotrophic factor (BDNF) processing (Anyetei-Anum et al., 2017; Wetsel et al., 2013). Furthermore, lack of embryonic lethality in PC7-null mice might be explained the redundant activity provided by overlapping PCs (Bessonnard et al., 2015). These data suggest that PC7 is involved in the maturation of non-essential substrates or is expressed in cells where substrates processing is mediated by redundant PCs (Taylor et al., 2003). PC7 shares several secretory substrates with other PC family members, both *in vitro* and *in vivo*, such as growth factors like the vascular endothelial growth factor-C (VEGF-C) or BMP-4 (Cui et al., 1998; Nelsen and Christian, 2009; Siegfried et al., 2003), proteases like disintegrin and metalloproteinases domain-containing 10 (ADAM10) and ADAM17 (Anders et al., 2001; Endres et al., 2003) and adhesion molecules like E-cadherin (Bessonnard et al., 2015). However, the redundancy is only partial, since PC7 cannot rescue embryonic lethality in other PCs knock-mice (Bessonnard et al., 2015; Creemers and Khatib, 2008; Roebroek et al., 1998; Scamuffa et al., 2006). Inactivation of PC in zebrafish resulted in various developmental defects suggesting that PC7 has a non-redundant and relevant function in ealry zebrafish development (Turpeinen et al., 2013). Furthermore, a recent genome-wide association study revealed a strong link between lower levels of the soluble form of the human transferrin receptor 1 (hTfR1) and a PC7-specific single nucleotide polymorphism (SNP) (Oexle et al., 2011). In addition, PC7 has been shown to mediate the shedding of the overexpressed hTfR1 in different cell lines (Guillemot et al., 2013), demonstrating its role in iron homeostasis. PC7 role in shedding the hTfR1, relies on its catalytic activity, but also on the presence of the cytosolic tail, which directs intracellular sorting and PC localization. Furthermore PC7 indirectly enhances maturation of epidermal growth factor precursor (proEGF) (Rousselet et al., 2011b), and can process overexpressed apolipoprotein-F (apo-F) and sortilin in mouse primary hepatocytes (Guillemot et al., 2014).

1.1.7 Proprotein Convertases in homeostasis and diseases

Several studies underline the importance of PC activities in development and under physiological conditions (reviewed in Seidah and Prat, 2012). The embryonic lethality of Furin, PC5 or SKI-1-null mice firmly indicate that their absence or underexpression result in defects in proper cellular or homeostasis organogenesis (Essalmani et al., 2008; Roebroek et al., 1998; Scamuffa et al., 2006). Although viable, knock-out mice of other family members showed defects in growth (PC1 and PC2) (Furuta et al., 1997; Zhu et al., 2002), in fertility (PC4) (Mbikay et al., 1997a), in development (PACE4) (Constam and Robertson, 2000), and in metabolism (PC2 and PCSK9) (Furuta et al., 1997; Rashid et al., 2005).

Due to their ability of cleaving a plethora of substrates, alteration in PCS activity or expression has been associated with several diseases. As previously discussed, Furin can activate bacterial toxins, and several viruses hijack host PC to cleave their glycoproteins (reviewed in Thomas, 2002). Furthermore, Furin and other family members are involved in neurodegenerative diseases due to their, although indirect, role in plaque formation (Bennett et al., 2000; Lopez-Perez et al., 1999). Some studies have reported their contribution in atherosclerosis by activation of membrane-bound matrix metalloproteinases (MT-MMPs) and αv-integrins in macrophages and in muscle cells (Stawowy and Fleck, 2005; Stawowy et al., 2005). Finally, PC are involved in different steps of cancer progression (reviewed in Artenstein and Opal, 2011; Jaaks and Bernasconi, 2017) and due to the wide range of activated substrates, their implication is discussed below.

1.1.8 Proprotein Convertases in cancer

Many of the *in vitro* and *in vivo* validated PC substrates are involved in the different steps of tumorigenesis, including transformation, proliferation, invasion, and metastasis formation (reviewed in Artenstein and Opal, 2011). Therefore, the increase in PC expression and activities is associated with progression and invasion in several types of cancer. In addition, PC expression varies between different tumors and it's intuitive to think that their contribution in cancer progression whether they activate oncogenic or tumor-suppressor proteins. I further aim to give a general overview of PC expression and their role in different tumor types.

Astrocytoma and cancer of the brain: PCs can promote the malignant phenotype of cancer of the central nervous system. Indeed, Furin is highly expressed in high grade astrocytoma, and its inhibition leads to reduced proliferation *in vitro* and tumor growth *in vivo*. This effect is due to the reduced processing of specific substrates, including MT-MMP1, the insulin receptor (IR) and transforming growth factor-β (TGFβ), that promotes proliferation of malignant gliomas (Mercapide et al., 2002). Moreover, Furin activity promotes glioma cell invasiveness *in vitro* (Wick et al., 2004).

Breast cancer: Many PC family members, including Furin, PACE4, and PC7 are expressed in both human tumors and breast cancer cell lines (Cheng et al., 1997). Overexpression of the inhibitory Furin prosegment in breast cancer cells results in reduction of tumor growth *in vivo* and impaired processing of the insulin-like growth factor 1 receptor (IGFR1) and the platelet-derived growth factor A (PDGF-A) (Scamuffa et al., 2014). Interestingly, inhibition of PACE4 by overexpression of its prosegment results in the opposite effect, suggesting different roles of PACE4 and Furin in breast cancer progression (Lapierre et al., 2007). In another *in vitro* study, Furin inhibition resulted in MT-MMP1 inactivation and in reduction of matrix

metalloproteinase 2 (MMP2) and MMP9 expression, suggesting a link between breast cancer cells motility and MMPs expression (Cepeda et al., 2017).

Cervical, endometrial and ovarian cancer: Increased motility and tumor growth of cervical cancer cells, both *in vitro* and *in vivo*, are dependent on NF-kB-dependent overexpression of Furin (Kumar et al., 2010). Among the family members, Furin is the most expressed in human endometrial tumors and cell lines (Singh et al., 2012). Furthermore, monitoring PC activity in endocervical swabs and in uterine lavage samples has been proposed as a non-invasive diagnostic tool for endometrial cancer since PC activity was higher in patient samples compared to healthy control (Heng et al., 2016a, 2016b). Finally, the importance of PCs in ovarian cancer has been investigated. Indeed, Furin is expressed in several stages of the disease, including ascites and metastasis. Furthermore, Furin activity is important for the proper processing of MT-MMP1 (Longuespée et al., 2014; Page et al., 2007). Interestingly, it has been shown that PACE4 expression in down-modulated in ovarian cancer cells (Fu et al., 2003).

Gastrointestinal cancer: PC1 and PC2 have been found upregulated in liver metastasis originating from colorectal cancer (Tzimas et al., 2005). However, Furin is the most overexpressed PC in tumors and cancer cell lines (Nakajima et al., 2002). Its inhibition by overexpression of Furin prosegment or by pan-PC inhibitor α1-antitrypsin Portland (α1-PDX) result in impaired processing of IGFR1, insulin growth factor-1 (IGF-1) and PDGF-A and leads to the decrease of tumor growth and number of metastasis *in vivo* (Khatib et al., 2001; Scamuffa et al., 2008, 2014). Moreover, Furin can activate the parathyroid hormone-related peptide (PTHrP), which in turn stimulates Furin expression and increases gastric cancer cells proliferation *in vitro* (Nakajima et al., 2002).

Head and neck squamous cell carcinomas (HNSCC): High PC expression is found to correlate with aggressiveness of head and neck derived squamous cell carcinoma *in vivo*, including PC5 and Furin, while PC7 is highly expressed in HNSCC cell lines *in vitro* (Bassi et al., 2001a, 2005). Several studies, showed that PC activities are important for HNSCC cells proliferation, motility and invasiveness both *in vitro* and *in vivo*. Furthermore, PCs have been shown to be required for proper activation of important proteins involved in HNSCC progression like VEGF-C, IGFR1, TGFβ, and MT-MMP1(Bassi et al., 2001b, 2003; De Cicco et al., 2005).

*Lung carcinomas***:** Furin was the first PC detected in non-small cell lung cancer (NSCLC) and its expression was found to be higher in adenocarcinomas and in squamous cell carcinoma compared to small-cell lung carcinoma (SCLCs) (Schalken et al., 1987). Furthermore, since Furin expression correlates with the invasiveness of NSCLS cell lines (Bassi et al., 2001a; López de Cicco et al., 2002), Furin has been proposed as a potential biomarker for this type

of tumor (Demidyuk et al., 2013). By constrast, other family members including PC1, PC2 and PACE4 are expressed only in SCLSs (Mbikay et al., 1997b; Rounseville and Davis). In addition, inhibition of PCs activities reduces cell proliferation and migration *in vitro*, as well as tumor formation *in vivo* (Bassi et al., 2016; Ma et al., 2014).

Prostate cancer: Two studies have elucidated the role of PACE4 in prostate cancer progression to a more aggressive grade (D'Anjou et al., 2011, 2014). Furthermore, it has been shown that both Furin and PC7 cannot substitute PACE4 activity in prostate cancer cell proliferation *in vivo*, positioning PACE4 as potential therapeutic target for prostate cancer (Couture et al., 2012).

Sarcomas: Although both Furin and PACE4 are found overexpressed in rhabdomyosarcoma (RMS), only the contribution of Furin in tumor progression has been investigated. Furin activity is required in RMS cell lines for proper maturation of cancer-related substrates including VEGF-C, IGF1R, PDGF-B and MT1-MMP, that play a role in proliferation, invasion and metastasis formation (Jaaks et al., 2016a). Another study revealed that Furin is expressed in almost 90% of pediatric RMS, and Furin silencing leads to complete remission of established RMS cell line tumors *in vivo* (Jaaks et al., 2016b). Preliminary i*n vitro* studies revealed PC contribution in cell motility in both fibrosarcoma and osteosarcoma (Liu et al., 2014a; Maquoi et al., 1998).

Skin cancer: Furin overexpression in epidermal basal layer of the skin increases number of high-grade squamous cell carcinoma after a two-step chemical carcinogenesis protocol *in vivo* (Fu et al., 2012). Similar results were obtained in mice exposed to UVB radiation in UV-induced skin carcinogenesis experiments (Fu et al., 2013). Another PC family member, PACE4, has been characterized in skin cancer. PACE4 overexpression results in increased skin cancer cell proliferation both *in vitro* and *in vivo* (Bassi et al., 2015). In addition, PC inhibition in human primary melanoma cells impairs processing of PDGF-A, IGFR-1 and MMPs and result in reduced cell invasion and migration *in vitro* (Lalou et al., 2010).

1.1.9 Proprotein Convertase substrates in cancer

Many precursor proteins involved tumorigenesis and metastasis formation are cleaved by one or several members of the PC family (Fig. 3). Here I will briefly describe some important cancer-related PC substrates.
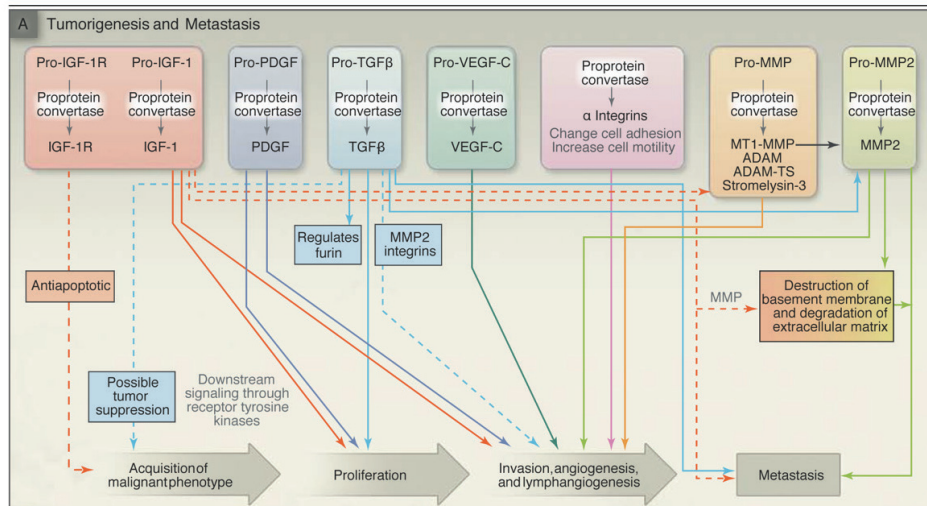

Figure 3. Proprotein convertases in tumorigenesis

In the processes of tumorigenesis and metastasis, proprotein convertases cleave a variety of precursors of distinct growth factors, receptors, adhesion molecules, and matrix metalloproteinases (MMPs). Each of these activated substrates has been shown to affect many of the pathways involved in tumor growth and progression (adapted from Artenstein and Opal, 2011)

ADAM metalloproteinases: The ADAMs (a disintegrin and metalloproteinases) are a family of secreted and membrane-associated metalloproteinases**,** which play important roles in cell adhesion, cell migration, proteolysis and signalling (reviewed in Edwards et al., 2009)**.** Their activity has been found to contribute to cancer progression and dissemination since they can cleave and activate several cancer-related proteins including Notch, epidermal growth factor, amphiregulin, tumor necrosis factor alpha, and transforming growth factor-alpha (reviewed in Duffy et al., 2009). As many other proteases, ADAMs family members are translated as inactive zymogens requiring posttranslational modifications to acquire proteolytic activity. For some members, this event consists in the removal of the inhibitory prodomain and is mediated by a PC. Both ADAM10 (Anders et al., 2001; Lopez-Perez et al., 2001) and ADAM17(Endres et al., 2003; Srour et al., 2003) are processed by PCs. However, while ADAM17 maturation is

blocked in the Furin-deficient LoVo cell line, suggesting that Furin is the main PC involved in ADAM17 maturation, ADAM10 processing occurs in LoVo cells suggesting a redundant activity of other PC family members. In addition, recent work has characterized a new upstream PC site located in the prodomain of ADAM9, ADAM10 and ADAM17. Cleavage of this upstream PC site appeared essential for proper activation of proADAM17 *in vitro* (Wong et al., 2015).

*Cadherins***:** These type-1 transmembrane proteins play important roles in cell adhesion, sorting and tissue morphogenesis (Halbleib and Nelson, 2006). The metastatic potential of cancer cells inversely correlates with cadherin expression (Vleminckx et al., 1991). PC-mediated activation of inactive cadherin precursor has been investigated only for two family members, epithelial-cadherin (E-cadherin) and neural-cadherin (N-cadherin). Both proteins are synthetized as inactive precursors that requires post-translation modification to acquire their activity. Removal of the prodomain enables calcium-dependent homotypic interaction (Ozawa and Kemler, 1990). Overexpression studies revealed that Furin can cleave and activate E-cadherin (Posthaus et al., 1998). However, the cleavage was not inhibited in Furin-deficient LoVo cells, suggesting that other PC family members might mediate the processing (Posthaus et al., 1998). Recent work in the lab has demonstrated that E-cadherin processing *in vivo* is mediated by Furin, PACE4 and PC7 (Bessonnard et al., 2015). In addition, E-cadherin has been extensively investigate as a potent tumor suppressor (Van Roy and Berx, 2008; Semb and Christofori, 1998) and loss of its expression correlates with poor prognosis and high tumor grade (Hirohashi, 1998; Perl et al., 1998).

Similar to E-cadherin, N-cadherin requires the removal of the inhibitory prodomain to acquire its activity (Tamura et al., 1998). Silencing experiments revealed that Furin is responsible for proper N-cadherin activation, and impaired processing results in accumulation of non-adhesive N-cadherin at the cell surface enhancing motility in tumor cells (Maret et al., 2010). In addition, the same group showed that N-cadherin can be inactivated by PC5 that cleaves an alternative PC-site different from the one recognized by Furin. This cleavage abolishes the adhesive N-cadherin function, favouring cell migration and motility *in vitro* (Maret et al., 2012). Interestingly, a switch from E-cadherin to N-cadherin expression called cadherin switching occurs in both developmental processes and tumorigenesis (Hao et al., 2012; Lade-Keller et al., 2013; Wheelock et al., 2008).

IGF1 and IGF1R: The insulin-like growth factor (IGF) signalling is important for growth and maintenance of many tissues. However, it has been shown to play a critical role in progression of several tumors through its ability to increase cell proliferation and anti-apoptotic signals (reviewed in Denduluri et al., 2015). Overexpression of both IGFR-1 and IGF-1 are associated with high risk of cancer and tumor progression (Chan et al., 1998; Kaleko et al., 1990). Both IGF-1 and IGF1-R are synthesized as a protein precursor and PC-cleavage for their activity

(Duguay et al., 1997; Lehmann et al., 1998; Scamuffa et al., 2008). In fact, PC-inhibition results in reduced tumor growth and cell proliferation *in vitro* through impaired activation of the IGF signalling (Khatib et al., 2001; Lalou et al., 2010; Scamuffa et al., 2008).

Integrins: Integrins are heterodimeric cell surface receptor binding specific proteins of the extracellular matrix (ECM) and providing the traction necessary for cell motility and invasion. In addition, integrins regulate tumor growth by increasing survival signalling and preventing pro-apoptotic events (reviewed in Desgrosellier and Cheresh, 2010). Each heterodimer is formed by two distinct chains named α and β subunits. Cleavage in the α subunit by Furin or PC5 has been shown to be required for their activation (Bergeron et al., 2003; Delwel et al., 1996; Lehmann et al., 1996; Lissitzky et al., 2000).

Matrix Metalloproteinases (MMPs): MMPs belong to a large family of calcium-dependent endopeptidases, that participate in the degradation or remodelling of the ECM (reviewed in Page-McCaw et al., 2007). More than 20 members have been identified in human, and all of them are synthesized as inactive zymogens. To acquire proteolytic activity, the zymogen undergoes a series of proteolytic events including a PC-mediated cleavage. In addition, elevated expression of MMPs correlates with poor prognosis in cancer patients (Egeblad and Werb, 2002). The membrane-anchored MT-MMP-1 is known to be cleaved by Furin (Yana and Weiss, 2000) and is involved in cancer invasion and tumorigenicity in several cancers (Bassi et al., 2001b; Lalou et al., 2010). Furthermore, PACE4 and Furin have been shown to cleave and activate stromelysin-3 (MMP-11) (Pei and Weiss, 1995; Santavicca et al., 1996). Contrary to MMP-11 and MT-MMP1, Furin-dependent cleavage inactivates the MMP-2 family member (Cao et al., 2005).

Notch: The evolutionary conserved Notch pathway play a crucial role in homeostasis and development in various organs and tissues (Artavanis-Tsakonas, 1999). In cancer, depending on the tissue or cellular context, Notch can act as an oncogene or a tumor suppressor gene (reviewed in Nowell and Radtke, 2017; reviewed in Radtke and Raj, 2003). The four mammalian Notch receptors (Notch1-4) are translated as precursor proteins that undergo sequential proteolytic events. The first proteolytic cleavage (S1) is mediated by PCs (Logeat et al., 1998), however the role of this proteolytic events remains controversial. Indeed, both mammalian and fly studies suggest that Furin-independent Notch might signal (Bush et al., 2001; Kidd and Lieber, 2002). On the other hand, Notch1 Furin-cleavage mutant has been shown to be less expressed at the cell surface and exhibits decreased ligand-mediated receptor activation (Gordon et al., 2009).

Platelet-derived growth factor (PDGF): Many studies about PDGF and their receptors (PDGFRs) have elucidated their role in cell proliferation, growth and differentiation (reviewed

in Andrae et al., 2008). Upregulation of the growth factors and their receptors has been found in several types of cancer and their inhibition has demonstrated potential benefit in preclinical and clinical trials (reviewed in Heldin, 2013). To acquire receptor-binding activity, both PDGF-A and PDGF-B prodomains are removed by PC-mediated cleavage. Although most of the basic PC are able to process PDGF-A and PDGF-B, Furin appears as the most potent member in PDGF processing (Siegfried et al., 2003, 2005).

Transforming growth factors β (TGF-β): TGF-β is the founding member of the TGF-β superfamily, which comprises at least 30 members in mammals, and regulates vital cellular processes including proliferation, migration, differentiation and death (reviewed in Weiss and Attisano, 2013)**.** In cancer, TGF-β acts as a tumor suppressor in the early stages of carcinogenesis by inhibition of cells growth and preventing cells dedifferentiation, whereas its behaves as a oncogene in the later stages promoting invasion and metastasis formation (reviewed in Massagué, 2008)**.** TGF-β1 is translated as homodimer requiring two proteolytic cleavages to become active. Although PACE4, PC5 and PC7 can process and maturate the precursor, Furin is considered as the main responsible of the cleavage *in vivo* (Dubois et al., 2001; Roebroek et al., 1998). In addition, TGF-β2 is insensitive to Furin processing, probably due to the tertiary structure of TGF-β2 prosegment (Kusakabe et al., 2008).

Vascular endothelial growth factors: VEGFs are growth factors involved in angiogenesis and lymphangiogenesis in both physiological and pathological conditions (reviewed in Carmeliet, 2005; reviewed in Hoeben et al., 2004). VEGFs are translated as homodimers and secreted as inactive precursors which requires removal of both the N- and C-terminal propeptide to acquire their mature form (Joukov et al., 1997; Stacker et al., 1999). Among the four family members (VEGF-A to D), VEGF-C and VEGF-D are processed by PCs. While Furin and PC5 cleaves proVEGF-D realising both the N- and the C-terminal propeptide (McColl et al., 2007), PC7 promotes cleavage of the C-terminal propeptide only (McColl et al., 2007). In addition, Furin, PC5 and PC7 can cleave only the C-terminal propeptide in VEGF-C precursor (Siegfried et al., 2003).

1.1.10 Proprotein Convertases Inhibitors

Considering PCs contributions in many diseases, several efforts were directed towards the designing and development of inhibition strategies. However, although both *in vitro* and *in vivo* experiments provided extensive evidence of their efficacy, until now few clinical studies support their use in therapeutic context.

Endogenous Inhibitor: Few endogenous PC inhibitors have been so far identified. The proprotein convertase subtilisin/kexin type 1 inhibitor (proSAAS) has been documented as

PC1 endogenous inhibitor with a K_i in the micromolar range (Fricker et al., 2000). Similar to PC1, PC2 was found to be inhibited by an endogenous protein called 7B2. Notably, pro7B2 is a Furin substrate (Paquet et al., 1994), and its C-terminal domain inhibits PC2 until the protease reaches the immature granules where PC2 becomes active (Zhu et al., 1996). Beside its inhibition function, the neuroendocrine 7B2 is essential for proper PC2 folding and activation (Westphal et al., 1999). In the past years, the plasminogen activator inhibitor-1 (PAI-1), which forms a sodium dodecyl sulfate (SDS)-stable complex with Furin thereby inhibiting its activity, has been proposed as potential endogenous Furin inhibitor (Bernot et al., 2011).

Chloromethylketones: The structure of these inhibitor contains the PC cleavage site, a N-terminal decanoyl extension to increase cell permeability and a C-terminal chloromethylketone to block potential degradation by proteases *in vivo*. The inhibitor acts in competitive manner binding with high affinity the catalytic domain forming a covalent PC-inhibitor complex (Garten et al., 1994). The most used and potent to block all PC activity is the decanoyl-Arg-Val-Lys-Arg-CMK (CMK)(Jean et al., 1998). The main caveat of this inhibitor is the lack of specificity for any PC family members and toxicity at high dose.

Poly-arginine derivatives: These suicide inhibitors represent an extension of the PC motif Arg-Arg-Arg-Arg (RRRR). The first inhibitor of this class to be synthesized was the hexa-D-arginine which effectively blocks Furin-activation of the PEA toxin *in vitro* and *in vivo* (Sarac et al., 2002). Another member of this class, poly-D-nonaarginine (D9R) was further synthetized and it has been proved to be a potent Furin inhibitor (K_i in nanomolar range) (Cameron et al., 2000; Kacprzak et al., 2004).

Streptamine derivatives: Docking experiments using the crystal structure of Furin have led to the modelling of non-peptide based PC inhibitors (Dahms et al., 2016b; Henrich et al., 2005). Guanidinilated derivatives of 2-dideoxystreptamine was shown to block PC activity *in vitro* (Jiao et al., 2006), and act in competitive and reversible manner binding the active site of the PC. Since these derivatives bind PACE4 and PC7 with ten or one hundred-fold lower efficiency, they are considered Furin or PC5 specific (Henrich et al., 2005). However, some of these inhibitors are not or poorly cell permeable, making them potential inhibitor of extracellular Furin activities.

Peptidomimetics: These are small molecules containing the PC motif and embedded in a peptide moiety (reviewed in Klein-Szanto and Bassi, 2017). The structure allows specific interactions outside the PC catalytic domain making each peptidomimetic able to bind specifically to each single PC and to inhibit PC activity in a competitive and reversible manner (Becker et al., 2012; Levesque et al., 2012). For example, *in vitro* experiments demonstrated

that the peptidomimetic called inhibitor 24 is more potent against Furin and PACE4 rather than PC7 (Becker et al., 2012).

Prosegment: As previously discussed, PC are synthetized as zymogens and to acquire their proteolytic activity they have to lose their inhibitory prosegment in specific subcellular compartment. Due to their intrinsic inhibitory nature, PC prosegment have been commonly used in several studies to investigate PC activity in physiological and in disease (Siegfried et al., 2003). Overexpression of Furin prosegment inhibits the processing of important cancer-related substrates in breast and gastrointestinal cancer, thereby reducing cancer proliferation and progression (Lapierre et al., 2007; Scamuffa et al., 2014).

α1-antitrypsin and derivative: While the α1-antitrypsin is a physiological inhibitor of neutrophil elastase, the α1-antitrypsin Portland (α1-PDX) is a bioengineered variant containing the PC recognition motif (Jean et al., 1998) which inhibits PC with a K_i in the nanomolar range (Benjannet et al., 1997; Jean et al., 1998). The α1-PDX acts as a suicide inhibitor. Indeed, it binds to PC active site and is cleaved by the PC generating a kinetically trapped SDS-stable complex with the enzyme (Dufour et al., 1998; Tsuji et al., 1999). The α1-PDX has been used to investigate PC contribution in many substrates processing like, MT-MMP1, VEGF and PDGF family members, IGF-1R, and in cancer progression (Khatib et al., 2001; McColl et al., 2007; Scamuffa et al., 2008; Siegfried et al., 2005).

nanobodies: Nanobodies consists in the variable region of the heavy chain of an antibody, and recently they have been designed against the P domain. The nanobody Nb14, specific for Furin P domain, has shown to block processing on PC substrates when overexpressed in cells. However, Nb14 inhibit processing of full PC substrates, whereas small molecules were properly cleaved (Zhu et al., 2012). This non-competitive inhibition strategy represents a promising approach.

PC inhibition in clinical trials: Many cancer cells overexpress the immunosuppressive PC substrates TGF-β1 and TGF-β2, which promote cancer cell proliferation and dissemination (Yoshimura and Muto, 2011). As previously discussed, Furin processing in indispensable for TGF-βs activities. Thus, blocking Furin might result in decreased TGF-β immunosuppressive activities and allow an effective immune response. This approach has been investigated in several types of cancer. In these studies, a cDNA encoding for the granulocyte–macrophage colony-stimulating factor (GM-CSF) and two copies of small hairpin Furin RNA were placed under the control of the strong cytomegalovirus promoter (Rao et al., 2010; Senzer et al., 2012). Patient-derived cancer cells were transfected with this construct and used as cellular vaccines (called FANG, and then named VIGIL in clinical trials) and injected back into the patients. The circulating cells produced elevated level of GM-CSF and low levels of TGF-β1

and TGF-β2. Although preliminary, this Furin-silencing approach seems to be promising in various malignancies including breast cancer, colon cancer, small cell lung cancer, liposarcoma, and ovarian cancer (Nemunaitis et al., 2014; Senzer et al., 2012). Furthermore, encouraging results, such as reduction in relapse rate, have been observed in patients diagnosed with ovarian cancer (Oh et al., 2016), Ewing's sarcoma (Ghisoli et al., 2015, 2016) and hepatocellular carcinoma (Nemunaitis et al., 2014).

1.2 Melanoma

Sadly, melanoma is one of the most aggressive and treatment-resistant human cancers. In 2017, an estimated 87,110 new case of invasive melanoma will be diagnosed and 9,730 deaths are expected (American Cancer Society).

1.2.1 Melanoma origin: melanocytes and MITF

Melanoma arise from malignant transformation of melanocytes, which are neural-crest derived cells that colonize the eye, the skin, the hair matrix, mucosal epithelia and meninges (Brito and Kos, 2008; Goldgeier et al., 1984; Haass et al., 2005; Mort et al., 2015; Tachibana, 1999; Yajima and Larue, 2008). Melanocytes are responsible for pigmentation and photoprotection. Indeed, these cells are specialized in producing two main types of pigments called red pheomelanin and the photoprotective pigment brown/black eumelanin (Valverde et al., 1995). These pigments are then provided to their neighbouring cells called keratinocytes that use them to protect their nucleus from DNA-damage induced by UV (Costin and Hearing, 2007; Kaidbey et al., 1979). Pigment synthesis is stimulated by binding of α-melanocyte stimulating hormone (α-MSH), which is secreted in response to UV radiation by keratinocytes in a p53-dependent manner, and which binds to melanocortin 1 receptor (MC1R) expressed on melanocytes (Cui et al., 2007). MC1R activates cyclic adenosine monophosphate (cAMP) production (Suzuki et al., 1996; Wong and Pawelek, 1973), which leads to activation of protein kinase A (PKA) and cAMP response element-binding protein (CREB)-mediated activation of microphtalmia-associated transcription factor (MITF) gene expression (Bertolotto et al., 1998a; Price et al., 1998).

MITF is a basic helix-loop-helix leucine zipper transcription factor (Hemesath et al., 1998; Hodgkinson et al., 1993; Hughes et al., 1993) discovered in a mouse lacking melanocytes (Hertwig, 1942) and has been named the master regulator of melanocytes (Levy et al., 2006). Furthermore, MITF is one of the potential regulator of the high plasticity in melanoma cells (Goding, 2011; Hoek and Goding, 2010). High levels of MITF are found in melanoma cells

exhibiting a proliferative phenotype, whereas more invasive cells exhibit low level of MITF (Hoek et al., 2006, 2008a). MITF expression is regulated by a number of transcription factors and signalling pathways (reviewed in Hartman and Czyz, 2015). In response to α-MSH signalling, the transcription factor SOX10 cooperates with CREB (Huber et al., 2003). A SOX10 response element was found in the *MITF* promoter (Verastegui et al., 2000) and both genes are found mutated in melanoma in a mutually exclusive manner (Cronin et al., 2009). Effectors of the wingless-type (Wnt) signalling pathway, β-catenin and lymphoid enhancer-binding factor 1 (LEF1) also regulate MITF expression (Eichhoff et al., 2011; Saito et al., 2002). Recently, the transcription factor zinc finger E-box binding protein 2 (ZEB2), involved in epithelial-mesenchymal transition (EMT) (Gheldof et al., 2012; Sánchez-Tilló et al., 2012; Tatari et al., 2014) has been shown to upregulate MITF expression (Denecker et al., 2014). In contrast, the transcription factor ZEB1 is found to repress MITF expression in retinal epithelium (Liu et al., 2009). Similar to ZEB1, the glioma-associated oncogene family member 2 (GLI2) inhibits MITF expression in a TGFβ-dependent manner (Pierrat et al., 2012). Intriguingly, the contribution of specific transcription factors is melanoma-specific. Indeed, while paired box 3 (PAX3) transcriptional activity induces MITF expression in melanocytes (Yang et al., 2008), in melanoma, PAX3 can negatively regulate MITF and this process is mediated by BRN2 protein (Bonvin et al., 2012; Eccles et al., 2013). In addition, several microRNAs, including miR-137 or miR-182, control expression of MITF protein acting on MITF transcript stability and degradation (Bell and Levy, 2011; Bemis et al., 2008; Craig and Spiegelman, 2012; Haflidadóttir et al., 2010; Luo et al., 2013; Segura et al., 2009; Yan et al., 2012). Furthermore, post-translational modifications including phosphorylation and SUMOylation regulate MITF transcriptional activity. In general MITF activity is enhanced by phosphorylation at specific residues (reviewed in Levy et al., 2006; Mansky et al., 2002), while SUMOylation modulates its activity. Indeed, MITF appeared more active for a set of specific target genes when it is not SUMOylated (Miller et al., 2005; Murakami and Arnheiter, 2005). MITF upregulates many genes of the melanocyte lineage involved in melanin synthesis and melanosome biogenesis (reviewed in Cheli et al., 2010), including dopachrome tautomerase (dct) and tyrosinase-related protein 1 (TYRP1) (Bertolotto et al., 1998b; Yavuzer et al., 1995), tyrosinase (Yasumoto et al., 1994) pigment cell-specific-pre-melanosomal protein 17 (PMEL17) (Baxter and Pavan, 2003) and Melan-A (Du et al., 2003). Furthermore, MITF can control *CDKN1A* and *CDKN2A* transcription and expression levels (Carreira et al., 2005; Loercher et al., 2005) or expression of *TBX2*, a transcription factor involved in senescence (Béjar et al., 2003; Carreira et al., 2000), indicating that MITF has a pivotal role in cell cycle progression and cell survival (reviewed in Cheli et al., 2010).

1.2.2 Melanoma: model of progression

Since melanocytes are present at different sites in the human body, different types of melanoma can arise. The most common are found on the skin and can be divided in two groups depending whether they are originated from skin that was or was not chronically sun damaged (CSD and non-CSD respectively) (reviewed in Shain and Bastian, 2016). Melanomas belonging to these two categories differ in sites of origin, oncogenic mutation, host age (Curtin et al., 2005; Long et al., 2011; Viros et al., 2008). For example, CDS melanomas arise from sites of the skin like head, neck and dorsal surface, that showed signs of long-term sun exposure of older people. These melanomas are found carrying neurofibromin 1 (NF1), KIT NRAS, BRAF^{nonV600E} mutations (Bastian, 2014). On the contrary, the non-CDS melanomas originate in the intermittently sun-exposed areas, such as the trunk, of younger people. The most common mutation identified in non-CDS melanomas is the BRAF^{V600E} (Bastian, 2014).

Classically, malignant transformation of melanocytes in melanoma cells is depicted using the Clark model (Clark et al., 1984). In this model, tumor progression is linear and consists in a series of different steps including successive formation of the benign precursor lesion (called melanocytic nevus), dysplastic nevus, progression to radial growth phase, progression to vertical growth phase and finally metastasis formation (Fig. 4). Genetic and epigenetic mutations accumulated during each step are though to drive tumor progression. However, melanoma can also arise *de novo* in normal skin (Clark et al., 1969; Weatherhead et al., 2007).
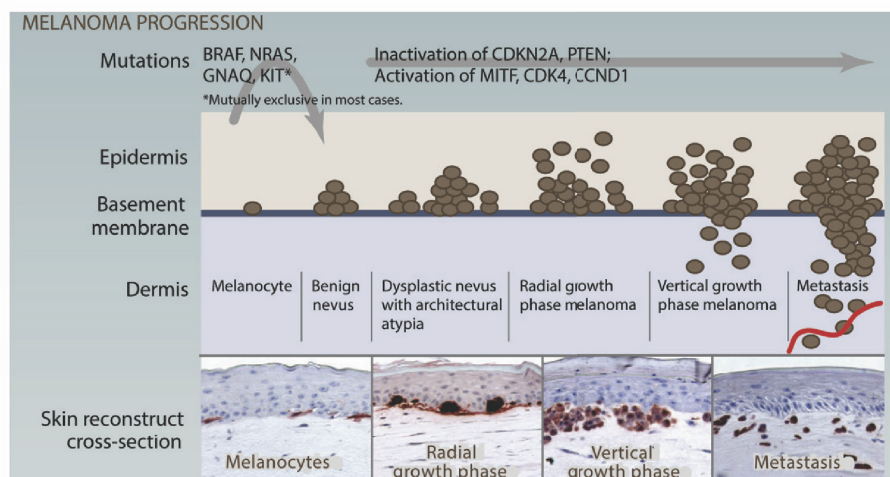

Figure 4. Melanoma progression.

Melanoma progresses in a stepwise fashion, accumulating more mutations during the process. BRAF mutations are the one of the initiating events in the transformation process. Additional mutations, such as inactivation of CDKN2A or PTEN, make cells acquiring malignant phenotype.

In the Clark model, the first step consists in the formation of benign nevi from melanocytes. This step is dependent on the abnormal activation of the mitogen-activated protein kinase (MAPK) signalling pathway (Lin et al., 1998; Welsh et al., 2001). The activation of MAPK signalling pathway, also called ERK (extracellular-related kinase) pathway, is the result of somatic mutation in genes encoding for the serine/threonine-specific protein kinase *BRAF* or for the G-like regulatory protein *NRAS*. Almost 15% of the malignant melanoma are associated with somatic NRAS mutations, while 50% with BRAF mutations (Albino et al., 1989; Davies et al., 2002; Omholt et al., 2003). Furthermore, depletion of both NRAS and BRAF suppresses melanoma growth *in vitro* (Eskandarpour et al., 2005; Hingorani et al., 2003; Hoeflich et al., 2006). According to the model, additional mutations are required for melanoma progression. In almost 40% of the cases, this mutations occur in the *CDKN2A* locus, which encodes for two proteins named p16^{INK4A} and p19^{ARF} (de Snoo et al., 2007). Both p16^{INK4A} and p19^{ARF} are known as tumor suppressor proteins (Kamb et al., 1994; Nobori et al., 1994) and are inactivated in several cancers (Kamb et al., 1994; Nobori et al., 1994; Serrano et al., 1993; Stott et al., 1998), including melanoma (Flores et al., 1996; Monahan et al., 2010; Walker et al., 1998). While p16^{INK4A} inhibits the CDK4/6-mediated phosphorylation of the tumor suppressor Rb (retinoblastoma) (Ortega et al., 2002; Serrano et al., 1993; Sharpless and Chin, 2003), p19^{ARF} regulates the p53 protein levels by sequestrating mouse double minute 2 protein (MDM2) and inhibiting MDM2-dependent p53 ubiquitination and degradation (reviewed in Harris and Levine, 2005; Pomerantz et al., 1998).

In another 50% of the malignant melanoma a different tumor suppressor gene, encoding for the phosphatase and tensin homologue (PTEN), is inactivated (Guldberg et al., 1997; Healy et al., 1995; Herbst et al., 1994; Parmiter et al., 1988). PTEN modulates a variety of growth factors signalling via dephosphorylation of phosphatidylinositol phosphate (PIP$_3$) into PIP$_2$. Increased level of PIP$_3$ leads to the activation of the protein kinase B (also called AKT) (Cantley, 2002; Maehama and Dixon, 1999) which in turns inactivates apoptotic factors or protein that suppress the cell cycle thereby increasing proliferation and cell survival (Nicholson and Anderson, 2002; Wu et al., 2003).

Then, to acquire more aggressive phenotypes, melanoma cells acquire more mutations in genes regulating cell differentiation. Loss of pigmentation is one feature of tumor dedifferentiation in melanoma (Bennett, 1983). Low level of MITF has been associated with melanoma characterized for more invasive phenotype (Hoek et al., 2008a), and amelanotic tumors are associated with poor prognosis (Hofbauer et al., 1998; Salti et al., 2000; Seiter et al., 2002). On the other hand, MITF overexpression is associated in tumor resistance to chemotherapy (Garraway et al., 2005).

Next, melanoma cells undergoes two different phases: escaping from the primary site and formation of metastasis in the secondary site (Hanahan and Weinberg, 2011). In the first step, cancer cells due to the lack of oxygen and nutrients induce neovascularization by expressing several angiogenic factors such as VEGF family members and fibroblast growth factors (Dvorak, 2002; Friesel and Maciag, 1995; Lázár-Molnár et al., 2000). Stromal cells like cancer-associated fibroblasts, myeloid cells and immune cells recruited to the primary site contribute to the process by producing pro-angiogenic factors (Kubota et al., 2009; Murdoch et al., 2008; Pietras et al., 2008; Watnick, 2012; Zumsteg and Christofori, 2009). However, tumor blood and lymphatic vessels are leaky and differ from normal counterpart by abnormal growth (Baluk et al., 2005; Nagy et al., 2009, 2010), which facilitate dissemination of cancer cells in the bloodstream (Baluk et al., 2005; Hanahan and Weinberg, 2011; Raza et al., 2010). Furthermore, to acquire their invasive capacity, cancer cells hijack the developmental process epithelial-mesenchymal transition (EMT) (Dissanayake et al., 2007; Kudo-Saito et al., 2009). This process is characterized by repression of cell adhesion molecules, like E-cadherins and integrins, which result in loss of cell-to-cell interaction and increase mobility (Kuphal et al., 2005; Yang and Weinberg, 2008). Furthermore, melanoma downregulate E-cadherin expression and upregulate N-cadherin. This switch has been shown to help and facilitate interaction between melanoma cells with fibroblast and endothelial cells (Villanueva and Herlyn, 2008).

Finally, cancer cells express molecules (ligand or receptor) that would preferentially home melanoma cells to one specific tissue. For example, some melanoma cells express many genes normally expressed in the brain, and this might partially explain the process of metastases in the brain (Cattell et al., 2002). In another case, the migration of circulating cancer cells towards a specific site e.g. the small intestine is explained by the highest expression of the cytokine CCL25 in this tissue which attracts cancer cells expressing the receptor CCR9 (Amersi et al., 2008). In addition, the liver is the most common metastatic site for uveal melanoma, Indeed, uveal melanoma cells express several receptors like IGF1R, c-Met or CXCR4, whereas the corresponding ligands are highly expressed in the liver (Bakalian et al., 2008; Lorigan et al., 1991).

1.2.3 Notch in melanocyte lineage and melanoma

Over the past two decades, several genes were identified to affect pigmentation of hair, fur or eyes in mice (Bennett and Lamoreux, 2003). Most of these genes are key components of distinct developmental pathways which regulates melanocytes homeostasis and are also implicated in pathological conditions such as melanoma (reviewed in Liu et al., 2014).

One such pathway is the evolutionary conserved Notch signalling. Notch proteins are highly conserved from nematode to vertebrates (Artavanis-Tsakonas, 1999). In mammals four Notch receptors (Notch1-4) have been identified, which function as ligand-activated transcription factors (Gordon et al., 2008). Notch receptors are translated as precursor proteins that undergo sequential proteolytic events. The first cleavage at site 1 (S1) mediated by proprotein convertases generates a heterodimeric Notch receptor composed of the Notch extracellular domain (NECD) that remains non-covalently bound to a transmembrane/intracellular fragment (TMIC) (Blaumueller et al., 1997; Logeat et al., 1998). The heterodimeric receptor binds specific membrane-bound ligands (Jagged 1,2 and DSL1,3,4) expressed on adjacent cells (reviewed in Kopan and Ilagan, 2009). Upon this interaction Notch receptors undergo a second additional proteolytic cleavage (S2), which is mediated by an ADAM family metalloproteinase. Recent finding suggest that ligand-dependent Notch activation relies almost only on ADAM10 (reviewed in van Tetering and Vooijs, 2011), since *ADAM10-/-*, but not *ADAM17-/-*, mimics the embryonic lethal *Notch1-/-* phenotype (Conlon et al., 1995; Hartmann et al., 2002; Peschon, 1998). Ligand-independent signalling relies on ADAM17, and does not result in ectodomain shedding, suggesting that ADAM17 does not cleave Notch at the cell surface (Bozkulak and Weinmaster, 2009). The S2 cleavage generates a substrate for a third proteolytic cleavage (S3) by γ-secretase, a protein complex comprising nicastrin, presenilin 1/2, Pen-2 and Aph-1 (Edbauer et al., 2003; Saxena et al., 2001). As result of the final cleavage the Notch intracellular domain (NICD) is released and enters the nucleus and by interaction with the DNA-binding protein RBPJ-k (also known as CSL, CBF1, Su(H) and LAG-1) and the coactivator Mastermind (MAML1-3), promotes the transcription of specific genes (Fryer et al., 2002; Henderson et al., 1994).

Due to difficulties in isolating or detecting melanocytes in situ, Notch signalling components expression data in this cell types are rare (Schouwey and Beermann, 2008).The role of Notch in pigmentation and melanocyte differentiation is supported by several *in vivo* studies using transgenic mouse models (Kumano et al., 2008; Moriyama et al., 2006; Schouwey et al., 2007). To overcome the embryonic lethality of *Notch1-/-* and *Notch2-/-* (Conlon et al., 1995; Hamada et al., 1999), key component of Notch signalling were conditionally ablated in the melanocyte lineage of mice expressing a *Cre* recombinase transgene under the control of the melanocyte-specific *Tyr* promoter (Delmas et al., 2003).

Hair graying and hair pigmentation defects were observed in conditional deletion of *RBP-Jk* in melanocyte lineage, revealing a role for Notch both in melanocyte precursors (melanoblasts) and melanocyte stem cells maintenance (Moriyama et al., 2006). Furthermore, conditional deletion of *Notch1* and *Notch2* revealed that the total dosage of these two genes determines the severity of the hair graying phenotype (Schouwey et al., 2007), and transgenic expression

of the NICD in *Notch1* and/or *Notch2* defective melanocytes rescues proper fur pigmentation (Schouwey et al., 2010a). In agreement with these results, mice carrying double heterozygous deletion of *Notch1* and *Notch2* show gradual hair graying after birth (Kumano et al., 2008). Since heterozygous deletion of *Notch1* with *Notch3*, and *Notch4* deletion, do not result in changes in pigmentation phenotype, only Notch1 and Notch2 are considered relevant in regulating hair pigmentation (Krebs et al., 2000, 2003).

Several studies have reported Notch signalling in different tumor types indicating that Notch can act as an oncogene or a tumor suppressor gene depending on the context. One of the best studied and characterized examples of how Notch signalling gain of function promotes cancer progression is T cell acute lymphoblastic leukaemia/lymphoma (reviewed in Demarest et al., 2008). By contrast, in the skin Notch has been described as a tumor suppressor gene (Nicolas et al., 2003), since deletion or inhibition of Notch signalling leads to the formation of spontaneous squamous cell carcinoma (Nicolas et al., 2003; Proweller et al., 2006).

Notch pathway receptors (Notch1 and Notch2) and ligands (Jagged-1, Jagged-2 and Delta-1) have been shown to be overexpressed in dysplastic nevi and melanoma compared to control melanocytes where Notch1 is undetectable (Balint et al., 2005; Bedogni et al., 2008; Massi et al., 2006; Pinnix and Herlyn, 2007). Furthermore, NICD overexpression in melanocytes promotes their transformation (Pinnix et al., 2009), while primary melanoma drives the progression toward a more aggressive phenotype (Liu et al., 2006). Due to the low expression in melanocytes, Notch signalling inhibition by γ-secretase tripeptide inhibitor, induces apoptosis in melanoma cells, whereas melanocytes were unaffected (Qin et al., 2004). Moreover, Notch inhibition enhances the effects of ERK inhibitor in BRAF-V600E melanoma cell lines, both *in vitro* and *in vivo* (Krepler et al., 2015). In addition, since Notch pathway relies on cell-cell interactions, stromal cells surrounding the tumor might participate in its regulation. In keeping with this concept, a recent study showed that non-invasive melanoma cells upon contact with differentiated keratinocytes, activate Notch signalling and become more aggressive in terms of invasivness (Golan et al., 2015). On the contrary Notch overexpression in stromal fibroblast decreased growth and angiogenesis of the surrounding melanoma cells (Shao et al., 2011).

Due to its role in cancer formation and progression, Notch signalling is intensely investigated as a potential therapeutic target. For example, an encouraging study supports evidences of anti-tumor activity, of the γ-secretase inhibitor RO4929097 in a phase I clinical trial for solid tumors, including melanoma (Tolcher et al., 2012).

1.3 FRET biosensors in life science

In a cell, nano-sized molecules like proteins, lipids and nucleic acids are involved in dynamic processes regulating physiological and pathological conditions. Understanding these processes is key to determine molecules functions and roles and in some cases design therapeutic approaches. Therefore, non-invasive approaches with nanometer resolution are required. One of the first methods described to reach nanometer resolution was based on the principle of Förster Resonance Energy Transfer (FRET) (Förster et al., 1939). FRET is a measurable physical energy transfer between an excited donor (D) fluorophore and an appropriate acceptor (A) protein or fluorophore. FRET occurs under specific conditions. The first requirement is an overlap between the donor emission spectrum and the acceptor excitation spectrum. The donor and acceptor (FRET-pair) have also to be in a sufficient spatial proximity, usually less than 10nm. The third condition for high FRET to occur is an appropriate orientation of dipole vectors. The most common FRET measurement approaches are the fluorescence intensity based approaches, the fluorescence lifetimes based approaches (Hinde et al., 2012; Wallrabe and Periasamy, 2005) and the fluorescence anisotropy approaches (Lidke et al., 2003).

Since most of this work is based on fluorescence intensity based approaches, only this type of method will be discussed.

The easiest method for rapid FRET measurements is the donor quenching method (Vereb et al., 2011). In this scenario, the donor intensity is reduced in the FRET-pair configuration compared to the donor only sample. Although simple, this method is error-prone because of inter-samples variability due to fluorophores expression levels and spectral cross-talk between FRET-pairs. Another approach is called acceptor photobleaching method (Szabà et al., 1992). In this method, FRET is measured by comparing donor intensity before and after acceptor photobleaching. In case of FRET the donor fluorescence intensity, which is quenched by the acceptor in FRET-pair configuration, will increase significantly. However, FRET microscopy based on acceptor photobleaching can lead to false positive FRET results due to the photoconversion of the acceptor in a donor-like protein (Seitz et al., 2012; Valentin, 2005) and due to an increase of the donor fluorescence under those conditions. Furthermore, it is known that CFP proteins under acceptor photobleaching conditions can increase their fluorescence intensities in a phenomenon named photoactivation (Malkani and Schmid, 2011). Furthermore, other drawbacks are photobleaching of the donor, incomplete photobleaching of the acceptor, as well as acceptor photodestruction precluding real-time or repeated measurements (Shrestha et al., 2015). Finally, the most reliable intensity-based approach is based the sensitized acceptor emission method (Jares-Erijman and Jovin, 2003; reviewed in Shrestha et

al., 2015). When FRET occurs, fluorescence intensity of the acceptor can be quantified as result of the radiation-free energy transfer of the excited donor. This method requires is to collect three independent signals from a FRET-pair expressing sample, consisting in the fluorescent intensities of the donor, the acceptor and the sensitized acceptor. To exclude drawbacks like fluorophores cross-talks, correction factors are calculated from independent single donor or single acceptor control samples (Xia and Liu, 2001).

Since FRET occurs over interatomic distances, it has been first used to visualize and monitor molecular interactions. The discovery of the green fluorescent protein (GFP) (Shimomura, 2009) and the generation of different fluorescent proteins (FPs) allowing to cover the entire visible spectrum (Olenych et al., 2007; Schmid and Neumeier, 2005) enable the development of more appropriate and suitable FRET-pairs. Furthermore, the FRET-pair can be linked with a spacer sequence that reacts to specific biological stimuli altering the distance between the fluorophores and resulting in FRET signal changes. These kinds of constructs are named intramolecular FRET-biosensors, since both donor and acceptor are part of the same protein. On the other hand, intermolecular FRET is mostly used to study interactions between two fluorescently-tagged proteins. Depending on the spacer linker which separates the FRET-pair, intramolecular FRET biosensor can serve as tool to investigate several biological processes both *in vitro* and *in vivo*.

For instance, FRET biosensors can be used to quantify metabolite concentrations including ATP, glucose, calcium and other molecules (Fehr et al., 2003; Imamura et al., 2009; Miyawaki et al., 1997; San Martín et al., 2013; Vevea et al., 2013). For such biosensors, bacterial domains able to recognize specific metabolites, are generally used as spacer in these biosensors configuration. Upon binding of the metabolite, a change in the spacer conformation leads to detectable change in FRET efficiency. Conformational change-based biosensors have been used also to study processes occurring in a tightly regulated manner such as cyclin or PKA activities in cell division (Gavet and Pines, 2010; Vandame et al., 2014) or spatiotemporal changes in signal transduction for specific pathways like, AKT (Miura et al., 2014), ERK (Kamioka et al., 2012) or GTPase (Komatsu et al., 2011). Notably, FRET biosensors have been used to study mechano-transduction forces (Seong et al., 2013; Wang et al., 2005), drug efficacy (Mizutani et al., 2010; Nobis et al., 2013) and T-cell interaction (Paster et al., 2009; Randriamampita et al., 2008).

Beside the conformational change-based biosensors, another class of intramolecular biosensor is represented by the cleavage-based FRET biosensors. In these cases, the spacer consists in a cleavable linker that can be processed by a specific protease. When the enzyme is active and co-localize with the biosensor, the cleavage of the linker occurs and drastically reduces the FRET signal. The first biosensor belonging to this class was developed in 1998

and comprises a BFP(blue)-GFP pair separated by a linker containing the specific Asp-Glu-Val-Asp (DEVD) motif, which is specifically recognized and cleaved by Caspase-3 (Xu et al., 1998). Novel and updated versions of Caspase-3 FRET-based biosensor (Tyas et al., 2000), or for other family members (Caspase-6,8 and 9) have been designed (Bozza et al., 2014; Kominami et al., 2012; Takemoto et al., 2003; Wu et al., 2006) to study apoptosis in physiological and pathological conditions. Another cellular relevant process that can be monitored by FRET-based cleavable biosensor is autophagy, a process involved specific organelles called autophagosome (Jin and White, 2007). Autophagosome biogenesis is depending on the processing of the autophagy-related protein 8 (Atg8) by Atg4 (Xie et al., 2008). Two different FRET-based biosensor shed light in the physiological level of autophagy and elucidate potential inhibitory mechanism (Li et al., 2012; Vezenkov et al., 2015). Although, these biosensors are commonly used in several contexts one intuitive drawback is the irreversibility of the cleavage. Besides these examples, other proteases whose roles and activities have been also characeterized by FRET-based biosensor are the MT1-MMP (Eichorst et al., 2012; Ouyang et al., 2008) and ADAM17 (Chapnick et al., 2015).

Finally, we developed the first PC-specific biosensor named cell-linked indicator of proteolysis version 1 (CLIPv1) (Mesnard and Constam, 2010). CLIPv1 consists of secreted eCFP and mCitrine fused together via a flexible linker containing the PC recognition motif Arg-Gln-Arg-Arg (RQRR), that can be cleaved by the most widespread PC family members such as Furin, PACE4, PC5 and PC7 both *in vitro* and *in vivo* (Bessonnard et al., 2015; Mesnard and Constam, 2010; Mesnard et al., 2011). A glycosylphospatidyl-inositol (GPI) anchor links the biosensor to the cholesterol-rich plasma membrane microdomains (lipid rafts) enabling us to detect both autocrine and paracrine secreted PC activities at the surface of cells and embryos (Mesnard and Constam, 2010; Mesnard et al., 2011). CLIPv1 analysis revealed a novel source of PC and functions during embryo development (Mesnard and Constam, 2010; Mesnard et al., 2011) and enable us to decipher single PC contribution in substrate cleavage *in vivo* (Bessonnard et al., 2015). However, the sensitivity of CLIPv1 analysis is limited by the relatively weak fluorescence of eCFP, especially in tissues with high autofluorescence. In addition, due to its configuration FRET can be measured only by sensitized acceptor emission and the GPI anchor limited the analysis only to lipid rafts, whereas PC activities in subcellular compartments of the secretory pathway were neglected.

2 Aim of the project

Members of the PC family, including Furin and PC7, determine the bioavailability and regulate the activities of many proteins such as Notch, E-cadherin, ADAM metalloproteinases and TGFβ family members, by mediating the cleavage of their inactive precursors. As proteolytic enzymes, PCs are considered attractive druggable targets for several diseases, including cancer. However, the major barrier to pharmacologically target any of these proteases is the insufficient knowledge of their individual contribution in substrate cleavage *in vivo* due to indistinguishable overlapping activities *in vitro*. Decipher and characterize the activity and the substrate specificities of each single PC is therefore fundamental to design therapeutic strategies to selectively target PC pathological functions. It has been hypothesized that PCs substrates specificity and their unique functions may reflect differences in their subcellular trafficking. However, direct evidences confirming this hypothesis are lacking.

The following work will address two different aspects of PC activities and functions:

1. PCs cleave and maturate precursor proteins during their transit in the different compartments of the secretory pathway. Knowing where exactly substrates cleavage occurs and which PC is responsible for such cleavage will inform better drug design. To discriminate individual PC contribution and to map their intracellular activity, we quantified PC activities in specific subcellular compartments of two unrelated cell lines (HEK293T and B16F1 mouse melanoma) using a ratiometric and a FRET-based PC biosensors, named CLIPv3 and CLIPv4 respectively. Then, we mapped individual PC contribution in substrates cleavage in B16F1 CRISPR-edited clones for endogenously expressed PCs.

2. Much evidence suggests that PCs are involved in tumorigenesis because of their roles in proteolytic maturation of cancer-related protein precursor. Although PC inhibition appears to repress cell proliferation and motility in melanoma and in other skin cancer cells *in vitro*, individual PC contribution in tumor progression *in vivo* is poorly studied. In this second part, we tried to investigate the individual contribution of Furin and PC7 in B16F1 proliferation and differentiation *in vivo*

3 Results

3.1 Imaging PC activities in different subcellular compartments

3.1.1 Novel CLIP version v3 and v4 and their variants containing distinct localization signals

The initial version (v1) of CLIP and a mutant control (mCLIP) without a PC cleavage motif are enriched at the cell surface by a glycosylphospatidyl-inositol (GPI) anchor (Bessonnard et al., 2015; Mesnard and Constam, 2010) (Fig. 5A,B), To improve the signal-to-noise ratio of CLIPv1 fluorescence, we replaced the FRET donor (eCFP) by monomeric TFP1-FLAG or by monomeric Cerulean (Rizzo et al., 2006; Salonikidis et al., 2011) and exchanged its position relative to monomeric Citrine (Fig. 5A, B). Of the resulting CLIPv3 and v4, we derived compartment-specific variants by replacing the GPI anchor using the transmembrane domain (TMD) and cytosolic tails of membrane proteins with well-defined trafficking signals (Table 1). To estimate baseline levels of PC-independent hydrolysis and to use them for signal normalization of RQRR-specific CLIP cleavage, we generated the corresponding PC-resistant mCLIP controls by mutating the RQRR linker sequences in all CLIPv3 and CLIPv4 variants to SQAG (Fig.5B).

To verify that alternative trafficking signals are functional, we monitored Citrine epifluorescence of mCLIPv3 variants in transfected human HEK293T cells that were co-labelled for specific markers by immunofluorescence staining. As described for CLIP version v1 (Mesnard and Constam, 2010), fusion to a GPI signal enriched mCLIPv3 at the plasma membrane (Fig. 5C). By contrast, fusion to a C-terminal KDEL sequence retained mCLIPv3-KDEL in the endoplasmic reticulum (ER) (Lewis and Pelham, 1990). Alternatively, fusion to the TMD and cytosolic tail of the *trans*-Golgi network (TGN) protein TGN38 (Bos et al., 1993) enriched mCLIPv3 in vesicles stained for TGN46 (Fig. 5D), whereas fusion of mCLIPv3 to the TMD and cytosolic tail of cation-dependent mannose-6-phosphate receptor (CD-M6PR) let to its colocalization with the endogenous late endosomal protein cation-independent mannose-6-phosphate receptor (CI-M6PR) (Ghosh et al., 2003) (Fig. 5E). These results show that the

localization signals examined are functional and enrich mCLIPV3 in distinct specific subcellular compartments.
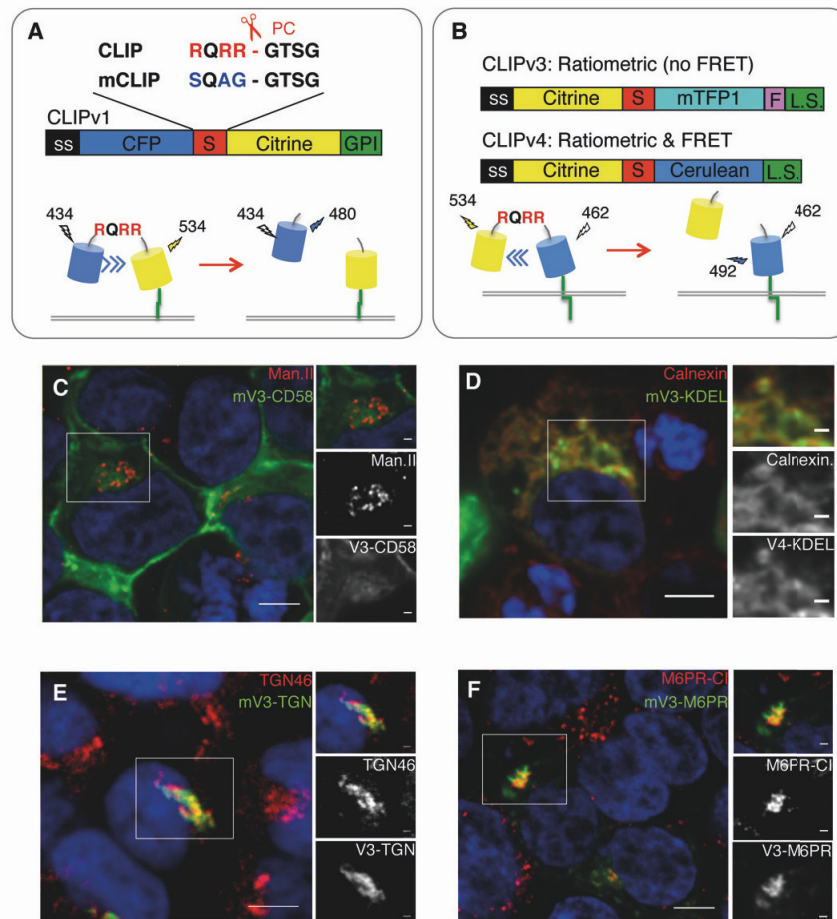
Figure 5. New versions v3 and v4 of the biosensor CLIP and differential localization of compartment-specific variants.

(A) Schematic representations of the initial version of the biosensor CLIPv1 and its cleavage mutant mCLIP. (B) Schematic representation of the novel derivatives CLIPv3 and CLIPv4 and their mCLIP controls. Compartment-specific variants were derived by adding specific localization signals (L.S.). ss: Secretory signal sequence; S: flexible linker comprising the PC cleavage site; F: Flag epitope. (C) Citrine fluorescence (green) of mCLIPv3-GPI in HEK293T cells counterstained by anti-human Mannosidase II antibody (red). (D) Citrine fluorescence (green) of mCLIPv3-KDEL in the endoplasmatic reticulum of HEK293T cells labeled by anti-human Calnexin immunostaining (red). (E) Citrine fluorescence (green) of mCLIPv3-TGN in HEK293T cells counterstained by anti-human TGN46 antibody (red). (F) Overlap of mCLIPv3-M6PR epifluorescence (green) with endogenous late endosomal cation-independent mannose 6 phosphate receptor M6PR-CI stained by immunofluorescence (in red) in HEK293T cells Size bars: 5µm and 1 µm.

Table 1. Localization signals to enrich CLIPv3 and CLIPv4 to distinct subcellular compartments

Name	Localization signal	Compartment	Reference
v4-sol	none	secreted	
v3/v4-CD58	GPI signal of CD58	lipid rafts	(Keller et al., 2001)
v3/v4-KDEL	KDEL	endoplasmic reticulum	(Lewis and Pelham, 1990)
v3/v4-TGN	TGN38	Trans Golgi Network	(Bos et al., 1993)
v3/v4-TFR	TFRC	early endosomes	(Van Dam et al., 2002)
v3/v4-M6PR	M6PR	late endosomes	(Ghosh et al., 2003)
v3/v4-M6PR(6Ala)	M6PR (6Ala)	plasma membrane	(Stockli, 2004)

3.1.2 Cleavage and ratiometric CLIPv3 imaging can estimate PC activity in exocytic compartments

To estimate maximal FRET efficiencies of uncleaved CLIPv3 and CLIPv4, we compared PC-resistant mCLIPv3 and mCLIPv4 by sensitized emission analysis in transfected HEK293T cells. FRET values acquired on live cells were processed using the ImageJ (National Institutes of Health) pixFRET plug-in and normalized as previously described (Feige et al., 2005; Xia and Liu, 2001). To prevent that shed Citrine escapes into the medium we chose the late endosomal M6PR-tagged variants. In mCLIPv4, but not in the cleavable control CLIPv4, excitation of Cerulean triggered robust Citrine emission while Cerulean emission was quenched by Citrine, indicating robust FRET specifically in the absence of biosensor cleavage (Fig. 6A, B). In sharp contrast, no FRET signal was detected upon excitation of TFP1 in mCLIPv3, although unexpected, confirms that the signal of mCLIPV4 was specific FRET (Fig. 6A, B).

Since Citrine and TFP1 fluorescence signals of mCLIPv3 were not skewed by FRET, we asked whether ratiometric imaging of cleavable CLIPv3 suffices to quantify PC activities. To test this and to evaluate potential effects of subcellular localization on biosensor cleavage, we analyzed CLIPv3 variants by ratiometric imaging and by immunoblotting using corresponding cleavage mutant mCLIPv3 variants as negative control. Despite detectable PC-independent cleavage of the negative control, ratiometric imaging in HEK293T cells showed that the mean Citrine/TFP1 fluorescence ratio of CLIPv3 was 2-fold below that of cleavage mutant mCLIPv3, irrespective of whether the sensor was targeted to the TGN or to the late endosomes (Fig. 7A, B). However, this quantification appears to be inaccurate because anti-Flag Western blot analysis in stable cell lines revealed that only 14±5% of the total CLIPv3-TGN in whole cell

lysates was actually cleaved compared to 56±5% of the total CLIPv3-M6PR (Fig. 7C). The cleaved fraction further increased to 73±5% in the case of GPI-anchored CLIPv3, whereas CLIPv3-KDEL containing the ER retention signal KDEL remained uncleaved. While confirming that endogenous PCs are activated in post-ER vesicles, these results provide direct evidence that the destination of a given substrate within TGN/endosomal subcompartments is rate-limiting for its cleavage.

To assess how much of the late endosomal CLIPv3-M6PR might be cleaved during transit at the cell surface, we substituted 6 residues of its localization signal by alanines such that it cannot interact with the clathrin machinery (Ghosh et al., 2003; Stockli, 2004) . Compared to the wild-type the mutated M6PR(6Ala) localization signal enriched CLIPv3 at the cell surface and significantly dimished the cleaved fraction from 56% to 36% of the total (Fig. 7C, D). Thus, CLIPv3-M6PR appears to be cleaved mostly within endosomes. Therefore, and since such vesicles retain both fluorophores even after cleavage (Fig. 7A), PC activity within endosomes cannot be quantified accurately by simple ratiometric imaging.
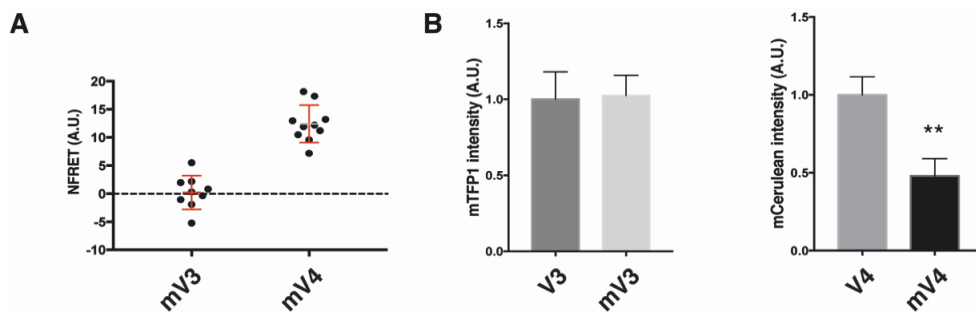
Figure 6. FRET analysis of CLIPv3 and CLIPv4 in HEK293T cells

(A) Maximal normalized FRET efficiencies of mCLIPv3 and mCLIPv4 quantified by sensitized emission analysis in endosomes of live HEK293T cells target by the localization signal M6PR. Data represent mean±s.e.m. of two independent experiments. (B) TFP fluorescence of CLIPv3-M6PR relative to that of cleavge mutant mCLIPv3-M6PR control (left), and Cerulean fluorescence of CLIPv4-M6PR relative to mCLIPv4-M6PR. Data represent mean±s.e.m. of two independent experiments (**p<0.01, t-test).
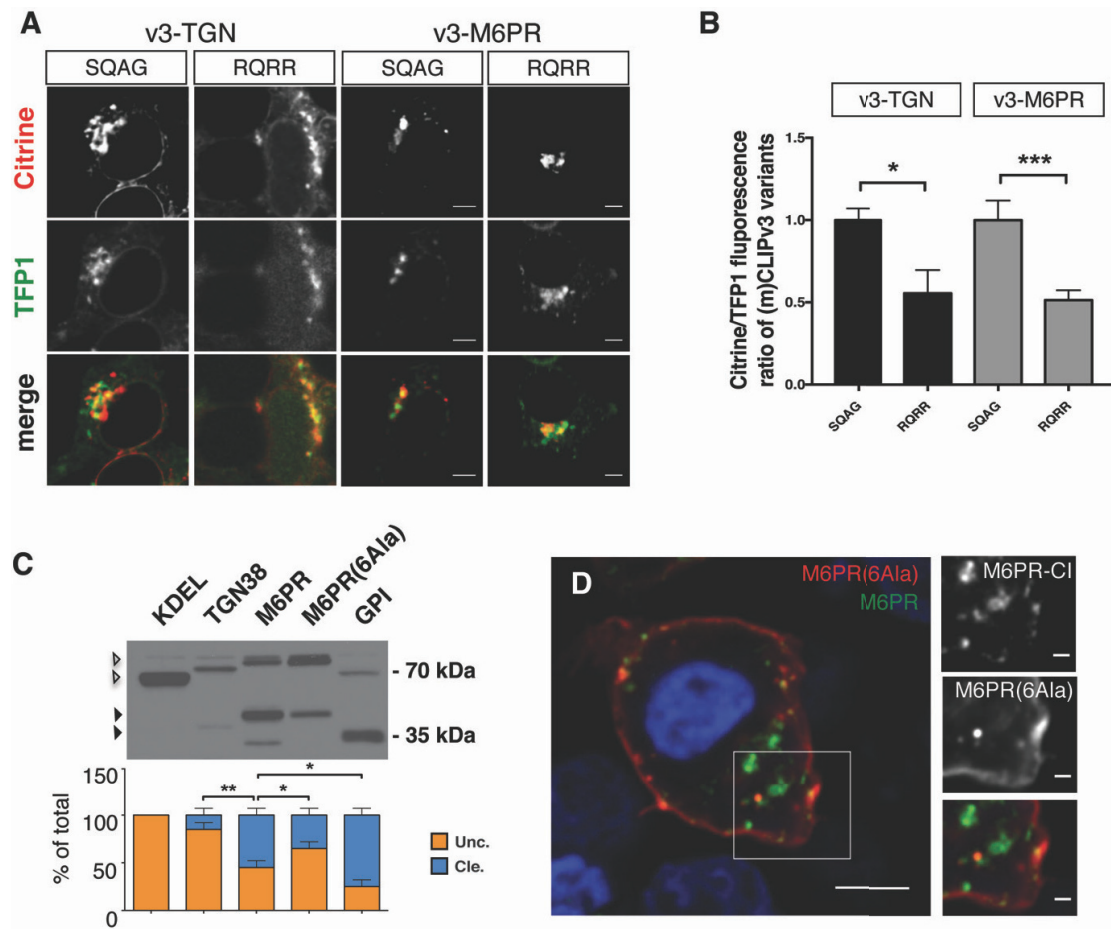
Figure 7. Ratiometric and Western blot analysis of CLIPv3 variants.

(A) Fluorescent images of CLIPv3-TGN and CLIPv3-M6PR(RQRR) and their corresponding PC-resistant mCLIPv3 controls (SQAG). (B) Average Citrine/TFP1 fluorescence ratios of CLIPv3-TGN and CLIPv3-M6PR relative to those of their mCLIPv3 controls. Data represent mean±s.e.m. of two independent experiments (*p<0.05 , **p<0.001, t-test). (C) Anti-Flag Western blot (top) of compartment-specific CLIPv3 variants in HEK293T cells lysates. Densitometric analysis is shown below. Uncleaved (Unc.) and cleaved (Cle.) forms of CLIPv3 variants fused to the indicated localization signals are marked in the top panel by open and closed arrowheads, respectively (*p>0.5, **p>0.001, t-test). Courtesy of Dr.P. Donovan. (D) Epifluorescence of Citrine-M6PR(6Ala) which is enriched at the plasma membrane due to the endocytosis-blocking FFWYLL to 6xAla mutation in its M6PR localization signal (in red), and of the late endosomal marker Cerulean-M6PR (in green).

3.1.3 FRET imaging of CLIPv4 reveals that endogenous Furin activity in HEK293T cells is highly enriched in late endosomes

Western blotting is suboptimal to quantify PC-mediated cleavage, also because it cannot take into account protein turnover. Since lysosomal delivery and degradation are unlikely slower in late endosomes than in the TGN, we were surprised that CLIPv3 nonetheless appeared up to 4-fold more cleaved in post-TGN compartments than in the TGN. To validate this conclusion, we quantified total PC activity in these and other compartments by FRET imaging of CLIPv4 variants. Their average FRET signals were normalized to the average maximal FRET of the corresponding non-cleavable mCLIPv4 variants. We found that the normalized FRET (NFRET) efficiency of CLIPv4-TGN was only 25±5% below that of PC-resistant mutant control mCLIPv4-TGN (Fig. 8A, left panel). By contrast, the average NFRET of CLIPv4-M6PR differed from that of mCLIPv4-M6PR by almost 50±10% (Fig. 8A, right panel). These results corroborate our conclusion that total PC activity is significantly higher in late endosomes and/or other post-TGN compartments than in the TGN. Although both compartments are thought to host functionally relevant PC activities, we were surprised by this result because we expected especially Furin and PC7 to be enriched in the TGN (Declercq et al., 2012, 2016; Rousselet et al., 2011a; Schäfer et al., 1995; Teuchert et al., 1999a).

HEK293T cells transcribe five PC family members (Bessonnard et al., 2015). To obtain an initial estimate of their relative contributions to total PC activity during endocytosis, we depleted *Furin* or *PC7* mRNAs in HEK293T cells expressing CLIPv4-M6PR using previously validated siRNAs (Bessonnard et al., 2015; Scamuffa et al., 2008). Compared to cells transfected with scrambled control siRNA, cells depleted of 64±10% of *Furin* mRNA significantly increased the average NFRET signal of CLIPv4-M6PR, whereas depletion of 56±10% of *PC7* mRNA did not (Fig. 8B). Depletion of *Furin* mRNA did not significantly increase *PC7* mRNA levels (Fig. 8B, C). Together, these results suggest that processing of the late endosomal PC biosensor CLIPv4-M6PR in HEK293T cells largely depends on Furin.
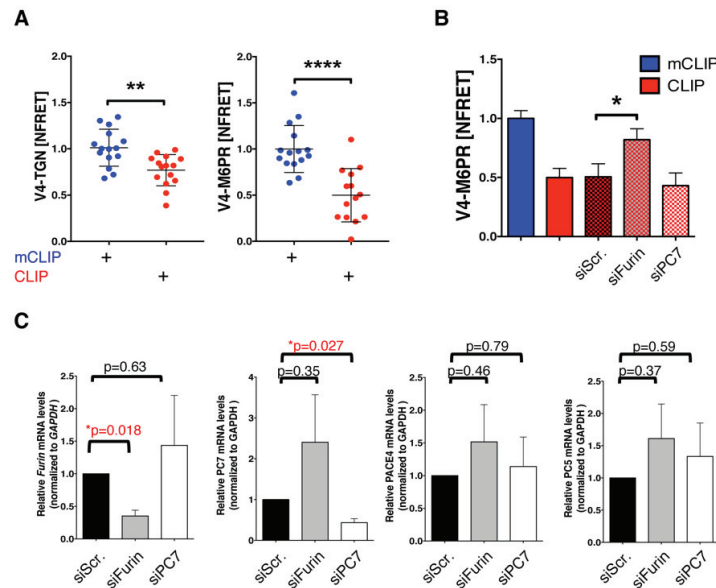
Figure 8. Detection of endogenous Furin activity in late endosomes of HEK293T cells.

(A) Relative NFRET efficiencies of CLIPv4-TGN and CLIPv4-M6PR. Each dot of the scatter plots represents the entire cytoplasmic region of one cell (**p<0.01, ***p<0.001, t-test). (B) Relative NFRET efficiencies of CLIPv4-M6PR in HEK293T cells transfected with or without the indicated siRNAs (*p<0.05, t-test). (C) RT-qPCR analysis of the relative expression of endogenous PCs in wild-type HEK293T cells transfected with the indicated siRNAs. The asterisk indicates a significant difference relative to the scrambled control (siScr) as determined by t-test (p-values are indicated).

3.1.4 CRISPR/Cas9 genome editing of endogenous PCs expressed in B16F1 melanoma cells

Since multiple overlapping bioactive PCs are coexpressed in most cells and tissues, their relative contribution to the cleavage of a given substrate are notoriously difficult to estimate. Tissue-specificity and/or cross-regulation among PC family members may further complicate the interpretation of experimental manipulation (Bessonnard et al., 2015; Lapierre et al., 2007). To reduce this complexity, we decided to image compartment-specific CLIPv4 variants in mouse B16F1 melanoma cells which express endogenous *Furin* and *PC7*, but no detectable *Pace4* and *PC5* mRNAs (Fig. 9A). To inactivate endogenous Furin and PC7, we mutated their genes adjacent to the start codons in B16F1 cells using CRISPR/Cas9 genome editing (Fig. 9B, C). Of 37 selected cell lines analysis 91% showed frameshift mutations in one or all alleles, resulting in premature stop codons and short inactive protein. We selected clones where no wild-type alleles were detected, including single mutant sgPC7-1, sgFurin-1sgFurin-2 cells and double knockout (sgDKO) cells (Fig. 9D, F). Immunoblotting of cells extracts from wild-type and CRISPR-edited clones confirmed loss of Furin protein expression specifically in
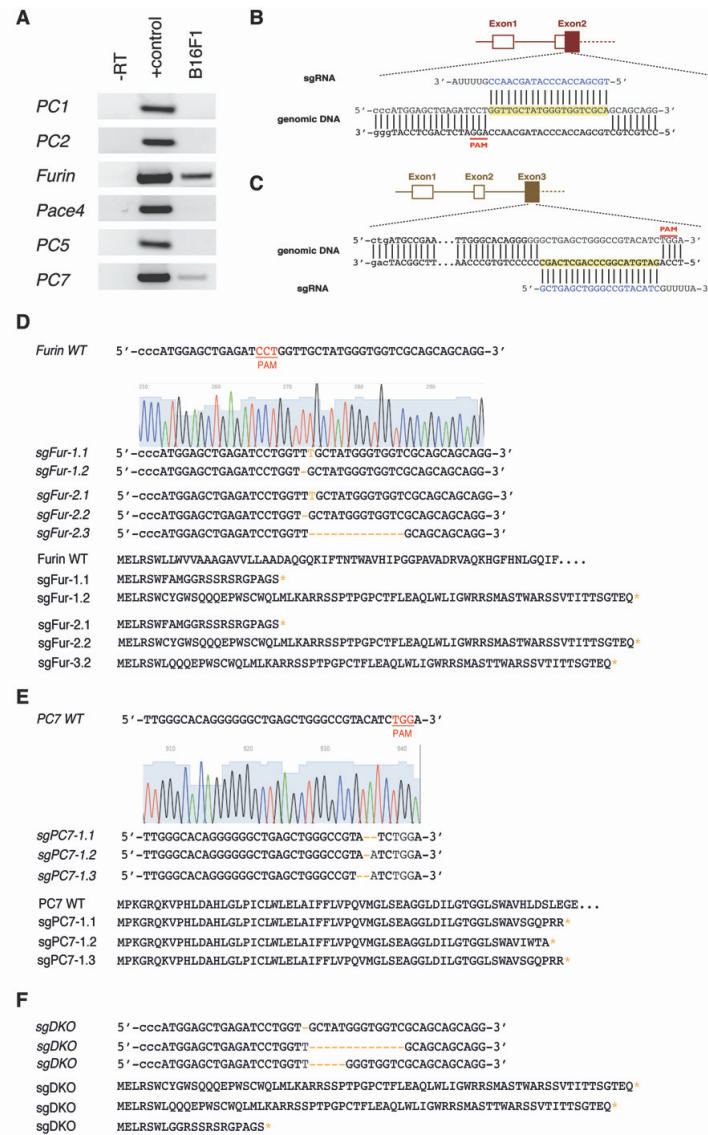
Figure 9. CRISPR/Cas9 genome editing of Furin and PC7 in B16F1 melanoma cells.

(A) RT-PCR analysis of PC mRNAs in B16F1 cells. Results are representative of three independent experiments. (B) Targeted region of mouse Furin locus. Yellow: targeted sequence. Blue: complementary sgRNA sequence. PAM: Protospacer adjacent motif. (C) Targeted region of the mouse PC7 locus. Yellow: targeted sequence. Blue: complementary sgRNA sequence. PAM: Protospacer adjacent motif. (D-E) Wild-type(top) and representative CRISPR-edited DNA sequences (below) of the second exon of mouse Furin (A), or the third exon of mouse PC7 (B) in genomic regions targeted as shown in B and C by sgFurin or sgPC7 single guide RNAs respectively. Representative fluorograms show one targeted allele per gene in clones sgFurin-1 and sgPC7-1. (F) Wild-type (top) and representative CRISPR-edited DNA sequences (below) of the second exon of mouse Furin in clone sgDKO that was derived from clone sgPC7-1 by Furin guide RNA transfection. Predicted protein sequences and their truncation by frame-shifting insertion-deletion mutations in sgRNA-treated cells are shown below.

sgFurin and sgDKO clones (Fig. 10A). PC7 antibody is not commercially available. However, RT-qPCR analysis showed that sgFurin1/2 and sgDKO clones continued to express *PC7*

mRNA or even significantly upregulated it compared to control cells (Fig. 10B, C). Conversely, expression of *Furin* mRNA was reduced 2-or 10-fold in the sgFurin1/2 and sgDKO clones, respectively, compared to control B16F1 cells, consistent with potential autoregulatory feedback (Blanchette et al., 2001; Qiu et al., 2015). Neither *Pace4* nor *PC5* mRNAs were detectable. These data suggest that B16F1 melanoma cells are viable independently of Furin and PC7, but that loss of one of these PCs may influence the expression of the other.
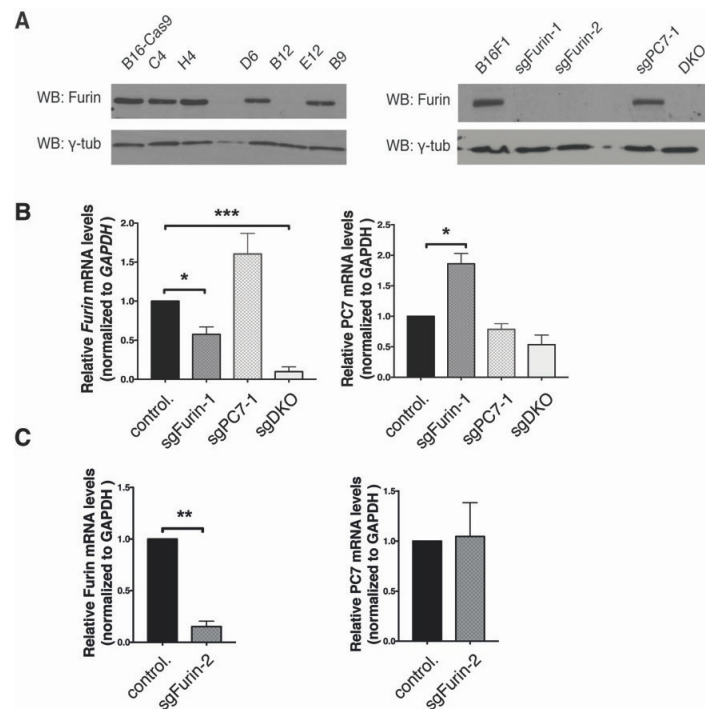
Figure 10. Furin and PC7 expression in CRISPR-edited B16F1 melanoma cells

(A) Western blot analysis of Furin protein levels in B16F1 cell clones before and after selection with Cas9 alone (B16-Cas9), or with Cas9 and sgFurin. Left panel: sgPC7 revealed no significant clonal variation in Furin expression among clones that retained functional Furin alleles. Right panel: Western blot of cell extracts from parental B16F1 cells and selected clones that were chosen for genotyping by DNA sequencing. γ-tubulin served as loading control. (B) RT-qPCR analysis of the relative expression of endogenous PC in B16F1 wild-type, sgFurin-1, sgPC7-1 and sgDKO cells (*p<0.05, ***p<0.001, t-test). (C) RT-qPCR analysis of the relative expression of endogenous PC in wild-type and sgFurin-2 B16F1 cells (**p<0.01, t-test).

3.1.5 CRISPR editing confirms that both endogenous Furin and PC7 in B16F1 melanoma cells are active

To verify that endogenous Furin and PC7 in B16F1 cells were functional, we analyzed processing of known substrates. First we transfected parental cells and CRISPR clones with

E-cadherin, a validated *in vivo* substrate of overlapping Furin, PC7 and Pace4 activities (Bessonnard et al., 2015). A cleavage mutant E-cadherin (cmEcad) where the PC recognition motif RQKR was mutated to SQAG served as a specificity control. Western blot analysis showed that 53% to 62% of the stably accumulating total E-cadherin was cleaved in B16F1 sgFurin, sgPC7 and control cells, compared to only 32% in DKO. The residual cleaved fraction of 32% in sgDKO was close to 20-27% observed with cleavage cmEcad in B16F1 cells irrespective of their genotype (Fig. 11A), indicating that it originated from PC-independent degradation. Thus endogenous Furin and PC7 appear to substitute for each other to cleave E-cadherin in B16F1 cells, similar to what we observed previously in mouse blastocysts (Bessonnard et al., 2015). Other substrates that may be shared by Furin and PC7 include the precursors of Notch1 and the disintegrin metalloproteinase ADAM10 (Anders et al., 2001; Logeat et al., 1998). Western blot analysis detected endogenous ADAM10 mainly in its mature form in control cells, whereas sgFurin-1, sgPC7-1 and sgDKO clones all enriched the uncleaved proADAm10 (Fig. 11B). Analysis of endogenous Notch 1 was hampered by frequent loss of expression in CRISPR clones (see section 3.2.4, Fig. 28A). However, Western blot analysis of transfected exogenous Notch1 revealed cleaved Notch1 p120 fragment specifically in control and in single mutant clones, whereas it was absent in sgDKO cells (Fig. 11C). These results indicate that both endogenous Furin and PC7 are functional in B16F1 cells and able to substitute for each other during E-cadherin, Nocth1 and ADAM10 precursor processing.
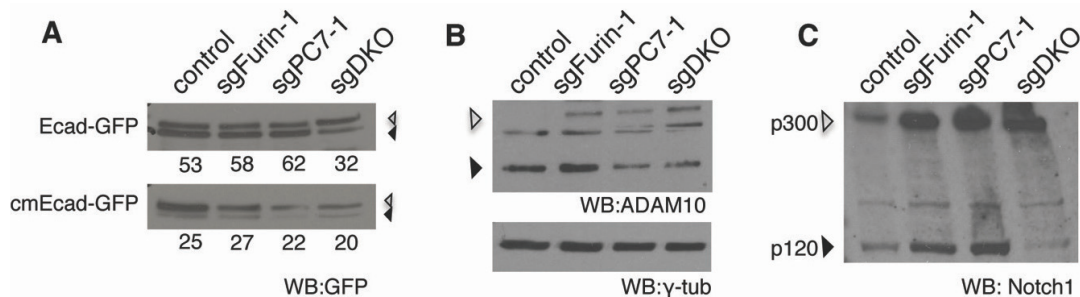
Figure 11. Furin and PC7 overlapping activities in CRISPR-edited B16F1 melanoma cells

(A) Western blot analysis of GFP-tagged wild-type E-cadherin (top) or cleavage mutant RQKR>SQAG derivative (bottom) in whole cell lysates of parental and sgFurin-1, sgPC7-1 and sgDKO B16F1 cell lines. Filled and open arrowheads indicate cleaved E-cadherin and uncleaved E-cadherin respectively (B) Western blot analysis of endogenous ADAM10 protein processing in B16F1 cell clones. Filled and open arrowheads indicate PC-cleaved ADAM10 and immature ADAM10 respectively. γ-tubulin served as loading control. (C) Western blot analysis of Notch1 protein processing in B16F1 cell clones. Filled and open arrowheads indicate PC-cleaved Notch1(p120) and uncleaved Notch1(p300) respectively.

3.1.6 PC inhibitor treatments and CRISPR editing confirms that both endogenous Furin and PC7 in B16F1 melanona cells cleave CLIPv4

To quantify the relative contribution of Furin and PC7 to total PC activity by CLIP imaging, we first wished to verify that CLIPv4 can be cleaved by both enzymes. In CLIPv1, the RQRR linker of CLIPv1 that is identical in all CLIPv3 and CLIPv4 variants is efficiently cleaved by both endogenous Furin and PC7 in diverse cell types in mouse embryos and *ex vivo* (Bessonnard et al., 2015; Mesnard and Constam, 2010). However, in B16F1 cells, CLIPv1 and other GPI-anchroed fluorophores such as Citrine-GPI or Cerulean-GPI failed to accumulate in B16F1 cells, both at the plasma membrane and in conditioned media (data not shown). Therefore, CLIPv1 was not suited as a positive control. As an alternative, we transfected cells with a soluble secreted CLIPv4 (Table1). We found that control, sgFurin-1 and sgPC7-1 single mutant B16F1 cells all released both uncleaved and cleaved CLIPv4-sol into the medium, and that mutation of *Furin* severely reduced or, in combination with loss of *PC7* entirely abolished cleavage (Fig. 12). By contrast, mutation of *PC7* alone did not diminish the amount of cleaved CLIPv4 in culture medium but rather increased it, correlating with upregulation of Furin mRNA (Fig. 10A). These data show that both Furin and PC7 can cleave CLIPv4.

To validate this conclusion by an independent approach that does not rely on clonal DKO cell lines, we took advantage of the fact that endogenous PC7 in cells and tissues is refractory to inhibition by the pan-PC inhibitor decanoyl-Arg-Val-Lys-Arg-CMK (CMK), even though CMK inhibits purified PC7 in cell-free assays more potently than any other PC (Jean et al., 1998). Treatment of CRISPR-edited and control B16F1 cells with CMK for 12 hours dose-dependently inhibited CLIPv4 cleavage both in parental and sgPC7-1 B16F1 cells. By contrast, cleavage of CLIPv4 in sgFurin-1 cells was not inhibited even at the maximal tolerated CMK dosage of 50 µM (Fig. 12). Besides confirming that endogenous PC7 is less sensitive to CMK inhibition than Furin, these results corroborate our previous conclusion that both Furin and PC7 are active in B16F1 cells.
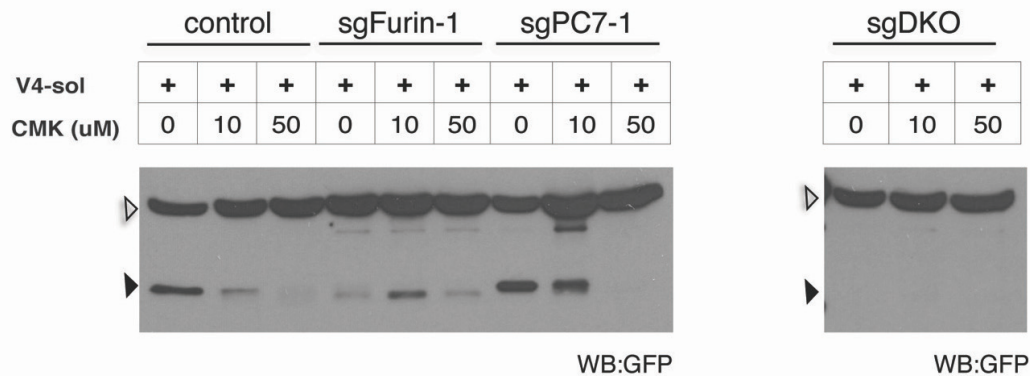
Figure 12. Furin and PC7 can cleave CLIPv4 biosensor in B16F1 melanoma cells.

Anti-GFP Western blots of conditioned media of the indicated B16F1 cell lines transfected with soluble CLIPv4 and treated with the pan-PC inhibitor decanoyl-Arg-Val-Lys-Arg-CMK (CMK) or empty vehicle. In keeping with a for PC7, residual CLIPv4 cleavage in sgFurin-1 cells was resistant to CMK treatment (Bessonnard et al., 2015), and blocked in sgDKO cells. Filled and open arrowheads indicate cleaved Citrine and uncleaved CLIPv4, respectively. Both blots were generated and processed in parallel but on two separate gels to accommodate all samples.

3.1.7 All PC activity in the TGN/endosomal system of B16F1 cells is mediated by Furin and not by endogenous PC7

Previous studies suggest that both Furin and PC7 cycle between the TGN, the plasma membrane and endosomes, at least upon overexpression (Declercq et al., 2012, 2016; Van De Loo et al., 1997; Molloy et al., 1999; Thomas, 2002). To explain the unexpected resistance to CMK treatment, we speculated that endogenous PC7 functions in an intracellular compartment distinct from Furin (Bessonnard et al., 2015). To test whether endogenous Furin and PC7 activities are differentially localized, we monitored their relative influence on CLIPv4 variants in CRISPR-edited B16F1 clones. In parental cells (WT), average NFRET of CLIPv4 was 60% below that of corresponding mCLIPv4 control when targeted to TGN (Fig. 13A), compared to an 80% difference when targeted to late endosomes by M6PR (Fig. 13B). By contrast, average NFRET of CLIPv4 was comparable to that of mCLIPv4 when the biosensor was retained in the ER by the KDEL sequence (Fig. 13C). Thus, in B16F1 cells, PCs are activated in post-ER compartments and total PC activity is higher in late endosome than in TGN, similar to what we described in HEK293T cells (Fig. 8A).

To quantify the relative contributions of Furin versus PC7, we imaged CLIPv4 variants in sgPC7-1 and sgFurin-1 cells. Average NFRET of CLIPv4-TGN and CLIPv4-M6PR did not significantly differ in sgPC7 from those in parental B16F1 cells or in Cas9 alone expressing clones (B16-Cas9) (Fig. 13A, B, D). By contrast, in two independent sgFurin clones, NFRET

of CLIPv4-TGN and CLIPv4-M6PR soared to maximal levels comparable to those of PC-resistant cleavage mutant control constructs (Fig. 13A, B, E). Average NFRET of CLIPv4-KDEL in CRISPR-edited clones did not differ from the one of mCLIPv4-KDEL control (Fig. 9C). These results agree with our observation in HEK293T cells that PC activity is enriched in endosomes compared to TGN and mediated in both compartments exclusively by Furin and not by PC7.

Since endogenous PC7 activity was not detected in the TGN and in late endosomes but able to cleave the soluble CLIPv4-sol, we wished to test whether it is activated specifically in endosomes that communicate with fluid phase. To target early endosomes, CLIPv4 and its cleavage mutant control were fused to the type II trans-membrane domain and cytosolic N-terminus of transferrin receptor (TfR) (Van Dam et al., 2002; Schlierf et al., 2000). In addition, we inverted the relative positions of the fluorophores to retain the FRET donor at the membrane (Table 1, Fig 13F). Immunostaining confirmed that the resulting CLIPv4-TfR co-localized with endogenous early endosome antigen-1 (EEA-1) (Fig. 13F). However, average NFRET efficiency of the resulting CLIPv4-TfR sensor only increased in sgFurin-1 and not in sgPC7-1 compared to control B16F1 cells (Fig. 13G). These results suggest that endogenous PC activity in early endosomes of B16F1 cells is mediated solely by Furin and not by PC7.
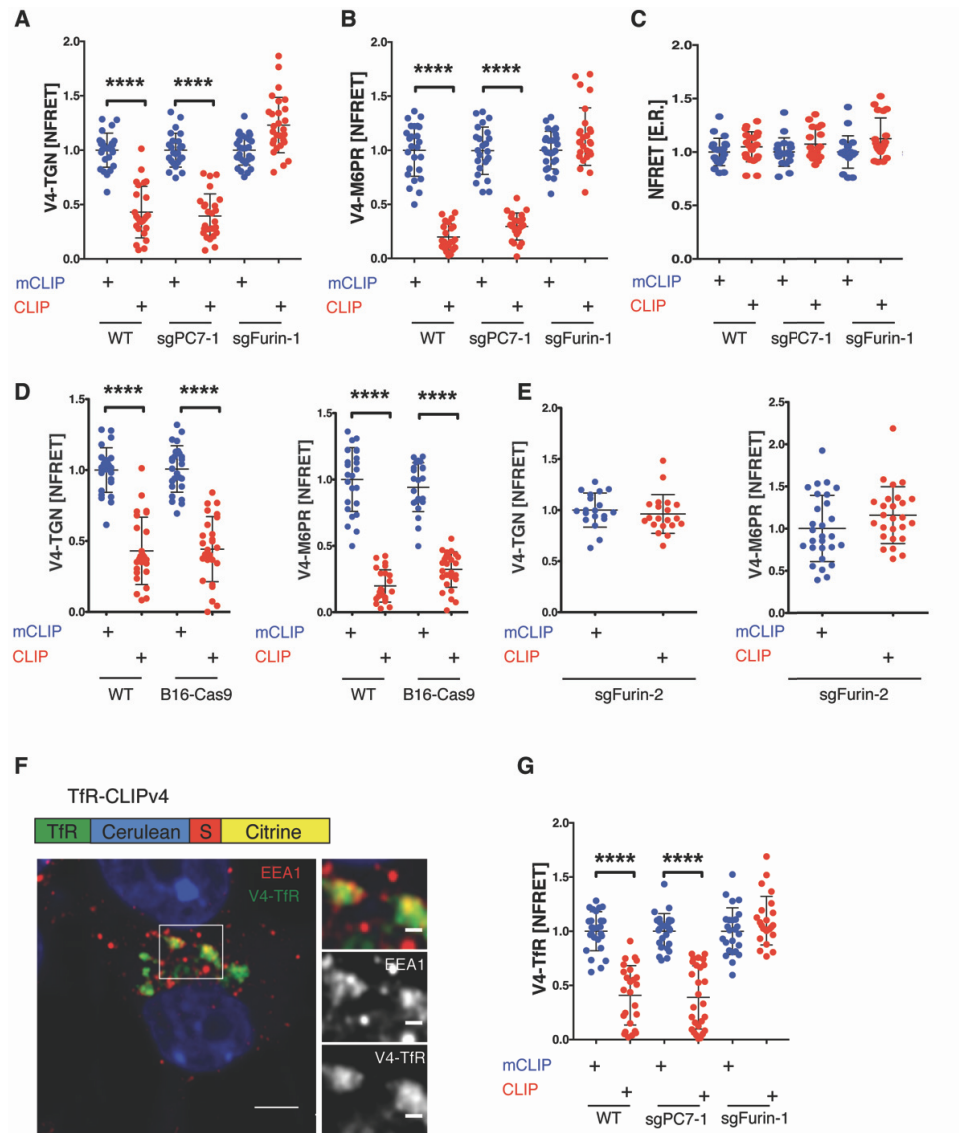
Figure 13. PC activity in the TGN/endosomal system is mediated by Furin but not by endogenous PC7.

*(A-C) Average NFRET efficiencies of A) CLIPv4-TGN, B) CLIPv4-M6PR, and C) CLIPv4-KDEL in control, sgFurin-1 and sgFurin-1 B16F1 cells. (****p<0.0001, t-test). (D) Average NFRET efficiencies of CLIPv4-TGN (left panel) and CLIPv4-M6PR (right panel) in Cas9-transfected control (B16-Cas9) versus parental B16F1 cells (****p>0.0001, t-test). (E) Average NFRET efficiencies of CLIPv4-TGN (left panel) and CLIPv4-M6PR (right panel) in sgFurin-2 and B16F1 cells. (F) Schematic representation of CLIPv4-TfR where the localization signal consisting of the cytosolic tail and type II trans-membrane domain of human transferrin receptor were fused to the N-terminus of monomeric Cerulean to ensure that PC cleavage solubilizes the FRET acceptor Citrine as in other CLIPv4 variants, and not the FRET donor. Below: B16F1 cells expressing mCLIPv4-TfR in early endosomes marked by anti-mouse EEA1 immunostaining. (G) NFRET efficiencies of CLIPv4-TfR in control, sgFurin-1 and sgPC7-1 B16F1 cells (****p<0.0001, t-test)*

3.1.8 Imaging of PC activity at the plasma membrane

The above findings revealed that Furin might cleave substrates during the transit in the TGN/endosomal system in B16F1 cells, whereas PC7 activity is restricted to other compartments. To identify such compartment(s), we assessed PC activity at the plasma membrane, where PC7 has been shown to transit (Declercq et al., 2012; Rousselet et al., 2011a). The mutated M6PR(6Ala) localization signal (Table 1) enriched CLIPv3 at the cell surface of both HEK293T and B16FI cells (Fig. 7D and Fig. 14A). In contrast, CLIPv4 failed to accumulate at the plasma membrane but accumulated intracellularly in both cell lines (Fig. 14B and data not shown). Since Citrine and TFP1 fluorescence of mCLIPv3 are not skewed by FRET (Fig. 6A), and since Citrine is released into the medium after the cleavage, we reasoned that cleavable CLIPv3-M6PR(6Ala) should suffice to quantify PC activity by ratiometric imaging at the plasma membrane.

Indeed, ratiometric imaging showed that the mean Citrine/TFP1 fluorescence ratio of CLIPv3 in wild-type B16F1 was 2-fold below that of cleavage mutant mCLIPv3, indicating robust PC activity at the plasma membrane (Fig. 14C). To quantify the relative contributions of endogenous Furin and PC7, we imaged CLIPv3- M6PR(6Ala) in sgPC7-1 and sgFurin-1 cells. Average Citrine/TFP fluorescence ratios of CLIPv3- M6PR(6Ala) were indistinguishable in sgPC7 from those in parental B16F1, whereas in sgFurin-1 cells they instead resembled those of PC-resistant cleavage mutant control. These results suggest that endogenous PC activity at the plasma membrane of B16F1 cells was mediated by Furin and not by PC7.
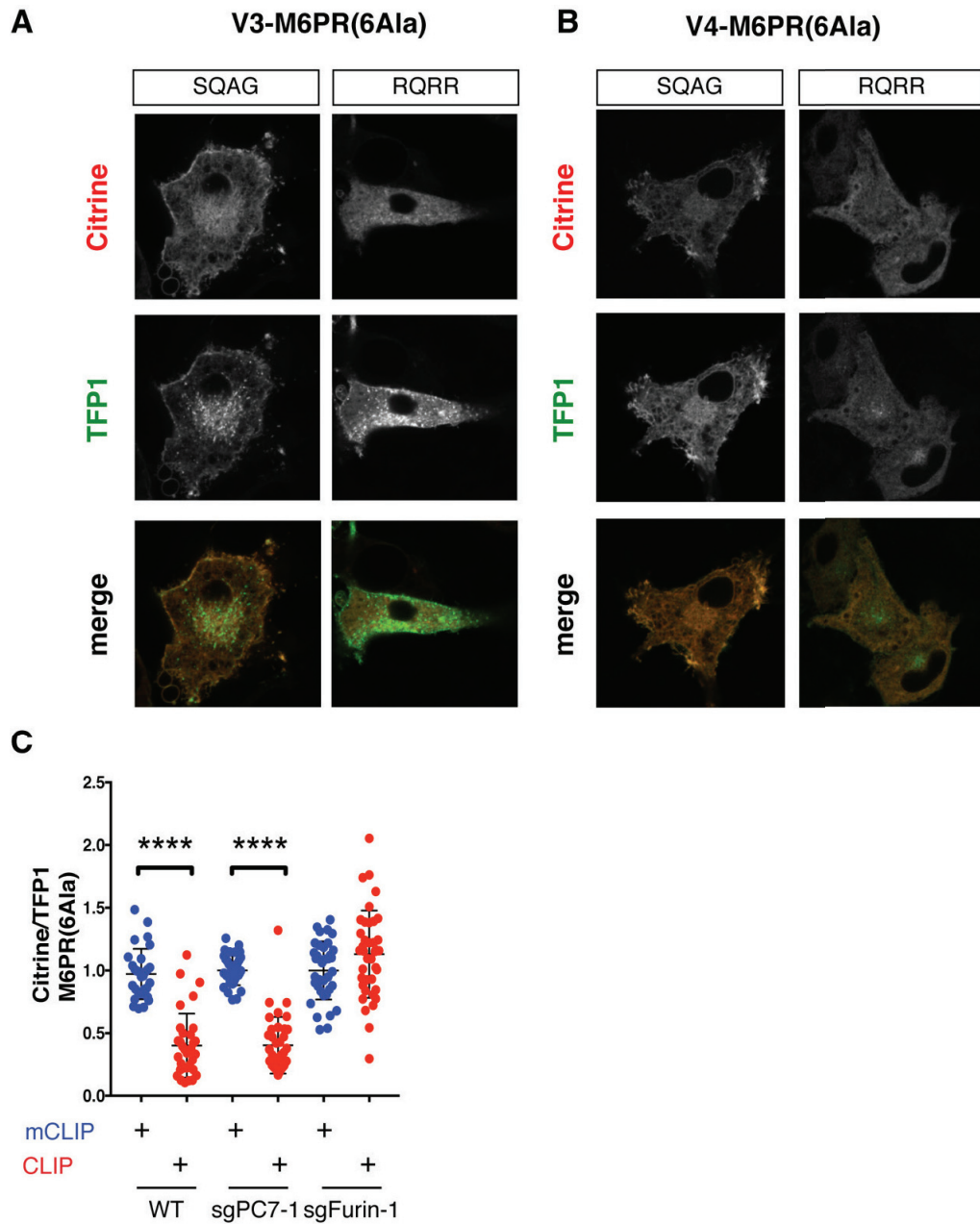
Figure 14. Furin but not PC7 is active in plasma membrane of B16F1 cells.

*(A) Fluorescent images of CLIPv3-M6PR(6Ala) and its corresponding PC-resistant mCLIPv3 controls (SQAG) in B16F1 cells. (B) Fluorescent images of CLIPv4-M6PR(6Ala) and its corresponding PC-resistant mCLIPv4 controls (SQAG) in B16F1 cells. Note that for unknown reasons, theM6PR(6Ala) signal only enriched v3 but not v4 sensors at the plasma membrane. (C) Average Citrine/TFP1 fluorescence ratios of CLIPv3- M6PR(6Ala) relative to that of its mCLIPv3 control (****p<0.0001, t-test).*

3.1.9 CLIPv4 fused to only the cytosolic tail of PC7 does not recapitulate PC7 trafficking and instead marks compartments harboring Furin

Since no endogenous PC7 activity in B16F1 cells was detected by membrane-bound CLIPv4 variants in the TGN/endosmal system and at the plasma membrane, we wondered whether its abodes might be uncovered by new CLIPv4 variant carrying the cytosolic tail and TMD of PC7 itself (Fig. 15A). Contrary to this prediction, co-transfection of CLIPv4-PC7 with Flag-tagged PC7 resulted in no significant co-localization of the two proteins. Instead, anti-Flag staining detected Flag-PC7 in peripheral cytoplasmic vesicles, whereas CLIPv4-PC7 showed a Golgi-like distribution near DAPI-stained nuclei (Fig. 15B). Furthermore, sensitized emission analysis revealed that the average NFRET efficiencies of CLIPv4-PC7 were 70±3% and 60±3% in B16F1 control and sgPC7-1 cells, respectively. By contrast, in sgFurin-1 cells, NFRET of CLIPv4-PC7 increased to 95±2%, suggesting that cleavage depended entirely on Furin (Fig. 15C). Taken together, these results show that fusion to the TMD and cytosolic domains of PC7 alone is not sufficient to route CLIPv4 to the PC7 compartments. Instead, it directs CLIPv4 to an alternative destination where it is cleaved by Furin.
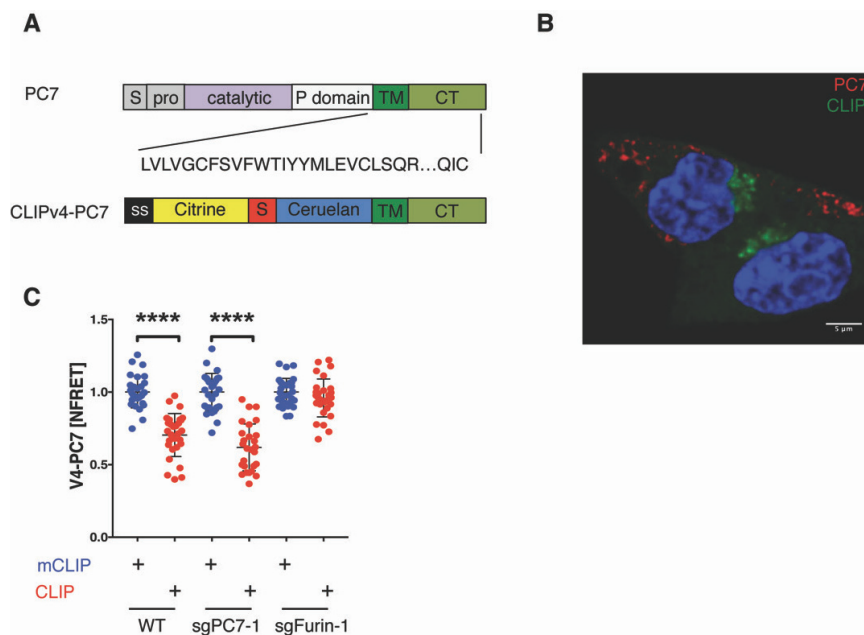
Figure 15. CLIPv4-PC7 marks compartments harboring Furin activity.

*(A) Schematic representation of the biosensor CLIPv4-PC7 containing the TM domain and cytosolic tail of PC7 as a localization signal. ss: secretory signal sequence; pro: propeptide; TM: transmembrane domain; CT: cytosolic tail. (B) Immunofluorescent staining of Flag-tagged mouse PC7 (red) in B16F1 cells shows no significant overlap with Citrine epifluorescence of mCLIPv4-PC7 (green). (C) Average NFRET efficiencies of CLIPv4-PC7 in parental versus sgFurin-1 or sgPC7-1 B16F1 cells (****p<0.0001, t-test)*

3.1.10 PC7 can only cleave TGN/endosomal and plasma membrane CLIPv4 variants when it is overexpressed

Our finding that endogenous PC7 activity was below detection in the TGN/endosomal agrees with reported differences in the sorting between endogenous PC7 and Furin in rat livers (Wouters et al., 1998), and that at least a fraction of overexpressed PC7 in KEK293 cells reached the cell surface by a TGN-independent route (Rousselet et al., 2011a). However, it contrasts previous data that overexpressed PC7 can reach the cell surface and recycle to the TGN (Declercq et al., 2012, 2016; Van De Loo et al., 1997; Rousselet et al., 2011a), cleaving substrates during transit in endosomes (Guillemot et al., 2013). To test if PC7 activity in any of these compartments depends on overexpression, we co-transfected sgDKO B16F1 cells with distinct CLIPv4 or v3 variants and Flag-PC7 or empty vector. Flag-Furin was transfected as a control. Anti-Flag Western blot analysis revealed no differences in Furin and PC7 expression levels (Fig. 16A). Overexpressed Furin reduced average NFRET, or in the case of CLIPv3, Citrine/TFP1 fluorescence ratios, in all compartments where endogenous Furin was active, as expected. Notably, overexpressed PC7 was similarly active in every compartment analyzed, including TGN, early and late endosomes, resulting in >59% inhibition of average NFRET in the corresponding CLIPv4 variants relative to their mCLIPv4 controls (Fig. 16B, C and D). Overexpressed PC7 was also active at the plasma membrane, resulting in almost 50% reduction of Citrine/TFP1 ratio compared to its mCLIPv3 control (Fig. 16E). These data show that, wild-type PC7 can restore CLIPv4 and v3 cleavage in DKO cells almost as efficiently as overexpressed Furin.

Prompted by this result, we tested whether overexpressed PC7 can also rescue the processing of substrates other than CLIP variants that normally are cleaved preferentially by Furin. To address this, we focused on the tumor necrosis factor-α converting enzyme (TACE or ADAM17)(Endres et al., 2003; Srour et al., 2003). While Western blot analysis detected endogenous ADAM17 mainly in its mature form both in control cells and in sgPC7-1, the uncleaved form accumulated specifically in sgFurin-1 and in sgDKO clones (Fig. 16F). Thus, in contrast to ADAM10 (Fig. 11B), ADAM17 is mainly cleaved by endogenous Furin. Nevertheless, ADAM17 cleavage in sgDKO cells could be restored by either Flag-Furin or Flag-PC7 overexpression (Fig. 16F) demonstrating that PC7 can substitute for Furin also during ADAM17 cleavage when overexpressed. However, in cells that endogenously express PC7 activity at physiological levels, ADAM17 cleavage depends on Furin.
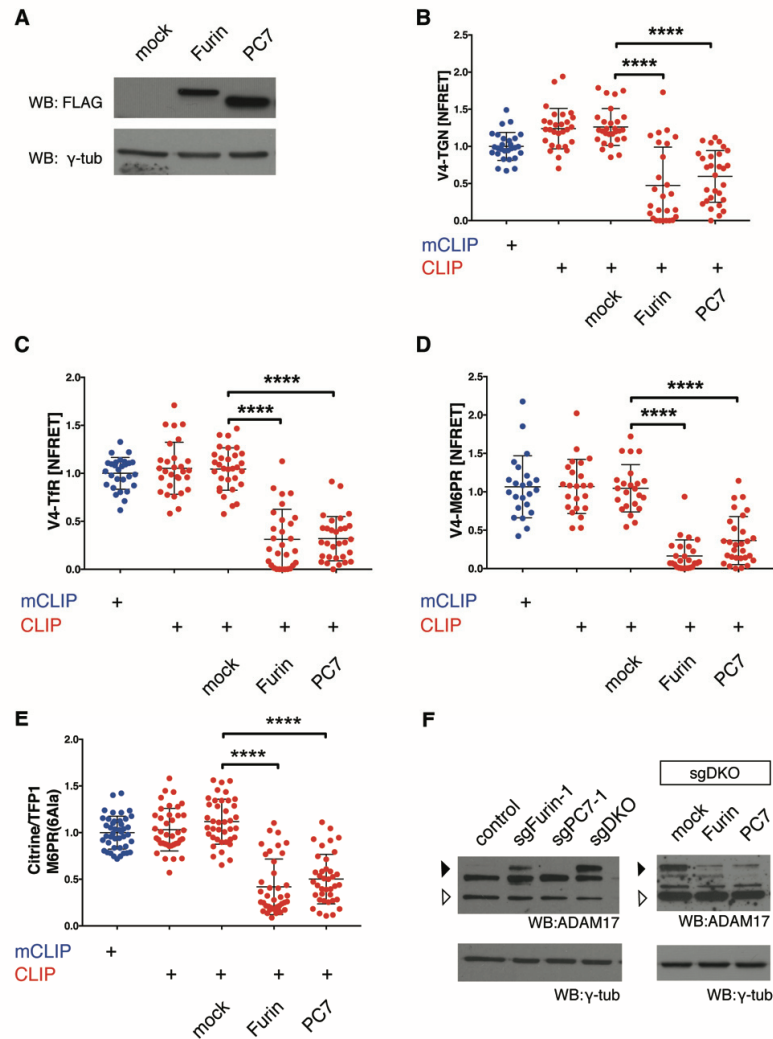
Figure 16. Overexpressed PC7 activity in TGN/endosomal and plasma membrane compartments.

(A) Representative Western blot of Flag-tagged Furin or PC7 in extracts of sgDKO B16F1 cells. γ-tubulin served as a loading control. (B-D) Live imaging of B) CLIPv4-TGN, C) CLIPv4-TfR and D) CLIPv4-M6PR in B16F1 cells cotransfected with Flag-tagged Furin or PC7. (E) Average Citrine/TFP1 fluorescence ratios of CLIPv3- M6PR(6Ala) relative to that of its mCLIPv3 control in B16F1 cells cotransfected with Flag-tagged Furin or PC7. (****p<0.0001, t-test). The asterisk indicates a significant difference with the mock control as determined by Mann-Whitney t-test (****p<0.0001). (F) Western blot analysis of endogenous ADAM17 protein processing in parental (left) and in sgDKO B16F1 cells transfected with the indicated plasmid (right). Filled and open arrowheads mark the positions of PC-cleaved ADAM17 and immature ADAM17, respectively. γ-tubulin served as a loading control.

3.1.11 Internalization of PC7 is required for its activity in exocytic compartments

Overexpressed PC7 uses both conventional and unconventional secretory pathways to reach the cell surface before internalization and re-cycling to the TGN (Declercq et al., 2012; Rousselet et al., 2011a). A short sequence in the cytosolic tail composed of the residues Pro^{724}, Leu^{725} and Cys^{726} is important to normally internalize PC7 from the plasma membrane (Declercq et al., 2012). To test whether this internalization signal regulates PC7 function, we replaced Pro^{724}, Leu^{725} and Cys^{726} in Flag-tagged mouse PC7 by alanine residues. The resulting mutant $PC7^{P>A}$ or wild-type PC7 were expressed in B16F1, and defects in trafficking were evaluated by antibody uptake experiments using a double labeling method as previously described to first label FLAG antibodies retained at the cell surface, followed by cell permeabilization and immunostaining of the internalized pool (Declercq et al., 2012). While the wild-type Flag-tagged PC7 mediated efficient antibody uptake and enrichment in Golgi-like structures, the mutant $PC7^{P>A}$ accumulated at the cell surface with few stained internalized vesicles (Fig. 17A). Furthermore, anti-Flag Western blot analysis revealed no adverse effect of the PLC>AAA mutation on PC7 expression (Fig. 17B). These results confirm that the PLC motif is important also in B16F1 cells to normally internalize overexpressed PC7 from the cell surface prior to its retrieval to the Golgi apparatus. To test potential effects on activity, wild-type PC7 or $PC7^{P>A}$ mutant were added back to PC7/Furin deficient sgDKO cells by co-transfection together with different CLIPv4 variants or the CLIPv3-M6PR(6Ala). While both wild-type PC7 and $PC7^{P>A}$ efficiently cleaved CLIPv3-M6PR (6Ala) at the plasma membrane and CLIPv4-M6PR in late endosomes, only wild-type PC7 but not $PC7^{P>A}$ rescued cleavage of CLIPv4 in the TGN (Fig. 17C). These results suggest that PLC motif-mediated internalization is essential for overexpressed PC7 activity to reach exocytic vesicles of the TGN.
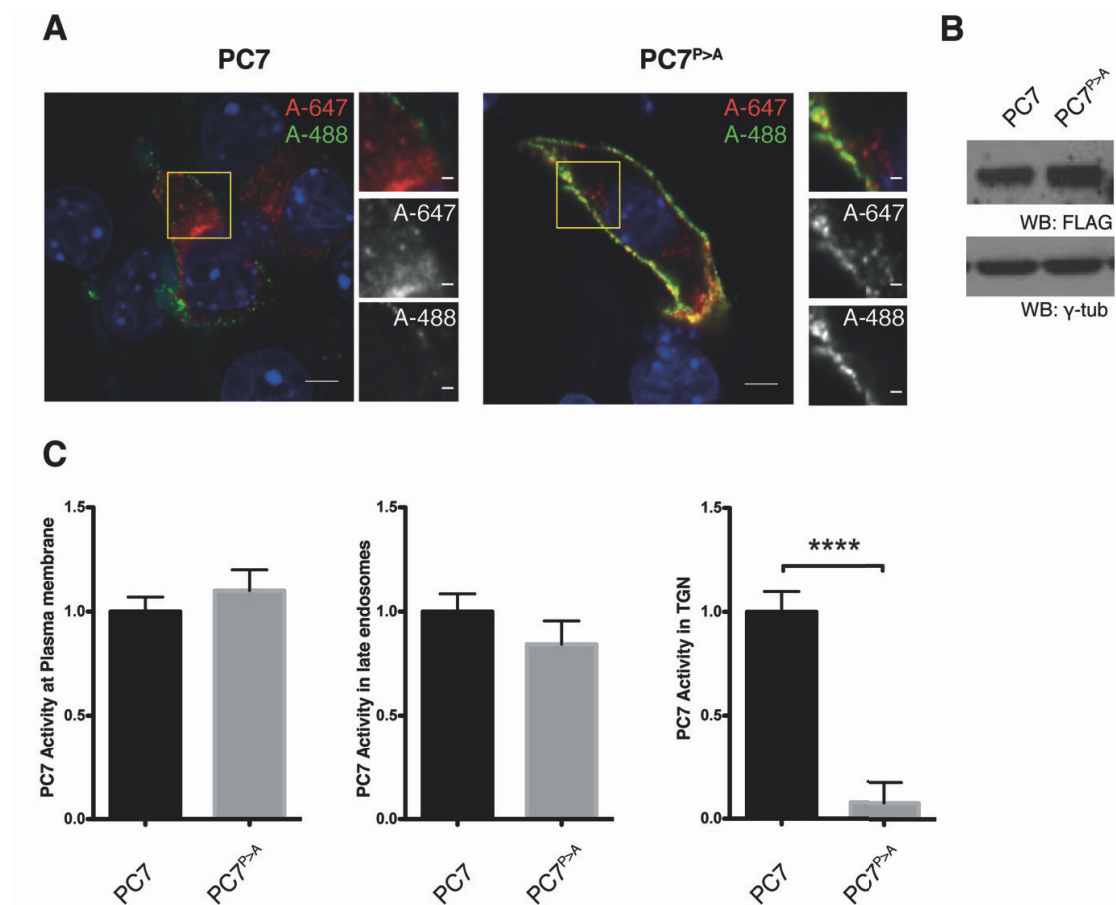
Figure 17. A cytosolic PLC motif is essential to recycle overexpressed PC7 to the TGN after its internalization from the cell surface.

(A) Representative images of M2 anti-Flag antibody uptake by sgDKO cells expressing wild-type PC7 (left) or mutant PC7$^{P>A}$ (right). FlagPC7-bound antibody was stained before and after cell permeabilization, in green and red, respectively to distinguish PC7 pools at the plasma membrane from those that were internalized. Size bars: 5µm and 1 µm. (B) Representative Western blot of Flag-tagged PC7 and PC7$^{P>A}$ in extracts of sgDKO B16F1 cells. γ-tubulin served as a loading control. (C) Activity of PC7$^{P>A}$ relative to that of wild-type PC7 plotted as NFRET difference in sgDKO cells co-expressing CLIPv4 at the plasma membrane (left), in late endosomes (center) or in the TGN (right). The activity of wild-type PC7 was defined as 1.0 after normalization to empty vector control (****p<0.0001; Mann-Whitney t-test).

3.1.12 Compartment-specific variants of the biosensor CLIPv4 quantify the efficacy of PC inhibitors and validate their access to specific intracellular destinations

Besides elucidating the spatial distribution of PC activities, we reasoned that CLIP imaging might be useful to characterize the efficacy and the tropism of PC inhibitors. As proof of principle, we compared CLIPv4 variants in TGN, early endosomes and late endosomes in

B16F1 treated with increasing concentrations of the inhibitor CMK. We found that CMK inhibited CLIPv4 cleavage in TGN with a half-maximal inhibitory concentration (IC_{50}) of 400 nM. By comparison, the IC50 concentrations of CMK required to inhibit CLIPv4 in early or late endosomes, respectively, were 3 µM and 7 µM, i.e. almost 10-or 20-fold higher dosage, respectively, than in the TGN (Fig. 18A). To validate this difference in CMK tropism and efficacy between different subcellualr compartments across different cell types, we also titrated CMK on HEK293T cell lines stably expressing CLIPv3-TGN, CLIPv3-M6PR or the endocytosis-deficient mutant derivative CLIPv3-M6PR(6Ala). The results showed that while a low concentration of 10 µM completely inhibited CLIPv3 processing in TGN and at the plasma membrane, a 10-fold higher dose (100 µM) was required to block cleavage in late endosomes (Fig. 18B). The reduced sensistivity of CLIPv4 to inhibition by CMK in endosomes compared to TGN and plasma membrane corroborates our earlier conclusion that it is mainly cleaved locally within endosomes. Since cleavage of CLIPv4 in all three compartments was mediated by Furin alone, CMK titration emerges as a new convenient criterion to evaluate where a given Furin substrate is cleaved within the TGN/endosomal system.

To test this idea on a physiological endogenous Furin substrate, we focused on the pigment cell-specific-pre-melanosomal protein (PMEL, also known as PMEL17 or gp100), which is important for melanin storage in melanocytes. Immature Pmel, called P1 form, is exported from ER to the Golgi apparatus where its oligosaccharides are modified to derive the higher molecular weight P2 form (Theos et al., 2005). The P2 form undergoes multiple proteolytic events, including PC-dependent cleavage which is essential to generate functional melanosomes (Berson et al., 2003). Western blot analysis revealed that the glycosylated uncleaved form (P2) is undetectable in parental cells but accumulated in sgFurin and in sgDKO clones cell lysates and condtioned media (Fig. 19A). This result indicates that Furin is the only PC able to process PMEL in B16F1 cells. Since PC cleavage of PMEL occurs during secretion independently of endocytic uptake (Leonhardt et al., 2011), we asked whether a low dose of CMK is sufficient to inhibit it. Confirming this prediction, the P2 form started to accumulate in cells treated with CMK concentration in the nanomolar range (Fig 19B), i.e. at concentration that are below those required to inhibit Furin activity in endosomes (Fig. 18A). To our knowledge, these data provide the first proof-of-concept that pharmacological PC inhibitors can be used to differentially target a subset of diverse intracellular PC compartments.
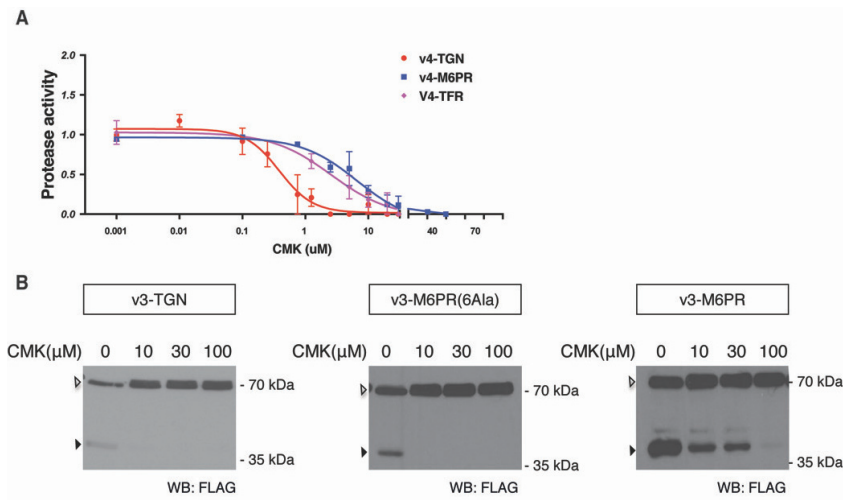
Figure 18. Tropism and efficacy of the PC inhibitor dec-RVKR-cmk (CMK) in B16F1 cells and HEK293T cells.

(A) Inhibition of protease activity, plotted as difference between mCLIP and CLIP NFRET efficiency, using increasing concentration of the pan-PC inhibitor CMK in B16F1 cells. Data for protease activity in TGN, early and late endosomes are shown in red, magenta and blue, respectively. Data represents means± SD of three experiments, normalized to vehicle control and scaled to 1 (maximum activity). Half maximal inhibitory concentrations (IC_{50}) of the PC-inhibitor CMK required to block cleavage of CLIPv4-TGN was 400 nM, whereas for CLIPv4-Tfr or CLIPv4-M6PR they were3 μM and7 μM, respectively. (B) Anti-Flag Western blot analysis of CLIPv3 in the TGN (v3-TGN), at the plasma membrane (v3-M6PR(6Ala)) or in late endosomes (v3-M6PR) of HEK293T cells treated with the indicated dosage of the pan-PC inhibitor CMK. Data in panel B are Courtesy of Dr. P. Donovan.
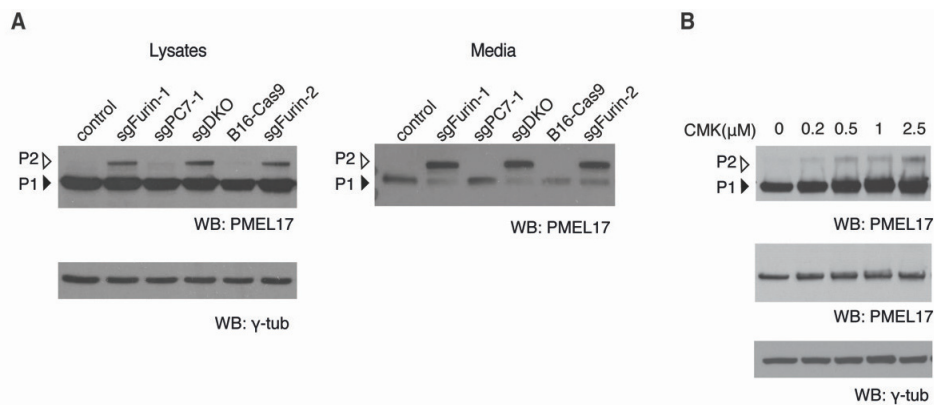
Figure 19. PMEL processing by Furin in CMK-sensitive exocytic vesicles and not by endogenous PC7.

(A) Western blot analysis of endogenous PMEL in B16F1 cell clones lysate (left panel) and conditioned media (right panel). Partially glycosylated P1 and post-Golgi P2 forms of uncleaved PMEL are indicated by filled and open arrowheads, respectively. γ-tubulin served as loading control. (B) Inhibition of endogenous PMEL processing in B16F1 cells treated with the indicated concentrations of the PC inhibitor CMK. Low exposure and γ-tubulin served as loading control.

Next, we asked whether other inhibitors showed similar tropism and efficacy as CMK. The inhibitor-24 (Inh.24) has recently been described as a potent and cell-permeable new inhibitor specific for basic PCs with the exception of PC2 and PC7 (Becker et al., 2012). To characterize Inh.24 tropism and efficacy, we compared CLIPv4-TGN and CLIPv4-M6PR in B16F1 treated with increasing concentration of the inhibitor. Preliminary experiments showed that a low concentration of Inh.24 (500 nM) was sufficient to rescue NFRET efficiencies of CLIPv4 in both TGN and late endosomes compartments (Fig. 20A). To further investigate Inh.24 efficacy, we also titrated Inh.24 on HEK293T cell lines stably expressing CLIPv3-TGN and CLIPv3-M6PR. The result showed that low concentration of Inh.24 (100 nM) was sufficient to block CLIPv3 processing in TGN, while a 10-fold higher dose (1 µM) was required to block cleavage in late endosomes (Fig. 20B). Taken together, these results indicate that specific PC inhibitor show different tropism and efficacy in distinct subcellular compartment, and their titration might be used to target a subcellular subset of PC activities in B16F1 cells.
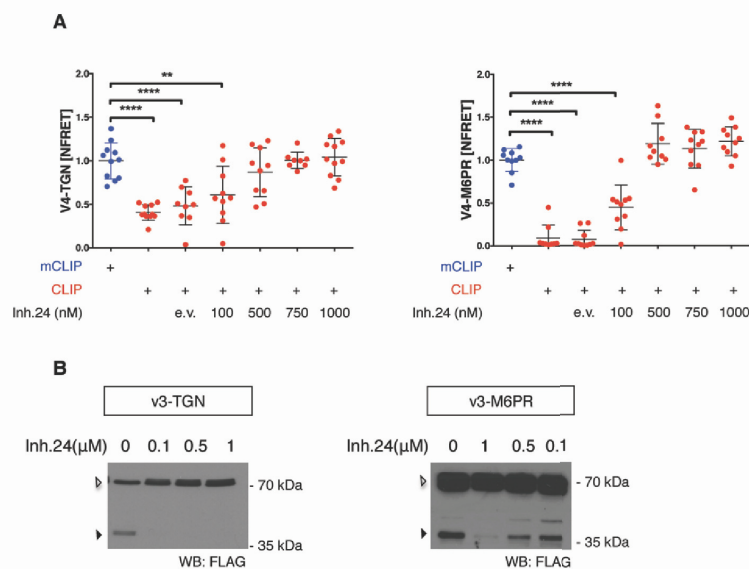
Figure 20. Tropism and efficacy of the PC Inhibitor-24 (Inh.24) in B16F1 cells and HEK293T cells.

(A) Live imaging of CLIPv4-TGN (left) and CLIPv4-M6PR (right) in B16F1 cells treated with the indicated dosage of the PC inhibitor Inh.24. (**p<0.01; ****p<0.0001; Mann-Whitney t-test). (B) Anti-Flag Western blot analysis of CLIPv3 in the TGN (v3-TGN), or in late endosomes (v3-M6PR) of HEK293T cells treated with the indicated dosage of the PC inhibitor Inh.24.

3.1.13 Spatial mapping of Furin and PC7 activities by compartment-specific CLIPv4 variants can explain differential substrate specificities

A longstanding enigma in proprotein processing is whether compartmentalization of PCs determines their substrate specificities, and if so, whether functional overlap between two PCs requires that shared substrates enter more than one PC compartment in parallel, or whether two PCs must co-localize in the same vesicles to substitute for each other. To address this question, we evaluated whether the spatial mapping of Furin and PC7 activities by CLIPv4 imaging can explain which of these endogenous PCs, if any, mediates cleavage of the transforming growth factor-β (TGFβ)-related Activin-A precursor. Activin-A is a multifunctional endocrine factor that regulates the menstrual cycle, bone and skeletal muscle formation (Chen et al., 2017) and inflammatory processes (Hedger et al., 2011; Sanchez-Duffhues et al., 2015) Depending on the context, Activin-A also mediates tumor suppressive or oncogenic functions (Loomans et al., 2014). E.g. in syngeneic B16F1 melanoma grafts, autocrine growth-inhibitory signalling is attenuated, while paracrine signalling promotes primary and metastatic growth by inhibiting tumor immunesurveillance (Donovan et al., 2017). However, how Activin-A precursor processing is regulated in this or other contexts is unknown (Antenos et al., 2008). To estimate the relative contributions of endogenous Furin and PC7 in Activin-A maturation, we transfected parental B16F1 cells and CRISPR clones with *INHβA* expression vector encoding Activin-A. Western blot analysis showed that conditioned media of control and sgPC7-1 single mutant B16F1 cells accumulated mature Activin-A (A30) consisting of a homodimer of the C-terminal INHβA fragment (28-30 kDa), together with dimers of one cleaved and one uncleaved INHβA subunit (A60) (Huylebroeck et al., 1990; Mason et al., 1996), but no precursor dimers (A110). By contrast, in sgFurin-1 and sgDKO cells, A110 was stabilized, and the 60 kDa processing intermediate was shifted to 70 kDa (Fig. 21A) or below detection (Fig. 21C). Mutation of the INHβA S1 site (cmβA) blocked the production of all processed forms (Fig. 21B), whereas add-back of Furin to INHβA-transfected sgFurin-1 cells restored A60 and A30 maturation, confirming specificity (Fig. 21C). These results demonstrate that proActivin-A is cleaved at the S1 site, and only in one INHβA subunit by an unknown protease independently of Furin and PC7. This was completely unexpected because sgFurin;sgPC7 DKO cells did not upregulate the expression of any other known PCs (Fig. 10).

Our finding that deletion of Furin blocks the conversion of A70 to A60 established that proActivin-A is cleaved at a PC7-resistant novel S2 site approximately 90 residues after the signal sequence. In this position, the βA chain has a dibasic motif (RR_{110}). While an RR motif at an analogous position is cleaved in the INHα chain (Sugino et al., 1992), this unstructured region in several other TGFβ family members instead harbors a metalloprotease cleavage site (Ge et al., 2005). Cleavage at this position severs the so-called latency lasso at the N-terminus,

which in crystals of uncleaved TGFβ precursor masks type II receptor binding epitopes in the C-terminal mature domain (Shi et al., 2011). The lasso of one TGFβ subunit contacts the mature region of the other in a 'cross-armed' conformation that is stabilized by covalent dimerization of the prodomain. However, in most other TGFβ family members, the prodomain may switch between cross- and open-arm conformations, with the latter masking binding sites of type I instead of type II receptors, and (in BMP9) the interface of a soluble antagonist (Mi et al., 2015). We hypothesize that cleavage of the S2 site favors an open-arm conformation.

We were surprised that endogenous PC7 in B16F1 cells failed to cleave Activin-A, because it was clearly active and able to compensate for the loss of Furin e.g. to process E-cadherin and Notch1 (Fig. 7). To test whether differential PC sorting accounted for substrate specificity, we examined the effect of the trafficking mutant PC7$^{P>A}$. Despite comparable expression, only wild-type PC7 and not PC7$^{P>A}$ efficiently rescued the conversion of A110 to mature Activin-A (A30). PC7$^{P>A}$ instead cleaved A110 only partially to rescue the production of A70, while releasing minimal amounts of A30 (Fig. 21C). An artifact linked to the P>A mutation is unlikely, since the P>A mutation did not significantly impair PC7-mediated cleavage of Notch1 (Fig. 21D). These results strongly suggest that PCs release A30 into the medium only if Activin-A enters the TGN via endosomes where the A70 intermediate is converted to A60. This retrograde processing route must be incredibly efficient because in Furin wild-type B16F1 cells, A110 is almost completely converted into A60 and A30, while in the absence of Furin, even A70 (together with uncleaved A110) re-cycles and is secreted into the medium. To confirm a role of endocytosis in Furin-mediated processing, we refrained from manipulating the endocytic machinery because of certain and uninterpretable indirect effects. Instead, we titrated the PC inhibitor CMK. A low CMK dose (5 µM) which blocks Furin in the TGN but not in endosomes (Fig. 18) stabilized the endosomally derived A60, thus allowing its re-cycling into the medium, whereas conversion of A70 to A60 was only inhibited by concentrations above 50 µM that block also endosomal Furin. A high dose of CMK was also needed in Furin WT cells to stabilize A110 (Fig. 21E). These data strongly corroborate our model that Furin first cleaves the S2 and the S1 site of at least one βA chain in endosomes, before it can cleave the S1 site of the second subunit in the TGN.
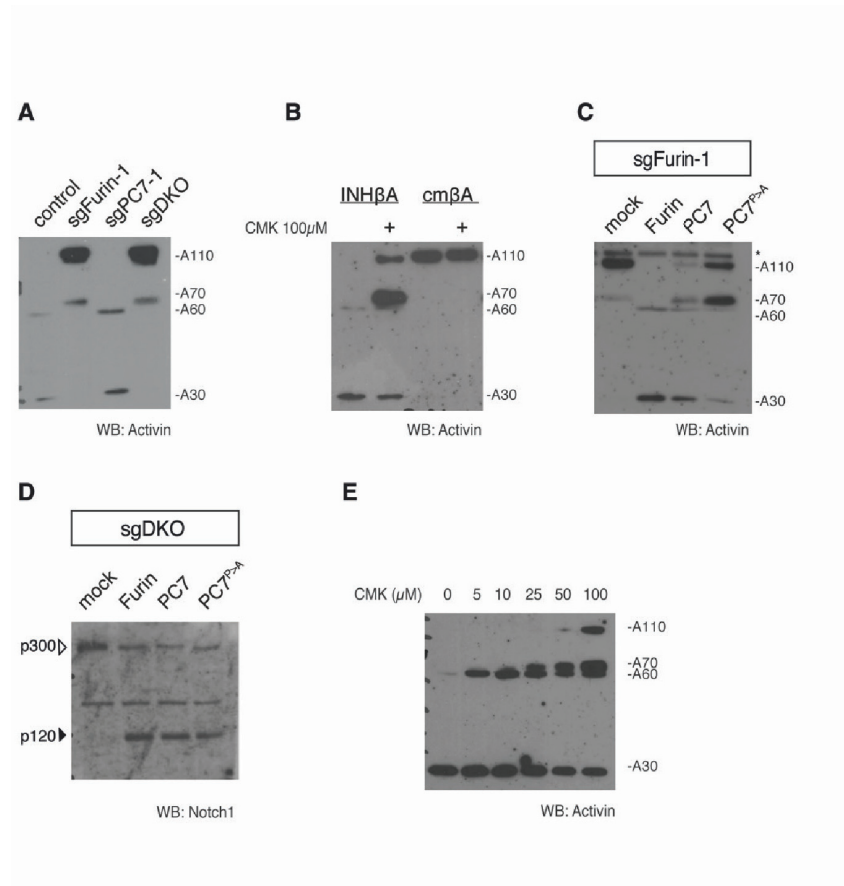
Figure 21. Activin-A processing in B16F1 cells.

(A) Western blot analysis, under non-reducing conditions, of conditioned media of the indicated B16F1 cells overexpressing Activin-A. Molecular weights of the cleaved products are indicated. (B) Western blot analysis, under non-reducing conditions, of conditioned media of control cells overexpressing Activin-A or the S1-mutant cmβA, treated or not with 100μM concentrations of the PC inhibitor CMK. (C) Western blot analysis, under non-reducing conditions, of conditioned media of sgFurin-1cells overexpressing Activin-A and co-transfected with the indicated PC. Molecular weights of the cleaved products are indicated, (*) non-specific band. (D) Western blot analysis of conditioned media of sgDKO-1cells overexpressing Notch-1 and co-transfected with the indicated PC. Filled and open arrowheads indicate PC-cleaved Notch1(p120) and uncleaved Notch1(p300) respectively. (E) Western blot analysis, under non-reducing conditions, of conditioned media of control cells overexpressing Activin-A treated with the indicated concentrations of the PC inhibitor CMK.

3.2 Roles of Furin and PC7 in B16F1 tumor growth and differentiation

3.2.1 Furin may promote B16F1 tumor growth

Mounting evidence suggests that PC play a crucial role in tumorigenesis by regulating the activation or inactivation of several cancer-related proteins (reviewed in Artenstein and Opal, 2011; Bassi et al., 2005; reviewed in Seidah and Prat, 2012). Elevated or altered PC expression have been associated with different types of cancer including melanoma (Bassi et al., 2001a; Cheng et al., 1997; Khatib et al., 2001; Lalou et al., 2010; Longuespée et al., 2014). However, the precise contributions of each single PC in acquisition of malignant properties in melanoma are unknown. To evaluate the role of Furin and PC7 in cancer progression of B16F1 tumors *in vivo*, B16F1 and CRISPR-edited clones were grafted intradermally in the right flank of 8-10 weeks old female C57BL/6 mice. Whereas control tumors of parental B16F1 cells or control wild-type CRISPR clones were strongly pigmented, tumors formed by sgFurin, sgPC7 and sgDKO cells were amelanotic (Fig. 22A, B, C,). Furthermore, while sgPC7-1 and sgDKO tumors grew as fast as the control ones, tumor growth of sgFurin-1 cells were significantly reduced (Fig. 22D, E). Viability of sgFurin-1 knockout cells was determined by Alamar assay *in vitro* (Fig. 22F). Although these data need to be confirmed by additional CRISPR clones, these results indicate that endogenous Furin may be limiting for tumor growth *in vivo*, but that its loss may be rescued by PC7 deletion. However, both Furin and PC7 are required for tumor pigmentation

One important determinant of tumor growth rate in B16 melanoma models is tumor immune surveillance mediated by both innate and adaptive immunity (Donovan et al., 2017; Smyth et al., 2006). To determine whether Furin may inhibit anti-tumor immunity, sgFurin-1 and control cells were intradermally inoculated on the right flank of 8-10 weeks old female Rag1$^{-/-}$ mice devoid of V-D-J recombination in antigen receptors. In mice lacking *Rag1*, sgFurin-1 tumors still grew significantly more slowly than control tumors and they remained amelanotic (Fig. 23A, B). However, compared to control tumors, sgFurin tumor volumes at the end of the experiment were only 2-fold reduced in Rag1-/- mice, compared to a 3-fold decrease in wild-type hosts, indicating a potential role of Furin in attenuating an immune response. Altogether, these data suggest that both Furin and PC7 are required for pigmentation. In addition, Furin may promote B16F1 tumor growth by antagonizing a tumor-suppressive function of PC7, although this preliminary conclusion requires further validation to rule out clonal artifacts. Finally, since the growth inhibition of sgFurin-1 tumors partly depended on functional T or B

cells, we cannot exclude that Furin promotes melanoma growth at least in part by inhibiting anti-tumor immunity.
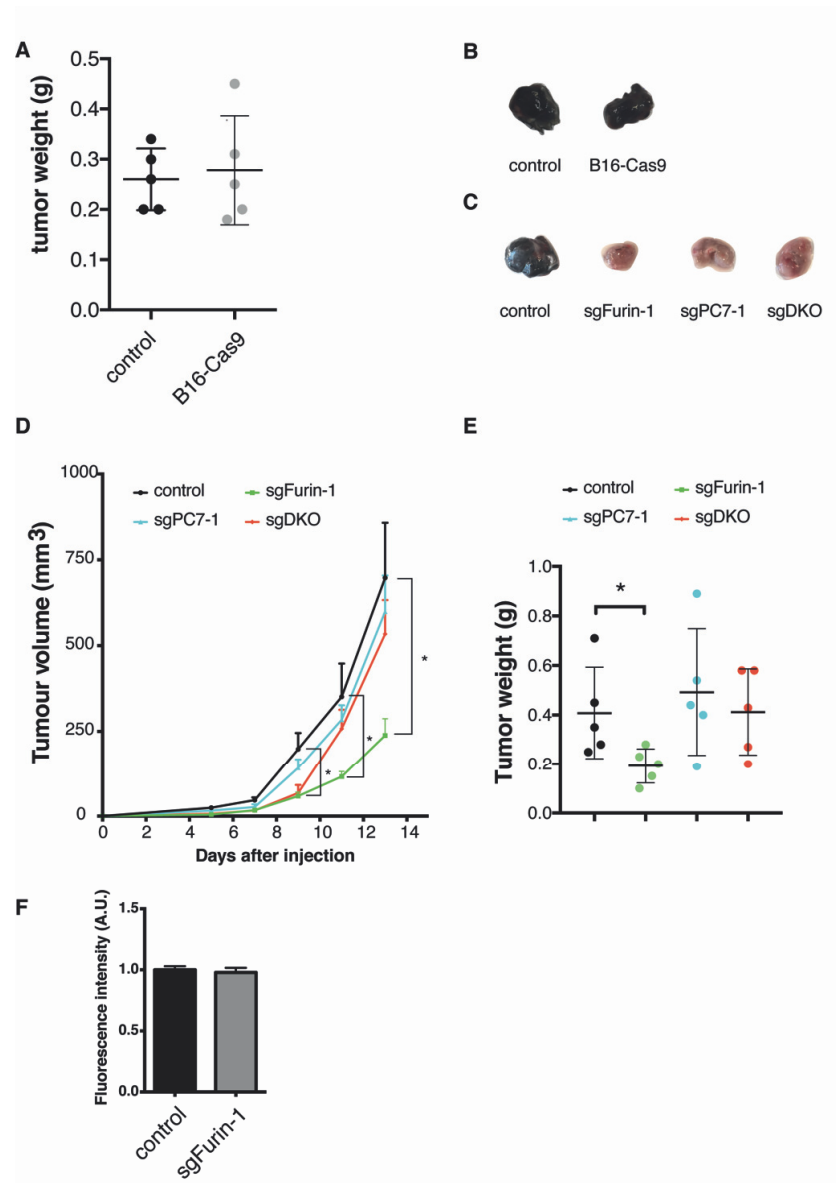
Figure 22. Roles of Furin and PC7 in B16F1 tumor differentiation and growth in immunocompetent syngenic hosts.

(A) Tumor weight of of syngenic control and B16-Cas9 grafts. (B) Representative images of control and B16-Cas9 tumor. (C) Representative images of B16-WT, sgFurin-1, sgPC7-1 and sgDKO tumor. (D) Growth curves of intradermal syngenic grafts of control, sgFurin-1, sgPC7-1 and sgDKO grafts in immunocompetent mice (n=5) (*p<0.05; Mann-Whitney t-test). (E) Tumor weight of intradermal syngenic grafts of control, sgFurin-1, sgPC7-1 and sgDKO grafts in immunocompetent mice. (*p<0.05; Mann-Whitney t-test). (F) Alamar blue assay of control and sgFurin-1 cells.
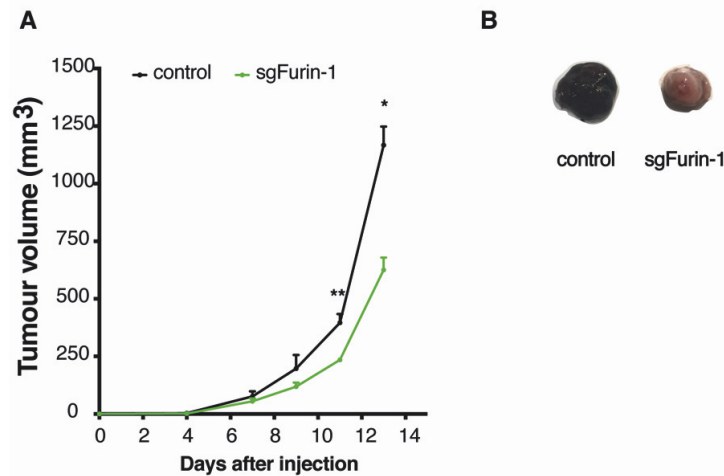
Figure 23. Role of Furin in B16F1 tumor growth in immunodeficient Rag1$^{-/-}$ mice.

(A) *Growth curves of intradermal syngenic grafts of control and sgFurin-1 grafts in Rag1$^{-/-}$ mice (n=5)* *(*p<0.05; **p<0.01; Mann-Whitney t-test).* **(B)** *Representative images of control and sgFurin-1 tumors.*

3.2.2 Furin but not PC7 is active in TGN of B16F1 tumors

Our CLIPv4 imaging results suggested that endogenous Furin, but not endogenous PC7, cleaves substrates in the TGN of B16F1 cells *in vitro*. To investigate whether Furin is the only PC active in TGN *in vivo*, we generated control and sgFurin-1 cell line stably expressing CLIPv3-TGN and its control mCLIPv3-TGN (Fig. 24A). Ratiometric imaging in B16F1 control cells showed that the mean Citrine/TFP1 fluorescence ratio of CLIPv3 was 10-fold below that of cleavage mutant mCLIPv3, whereas in sgFurin-1 cells, the mean Citrine/TFP1 fluorescence ratio of CLIPv3 were comparable to each other (Fig. 24B). These results show that only Furin cleaves CLIPv3 in TGN, in agreement with CLIPv4 data (Fig. 13A). Moreover, shedding of cleaved Citrine into the medium reduced intracellular Citrine/TFP1 ratio by more than 90±6% (Fig. 24A, B), in contrast to HEK293T cells where Citrine partly remained trapped in intracellular vesicles (Fig. 5D). Since B16F1 cells only trapped trace amounts of cleaved Citrine in intracellular vesicles, we reasoned that ratiometric imaging should suffice to accurately estimate CLIPv3 cleavage. Thus, to estimate PC activity in B16F1 tumors *in vivo*, we syngeneically grafted controls or sgFurin-1 cells expressing CLIPv3-TGN or its cleavage mutant control on the right flank of 8-10 weeks old female mice. Similar to previous results (Fig. 22), sgFurin-1 tumors were smaller than controls (Fig. 25A). Furthermore, cryosectioning of fixed samples revealed that, in agreement with the *in vitro* data, Citrine fluorescence of CLIPv3 was diminished to background levels in control tumors, whereas sgFurin-1 tumors retained Citrine in TGN-like intracellular vesicles (Fig. 25B, C). These data suggest that Furin is the only PC active in TGN in B16F1 *in vivo*. Although, we do not rule out that in specific

tumor areas, B16F1 cells may be exposed to host-derived PCs, or even internalize and recycle them to the TGN.
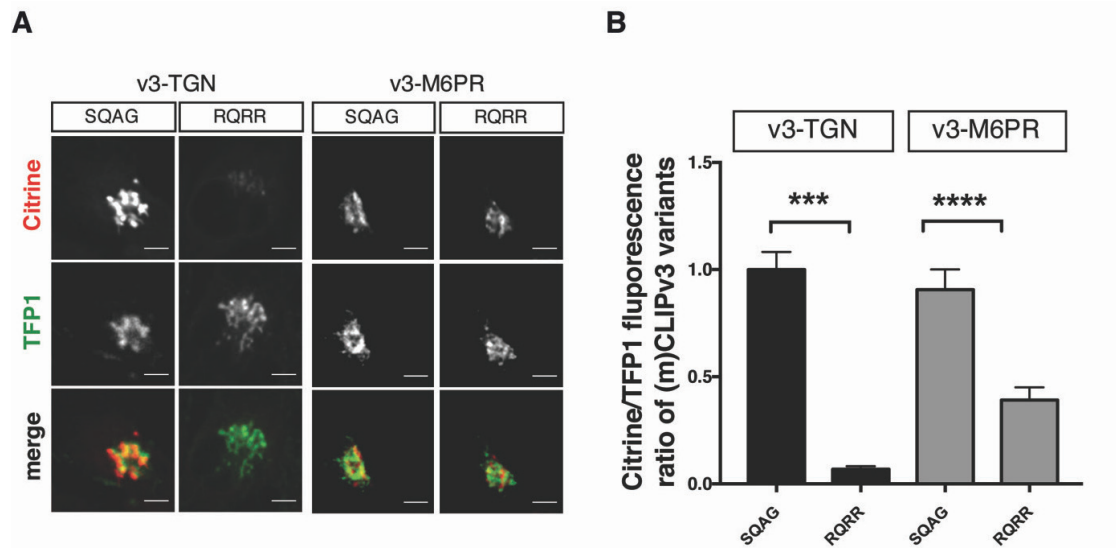
Figure 24. CLIPv3-TGN ratiometric analysis in B16F1 cells in vitro.

(A) Fluorescent images of CLIPv3-TGN (RQRR) and its corresponding PC-resistant mCLIPv3 control (SQAG) in cultured B16F1 cells. (B) Average Citrine/TFP1 fluorescence ratios of CLIPv3-TGN relative to that of its mCLIPv3 controls. Data represent mean±s.e.m. of 3 experiments (*p<0.05, ***p<0.001, t-test).
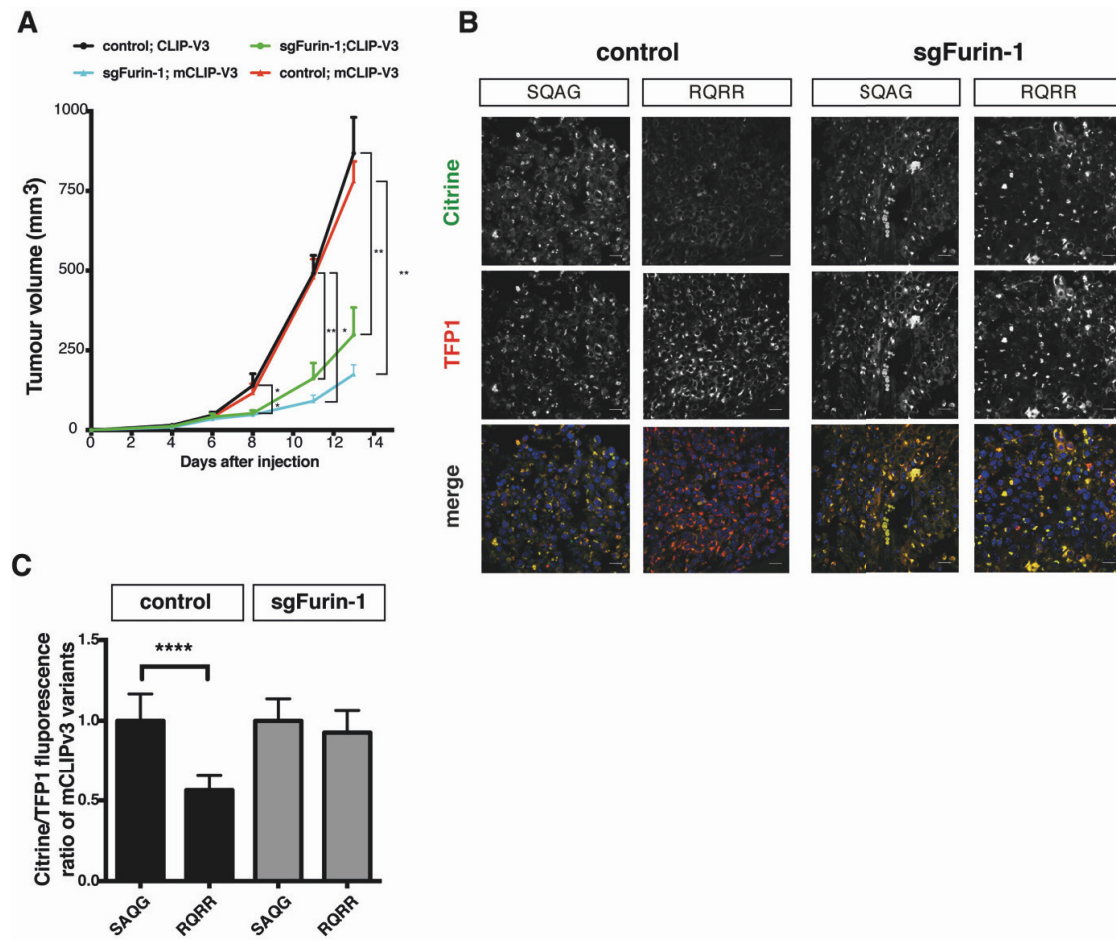
Figure 25. Furin activity in the TGN of B16F1 cancer cells in syngenic tumor grafts.

*(A) Growth curves of intradermal syngenic grafts of B16-WT and sgFurin-1expressing CLIPv3-TGN or its control mCLIPv3-TGN in immunocompetent mice (n=5) (*p<0.05; **p<0.01; Mann-Whitney t-test).
(B) Representative fluorescent images of CLIPv3-TGN and its corresponding PC-resistant mCLIPv3-TGN control in tumor section of wild-type and sgFurin-1 B16F1-derived tumors. Color channel was inverted compared to Fig. 24 to improve contrast in merge image (C) Average Citrine/TFP1 fluorescence ratios of CLIPv3-TGN relative to mCLIPv3 controls in tumor sections derived from B16F1-WT and sgFurin-1 tumors (****p<0.0001, t-test).*

3.2.3 Contribution of Furin in B16F1 cell differentiation in vitro and in vivo

Since Furin deletion resulted in formation of smaller tumors in grafts expressing bioactive PC7, we wished to validate whether expression of FurinGFP was sufficient to rescue tumor growth in sgFurin-1 grafts. For this purpose, we transduced sgFurin-1 cells with lentivirus expressing a doxycycline-inducible FurinGFP transgene (sgFurin-1;tetO-FurinGFP;rtTA). Induction of FurinGFP by doxycycline was confirmed by anti-GFP Western blot analysis of cell lysate and

conditioned media, and by monitoring GFP epifluorescence (Fig. 26A, B). To confirm that FurinGFP was functional, we analyzed processing of endogenous Furin substrate PMEL17 (Fig. 19). Expression of FurinGFP reduced the level of the P2 uncleaved PMEL form in both in cell lysate and in conditioned media (Fig. 26C), suggesting complete rescue of PMEL processing. Induction of FurinGFP in sgFurin-1 cells also restored pigment secretion into conditioned media. These results suggest that FurinGFP is active and can rescue pigment storage and secretion in sgFurin-1 cells.

To evaluate if induction of FurinGFP can rescue tumor growth in sgFurin-1 tumors, we grafted sgFurin-1;tetO-FurinGFP;rtTA cells intradermally in syngenic C57BL/6 mice, followed by treatment with doxycycline or empty vehicle. Interestingly, treatment restored pigmentation in only two out of five sgFurin-1 tumor grafts, and it failed to significantly increase average tumor growth (Fig. 27A, B). To assess whether doxycycline treatment was effective, we monitored FurinGFP expression in tumor sections of grafted sgFurin-1;tetO-FurinGFP;rtTA treated with doxycycline or vehicle. FurinGFP epifluorescence was clearly detectable in doxycycline treated tumors that rescued tumor pigmentation, whereas no GFP was observed in any doxycycline-treated grafts that remained amelanotic, or in vehicle-treated controls (Fig. 27B). Although preliminary, these data suggest that FurinGFP expression in sgFurin-1;tetO-FurinGFP;rtTA grafts can restore melanoma differentiation marked by pigment synthesis, but not tumor growth.
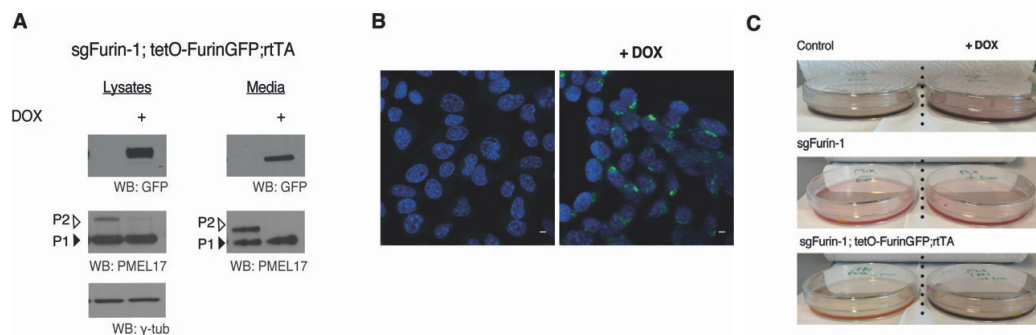
Figure 26. Inducible FurinGFP activity in vitro.

(A) Representative Western blots of PMEL17 and GFP in lysates and conditioned media of sgFurin-1;tetO-FurinGFP;rtTA cells treated or not with 250µg/mlDoxycycline. γ-tubulin served as a loading control. (B) Fluorescent images of sgFurin-1;tetO-FurinGFP;rtTA cells treated or not with 250µg/mlDoxycycline. (C). Conditioned media of B16-WT, sgFurin and inducible sgFurin-1;tetO-FurinGFP;rtTA cells cells treated or not with 250µg/mlDoxycycline .
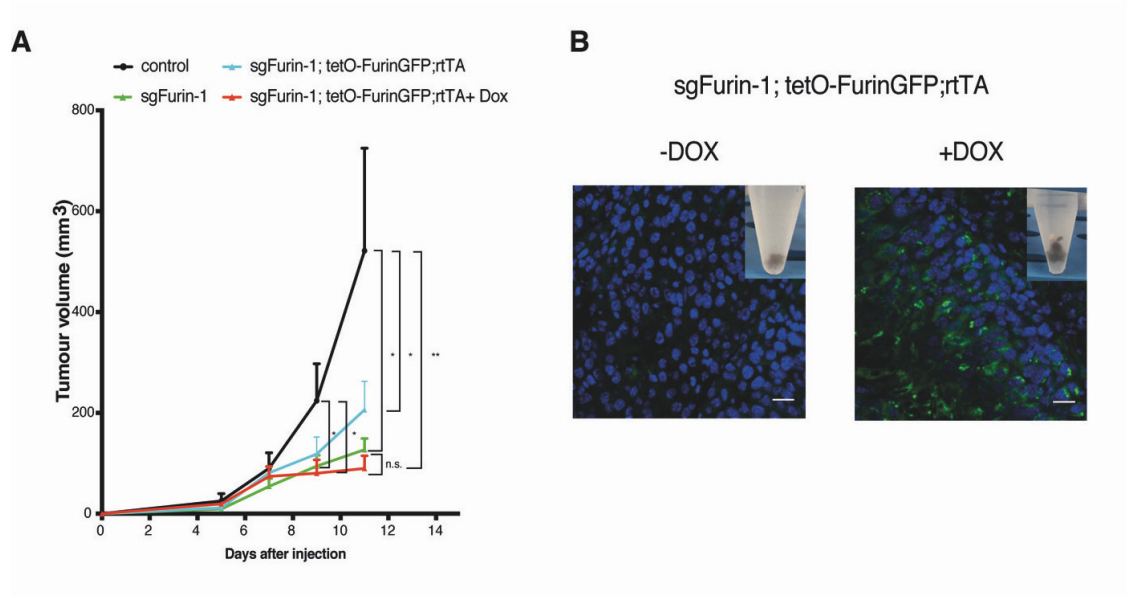
Figure 27. Inducible FurinGFP activity in vivo.

(A) Growth curves of intradermal syngenic grafts of B16F1-WT, sgFurin-1 and sgFurin-1;tetO-FurinGFP;rtTA cells (n=5) (*p<0.05; **p<0.01; Mann-Whitney t-test). (B) FurinGFP expression in syngeneic sgFurin-1;tetO-FurinGFP;rtTA tumors expressing FurinGFP (+Dox) or not . Insets show representative images of sgFurin-1;tetO-FurinGFP;rtTA tumors expressing FurinGFP (+Dox) or not.

3.2.4 Contribution of Notch1 to tumor pigmentation

The pigmentation system is regulated by several developmental pathways in both melanocytes and melanoma (reviewed in Liu et al., 2014). The evolutionarily conserved Notch signalling pathway has been described to be upregulated in melanoma cells line compared to control melanocytes (Hoek et al., 2004). Furthermore, inhibition of Notch signalling by Notch receptors alleles deletion or by treatment with γ-secretase inhibitor in melanocyte lineage resulted in hair graying and melanocytes loss. (Kumano et al., 2008; Schouwey et al., 2007). Rescue experiments using a mouse line expressing the Notch intracellular domain (NICD) have been reported to rescue those phenotypes, demonstrating that Notch signalling is RBP-JK dependent (Schouwey et al., 2010b). Our finding that pigmentation of B16F1 tumors requires both Furin and PC7 raised the question why these PCs cannot efficiently substitute for each other. Do they each cleave unique substrates that act in parallel to induce pigment *e.g.* PMEL (cleaved only by Furin) and an unknown PC7 substrate? Or do both Furin and PC7 cooperate to activate one shared substrate such as Notch1 in sufficient amounts? Since our data showed that overexpressed Notch1 can be cleaved by both Furin and PC7 (Fig. 11C), we asked whether Notch signalling is impaired in sgFurin-1, sgPC7-1 and sgDKO clones. First, we compared Notch mRNA levels in CRISPR-edited and in control cells by RT-qPCR analysis. Notch1 mRNA was reduced in all CRISPR-edited clones except for sgFurin-2 cell (Fig. 28A).

Western blot analysis confirmed loss of Notch-1 expression in sgFurin-1, sgPC7-1 and sgDKO-1 clones.

Unexpectedly, Notch1 protein similarly decreased in a B16F1-Cas9 control clone, indicating that B16F1 cells may be heterogenous, with some cells expressing Notch1 receptor and others expressing ligand, or that clonal variation may result from Cas9 treatment alone. In keeping with the former hypothesis and arguing against the latter, both p300 and p120 forms were still expressed in lysates of sgFurin-2 B16F1 cells (Fig. 28B) presumably because endogenous PC7 was sufficiently active in this clone to maintain Notch1 processing and autoregulation (Yashiro-Ohtani et al., 2009).

To test whether inhibition of Notch signalling is required for B16F1 cell pigmentation, we treated control cells with increasing concentration of the γ-secretase inhibitor N-[N-(3,5-Difluorophenacetyl)-L-alanyl]-S-phenylglycine t-butyl ester (DAPT). In line with our prediction, Western blot analysis of Notch1 revealed that DAPT treatment increased the levels of the transmembrane p120 Notch form (Fig. 28C). DAPT treatment also diminished the secretion of pigment into conditioned media (Fig. 28D). To assess how Notch signalling regulates B16F1 pigmentation we assessed the expression levels of PMEL17 and microphthalmia-associated transcription factor (MITF) proteins, which are involved in melanosomes biogenesis and melanocyte differentiation (Goding, 2000; Liu et al., 2014b; Raposo and Marks, 2007), and alteration in their function leads to defect in pigmentation and melanogenesis (Berson et al., 2003; Yajima et al., 1999). Treatment with low (5 µM) or high (20 µM) concentration of DAPT increased PMEL17 expression, whereas MITF protein levels only increased in cells trated with the lower concentration (5 µM) (Fig. 28E). In sharp contrast, MITF protein levels increased in both sgPC7-1 and in sgDKO cell lines (Fig. 28F) suggesting an inverse correlation between MITF and Notch expression. Taken together, these preliminary results suggest that Notch signalling influences B16F1 pigmentation *in vitro* and it can modulate expression of the master regulator of melanocyte differentiation MITF.
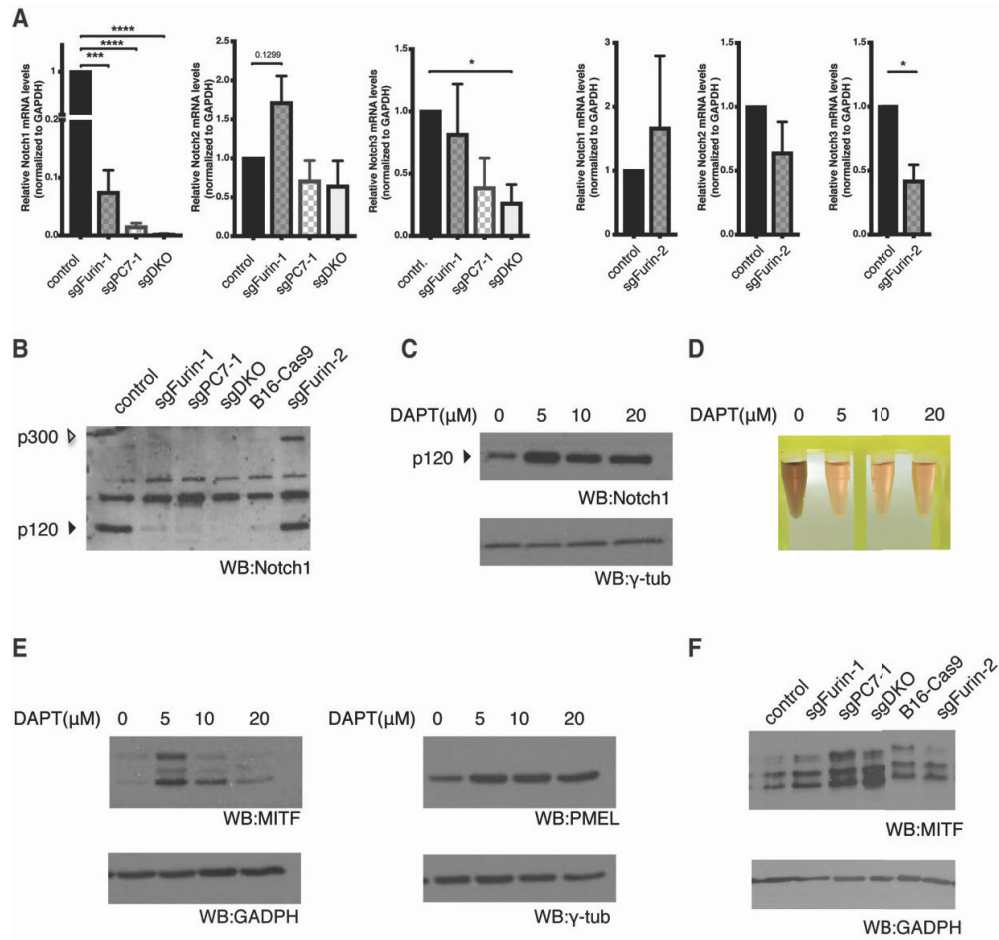
Figure 28. Notch inhibition.

(A) RT-qPCR analysis of the relative expression of endogenous Notch1, Notch2 and Notch3 in B16F1 wild-type, sgFurin-1/2, sg-PC7-1 and sgDKO cells (*p<0.05; ***p<0.001, ****p<0.0001t-test). (B) Representative Western blot of endogenous Notch1 in CRISPR-edited clones. (C) Conditioned media of B16F1 wild-type cells treated with the indicated dosage of the γ-secretase inhibitor (DAPT). (D) Western blot of endogenous Notch1 in B16F1 wild type cells treated with the indicated dosage of the gamma-secretase inhibitor (DAPT). γ-tubulin served as loading control. (E) Western blot of endogenous MITF and PMEL in B16F1 wild type cells treated with the indicated dosage of the gamma-secretase inhibitor (DAPT). γ-tubulin and GADPH served as loading control.

4 Discussion

In the present study, I investigated whether PC activities and the activity of specific inhibitors can be quantified at subcellular resolution using the new CLIP versions v3 or v4. My results show that fusion of CLIPv3 or CLIPv4 to different localization signals can enrich these biosensors in specific subcellular compartments, and that FRET imaging of compartment-specific variants of CLIPv4 can quantitatively map endogenous and overexpressed PC activities in the TGN/endosomal system of two unrelated cell lines (HEK293T and in B16F1 mouse melanoma). By contrast, CLIPv3, which elicited no FRET, emerged as a ratiometric biosensor that was useful to quantify PCs at the cell surface, where the citrine moiety can freely diffuse away after shedding. In addition, a Flag tag in CLIPv3 variants allows to estimate their cleavage in different compartment by Western blot analysis. Western blot analysis of CLIPv3 in HEK293T cells and live imaging of CLIPv4 in B16F1 melanoma cells revealed an unexpected enrichment of PC activity in endosomes compared to TGN vesicles in both cell lines. Furthermore, CRISPR editing of Furin and PC7 in B16F1 cells established that PC activity in the TGN/endosomal system was mediated solely by Furin, whereas endogenous PC7 activity was restricted to a distinct exocytic compartment resistant to the pan-PC inhibitor CMK. Thus, by manipulating the localization of one shared Furin/PC7 reporter substrate, our experiments directly demonstrate for the first time that endogenous Furin and PC7 are biologically active in distinct vesicles, and that the localization of substrate (and not only the amino acid sequence of its PC recognition motif) is indeed rate-limiting for its cleavage. These findings will be important to develop future strategies how Furin and PC7 may be targeted pharmacologically to preferentially block the processing of unique or shared substrates, respectively. Furthermore, our preliminary data *in vivo* suggested that Furin and PC7 are implicated in B16F1 graft growth, and that both regulate B16F1 pigmentation *in vivo.*

4.1 CLIPv3 and CLIPv4 as new live imaging tools to image endogenous and overexpressed PC activities

We previously invented an initial version v1 of the PC-specific biosensor CLIP to image endogenous PC activities in transgenic mice at the cell and tissue level (Mesnard and Constam, 2010). CLIPv1 consists of secreted eCFP fused via a PC-cleavable linker (RQRR) to mCitrine that was targeted to the cell surface by a GPI anchor. Previous result established that CLIPv1 can be cleaved by all four of the widespread PC family members Furin, Pace4, PC5 and PC7 *in vivo* and in several mammalian cell lines including mouse ES cells, human

HEK293T and in human HepG2 cells (Bessonnard et al., 2015; Mesnard and Constam, 2010). Imaging of CLIPv1 at the plasma membrane in regions of interest can detect both autocrine and paracrine secreted PC activities (Mesnard et al., 2011). However, CLIPv1 cannot distinguish contributions of PC activities at the plasma membrane from those in intracellular vesicles. Here, compartment-specific variants of CLIPv3 and CLIPv4 provided a detailed spatial map of endogenous PC activities in exocytic and endocytic vesicles. Furthermore, the sensitivity and the specificity of CLIPv3 and CLIPv4 were stringently validated in CRISPR-edited clones and by pharmacological inhibition of endogenous basic amino acid-specific PCs. Since both HEK293T and B16F1 cells express bioactive Furin and PC7, the ratiometric CLIPv3 and FRET-based CVLIPv4 biosensors emerge as new tools to study intracellular proteolytic activities of endogenous Furin and PC7 in live cells and in fixed tissues.

The first biosensors to quantify basic amino acid-specific PC activities monitored the release of alkaline phosphatase from a Golgi-associated sensor into the medium (Coppola et al., 2007), or the internalization of a tagged ligand of processed anthrax protective antigen (Hobson et al., 2006). In addition, PC activity has been detected at the cell-surface by incubating cells with a cell-impermeable FRET biosensor (Gawlik et al., 2010). Our data suggest that these methodologies each detect only a minor fraction of PC activity due to local confinement of the sensors to the Golgi apparatus or at the cell surface, respectively. Other systems were based on caged bioluminescent substrates specifically activated by Furin, and in the presence of firefly luciferase, able to produce bioluminescence emission (Dragulescu-Andrasi et al., 2009), or photoacoustic imaging where specific probes oligomerize after Furin-based cleavage, and generate ultrasonic waves that can be analysed to produce images and to localize Furin activity (Dragulescu-Andrasi et al., 2013). Although these methods were able to detect PC activity both *in vitro* and *in vivo* and can be used to screen general PC inhibitors, none of them provided information on the relative contributions of individual endogenous PCs in the processing of a given substrate. Furthermore, both Hobson's and Gawlik's biosensors contain sequences that are sensitive and selective mostly to the proteolytic activity of Furin (Gawlik et al., 2010; Hobson et al., 2006) and were partially or less sensitive to others redundant PC activities, e.g. PC7 (Remacle et al., 2008).

Our data established as proof-of-principle that ratiometric or FRET imaging of CLIP sensors can measure PC activities *in vitro* and in tissue sections (Bessonnard et al., 2015; Mesnard and Constam, 2010). However, as an alternative method, we propose that future studies should investigate the use of multiphoton imaging techniques for improved analysis of thick tissue sections or *in vivo* imaging of whole organs or tumors. Multiphoton Fluorescence-lifetime imaging microscopy (FLIM)-FRET imaging technique has previously been used to measure

the spatiotemporal regulation of Rac activity in primary cell cultures as well as intact tissues and organs (Johnsson et al., 2014), and to image presynaptic SNARE complexes in hippocampal slice cultures (Takahashi et al., 2015). Although, mCerulean has been widely chosen as a FRET-donor (Rizzo et al., 2004), its use as a FRET donor for FLIM-FRET measurements is limited, since mCeruelan show a biexponential decay (Millington et al., 2007). However, improved mCeruelan variant (mCerulean3) with single exponential decay has been generated by site-directed mutagenesis experiments (Markwardt et al., 2011), therefore it seems reasonable and possible to exchange the donor with an improved version for proper FLIM-FRET measurements.

4.2 The subcellular localization of reporter substrate is rate-limiting for its proteolysis

Our analysis revealed that subcellular localization dramatically influenced the processing of both CLIPv3 and CLIPv4. This was deduced first from our experiments in HEK293T cells, where CLIPv3 processing increased up to 4-fold in endosomal compartments compared to TGN processing. Similar results were obtained by FRET imaging of CLIPv4 both in HEK293T and B16F1 cells. CLIPv4 processing, measured as reduction in FRET efficiency, increased 2- or 4-fold in endosomes compared to exocytic compartments in both cell lines. Since all compartment-specific variants of CLIPv3 and CLIPv4 share the same PC recognition motif, this observation implies that how efficiently a substrate is cleaved might depend also on its trafficking and localization.

Substrate trafficking and localization might also influence PC substrates specificity. However, deciphering substrate specificity is a real challenge due to PC overlapping activities both *in vitro* and *in vivo*. Although multiple PCs may cleave a given substrate *in vitro*, this might not be the case *in vivo* where only one PC might be responsible for substrate maturation. On the other hand, overlapping and redundancy proteolytic activities have been described *in vivo* (Bessonnard et al., 2015; Mesnard and Constam, 2010; Roebroek et al., 2004). Several attempts were made to define, for each PC family member, substrate specificities. Most of these studies describe methods and algorithms that enable to predict Furin or PC cleavage sites (Duckert et al., 2004; Remacle et al., 2008; Tian et al., 2012). Although predictive, these methods ignore the cellular context and the possible physiological factors which may influence PC activities. To cleave a given substrate, it is necessary that the PC and the substrate co-localize in the same compartments of the secretory pathway. In keeping with this concept, several studies have attempted to define subcellular localization of endogenous PC. However, due to their low expression and lack of specific antibodies, localization of endogenous PC results, so far, an arduous challenge. For this reason, PC localization and activity has been

studied by overexpression systems where PC-tagged proteins where overexpressed in a given cell line (Declercq et al., 2012; Molloy et al., 1994; Rousselet et al., 2011a; Teuchert et al., 1999b).

Localization of overexpressed PCs by immunostaining remains technically challenging due to lack of specific antibodies, and it cannot discriminate between inactive and mature active forms. By contrast, in the present study, CLIPv3/v4 imaging enabled us to map and quantify endogenous PC activities in different subcellular compartments. A role for trafficking of substrate in conferring specificity of processing by specific PCs has been suggested by studies investigating processing and activation of the pro-β-secretase (Bace). While redundant overexpressed PCs cleaved wild type Bace, a soluble mutant form of Bace missing the trans-membrane domain was processed only by Furin (Creemers et al., 2001). This result implies that soluble Bace can only reach the Furin compartment, while the wild type is guided by the trans-membrane domain to compartments where other PCs are active. Alternatively, a given substrate or a given PC can be sorted in specific compartments by adaptor proteins. Previous work revealed the role of the glycosylphosphatidylinositol (GPI)-anchored protein Cripto to localize PC-mediated Nodal processing to specific lipid rafts microdomains (Blanchet et al., 2008a, 2008b). Similar to Nodal processing, Cripto has been shown to enhance Notch signaling by facilitating PC-mediated processing of the Notch-1 receptor (Watanabe et al., 2009).

Proteolytic events occur when a bioactive PC encounters a specific substrate. Sorting of PCs is regulated by the interaction with other proteins, GPI-anchor protein like Cripto or heparan sulphate proteoglycans (Blanchet et al., 2008b; Mayer et al., 2008; Nour et al., 2005) or by specific signal sequences in their cytosolic tails (Declercq et al., 2012, 2016; Rousselet et al., 2011a; Teuchert et al., 1999a, 1999b). Our results provide evidence that the PC trafficking and localization are relevant for proper substrate cleavage. While overexpressed PC7 can rescue Activin-A processing resulting in accumulation of the secreted A30 form, the PC7$^{P>A}$ mutant, which accumulated at the plasma membrane of B16F1 expressing cells, barely rescued A30 secretion. Thus, our results suggest that substrate specificity of a given PC depends on its trafficking and sorting even when it is overexpressed, and that Activin-A complete maturation relies on sorting to the TGN, highlighting the importance of substrates trafficking in substrates processing.

To define the relative contributions of individual endogenous PCs to total processing activity in various subcellular compartments, I deleted *Furin* or *PC7* or both in B16F1 cells. I chose B16F1 cells in part because they do not express other known PCs.

Analysis of physiological substrates such as PMEL, E-cadherin, Notch1, ADAM10 and ADAM17 either at endogenous levels or after overexpression indicated that both endogenous Furin and PC7 are active in B16F1 cells. Confirming this conclusion, cleavage of the soluble CLIPv4 reporter substrate in B16F1 cells was mediated by overlapping Furin and PC7 activities. Surprisingly, however, CLIPv3/CLIPv4 imaging detected only Furin and no PC7 activity in the TGN, endosomes and at the plasma membrane. While Furin is the most studied PC and its activity and has been described in several compartments of the secretory pathway (Blanchet et al., 2008b; Chiron et al., 1994; Degnin, 2004; Leonhardt et al., 2011; Logeat et al., 1998; Mesnard and Constam, 2010), PC7 activity and trafficking is poorly defined. Previous studies about the activity and trafficking of PC7 mostly relied on overexpression of PC7 together with various substrates of interest (Declercq et al., 2012, 2016; Endres et al., 2003; Guillemot et al., 2013, 2014; Lopez-Perez et al., 1999; Rousselet et al., 2011a, 2011b; Siegfried et al., 2003). While such studies can provide some useful information, they are not fully informative about endogenous activities and localization. Overexpressed proteins might not recapitulate the trafficking behavior and the activity of the endogenous counterparts. Indeed, our data showed that overexpressed PC7, contrary to the endogenous PC7, can cleave CLIPv4 in TGN, endosomes and plasma membrane. In addition, overexpressed PC7 was able to process substrates that normally are spared by the endogenous counterpart, including ADAM17 and Activin-A. A likely explanation is that overexpressed PC7 leaks into compartments where the endogenous bioactive PC7 might not accumulate in sufficient amounts to be functional. However, the spatial segregation of endogenous Furin and PC7 activities that I observed here by CLIP imaging is consistent with earlier density fractionation studies which indicated that endogenous Furin and PC7 partition to distinct vesicular compartments in alcohol-loaded rat livers (Leonhardt et al., 2010; Wouters et al., 1998).

In summary, CLIP imaging revealed redundant activity of overexpressed but not endogenous Furin and PC7 in B16F1 cells. We hypothesize that Furin and PC7 are active in distinct subcellular compartments and that PC7 acquires the ability to process in Furin compartments only when overexpressed. In addition, some substrates like Notch, ADAM10 or E-cadherin transit both Furin and PC7 compartments, whereas others like ADAM17 or PMEL17 reach only the Furin compartments, and therefore cannot be processed redundantly by both PCs. The difference in substrate cleavage observed between Furin and PC7 in B16F1 cells, might provide explanations on the partially or absent rescue among these PCs *in vivo* (reviewed in Scamuffa et al., 2006). While our PC7 knockout mice show no abnormal phenotype, except for learning and memory defects (Anyetei-Anum et al., 2017; Villeneuve et al., 2002; Wetsel et al., 2013), Furin knockout mice die by embryonic day E10.5 due to ventral closure defects and associated cardia bifida and failure of heart looping (Roebroek et al., 1998). By contrast, $Furin^{-/-};PC7^{-/-}$ double knockout embryos show a delay in morula compaction, and they arrest

development at the implanted blastocyst stage around E4.5 (Bessonnard et al., 2015), suggesting that Furin and PC7 functionally overlap *in vivo* and can partially compensate for each other when only one of them is deleted. The incompleteness of functional redundancy might reflect the intracellular spatial segregation of Furin and PC7 activities. In future studies, CLIPv3/v4 compartments-variants imaging can be used to characterize endogenous PC activities and contribution in embryo development, to disclose where important substrates are processed.

4.3 Furin activity is low in exocytic vesicles of the trans-Golgi network compared to early and late endosomes

Our findings revealed that Furin activities are unevenly distributed both in B16F1 and in HEK293T cells. Specifically, analysis of CLIPv3 processing and PC knock-down experiments revealed that endogenous Furin activities largely accumulate in endosomal compartments in HEK293T cells. In agreement with this result, FRET imaging of CLIPv4 compartment-specific biosensors revealed more PC-mediated cleavage in endosomes compared to exocytic vesicle of the TGN. Furthermore, pharmacological inhibition experiments indicated that the most widely used pan-PC inhibitor inhibits Furin ten times more potently in the TGN than in endosomes. Since Furin localizes at steady state to the TGN (Molloy et al., 1994; Schäfer et al., 1995; Wouters et al., 1998) and cleaves substrates within this compartment (Degnin, 2004; Leonhardt et al., 2011; Logeat et al., 1998; Schäfer et al., 1995; Vischer and Wagner, 1994), we were surprised to detect higher activity in endosomes. Although several studies already demonstrated that Furin is active in several post-TGN compartments such as plasma membrane (Gawlik et al., 2010; Klimpel et al., 1992), endosomes (Chiron et al., 1994; Garred et al., 1995; Tsuneoka et al., 1993), and in membrane microdomains known as lipid rafts (Blanchet et al., 2008a, 2008b; Mesnard and Constam, 2010; Watanabe et al., 2009), our work reveals for the first time important quantitative differences among Furin activities in distinct subcellular compartments of the same cell line.

Previous studies have suggested that processing of Furin substrates, such as plasma gelsolin or the Semliki Forest virus (SFV) glycoprotein precursor p62, are sensitive to endosomal Furin recycling (Band et al., 2001; Chen et al., 2001; reviewed in Thomas, 2002). The maturation of both of gelsolin or viral glycoprotein p62 appeared to occur in compartments generated by the fusion of endocytic Furin-containing vesicles with TGN-derived structures containing the substrates (Band et al., 2001; Chen et al., 2001), indicating that it is endosomal Furin and not TGN-resident counterpart able to cleave and to process such substrates. Which factors contribute to the difference is proteolytic activity among endosomal Furin and TGN-localized counterpart is not clear. Furin activation requires two compartment-specific autoproteolytic

events that are regulated by pH: While the first autocleavage occurs in the Endoplasmic reticulum (ER) (Anderson et al., 2002), a second autocleavage that releases the prodomain to generate bioactive Furin requires transit through mildly acidic TGN/endosomal compartments (Feliciangeli et al., 2006). Therefore, it is plausible that Furin activity increases in endosomes compared to TGN because complete activation is not completely achieved in the TGN environment, and because re-cycling of endosomal bioactive Furin to the TGN may be limited, e.g. by shedding of the Furin trans membrane domain and cytosolic tail, a process that also depends on endosomal acidification (Blanchet et al., 2008b). Trapping the viral glycoprotein p62 in the TGN by inhibition of membrane fusions avoids p62 transit in the endosomes, and its Furin-dependent maturation, suggesting the relevance of endosomal Furin activity (Band et al., 2001). Endosomal sorting also regulate activation of other proteases such as β-secretase (Rajendran et al., 2008). β-secretase is involved in the formation of the neurotoxic amyloid- β-peptide (Vassar, 2002), and is sorted from the cell surface to early endosomes where it acquires activity due to the lower acidic pH (Rajendran et al., 2006). In addition, even mild acidification of the pH can induce conformational changes in substrates (Hanč et al., 2016; Paulino and Kühlbrandt, 2014). Such pH-dependent conformational changes are suggested to occur in the known PC substrate Pseudomonas exotoxin, favouring proper processing (Chiron et al., 1994).

Alternatively, Furin activity in a given compartment may vary depending on the lifetime of this type of vesicle. Since TGN vesicles fuse with the plasma membrane within minutes (Schmoranzer and Simon, 2003), Furin within the TGN only has a limited opportunity to cleave any specific cargo compared to a pool of Furin in endosomes that may persist for hours before its passed on to other locations. In another mutually non-exclusive scenario, proteolytic activity of TGN-resident Furin may be kept at low levels by potential endogenous Furin inhibitors. The Golgi microenviroment has been suggested to provide optimal conditions for the inhibition of Furin by plasminogen activator inhibitor 1 (PAI-1) (Bernot et al., 2011). It is tempting to speculate that PAI-1 binds Furin preferentially in the TGN and that this interaction is lost when Furin reaches endosomal compartments. Further experiments will be needed to validate whether PAI-1 is expressed in B16F1 and HEK293T cells, or whether other proteins can act as Furin inhibitors in a manner reminiscent of PAI-1.

In summary, our findings imply that Furin is most active in late endosomes and this may be due to the slightly more acidic environment encountered in those compartment (reviewed in Faundez and Hartzell, 2004; Machen et al., 2003; Yamashiro and Maxfield, 1987). Accordingly, we hypothesize that endosomal transit and subsequent recycling of Furin to the TGN are key for proper regulation of Furin activity. This conclusion is in agreement with the previously proposed role of recycling in mediating the localization of Furin to the TGN (reviewed in

Thomas, 2002). Accordingly, the TGN might be regarded primarily as a strategic reservoir of inactive Furin molecules that may be sorted to endosomes and re-cycled to the TGN according to the demand for processing to reach specific compartments for proper activation and to mediate specific substrate processing events (Blanchet et al., 2008b; Watanabe et al., 2009).

4.4 Pharmacological targeting of PC in specific compartments

Accumulating evidence has confirmed a role for PCs in specific diseases such such as cancer and infections. Therefore, and because of their enzymatic nature, PCs are considered as attractive drug targets. However, pharmacological inhibition is challenging due to the similar substrate specificities *in vivo* and overlapping activities of several PCs *in vitro*, which severely complicates the task of delineating the physiological and the pathological PC activities. Here, besides providing information on the spatial distribution of individual PC activities, my CLIPv3 analysis and CLIP4 imaging demonstrated that, at a given concentration, the pan-PC inhibitor dec-RVKR-CMK (CMK) can be used to selectively block Furin activity in TGN in both HEK293T and B16F1 cell lines *in vitro*.

In recent years, several studies have reported that PCs also play important roles in different cancer types to regulate tumor progression and invasiveness. Pan-PC specific inhibitors such as the engineered α1-antitrypsin derivative α1-PDX or CMK have been shown to reduce proliferation and migration of cancer cells both *in vitro* and *in vivo*. For example, transgenic expression of α1-PDX in human colon carcinoma cell lines or human primary melanoma cell drastically reduced tumor growth and metastasis formation (Khatib et al., 2001; Lalou et al., 2010; Scamuffa et al., 2008). Similar results were obtained in osteosarcoma and in breast cancer cell lines (Liu et al., 2014a; Willson et al., 2017). Similarly, PC inhibition by CMK treatment affected tumor progression and invasion in several tumor types both *in vitro* and mouse tumor models (Bassi et al., 2010, 2016; Hajdin et al., 2010; Lee et al., 2016; Ma et al., 2014; Nejjari et al., 2004). The impact of PC inhibition on tumorigenesis is explained by the partial or reduced maturation of specific oncogenic PC substrates (reviewed in Artenstein and Opal, 2011; Bassi et al., 2016; Lee et al., 2016; Ma et al., 2014; Scamuffa et al., 2008). In addition, Furin has been shown to elicit essential functions in peripheral tolerance. In particular, Furin inhibition might promote autoimmunity and boost immune response against cancer cells (Pesu et al., 2008).

However, PCs also activate tumor suppressive proteins such as E-cadherin or can regulate the expression of stable and functional major histocompatibility complex-I (MHC-I) (Bessonnard et al., 2015; Leonhardt et al., 2010). Furthermore, some reports suggest protective Furin role against hepatocellular carcinoma, since its overexpression suppresses tumor growth (Huang et al., 2012). In agreement with this report, liver specific inactivation of

Furin leads to increased tumor growth (Declercq et al., 2015). In addition, human intestinal cancer showed systematic down-regulation of PC5, and PC5 inactivation in enterocytes in mouse model for intestinal adenocarcinoma was associated with higher tumor number and premature mortality, suggesting a potential protective role pf PC5 in this context (Sun et al., 2009). The contradictory effects of PC inhibition as anticancer therapy are intriguing. The circumstances that make PCs inhibition an advantageous therapy are poorly investigated and defined. It seems intuitive that depending on which substrates are processed and activated, PCs can mediate oncogenic or tumor suppressive functions. Moreover, alternative proteolytic processing mediated by different PCs might determine the function of the substrate. For example, in human malignant glioma cell lines processing of the N-cadherin precursor (proNCAD) can be mediated by two PCs, Furin and PC5 at two different cleavage sites. Furin-mediated cleavage activates proNCAD enabling the formation of hemophilic interactions between adjacent cells. By contrast, PC5-dependent processing generates nonfunctional NCAD (Maret et al., 2012). Stable intercellular interactions contribute to maintain the tumor cells in the original site. When these interactions are lost, the tumor cells are able to detach and disseminate. In this case, therapies aimed at blocking tumor detachment and dissemination should target only PC5 sparing Furin. Understanding where Furin and PC5 activities are spatially distributed will help us to define the best therapeutic strategy.

Since a given cell might express one or more PCs, inhibitor titration is required to determine for each cell line the optimum inhibitory concentration to block PC activities in compartment-specific fashion. In our experiments, the optimum concentration to block compartment-specific PC activities slightly differed between HEK293T and B16F1 cells. However, in both cell lines, CMK blocked Furin activities more potently in the TGN than in endosomes. Likewise, preliminary results in HEK293T cells revealed that the inhibitor-24 (Inh.24) blocked PC activities more potently in TGN than in endosomes, whereas in B16F1 both TGN and endosomal Furin activities were blocked by the same inhibitor concentration. From our results, we hypothesize that different concentration of the same PC inhibitor can be used to target PC activities in distinct subcellular compartments. The optimum inhibitory concentration has to be calculated depending on the inhibitor and on the cell line. Furthermore, our experiments established proof of concept that inhibitor titration combined with CLIP imaging can shed important light on where the cleavage of a specific substrates occurs. Using this two-pronged approach, I confirmed that PMEL17 is processed by Furin during its route in the secretory pathway, whereas Activin-A processing takes place stepwise in TGN and endosomal compartments. Although preliminary, our results might inspire future therapeutic approaches based on subcellular compartments drug delivery system (reviewed in Rajendran et al., 2010) targeting the compartment enriched by oncogenic PC activities or the compartments where the maturation or activation of oncogenic factor occurs.

4.5 PC7 activity is restricted to specific compartments

The spatial segregation of endogenous PC activities in B16F1 cells suggests that while Furin is able to cleave its substrates in the main subcellular sites of the secretory pathway, PC7 activity localizes in specific compartment(s). Indeed, we have found that in cells devoid of Furin the endogenous PC7, albeit able to cleave endogenous and overexpressed substrates, failed to rescue CLIPv4 processing in TGN, endosomes and at the cell surface. In contrast, overexpressed PC7 can fully compensate for Furin in CLIPv4 processing in all these compartments. Although apparently controversial, our results mirrored the behaviour of both endogenous and overexpressed PC7 described in the literature. Indeed, intracellular endogenous PC7 enriched vesicles are spatially separated from Furin ones (Leonhardt et al., 2010; Wouters et al., 1998). This might explain why PC7 cannot redundantly process Furin substrates, even though PC7 activities have been shown to overlap with Furin in lipid rafts domains *in vivo* (Bessonnard et al., 2015). Similarly to our findings, overexpressed PC7 is sorted and active in TGN-endosomal compartments (Declercq et al., 2012; Rousselet et al., 2011a, 2011b), where it can cleave endogenous substrates spared by the endogenous counterpart, such as ADAM17. Furthermore, the trafficking mutant PC7[P>A] (Declercq et al., 2012) recycled back to the cell surface in B16F1 cells, and cleaved reporter substrates at plasma membrane and in endosomes but not in TGN. These results confirm that PC7 does not follow the conventional ER/TGN secretory route but reaches post-Golgi compartments after recycling from the plasma membrane (Rousselet et al., 2011a). In addition, the difference in localization between overexpressed full-length PC7 and CLIPv4-PC7, indicated that, besides the transmembrane domain and the cytosolic tail, other motif(s) are regulating PC7 trafficking and localization. PCs trafficking is regulated by several factors, including interaction with adaptor proteins or specific PC receptor like Cripto (reviewed in Constam, 2009; reviewed in Seidah and Prat, 2012). The GPI-anchor protein Cripto can recruit both Furin and PC7 through interaction with their P domain, localizing both convertases with the substrate Nodal (Blanchet et al., 2008b). Further experiments are required to understand whether PC7 trafficking is partly or totally regulated by interaction with specific proteins.

How overexpressed PC7 acquired activity in compartments where the endogenous counterpart is not active remains unclear. One possible explanation might be the leaking of overexpressed PC7 in those compartments. Since an antibody specific for PC7 is not commercially available, further experiments are required to elucidate this difference. The idea that endogenous PC7 is segregated in a specific compartment is further corroborated by our pharmacological experiments. While Furin-mediated soluble CLIPv4 processing was blocked by the pan-PC inhibitor CMK in PC7 knock-out cells, in cells devoid of Furin soluble CLIPv4 processing occurred regardless of the presence of the inhibitor. This results supported our

previous data suggesting that PC7 localizes in intracellular CMK-resistant compartments (Bessonnard et al., 2015). Whether PC7 acquires CMK-resistance in this compartment and how PC7 reaches such compartment has to be defined. We propose that one possible way to reveal the PC7 CMK-resistant compartment would be to design CLIP variants that specifically follow the trafficking and route of substrates, like Notch, E-cadherin and ADAM10, that are cleaved by the endogenous PC7.

In summary, CLIPv3/v4 compartments imaging in B16F1 cells, revealed that endogenous PC7 is probably active in a CMK-resistant compartment. Some PC substrates such as Notch-1, ADAM10, E-cadherin might transit into this compartment while others, like Activin-A or ADAM17, follow alternative pathways. Furthermore, since overexpressed PC7 does not recapitulate the endogenous activity, investigating PC7 substrate specificity by overexpression might lead to improper conclusion.

4.6 Furin and PC7 in B16F1 tumor growth and pigmentation

In the present study, we investigated the contribution of Furin and/or PC7 in B16F1 tumor growth. Our preliminary data revealed that tumor volume was reduced only upon Furin deletion. Intriguingly, tumor volume of sgDKO grafted cells was comparable to the control, while expression of the Cas9 alone did not produce any effect in B16-Cas9 tumors. The reduction in tumor volume of sgFurin-1 grafts is consistent with previous reports where inhibition of PC activities reduced progression in xenograft models (Bassi et al., 2016; Hajdin et al., 2010; Jaaks et al., 2016a; Scamuffa et al., 2008). Since sgFurin-1 cell proliferated normally *in vitro*, the reduced proliferation *in vivo* might be attributed to interactions between tumor and the stromal cells. Furin can cleave and activate the immunosuppressive transforming growth factor-β1 (TGF-β1) (Dubois et al., 2001) and Furin deletion might elicit immune response (Pesu et al., 2008), therefore reduction in tumor volume in sgFurin-1 derived tumors would indicate a more effective tumor-specific immune response. However, in syngeneic Rag1+ hosts lacking both T- and B-lymphocytes, the sgFurin-1 derived tumor volume was reduced only 2-fold compared to the 3-fold reduction observed in C57BL/6 mice, suggesting that Furin did not have striking immune suppressive function.

In addition, sgDKO cells proliferated at the same rate as the wild type *in vivo*. This result might be explained by the expression in sgDKO cells *in vivo* of one or more redundant PC family members. On the other side, Furin and PC7 might antagonize each other cleaving substrates with opposite functions *in vivo*. In keeping with this concept, it is intuitive to hypothesize that treatment with pan-PC inhibitors will not be convenient, whereas targeting only Furin activities might result as more effective therapeutic approach. Finally, it's interesting to note that tumor growth was uncoupled from pigmentation in both C57BL/6 and Rag1+ hosts, suggesting that

amelanotic tumor retains proliferative signature. However, in order to exclude technical artefact arising from clonal effect, further experiments with more CRISPR-edited clones are needed.

Furthermore, sgFurin-1, sgPC7-1 and sgDKO tumors were amelanotic compared to the highly pigmented B16-Cas9 and control tumors. Loss of pigmentation is one feature of tumor dedifferentiation in melanoma (Bennett, 1983), and cancer dedifferentiation has been proposed to play an important role in tumor progression and invasion (reviewed in Friedmann-Morvinski and Verma, 2014; Gabbert et al., 1985).

Many genes are involved in pigmentation and differentiation in both melanocytes and melanoma (Liu et al., 2014b). Some of these melanocyte-lineage specific genes encode for proteins implicated in melanosomes biogenesis, such as PMEL17. Since accumulation of unprocessed PMEL17 disrupts melanosome morphology and alters its maturation (Berson et al., 2003), we showed that sgFurin-1 cells failed to mature the melanocyte-specific protein PMEL17. Doxycycline-inducible FurinGFP rescued both PMEL17 processing and media pigmentation *in vitro*, whereas in preliminary *in vivo* experiments did not efficiently rescue tumor growth. Further observations are needed to explain the discrepancy between the *in vitro* and the *in vivo* results of the doxycycline-inducible FurinGFP activity.

Other important genes involved both in melanoma progression and in pigmentation belong to the Notch signalling pathway (Hoek et al., 2004; Kumano et al., 2008). To our surprise all the CRISPR-edited clones, except for sgFurin-2 cells, lost *Notch-1* mRNA expression. Whether this loss is due to the heterogeneity of Notch expression in B16F1 cells or is a Cas9 clonal effect we are not able to confirm. However, both pigmentation and cell proliferation were not affected by loss of Notch-1 in B16-Cas9 *in vivo*, suggesting that other genes might be involved in proper tumor progression and cells differentiation. Intriguingly, both treatment with the γ-secretase DAPT at lower concentration and loss of Notch-1 in CRISPR-edited clones resulted in increased protein level of the microphthalmia-associated transcription factor (MITF). By activation of many genes, MITF is involved in several regulatory pathways in melanocytes and in melanoma (Giuliano et al., 2010; Hoek et al., 2008b; Widmer et al., 2012). Due to its function in driving melanoma progression, MITF has been described as an oncogene (Garraway et al., 2005), although other reports have shown its tumor suppressor activity (Cheli et al., 2012; Levy et al., 2010; Pinner et al., 2009; Thurber et al., 2011). Furthermore, several reports proposed that tumor with low levels of MITF are more invasive, while tumor expressing higher level of MITF are more proliferative (Carreira et al., 2006; Goodall et al., 2008; Hoek et al., 2008a). In keeping with this classification, we propose that proliferation rate of sgPC7-1 and sgDKO cells *in vivo* might be explained by an increased expression of MITF as detected *in vitro*.

We have demonstrated that Furin is active in exocytic and endocytic compartments of B16F1 cells *in vitro*, we cannot exclude compensatory upregulation of redundant PC family member or contribution of stromal-derived PC in substrates processing. Ratiometric analysis of CLIPv3-TGN in tumor sections, revealed no CLIPv3 cleavage in sgFurin-1 tumors. Then, our findings suggested that in some tumor areas Furin is the only active PC detected in the TGN of B16F1 cells *in vivo* and that no other endogenously expressed or host-derived PCs can cleave substrates in the TGN. Further observations are needed to investigate potential rescue mechanisms of PC activities in other compartments *in vivo*, for example in endosomes. Furthermore, CLIP imaging might serve as a tool to reveal changes in both distribution and localization of endogenous PC activities *in vivo* due to extrinsic factors, such as hypoxia. Hypoxia is essential for melanocyte differentiation and melanoma progression (Bedogni et al., 2005). It has been shown that increased Notch-1 and reduced MITF levels enhanced metastatic potential of melanoma cells (Bedogni et al., 2008; Cheli et al., 2012). In a recent report, upon subcutaneous or tail-vein injections, B16F10 cells pre-cultured in hypoxic conditions produced bigger tumors and formed more lung metastasis compared to cells pre-cultured in normoxic conditions (Cheli et al., 2012). Furthermore, hypoxia induced expression of Furin (McMahon et al., 2005) and relocated overexpressed Furin from TGN to endosomes, enhancing cancer cell invasion *in vitro* (Arsenault et al., 2012). Whether cancer cells optimize processing of oncogenic substrates in endosomes and whether this happens *in vivo* has to be further examined.

4.7 Conclusion and outlook

PC trafficking and localization likely regulate whether and where potential substrates are cleaved during or after exocytosis, but tools to directly test this hypothesis have been lacking. Here, I found that the novel PC specific biosensors CLIPv3 and CLIPv4 and their variants carrying different compartment-specific localization signals can for the first time quantitatively map endogenous and overexpressed PC activities in the TGN/endosomal system of two unrelated cell lines (HEK293T and in B16F1 mouse melanoma). Live imaging in CRISPR edited clones revealed that endogenous Furin and PC7 are biologically active in distinct vesicles. While Furin activity is enriched in endosomes compared to exocytic vesicles, PC7 activity was confined to a distinct compartment resistant to the pan-PC inhibitor CMK.

Determining which PC is responsible for a given cleavage in a specific subcellular compartment would be informative for better comprehension of PC functions and to improve rational drug design. Furthermore, to better understand PC contribution in both physiological and pathological processes, it is essential to define where in the cell a specific substrate is cleaved. In this study, inhibitor titration in combination with CLIPv4 imaging emerged as new

criteria to define where a given substrate is processed. Applying these approaches in different cell lines and tissues might improve our understanding of PC biology and the design of selective inhibitor that might preferentially block the processing of specific substrates.

PC inhibition has been shown to reduce proliferation and invasive potential of different cancer cell lines both *in vitro* and *in vivo*. However, the contribution of each PC family member in tumorigenesis is poorly defined. Here, I investigated Furin and PC7 roles in progression of B16F1 mouse tumor model *in vivo*. While both PCs were important for proper tumor pigmentation, tumor growth resulted impaired only in tumor devoid of Furin, whereas both Furin and PC7 deletion had not effect. This data suggest that, to block cancer cell proliferation, it is necessary to preferentially block only a specific subset of PC activities, while therapies unable to discriminate individual PC might not result effective.

5 Materials and Methods

5.1 Cell lines

HEK293T cells and B16F1 melanoma cells (ATCC) were maintained in Dulbecco's modified Eagle's medium (Sigma) supplemented with 10% fetal bovine serum, 1% gentamicin and 1% GlutaMAX (GIBCO Invitrogen). HEK293T cells stably transduced with lentiviral CLIPv3 reporter were maintained in the same medium supplemented with Puromycin (2 µg/ml) (GIBCO Invitrogen). Where indicated, decanoyl-RVKR-CMK (Enzo life sciences) was added at the indicated concentrations and replaced every 12 hrs. IC50 values were calculated using Prism (Graph-Pad Software) Where indicated, Inhibitor 24 (Calbiochem 537076) or the, γ-secretase inhibitor N-[N-(3,5-Difluorophenacetyl)-L-alanyl]-S-phenylglycine t-butyl ester (DAPT) was addede at the indicated concentration. Where indicated cells were incubated with 250ng/ml doxycycline.

5.2 Cell transfection and Western blot analysis

HEK293T cells were seeded in 6-well plates at a density of 6×10^5 cells/well and transfected the next day with a 2:1 mixture of JetPei and CLIPv4 or empty vectors (2 µg) (Polyplus). After 4 hrs, conditioned media were replaced with fresh complete media. For transient transfection, B16F1 were seeded in 6-well plates at a density of 6×10^5 cells/well. The next day, cells were incubated with plasmid (2 µg/well) in Lipofectamine 2000 (invitrogen) during 4-6 hrs in OptiMEM medium (Invitrogen). Thereafter the medium was replaced with fresh complete medium. For both cell lines r 24 hrs post transfection, proteins were extracted in lysis buffer (PBS supplemented with 0.5% (vol/vol) Triton X-100, 1 mM EDTA and protease inhibitor cocktail (Roche). Proteins in conditioned media were precipitated with cold acetone and resuspended in lysis buffer. Proteins were separated in on SDS-PAGE gel under reducing and non-reducing conditions. CLIP and E-cadherin expression and processing were monitored by chemiluminescent immunoblotting using monoclonal anti-GFP antibody (Sigma-Aldrich) or mouse anti-Flag M2 (Sigma-Aldrich) and HRP-conjugated anti-mouse secondary antibodies (GE Healthcare). Expression of endogenous proteins was visualized using rabbit anti-Furin (Abcam 3467), mouse anti-γ-tubulin (Sigma-Aldrich), rabbit anti-ADAM10 (Abcam 1997), rabbit anti-ADAM17 (Abcam 2051), rabbit anti-PMEL17 (Abcam 137078), mouse anti-MITF (C5; MA5-14146 Thermo Fisher), rabbit anti-GADPH (Abcam 70699), goat anti-Notch1 (C-20:sc-6014) and mouse anti-Activin-A (Abcam 89307) respectively. HRP-conjugated secondary anti-mouse, anti-rabbit (GE Healthcare) or anti-goat (Santa Cruz Biotechnology)

were used. Expression of overexpressed PCs (wild-type Furin, wild-type PC7 and PC7[P>A] mutant) was monitored using mouse anti-Flag M2 (Sigma-Aldrich) and HRP-conjugated anti-mouse secondary antibody (GE Healthcare).

5.3 Expression vectors and cloning

CLIP and mCLIP expression vectors were generated in pcDNA3.1 (Invitrogen). In brief, cDNA fragments comprising the signal sequence of lactase-phlorizin hydrolyse, mCitrine, a linker region, mTFP1 or mCeruelan were amplified by PCR and ligated in frame to a Flag epitope and the GPI attachment signal sequence of lymphocyte function-associated antigen 3 (Keller et al., 2001). Alternatively, to retain biosensors in the endoplasmatic reticulum, their C-terminus was fused to a KDEL tetrapeptide (Lewis and Pelham, 1990). To enrich biosensors in the TGN or endosomes, they were fused to the trans-membrane domain and cytosolic tail of TGOLN2 (Ladinsky and Howell, 1993; Luzio et al., 1990), TFRC (Van Dam et al., 2002; Harding et al., 1983; Schlierf et al., 2000), CD-M6PR (Duncan and Kornfeld, 1988; Ghosh et al., 2003), or its endocytosis-deficient mutant derivative CD-M6PR(6Ala) (Ghosh et al., 2003; Stockli, 2004). Localization signals in the TM domain and cytosolic tail of mouse PC7 were fused to the biosensors using the PCR primers: 5'- GAGAGCGGCCGCTCTTGTGCTGGTAGGCTGCTTC-3 and 5'-GAGATCTAGATCAGCAAATCTGCCCGCTC-3. To estimate maximal FRET, the Acceptor-linker-Donor sequence in CLIPv4 and in corresponding control constructs was replaced by monomeric forms of Citrine, Cerulean or TFP1. Linkers comprising the PC consensus cleavage site RQRR or the cleavage-resistant control sequence SQAG were described previously (Mesnard and Constam, 2010).

Expression vectors of of full-length mouse PCs containing CMV or EF1α promoters were described previously (Mesnard and Constam, 2010). To generate mutant PC7[P>A] construct, residues Pro[724], Leu[725] and Cys[726] in the cytosolic tail were replaced by alanine using overlap extension PCR with the following primers:

5'-GAGACTCGAGGTCGACCACCATGCCG-3',

5'- TTGCTGCTGGCCGCTGCCATTGATTCTAGTGCTGTCC-3',

5'- AATCAATGGCAGCGGCCAGCAGCAAGGACCTGGATGG-3' and

5'- GAGATCTAGAACTAGTGGATCCCCC-3'.

Plasmid encoding mouse Ecadherin fused to the N-terminus of GFP was a gift from Marc Stemmler (Max Planc Inst. Freiburg).

To generate mutant Ecadherin-GFP, RQKR PC recognition site was replaced by the PC resistant sequence SQAG using overlap extension PCR with the following primers:

5'-TCTAAAGCTCCACAAGCTGGA-3',

5'-CCAGCGTGTACCCAGGTCTCAGAAGCCAGGCCGGCGACTGGGTCATCCCTCCC-3',

5'-ATGGGAGGGATGACCCAGTCGCCGGCCTGGCTTCTGAGACCTGGGTACACGCTG-3'

 and 5'-CTTCTCCACCTCCTTCTTCAT-3'.

Plasmid encoding murine Notch1 cDNA (gift from Jeffrey S. Nye) has been described (Artavanis-Tsakonas and Simpson, 1991).Plasmid encoding for INHβA cDNA has been previously described (Donovan et al., 2017). For CRISPR/Cas9 editing, we used Addgene plasmid # 48138 containing pSpCas9(BB)-2A-GFP (PX458).

CLIPv3-TGN lentivector was generated by cloning CLIPv3-TGN as an NheI-XbaI fragment into Nhe-I-XbaI site of the pLenti hEF1α-MCS//SV40-PuroR (pCF519). To generate CLIPv3-M6PR lentivector, sequence encoding mTFP1and the trans-membrane domain and cytosolic tail of M6PR were cloned into ClaI-XbaI of pLenti hEF1α-CLIPv3-TGN//SV40-PuroR. Similarly, to generate CLIPv3-M6(6Ala) sequence encoding mTFP1and the mutated trans-membrane domain and cytosolic tail of M6PR were cloned into ClaI-XbaI of pLenti hEF1α-CLIPv3-TGN//SV40-PuroR. Similar strategy was adapted to generate CLIPv3-KDEL lentivector, where mTFP1 and the terminal KDEL tetrapeptide were cloned into ClaI-XbaI of pLenti hEF1α-CLIPv3-TGN//SV40-PuroR. pCF519 has been previously described (Fuerer et al., 2010, 2014).

To generate the lentiviral vector pLV-TRE- FurinGFP-hPGK-tTA2-M2, FurinGFP (Mesnard et al., 2011) was amplified using the following primers:

5'- GAGAGCTAGCCACCATGGAGCTGAGATCCTGGTT-3' and

5'- GAGAAATCGATTTCAAAGGGCGCTCTGGTCTT-3'.

The amplicon was cloned into NheI-ClaI sites of pLV-TRE-hPGK- tTA2-M2. The lentivector pLV-TRE-hPGK- tTA2-M2 was originated by excision of mSEAP insert from TMPrTA2 vector (gift from Isabelle Barde) and has been described (Barde et al., 2006).

5.4 Lentiviral transduction

Lentiviruses were produced by transient transfection of HEK293T with 5:3.25:1.75 mixture of lentivirus:packaging envelope vectors, CMVΔR8.74 (Addgene 22036) and pMD2.VSVg (Addgene 12259) (Fuerer et al., 2014). Cell supernatants were sterile-filtered (0.45 µm) and used directly or after 50'000 x g ultracentrifugation and resuspension with 0.1% bovine serum

albumin in PBS to transduce HEK293T cells. Cells stably expressing CLIPv3 variants were selected in 2 µg/ml puromycin (GIBCO) starting 2 days after transduction. B16F1 stably expressing inducible FuriGFP were FACS-sorted for GFP expression.

5.5 Gene expression analysis

Total mRNA was isolated using TRIzol, reverse transcribed using Superscript III (Invitrogen), and analyzed using SYBR green PCR Master Mix (Applied Biosyszem) coupled with 7900ht Fast RT_PCR system (Applied Biosystems). Human and mouse qRT-PCR primers for prorpotein convertase and Notch receptor were previously described (Bessonnard et al., 2015; Briot et al., 2014) and listed in table 2. For RT-PCR, the program was 95°C for 2 min; 30 cycles of 95°C for 1 min, 62°C for 2 min, 72°C for 2 min; and 72°C for 3 min. From 50µl PCR reaction, 25 µl were resolved on 1%agarose gel. Specific siRNAs against PCs (Scamuffa et al., 2008) were purchased from Ambion and transfected using Lipofectamine RNAiMAx. Sequences of siRNA are listed in table 3.

5.6 CRISPR/Cas9 editing

The designed guide RNA sequences 5'-TGCGACCACCCATAGCAACC-3' or 5'-GGTGGAGGCCATGCGGCAAC-3' targeting murine *Furin* or *PC7*, respectively, near their start codon were cloned into the expression vector PX458 containing GFP-tagged Cas9 (Ran et al., 2013). The resulting sgRNA/Cas9 expression vector were transfected in B16F1 cells. After 24h, the cells were trypsinized, washed with PBS and resuspended in PBS/1% FBS for single cell sorting for GFP by FACS into 96-well plate containing complete medium. Clonal cell lines were expanded and screened by anti-Furin by Western blot. To characterize the mutations, genomic DNA was purified using QuickExtract™ DNA Extraction Solution (Epicentre), and the region surrounding the protospacer adjacent motif (PAM) was amplified using PfuUltra II Fusion HS DNA polymerase (Agilent) using the primers:

Furin forward: 5'-TTTTAGGCTCAGCCGTGAGG-3'

Furin reverse: 5'-GTTACGGATCCCATCCCACC-3'

PC7 forward: 5'- ACAGACCCTGGTTCCTGTCTGA-3'

PC7 reverse: 5'- CTCTTCAGCAGCGTTTGCTC-3'

PCR products were purified using NucleoSpin® Gel and PCR Clean-up kits (Macherey-Nagel) and cloned into pCR™4-TOPO® TA vector for sequencing. For each cell line, at least 12-15 bacterial colonies were expanded to sequence their plasmid DNA.

5.7 Ratiometric imaging and FRET analysis

For live-cell imaging, transfected cells on coverslips in 3.5 cm dishes were transferred in buffered OptiMEM medium while the temperature was maintained at 37°C throughout the imaging process. Single cells images were acquired using a W N-Achromat 63x/0.9 objective on a confocal microscope (Zeiss LSM 710) at the following settings: Cerulean (or TFP1) channel, 458-nm excitation and 458-510-nm (463-514-nm) emission; FRET channel 458-nm excitation and 530-600-nm emission; and Citrine channel at 514-nm excitation and 530-600-nm emission. NFRET efficiency was calculated as described (Xia and Liu, 2001) by normalizing the corrected FRET signal to the square root of the product between Cerulean and Citrine intensities. Owing to this normalization, NFRET is independent of local fluorophore concentration and potential FRET between cell-linked Cerulean and soluble Citrine trapped in vesicles was accounted for. Correction factors accounting for spectral bleed through were determined independently on cells transfected with Cerulean or Citrine alone. Images of 5 to 15 reporter cells per condition were analyzed using ImageJ PixFRET plug-in to quantify NFRET in all regions defined by a mask of significant Cerulean signal above an arbitrary threshold (Feige et al., 2005). Each dot of the scatter plots represents the entire cytoplasmic region of one cell. For ratiometric analysis, the mean of TFP1 and Citrine background fluorescence were measured in untransfected cells. For each CLIPv3 expressing cell a mask was generated using the mTFP1 channel and overlaid with the channels of interest (mTFP1 and Citrine). Mean fluorescent intensities, after background subtraction, were measured and Citrine values were divided with the corresponding TFP1 values to obtain individual Citrine/TFP1 ratios.

5.8 Immunofluorescent staining

Transfected cells on coversplis were fixed with 4% paraformaldehyde for 12 min, permeabilized with cold methanol at -20°C for 2 min or with 0.5% Triton X-100 in PBS1X, and blocked with 10% FBS or 3% BSA in PBS 1X for 1 h. Primary antibodies were incubated overnight at 4°C. Antibodies included anti-Calnexin (Abcam 22595), anti-Mannosidase II (Abcam 24565), anti-TGN46 (abcam 2809), anti-M6PR (Abcam 2733) anti-EEA1 (Abcam 2900) and anti-Flag M2 (Sigma-Aldrich). After washing three times with PBS containing 10% FBS, coverslips were incubated with secondary antibodies coupled to Alexa-647 (Jackson ImmunoResearch Laboratories, Inc.) and DAPI at room temperature for 1 h. rinsed 3 times and mounted in DABCO mounting medium for confocal microscopy analysis (Zeiss LSM 710). Images were prepared using ImageJ software.

5.9 Antibody uptake experiments

Transfected B16F1 cells were washed and incubated with serum-free DMEM medium containing 1µg/ml anti-Flag M2 (Sigma-Aldrich) for 30 minutes at 4°C followed by 15 minutes at 37°C. After incubation with the antibody, the cells were washed with ice-cold PBS and fixed with 4% paraformaldehyde for 12 min. Double labelling method, as previously described (Declercq et al., 2012), was performed to discriminate between plasma membrane and internalized overexpressed Flag-tagged proteins. The cells were incubated 1 hour at room temperature with secondary anti-mouse coupled to Alexa-488 (Jackson ImmunoResearch Laboratories, Inc.) in PBS containing 10%FBS. Then, the cells were washed three times with PBS and incubated with secondary anti-mouse coupled to Alexa-647 (Jackson ImmunoResearch Laboratories, Inc.) and DAPI for 1 hour at room temperature in PBS containing 10%FBS and 0.2% Triton X-100. Finally, coversplis were washed three times and mounted in DABCO mounting medium for confocal microscopy analysis (Zeiss LSM 710). Images were prepared using ImageJ software. Using this two-step method, surface localized Flag-M2 was labelled with Alexa-488, while internalized Flag-M2 was labelled with Alexa-647.

5.10 Cell viability

5X103 cell were seeded in 96-well plates and cultured for 3 days. AlamarBlue® (Invitrogen, DAL1025) was added to wells 4 hours before fluorescent measurements at excitation wave length of 560 and 590nm, respectively.

5.11 Melanoma grafts

$1X10^6$ or $4X10^5$ B16F1 cells were injected intradermally into the right flank of 8-12 weeks old female wild-type (Harlan) or Rag1$^{-/-}$ C57BL/6 (EPFL animal core facility) syngenic hosts. Animal body weights and tumor sizes were measured every two days. Tumor volumes were calculated using the formula *length x width x depth* (Feldman and Goldwasser, 2009). Where indicated, animals were fed with chow containing 0.625g/Kg doxycycline (Provimi Kliba AG, Switzerland). All procedures were according with Swiss legislation and approved by the cantonal veterinary administration.

5.12 Whole mount staining

Tumors were fixed with 4%PFA overnight and cryoprotected with 20-30% sucrose in PBS and embedded in OCT. Free-floating thick cryosections (120µm) were rinsed in PBS for 10

minutes, followed by DAPI staining. Images were acquired using confocal microscope (Zeiss LSM 710) and processed using ImageJ software.

5.13 Statistical analysis

Statistical tests were performed using Prism (Graph-Pad Software). Unless indicated otherwise, data represent means±SD of at least 3 independent experiments. One-way ANOVA test was used to compare groups of unpaired values and when significant differences were observed, individual means were compared by unpaired Student's *t* test. The normal distribution of Citrine/TFP1 ratios and of normalized NFRET values were verified with the Shapiro-Wilk normality test, and the results were analyzed by Mann-Whitney or by a Student's *t* test depending on previous results. A p-values <0.05 was considered significant.

Table 2 Primers used for RT-PCRs and qRT-PCRs

Gene	Sequence (5'-3')
mouse Notch1	CCCTTGCTCTGCCTAACGC GGAGTCCTGGCATCGTTGG
mouse Notch2	GGAATGGTGGCAGAGTTGAT TCGCCTCCACATTATTGACA
mouse Notch3	GGACAAGATGCACTGGGAAT AGTCTCTTGGCCTCTGGACA
mouse Notch4	TTCTCGTCCTCCAGCTCATT CCACTCCATCCTCATCCACT
mouse Furin	TCC CCAGGATCTGGCCCTTA CGACCACCCATAGCAACCAG
mouse PC7	CGAGAGTTTCCGTAGGGTGG CATCAGAACAGCAGGCTGGG
mouse PACE4	CGGAAGATCGTCACCACAGA TTTATGCCCAGCTCCGTTGA
mouse PC5	CCCGTAACAAGGGTCTTGGA TCCCTTGGCAGGATAATGGC
mouse PC1	TGATGATCGTGTGACGTGGG CACTCCAAGCCATCATCCAGT
mouse PC2	ACAGCCCCACTTTTCACTCC CAAAGGGGAGCTTTCGGACT
mouse PC4	ACCCTGGGCCTGGAGAATAA GAGGGGACTGTGACTTTCCTG
mouse GADPH	ACTGAGGACCAGGTTGTCTCC GTTGGGATAGGGCCTCTCTTGC
human FURIN	GATGGTGAAGGTCGGCACTC TTGCTGCTACCACCCATAGC
human PC7	GGGGCACTACCTCTTTGTCC TCCGTCGGTTATTCAGGTGC
human PACE4	TGAGCCAGGCACCTACTTTG CTCGTCACACCTTCGACACA
human PC5	TCTCTTAGGTGGCAGTTGTGT TCATTCCAGAATTTGCCCTCC
Human GADPH	GTG CGAGGAGATCGCCATTA- GACTGCCGAAGTCCAAAAGC

Table 3. siRNA sequences used for Knockdown of human target genes

siRNA	Sequence (5'-3')
siFurin (sense)	CAGCUGCGCUCUGGCUUUAUU
siFurin (antisense)	UAAAGCCAGAGCGCAGCUGUU
siPC7 (sense)	CUACGUCAGUCCCGUGUUAUU
siPC7 (antisense)	UAACACGGGACUGACGUAGUU
siscramble	D-001810-01-20

References

Abrami, L., Fivaz, M., Decroly, E., Seidah, N.G., Jean, F., Thomas, G., Leppla, S.H., Buckley, J.T., and Van Der Goot, F.G. (1998). The pore-forming toxin proaerolysin is activated by furin. J. Biol. Chem. *273*, 32656–32661.

Albino, A.P., Nanus, D.M., Mentle, I.R., Cordon-Cardo, C., McNutt, N.S., Bressler, J., and Andreeff, M. (1989). Analysis of ras oncogenes in malignant melanoma and precursor lesions: correlation of point mutations with differentiation phenotype. Oncogene *4*, 1363–1374.

Amersi, F.F., Terando, A.M., Goto, Y., Scolyer, R.A., Thompson, J.F., Tran, A.N., Faries, M.B., Morton, D.L., and Hoon, D.S.B. (2008). Activation of CCR9/CCL25 in cutaneous melanoma mediates preferential metastasis to the small intestine. Clin. Cancer Res. *14*, 638–645.

Anders, A., Gilbert, S., Garten, W., Postina, R., and Fahrenholz, F. (2001). Regulation of the α-secretase ADAM10 by its prodomain and proprotein convertases. FASEB J. *15*, 1837–1839.

Anderson, E.D., Molloy, S.S., Jean, F., Fei, H., Shimamura, S., and Thomas, G. (2002). The ordered and compartment-specific autoproteolytic removal of the furin intramolecular chaperone is required for enzyme activation. J. Biol. Chem. *277*, 12879–12890.

Andrae, J., Gallini, R., and Betsholtz, C. (2008). Role of platelet-derived growth factors in physiology and medicine. Genes Dev. *22*, 1276–1312.

Antenos, M., Zhu, J., Jetly, N.M., and Woodruff, T.K. (2008). An activin/furin regulatory loop modulates the processing and secretion of inhibin α- and βB-subunit dimers in pituitary gonadotrope cells. J. Biol. Chem. *283*, 33059–33068.

Anyetei-Anum, E.N., Blum, A., Seidah, N.G., and Beinfeld, M.C. (2017). Prohormone convertase 7 is necessary for the normal processing of cholecystokinin in mouse brain. Biochem. Biophys. Res. Commun. *482*, 1190–1193.

Arsenault, D., Lucien, F., and Dubois, C.M. (2012). Hypoxia enhances cancer cell invasion through relocalization of the proprotein convertase furin from the trans-golgi network to the cell surface. J. Cell. Physiol. *227*, 789–800.

Artavanis-Tsakonas, S. (1999). Notch Signaling: Cell Fate Control and Signal Integration in Development. Science (80-.). *284*, 770–776.

Artavanis-Tsakonas, S., and Simpson, P. (1991). Choosing a cell fate: a view from the Notch locus. Trends Genet. *7*, 403–408.

Artenstein, A.W., and Opal, S.M. (2011). Proprotein Convertases in Health and Disease. N.

Engl. J. Med. *365*, 2507–2518.

Bakalian, S., Marshall, J.-C., Logan, P., Faingold, D., Maloney, S., Di Cesare, S., Martins, C., Fernandes, B.F., and Burnier, M.N. (2008). Molecular pathways mediating liver metastasis in patients with uveal melanoma. Clin. Cancer Res. *14*, 951–956.

Balint, K., Xiao, M., Pinnix, C.C., Soma, A., Veres, I., Juhasz, I., Brown, E.J., Capobianco, A.J., Herlyn, M., and Liu, Z.J. (2005). Activation of Notch1 signaling is required for β-catenin-mediated human primary melanoma progression. J. Clin. Invest. *115*, 3166–3176.

Baluk, P., Hashizume, H., and M, D.M. (2005). Cellular abnormalities of blood vessels as targets in cancer. Curr. Opin. Genet. Dev. *15*, 102–111.

Band, A.M., Määttä, J., Kääriäinen, L., and Kuismanen, E. (2001). Inhibition of the membrane fusion machinery prevents exit from the TGN and proteolytic processing by furin. FEBS Lett. *505*, 118–124.

Barde, I., Zanta-Boussif, M.A., Paisant, S., Leboeuf, M., Rameau, P., Delenda, C., and Danos, O. (2006). Efficient control of gene expression in the hematopoietic system using a single Tet-on inducible lentiviral vector. Mol. Ther. *13*, 382–390.

Barr, V., Phillips, S., Taylor, S., and Haft, C. (2000). Overexpression of a novel sorting nexin, SNX15, affects endosome morphology and protein trafficking. Traffic *1*, 904–916.

Basak, a, Touré, B.B., Lazure, C., Mbikay, M., Chrétien, M., and Seidah, N.G. (1999). Enzymic characterization in vitro of recombinant proprotein convertase PC4. Biochem. J. *343 Pt 1*, 29–37.

Bassi, D.E., Mahloogi, H., Al-Saleem, L., De Cicco, R.L., Ridge, J.A., and Klein-Szanto, A.J.P. (2001a). Elevated furin expression in aggressive human head and neck tumors and tumor cell lines. Mol. Carcinog. *31*, 224–232.

Bassi, D.E., Lopez De Cicco, R., Mahloogi, H., Zucker, S., Thomas, G., and Klein-Szanto, A.J. (2001b). Furin inhibition results in absent or decreased invasiveness and tumorigenicity of human cancer cells. Proc. Natl. Acad. Sci. U. S. A. *98*, 10326–10331.

Bassi, D.E., Mahloogi, H., Lopez De Cicco, R., and Klein-Szanto, A. (2003). Increased Furin Activity Enhances the Malignant Phenotype of Human Head and Neck Cancer Cells. Am. J. Pathol. *162*, 439–447.

Bassi, D.E., Fu, J., De Cicco, R.L., and Klein-Szanto, A.J.P. (2005). Proprotein convertases: "Master switches" in the regulation of tumor growth and progression. Mol. Carcinog. *44*, 151–161.

Bassi, D.E., Zhang, J., Cenna, J., Litwin, S., Cukierman, E., and Klein-Szanto, A.J.P. (2010). Proprotein convertase inhibition results in decreased skin cell proliferation, tumorigenesis, and

metastasis. Neoplasia *12*, 516–526.

Bassi, D.E., Cenna, J., Zhang, J., Cukierman, E., and Klein-Szanto, A.J. (2015). Enhanced aggressiveness of benzopyrene-induced squamous carcinomas in transgenic mice overexpressing the proprotein convertase PACE4 (PCSK6). Mol. Carcinog. *54*, 1122–1131.

Bassi, D.E., Zhang, J., Renner, C., and Klein-Szanto, A.J. (2016). Targeting proprotein convertases in furin-rich lung cancer cells results in decreased in vitro and in vivo growth. Mol. Carcinog. *56*, 1182–1188.

Bastian, B.C. (2014). The Molecular Pathology of Melanoma: An Integrated Taxonomy of Melanocytic Neoplasia. Annu. Rev. Pathol. Mech. Dis. *9*, 239–271.

Baxter, L.L., and Pavan, W.J. (2003). Pmel17 expression is Mitf-dependent and reveals cranial melanoblast migration during murine development. Gene Expr. Patterns *3*, 703–707.

Becker, G.L., Lu, Y., Hardes, K., Strehlow, B., Levesque, C., Lindberg, I., Sandvig, K., Bakowsky, U., Day, R., Garten, W., et al. (2012). Highly potent inhibitors of proprotein convertase furin as potential drugs for treatment of infectious diseases. J. Biol. Chem. *287*, 21992–22003.

Bedogni, B., Welford, S.M., Cassarino, D.S., Nickoloff, B.J., Giaccia, A.J., and Powell, M.B. (2005). The hypoxic microenvironment of the skin contributes to Akt-mediated melanocyte transformation. Cancer Cell *8*, 443–454.

Bedogni, B., Warneke, J.A., Nickoloff, B.J., Giaccia, A.J., and Powell, M.B. (2008). Notch1 is an effector of Akt and hypoxia in melanoma development. J. Clin. Invest. *118*, 3660–3670.

Béjar, J., Hong, Y., and Schartl, M. (2003). Mitf expression is sufficient to direct differentiation of medaka blastula derived stem cells to melanocytes. Development *130*, 6545–6553.

Bell, R.E., and Levy, C. (2011). The three M's: Melanoma, microphthalmia-associated transcription factor and microRNA. Pigment Cell Melanoma Res. *24*, 1088–1106.

Bemis, L.T., Chen, R., Amato, C.M., Classen, E.H., Robinson, S.E., Coffey, D.G., Erickson, P.F., Shellman, Y.G., and Robinson, W.A. (2008). MicroRNA-137 targets microphthalmia-associated transcription factor in melanoma cell lines. Cancer Res. *68*, 1362–1368.

Benjannet, S., Rondeau, N., Paquet, L., Boudreault, A., Lazure, C., Chrétien, M., and Seidah, N.G. (1993). Comparative biosynthesis, covalent post-translational modifications and efficiency of prosegment cleavage of the prohormone convertases PC1 and PC2: glycosylation, sulphation and identification of the intracellular site of prosegment cleavage of PC1 and P. Biochem. J. *294 (Pt 3*, 735–743.

Benjannet, S., Savaria, D., Laslop, A., Munzer, J.S., Chrétien, M., Marcinkiewicz, M., and Seidah, N.G. (1997). alpha1-antitrypsin portland inhibits processing of precursors mediated by

proprotein convertases primarily within the constitutive secretory pathway. J. Biol. Chem. *272*, 26210–26218.

Benjannet, S., Rhainds, D., Essalmani, R., Mayne, J., Wickham, L., Jin, W., Asselin, M.C., Hamelin, J., Varret, M., Allard, D., et al. (2004). NARC-1/PCSK9 and its natural mutants: Zymogen cleavage and effects on the low density lipoprotein (LDL) receptor and LDL cholesterol. J. Biol. Chem. *279*, 48865–48875.

Bennett, D.C. (1983). Differentiation in mouse melanoma cells: Initial reversibility and an on-off stochastic model. Cell *34*, 445–453.

Bennett, D.C., and Lamoreux, M.L. (2003). The Color Loci of Mice - A Genetic Century. Pigment Cell Res. *16*, 333–344.

Bennett, B.D., Denis, P., Haniu, M., Teplow, D.B., Kahn, S., Louis, J.C., Citron, M., and Vassar, R. (2000). A furin-like convertase mediates propeptide cleavage of BACE, the Alzheimer's β-secretase. J. Biol. Chem. *275*, 37712–37717.

Bergeron, E., Basak, A., Decroly, E., and Seidah, N.G. (2003). Processing of alpha4 integrin by the proprotein convertases: histidine at position P6 regulates cleavage. Biochem. J. *373*, 475–484.

Bernot, D., Stalin, J., Stocker, P., Bonardo, B., Scroyen, I., Alessi, M.-C., and Peiretti, F. (2011). Plasminogen activator inhibitor 1 is an intracellular inhibitor of furin proprotein convertase. J. Cell Sci. *124*, 1224–1230.

Berson, J.F., Theos, A.C., Harper, D.C., Tenza, D., Raposo, G., and Marks, M.S. (2003). Proprotein convertase cleavage liberates a fibrillogenic fragment of a resident glycoprotein to initiate melanosome biogenesis. J. Cell Biol. *161*, 521–533.

Bertolotto, C., Abbe, P., Hemesath, T.J., Bille, K., Fisher, D.E., Ortonne, J.P., and Ballotti, R. (1998a). Microphthalmia gene product as a signal transducer in cAMP-induced differentiation of melanocytes. J. Cell Biol. *142*, 827–835.

Bertolotto, C., Buscà, R., Abbe, P., Bille, K., Aberdam, E., Ortonne, J.P., and Ballotti, R. (1998b). Different cis-acting elements are involved in the regulation of TRP1 and TRP2 promoter activities by cyclic AMP: pivotal role of M boxes (GTCATGTGCT) and of microphthalmia. Mol. Cell. Biol. *18*, 694–702.

Bessonnard, S., Mesnard, D., and Constam, D.B. (2015). PC7 and the related proteases Furin and Pace4 regulate E-cadherin function during blastocyst formation. J. Cell Biol. *210*, 1185–1197.

De Bie, I., Marcinkiewicz, M., Malide, D., Lazure, C., Nakayama, K., Bendayan, M., and Seidah, N.G. (1996). The isoforms of proprotein convertase PC5 are sorted to different subcellular compartments. J. Cell Biol. *135*, 1261–1275.

Blanchet, M.-H., Le Good, J.A., Oorschot, V., Baflast, S., Minchiotti, G., Klumperman, J., and Constam, D.B. (2008a). Cripto localizes Nodal at the limiting membrane of early endosomes. Sci. Signal. *1*, ra13.

Blanchet, M.H., Le Good, J.A., Mesnard, D., Oorschot, V., Baflast, S., Minchiotti, G., Klumperman, J., and Constam, D.B. (2008b). Cripto recruits Furin and PACE4 and controls Nodal trafficking during proteolytic maturation. EMBO J. *27*, 2580–2591.

Blanchette, F., Rudd, P., Grondin, F., Attisano, L., and Dubois, C.M. (2001). Involvement of Smads in TGFβ1-induced furin (fur) transcription. J. Cell. Physiol. *188*, 264–273.

Blaumueller, C.M., Qi, H., Zagouras, P., and Artavanis-Tsakonas, S. (1997). Intracellular cleavage of Notch leads to a heterodimeric receptor on the plasma membrane. Cell *90*, 281–291.

Bonvin, E., Falletta, P., Shaw, H., Delmas, V., and Goding, C.R. (2012). A Phosphatidylinositol 3-Kinase-Pax3 Axis Regulates Brn-2 Expression in Melanoma. Mol. Cell. Biol. *32*, 4674–4683.

Bos, K., Wraight, C., and Stanley, K.K. (1993). TGN38 is maintained in the trans-Golgi network by a tyrosine-containing motif in the cytoplasmic domain. EMBO J. *12*, 2219–2228.

Bozkulak, E.C., and Weinmaster, G. (2009). Selective Use of ADAM10 and ADAM17 in Activation of Notch1 Signaling. Mol. Cell. Biol. *29*, 5679–5695.

Bozza, W.P., Di, X., Takeda, K., Rosado, L.A.R., Pariser, S., and Zhang, B. (2014). The use of a stably expressed FRET biosensor for determining the potency of cancer drugs. PLoS One *9*, e107010.

Briot, A., Jaroszewicz, A., Warren, C.M., Lu, J., Touma, M., Rudat, C., Hofmann, J.J., Airik, R., Weinmaster, G., Lyons, K., et al. (2014). Repression of Sox9 by Jag1 is continuously required to suppress the default chondrogenic fate of vascular smooth muscle cells. Dev. Cell *31*, 707–721.

Brito, F.C., and Kos, L. (2008). Timeline and distribution of melanocyte precursors in the mouse heart. Pigment Cell Melanoma Res. *21*, 464–470.

Bruzzaniti, A., Goodge, K., Jay, P., Taviaux, S.A., Lam, M.H., Berta, P., Martin, T.J., Moseley, J.M., and Gillespie, M.T. (1996). PC8 [corrected], a new member of the convertase family. Biochem J *314 (Pt 3*, 727–731.

Bürkle, A. (2001). Posttranslational Modification. In Encyclopedia of Genetics, (Elsevier), p. 1533.

Bush, G., DiSibio, G., Miyamoto, A., Denault, J.-B., Leduc, R., and Weinmaster, G. (2001). Ligand-Induced Signaling in the Absence of Furin Processing of Notch1. Dev. Biol. *229*, 494–502.

References

Cameron, A., Appel, J., Houghten, R.A., and Lindberg, I. (2000). Polyarginines are potent furin inhibitors. J. Biol. Chem. *275*, 36741–36749.

Cantley, L.C. (2002). The phosphoinositide 3-kinase pathway. Science *296*, 1655–1657.

Cao, J., Rehemtulla, A., Pavlaki, M., Kozarekar, P., and Chiarelli, C. (2005). Furin directly cleaves proMMP-2 in the trans-golgi network resulting in a nonfunctioning proteinase. J. Biol. Chem. *280*, 10974–10980.

Carmeliet, P. (2005). VEGF as a key mediator of angiogenesis in cancer. Oncology *69*, 4–10.

Carreira, S., Liu, B., and Goding, C.R. (2000). The gene encoding the T-box factor Tbx2 is a target for the microphthalmia-associated transcription factor in melanocytes. J. Biol. Chem. *275*, 21920–21927.

Carreira, S., Goodall, J., Aksan, I., La Rocca, S.A., Galibert, M.-D., Denat, L., Larue, L., and Goding, C.R. (2005). Mitf cooperates with Rb1 and activates p21Cip1 expression to regulate cell cycle progression. Nature *433*, 764–769.

Carreira, S., Goodall, J., Denat, L., Rodriguez, M., Nuciforo, P., Hoek, K.S., Testori, A., Larue, L., and Goding, C.R. (2006). Mitf regulation of Dia1 controls melanoma proliferation and invasiveness. Genes Dev. *20*, 3426–3439.

Cattell, E., Kelly, C., and Middleton, M.R. (2002). Brain metastases in melanoma: A European perspective. Semin. Oncol. *29*, 513–517.

Cepeda, M.A., Evered, C.L., Pelling, J.J.H.., and Damjanovski, S. (2017). Inhibition of MT1-MMP proteolytic function and ERK1/2 signalling influences cell migration and invasion through changes in MMP-2 and MMP-9 levels. J. Cell Commun. Signal. *11*, 167–179.

Chan, J.M., Stampfer, M.J., Giovannucci, E., Gann, P.H., Ma, J., Wilkinson, P., Hennekens, C.H., and Pollak, M. (1998). Plasma insulin-like growth factor-I and prostate cancer risk: a prospective study. Science (80-.). *279*, 563–566.

Chapnick, D.A., Bunker, E., and Liu, X. (2015). A biosensor for the protease TACE reveals actin damage induced TACE activation. Sci. Signal.

Cheli, Y., Ohanna, M., Ballotti, R., and Bertolotto, C. (2010). Fifteen-year quest for microphthalmia-associated transcription factor target genes. Pigment Cell Melanoma Res. *23*, 27–40.

Cheli, Y., Giuliano, S., Fenouille, N., Allegra, M., Hofman, V., Hofman, P., Bahadoran, P., Lacour, J.-P., Tartare-Deckert, S., Bertolotto, C., et al. (2012). Hypoxia and MITF control metastatic behaviour in mouse and human melanoma cells. Oncogene *31*, 2461–2470.

Chen, C. Di, Huff, M.E., Matteson, J., Page, L., Phillips, R., Kelly, J.W., and Balch, W.E. (2001). Furin initiates gelsolin familial amyloidosis in the golgi through a defect in Ca2+ stabilization.

EMBO J. *20*, 6277–6287.

Chen, J.L., Walton, K.L., Hagg, A., Colgan, T.D., Johnson, K., Qian, H., Gregorevic, P., and Harrison, C.A. (2017). Specific targeting of TGF-β family ligands demonstrates distinct roles in the regulation of muscle mass in health and disease. Proc. Natl. Acad. Sci. 201620013.

Cheng, M., Watson, P.H., Paterson, J. a, Seidah, N., Chrétien, M., and Shiu, R.P. (1997). Pro-protein convertase gene expression in human breast cancer. Int. J. Cancer *71*, 966–971.

Chiron, M.F., Fryling, C.M., and Fitzgerald, D.J. (1994). Cleavage of pseudomonas exotoxin and diphtheria toxin by a furin-like enzyme prepared from beef liver. J. Biol. Chem. *269*, 18167–18176.

De Cicco, R.L., Bassi, D.E., Zucker, S., Seidah, N.G., and Klein-Szanto, A.J.P. (2005). Human carcinoma cell growth and invasiveness is impaired by the propeptide of the ubiquitous proprotein convertase furin. Cancer Res. *65*, 4162–4171.

Clark, W.H., From, L., Bernardino, E.A., and Mihm, M.C. (1969). The Histogenesis and Biologic Behavior of Primary Human Malignant Melanomas of the Skin. Cancer Res. *29*, 705–727.

Clark, W.H., Elder, D.E., Guerry, D., Epstein, M.N., Greene, M.H., and Van Horn, M. (1984). A study of tumor progression: the precursor lesions of superficial spreading and nodular melanoma. Hum. Pathol. *15*, 1147–1165.

Conlon, R. a, Reaume, a G., and Rossant, J. (1995). Notch1 is required for the coordinate segmentation of somites. Development *121*, 1533–1545.

Constam, D.B. (2009). Riding shotgun: A dual role for the epidermal growth factor-Cripto/FRL-1/ Cryptic protein cripto in nodal trafficking. Traffic *10*, 783–791.

Constam, D.B., and Robertson, E.J. (2000). SPC4/PACE4 regulates a TGFbeta signaling network during axis formation. Genes Dev. *14*, 1146–1155.

Constam, D.B., Calfon, M., and Robertson, E.J. (1996). SPC4, SPC6, and the novel protease SPC7 are coexpressed with bone morphogenetic proteins at distinct sites during embryogenesis. J. Cell Biol. *134*, 181–191.

Constam, D.B., Robertson, E.J., Ang, S.L., Rossant, J., Arceci, R.J., King, A.A., Simon, M.C., Orkin, S.H., Wilson, D.B., Beddington, R.S., et al. (2000). Tissue-specific requirements for the proprotein convertase furin/SPC1 during embryonic turning and heart looping. Development *127*, 245–254.

Coppola, J.M., Hamilton, C.A., Bhojani, M.S., Larsen, M.J., Ross, B.D., and Rehemtulla, A. (2007). Identification of inhibitors using a cell-based assay for monitoring Golgi-resident protease activity. Anal. Biochem. *364*, 19–29.

Costin, G.-E., and Hearing, V.J. (2007). Human skin pigmentation: melanocytes modulate skin

color in response to stress. FASEB J. *21*, 976–994.

Couture, F., D'Anjou, F., Desjardins, R., Boudreau, F., and Day, R. (2012). Role of proprotein convertases in prostate cancer progression. Neoplasia *14*, 1032–1042.

Craig, E.A., and Spiegelman, V.S. (2012). Inhibition of coding region determinant binding protein sensitizes melanoma cells to chemotherapeutic agents. Pigment Cell Melanoma Res. *25*, 83–87.

Creemers, J.W.M., and Khatib, A.-M. (2008). Knock-out mouse models of proprotein convertases: unique functions or redundancy? Front. Biosci. *13*, 4960–4971.

Creemers, J.W.M., Van De Loo, J.W.H.P., Plets, E., Hendershot, L.M., and Van De Ven, W.J.M. (2000). Binding of BiP to the processing enzyme lymphoma proprotein convertase prevents aggregation, but slows down maturation. J. Biol. Chem. *275*, 38842–38847.

Creemers, J.W.M., Dominguez, D.I., Plets, E., Serneels, L., Taylor, N.A., Multhaup, G., Craessaerts, K., Annaert, W., and De Strooper, B. (2001). Processing of β-Secretase by Furin and Other Members of the Proprotein Convertase Family. J. Biol. Chem. *276*, 4211–4217.

Cronin, J.C., Wunderlich, J., Loftus, S.K., Prickett, T.D., Wei, X., Ridd, K., Vemula, S., Burrell, A.S., Agrawal, N.S., Lin, J.C., et al. (2009). Frequent mutations in the MITF pathway in melanoma. Pigment Cell Melanoma Res. *22*, 435–444.

Crump, C.M., Xiang, Y., Thomas, L., Gu, F., Austin, C., Tooze, S.A., and Thomas, G. (2001). PACS-1 binding to adaptors is required for acidic cluster motif-mediated protein traffic. EMBO J. *20*, 2191–2201.

Cui, R., Widlund, H.R., Feige, E., Lin, J.Y., Wilensky, D.L., Igras, V.E., D'Orazio, J., Fung, C.Y., Schanbacher, C.F., Granter, S.R., et al. (2007). Central Role of p53 in the Suntan Response and Pathologic Hyperpigmentation. Cell *128*, 853–864.

Cui, Y., Jean, F., Thomas, G., and Christian, J.L. (1998). BMP-4 is proteolytically activated by furin and/or PC6 during vertebrate embryonic development. EMBO J. *17*, 4735–4743.

Cunningham, D., Danley, D.E., Geoghegan, K.F., Griffor, M.C., Hawkins, J.L., Subashi, T.A., Varghese, A.H., Ammirati, M.J., Culp, J.S., Hoth, L.R., et al. (2007). Structural and biophysical studies of PCSK9 and its mutants linked to familial hypercholesterolemia. Nat. Struct. Mol. Biol. *14*, 413–419.

Curtin, J.A., Fridlyand, J., Kageshita, T., Patel, H.N., Busam, K.J., Kutzner, H., Cho, K.-H., Aiba, S., Bröcker, E.-B., LeBoit, P.E., et al. (2005). Distinct Sets of Genetic Alterations in Melanoma. N. Engl. J. Med. *353*, 2135–2147.

D'Anjou, F., Routhier, S., Perreault, J.-P., Latil, A., Bonnel, D., Fournier, I., Salzet, M., and Day, R. (2011). Molecular Validation of PACE4 as a Target in Prostate Cancer. Transl. Oncol.

4, 157–IN9.

D'Anjou, F., Couture, F., Desjardins, R., and Day, R. (2014). Knockdown Strategies for the Study of Proprotein Convertases and Proliferation in Prostate Cancer Cells. In Methods in Molecular Biology (Clifton, N.J.), pp. 67–82.

Dahms, S.O., Creemers, J.W.M., Schaub, Y., Bourenkov, G.P., Zögg, T., Brandstetter, H., and Than, M.E. (2016a). The structure of a furin-antibody complex explains non-competitive inhibition by steric exclusion of substrate conformers. Sci. Rep. *6*, 34303.

Dahms, S.O., Arciniega, M., Steinmetzer, T., Huber, R., and Than, M.E. (2016b). Structure of the unliganded form of the proprotein convertase furin suggests activation by a substrate-induced mechanism. Proc. Natl. Acad. Sci. *113*, 11196–11201.

Van Dam, E.M., Ten Broeke, T., Jansen, K., Spijkers, P., and Stoorvogel, W. (2002). Endocytosed transferrin receptors recycle via distinct dynamin and phosphatidylinositol 3-kinase-dependent pathways. J. Biol. Chem. *277*, 48876–48883.

Davies, H., Bignell, G.R., Cox, C., Stephens, P., Edkins, S., Clegg, S., Teague, J., Woffendin, H., Garnett, M.J., Bottomley, W., et al. (2002). Mutations of the BRAF gene in human cancer. Nature *417*, 949–954.

Day, R., Schafer, M.K., Watson, S.J., Chrétien, M., and Seidah, N.G. (1992). Distribution and regulation of the prohormone convertases PC1 and PC2 in the rat pituitary. Mol. Endocrinol. *6*, 485–497.

Declercq, J., Meulemans, S., Plets, E., and Creemers, J.W.M. (2012). Internalization of proprotein convertase PC7 from plasma membrane is mediated by a novel motif. J. Biol. Chem. *287*, 9052–9060.

Declercq, J., Brouwers, B., Pruniau, V.P.E.G., Stijnen, P., Tuand, K., Meulemans, S., Prat, A., Seidah, N.G., Khatib, A.M., and Creemers, J.W.M. (2015). Liver-specific inactivation of the proprotein convertase FURIN leads to increased hepatocellular carcinoma growth. Biomed Res. Int. *2015*, 148651.

Declercq, J., Ramos-Molina, B., Sannerud, R., Brouwers, B., Pruniau, V.P.E.G., Meulemans, S., Plets, E., Annaert, W., and Creemers, J.W.M. (2016). Endosome to trans-Golgi network transport of Proprotein Convertase 7 is mediated by a cluster of basic amino acids and palmitoylated cysteines. Eur. J. Cell Biol.

Degnin, C. (2004). Cleavages within the Prodomain Direct Intracellular Trafficking and Degradation of Mature Bone Morphogenetic Protein-4. Mol. Biol. Cell *15*, 5012–5020.

Delmas, V., Martinozzi, S., Bourgeois, Y., Holzenberger, M., and Larue, L. (2003). Cre-mediated recombination in the skin melanocyte lineage. Genesis *36*, 73–80.

References

Delwel, G.O., Hogervorst, F., and Sonnenberg, A. (1996). Cleavage of the alpha6A subunit is essential for activation of the alpha6Abeta1 integrin by phorbol 12-myristate 13-acetate. J Biol Chem *271*, 7293–7296.

Demarest, R.M., Ratti, F., and Capobianco, A.J. (2008). It's T-ALL about Notch. Oncogene *27*, 5082–5091.

Demidyuk, I. V., Shubin, A. V., Gasanov, E. V., Kurinov, A.M., Demkin, V. V., Vinogradova, T. V., Zinovyeva, M. V., Sass, A. V., Zborovskaya, I.B., and Kostrov, S. V. (2013). Alterations in Gene Expression of Proprotein Convertases in Human Lung Cancer Have a Limited Number of Scenarios. PLoS One *8*, e55752.

Denduluri, S.K., Idowu, O., Wang, Z., Liao, Z., Yan, Z., Mohammed, M.K., Ye, J., Wei, Q., Wang, J., Zhao, L., et al. (2015). Insulin-like growth factor (IGF) signaling intumorigenesis and the development ofcancer drug resistance. Genes Dis. *2*, 13–25.

Denecker, G., Vandamme, N., Akay, Ö., Koludrovic, D., Taminau, J., Lemeire, K., Gheldof, A., De Craene, B., Van Gele, M., Brochez, L., et al. (2014). Identification of a ZEB2-MITF-ZEB1 transcriptional network that controls melanogenesis and melanoma progression. Cell Death Differ. *21*, 1250–1261.

Desgrosellier, J.S., and Cheresh, D.A. (2010). Integrins in cancer: biological implications and therapeutic opportunities. Nat. Rev. Cancer *10*, 9–22.

Dissanayake, S.K., Wade, M., Johnson, C.E., O'Connell, M.P., Leotlela, P.D., French, A.D., Shah, K. V., Hewitt, K.J., Rosenthal, D.T., Indig, F.E., et al. (2007). The Wnt5A/protein kinase C pathway mediates motility in melanoma cells via the inhibition of metastasis suppressors and initiation of an epithelial to mesenchymal transition. J. Biol. Chem. *282*, 17259–17271.

Dittié, A.S., Thomas, L., Thomas, G., and Tooze, S.A. (1997). Interaction of furin in immature secretory granules from neuroendocrine cells with the AP-1 adaptor complex is modulated by casein kinase II phosphorylation. EMBO J. *16*, 4859–4870.

Dong, W., Marcinkiewicz, M., Vieau, D., Chrétien, M., Seidah, N.G., and Day, R. (1995). Distinct mRNA expression of the highly homologous convertases PC5 and PACE4 in the rat brain and pituitary. J. Neurosci. *15*, 1778–1796.

Donovan, P., Dubey, O.A., Kallioinen, S., Rogers, K.W., Muehlethaler, K., Müller, P., Rimoldi, D., Constam, D.B., and Daniel, B. (2017). Paracrine Activin-A signaling promotes melanoma growth and metastasis through immune evasion. J. Invest. Dermatol.

Dragulescu-Andrasi, A., Liang, G., and Rao, J. (2009). In vivo bioluminescence imaging of furin activity in breast cancer cells using bioluminogenic substrates. Bioconjug. Chem. *20*, 1660–1666.

Dragulescu-Andrasi, A., Kothapalli, S.R., Tikhomirov, G.A., Rao, J., and Gambhir, S.S. (2013).

Activatable oligomerizable imaging agents for photoacoustic imaging of furin-like activity in living subjects. J. Am. Chem. Soc. *135*, 11015–11022.

Du, J., Miller, A.J., Widlund, H.R., Horstmann, M.A., Ramaswamy, S., and Fisher, D.E. (2003). MLANA/MART1 and SILV/PMEL17/GP100 Are Transcriptionally Regulated by MITF in Melanocytes and Melanoma. Am. J. Pathol. *163*, 333–343.

Dubois, C.M., Blanchette, F., Laprise, M.H., Leduc, R., Grondin, F., and Seidah, N.G. (2001). Evidence that furin is an authentic transforming growth factor-β1-converting enzyme. Am. J. Pathol. *158*, 305–316.

Duckert, P., Brunak, S., and Blom, N. (2004). Prediction of proprotein convertase cleavage sites. Protein Eng. Des. Sel. *17*, 107–112.

Duffy, M.J., McKiernan, E., O'Donovan, N., and McGowan, P.M. (2009). Role of ADAMs in cancer formation and progression. Clin. Cancer Res. *15*, 1140–1144.

Dufour, E.K., Denault, J.B., Hopkins, P.C.R., and Leduc, R. (1998). Serpin-like properties of α1-antitrypsin Portland towards furin convertase. FEBS Lett. *426*, 41–46.

Duguay, S.J., Milewski, W.M., Young, B.D., Nakayama, K., and Steiner, D.F. (1997). Processing of wild-type and mutant proinsulin-like growth factor-IA by subtilisin-related proprotein convertases. J. Biol. Chem. *272*, 6663–6670.

Duncan, J.R., and Kornfeld, S. (1988). Intracellular movement of two mannose 6-phosphate receptors: Return to the Golgi apparatus. J. Cell Biol. *106*, 617–628.

Dvorak, H.F. (2002). Vascular permeability factor/vascular endothelial growth factor: A critical cytokine in tumor angiogenesis and a potential target for diagnosis and therapy. J. Clin. Oncol. *20*, 4368–4380.

Eccles, M.R., He, S., Ahn, A., Slobbe, L.J., Jeffs, A.R., Yoon, H.-S., and Baguley, B.C. (2013). MITF and PAX3 Play Distinct Roles in Melanoma Cell Migration; Outline of a "Genetic Switch" Theory Involving MITF and PAX3 in Proliferative and Invasive Phenotypes of Melanoma. Front. Oncol. *3*, 229.

Edbauer, D., Winkler, E., Regula, J.T., Pesold, B., Steiner, H., and Haass, C. (2003). Reconstitution of gamma-secretase activity. Nat. Cell Biol. *5*, 486–488.

Edwards, D.R., Handsley, M.M., and Pennington, C.J. (2009). The ADAM metalloproteinases. Mol. Aspects Med. *29*, 258–289.

Egeblad, M., and Werb, Z. (2002). New functions for the matrix metalloproteinases in cancer progression. Nat. Rev. Cancer *2*, 161–174.

Eichhoff, O.M., Weeraratna, A., Zipser, M.C., Denat, L., Widmer, D.S., Xu, M., Kriegl, L., Kirchner, T., Larue, L., Dummer, R., et al. (2011). Differential LEF1 and TCF4 expression is

involved in melanoma cell phenotype switching. Pigment Cell Melanoma Res. *24*, 631–642.

Eichorst, J.P., Clegg, R.M., and Wang, Y. (2012). Red-shifted fluorescent proteins monitor enzymatic activity in live HT-1080 cells with fluorescence lifetime imaging microscopy (FLIM). J. Microsc. *248*, 77–89.

Elagoz, A., Benjannet, S., Mammarbassi, A., Wickham, L., and Seidah, N.G. (2002). Biosynthesis and cellular trafficking of the convertase SKI-1/S1P. Ectodomain shedding requires SKI-1 activity. J. Biol. Chem. *277*, 11265–11275.

Endres, K., Anders, A., Kojro, E., Gilbert, S., Fahrenholz, F., and Postina, R. (2003). Tumor necrosis factor-α converting enzyme is processed by proprotein-convertases to its mature form which is degraded upon phorbol ester stimulation. Eur. J. Biochem. *270*, 2386–2393.

Eskandarpour, M., Kiaii, S., Zhu, C., Castro, J., Sakko, A.J., and Hansson, J. (2005). Suppression of oncogenic NRAS by RNA interference induces apoptosis of human melanoma cells. Int. J. Cancer *115*, 65–73.

Espenshade, P.J., Cheng, D., Goldstein, J.L., and Brown, M.S. (1999). Autocatalytic processing of site-1 protease removes propeptide and permits cleavage of sterol regulatory element-binding proteins. J. Biol. Chem. *274*, 22795–22804.

Essalmani, R., Hamelin, J., Marcinkiewicz, J., Chamberland, A., Mbikay, M., Chretien, M., Seidah, N.G., and Prat, A. (2006). Deletion of the Gene Encoding Proprotein Convertase 5/6 Causes Early Embryonic Lethality in the Mouse. Mol. Cell. Biol. *26*, 354–361.

Essalmani, R., Zaid, A., Marcinkiewicz, J., Chamberland, A., Pasquato, A., Seidah, N.G., and Prat, A. (2008). In vivo functions of the proprotein convertase PC5/6 during mouse development: Gdf11 is a likely substrate. Proc. Natl. Acad. Sci. USA *105*, 5750–5755.

Essalmani, R., Susan-Resiga, D., Chamberland, A., Abifadel, M., Creemers, J.W., Boileau, C., Seidah, N.G., and Prat, A. (2011). In vivo evidence that furin from hepatocytes inactivates PCSK9. J. Biol. Chem. *286*, 4257–4263.

Faundez, V., and Hartzell, H.C. (2004). Intracellular chloride channels: determinants of function in the endosomal pathway. Sci. STKE *2004*, re8.

Fehr, M., Lalonde, S., Lager, I., Wolff, M.W., and Frommer, W.B. (2003). In vivo imaging of the dynamics of glucose uptake in the cytosol of COS-7 cells by fluorescent nanosensors. J. Biol. Chem. *278*, 19127–19133.

Feige, J.N., Sage, D., Wahli, W., Desvergne, B., and Gelman, L. (2005). PixFRET, an ImageJ plug-in for FRET calculation that can accommodate variations in spectral bleed-throughs. Microsc. Res. Tech. *68*, 51–58.

Feldman, J.P., and Goldwasser, R. (2009). a Mathematical Model for Tumor Volume

Evaluation Using Two-Dimensions. Jpurnal Appl. Quant. Methods *4*, 455–462.

Feliciangeli, S.F., Thomas, L., Scott, G.K., Subbian, E., Hung, C.H., Molloy, S.S., Jean, F., Shinde, U., and Thomas, G. (2006). Identification of a pH sensor in the furin propeptide that regulates enzyme activation. J. Biol. Chem. *281*, 16108–16116.

Flores, J.F., Walker, G.J., Glendening, J.M., Haluska, F.G., Castresana, J.S., Rubio, M.P., Pastorfide, G.C., Boyer, L.A., Kao, W.H., Bulyk, M.L., et al. (1996). Loss of the p16(INK4a) and p15(INK4b) genes, as well as neighboring 9p21 markers, in sporadic melanoma. Cancer Res. *56*, 5023–5032.

Förster, T., Energiewanderung, Z., and Von, F. (1939). Zwischenmolekulare Energiewanderung und Fluoreszenz. Ann. Phys. *248*, 55–75.

Fricker, L.D., McKinzie, a a, Sun, J., Curran, E., Qian, Y., Yan, L., Patterson, S.D., Courchesne, P.L., Richards, B., Levin, N., et al. (2000). Identification and characterization of proSAAS, a granin-like neuroendocrine peptide precursor that inhibits prohormone processing. J. Neurosci. *20*, 639–648.

Friedmann-Morvinski, D., and Verma, I.M. (2014). Dedifferentiation and reprogramming: origins of cancer stem cells. EMBO Rep. *15*, 244–253.

Friesel, R.E., and Maciag, T. (1995). Molecular mechanisms of angiogenesis: fibroblast growth factor signal transduction. FASEB J. *9*, 919–925.

Fryer, C.J., Lamar, E., Turbachova, I., Kintner, C., and Jones, K.A. (2002). Mastermind mediates chromatin-specific transcription and turnover of the notch enhancer complex. Genes Dev. *16*, 1397–1411.

Fu, J., Bassi, D.E., Zhang, J., Li, T., Nicolas, E., and Klein-Szanto, A.J.P. (2012). Transgenic Overexpression of the Proprotein Convertase Furin Enhances Skin Tumor Growth. Neoplasia *14*, 271–282.

Fu, J., Bassi, D.E., Zhang, J., Li, T., Cai, K.Q., Testa, C.L., Nicolas, E., and Klein-Szanto, A.J. (2013). Enhanced UV-Induced Skin Carcinogenesis in Transgenic Mice Overexpressing Proprotein Convertases. Neoplasia *15*, 169–179.

Fu, Y., Campbell, E.J., Shepherd, T.G., and Nachtigal, M.W. (2003). Epigenetic regulation of proprotein convertase PACE4 gene expression in human ovarian cancer cells. Mol. Cancer Res. *1*, 569–576.

Fuerer, C., Habib, S.J., and Nusse, R. (2010). A study on the interactions between heparan sulfate proteoglycans and Wnt proteins. Dev. Dyn. *239*, 184–190.

Fuerer, C., Nostro, M.C., and Constam, D.B. (2014). Nodal·Gdf1 heterodimers with bound prodomains enable serum-independent nodal signaling and endoderm differentiation. J. Biol.

Chem. *289*, 17854–17871.

Fuller, R.S., Sterne, R.E., and Thorner, J. (1988). Enzymes required for yeast prohormone processing. Annu. Rev. Physiol. *50*, 345–362.

Furuta, M., Yano, H., Zhou, A., Rouille, Y., Holst, J.J., Carroll, R., Ravazzola, M., Orci, L., Furuta, H., and Steiner, D.F. (1997). Defective prohormone processing and altered pancreatic islet morphology in mice lacking active SPC2. Proc. Natl. Acad. Sci. *94*, 6646–6651.

Gabbert, H., Wagner, R., Moll, R., and Gerharz, C.D. (1985). Tumor dedifferentiation: An important step in tumor invasion. Clin. Exp. Metastasis *3*, 257–279.

Garraway, L.A., Widlund, H.R., Rubin, M.A., Getz, G., Berger, A.J., Ramaswamy, S., Beroukhim, R., Milner, D.A., Granter, S.R., Du, J., et al. (2005). Integrative genomic analyses identify MITF as a lineage survival oncogene amplified in malignant melanoma. Nature *436*, 117–122.

Garred, O., Van Deurs, B., and Sandvig, K. (1995). Furin-induced cleavage and activation of shiga toxin. J. Biol. Chem. *270*, 10817–10821.

Garten, W., Hallenberger, S., Ortmann, D., Schäfer, W., Vey, M., Angliker, H., Shaw, E., and Klenk, H.D. (1994). Processing of viral glycoproteins by the subtilisin-like endoprotease furin and its inhibition by specific peptidylchloroalkylketones. Biochimie *76*, 217–225.

Gavet, O., and Pines, J. (2010). Progressive Activation of CyclinB1-Cdk1 Coordinates Entry to Mitosis. Dev. Cell *18*, 533–543.

Gawlik, K., Remacle, A.G., Shiryaev, S.A., Golubkov, V.S., Ouyang, M., Wang, Y., and Strongin, A.Y. (2010). A femtomol range FRET biosensor reports exceedingly low levels of cell surface furin: Implications for the processing of anthrax protective antigen. PLoS One *5*.

Ge, G., Hopkins, D.R., Ho, W.-B., and Greenspan, D.S. (2005). GDF11 forms a bone morphogenetic protein 1-activated latent complex that can modulate nerve growth factor-induced differentiation of PC12 cells. Mol. Cell. Biol. *25*, 5846–5858.

Gheldof, A., Hulpiau, P., van Roy, F., De Craene, B., and Berx, G. (2012). Evolutionary functional analysis and molecular regulation of the ZEB transcription factors. Cell. Mol. Life Sci. *69*, 2527–2541.

Ghisoli, M., Barve, M., Schneider, R., Mennel, R., Lenarsky, C., Wallraven, G., Pappen, B.O., LaNoue, J., Kumar, P., Nemunaitis, D., et al. (2015). Pilot Trial of FANG Immunotherapy in Ewing's Sarcoma. Mol. Ther. *23*, 1103–1109.

Ghisoli, M., Barve, M., Mennel, R., Lenarsky, C., Horvath, S., Wallraven, G., Pappen, B.O., Whiting, S., Rao, D., Senzer, N., et al. (2016). Three-year Follow up of GMCSF/bi-shRNA furin DNA-transfected Autologous Tumor Immunotherapy (Vigil) in Metastatic Advanced Ewing's

Sarcoma. Mol. Ther. *24*, 1478–1483.

Ghosh, P., Dahms, N.M., and Kornfeld, S. (2003). Mannose 6-phosphate receptors: new twists in the tale. Nat. Rev. Mol. Cell Biol. *4*, 202–213.

Giuliano, S., Cheli, Y., Ohanna, M., Bonet, C., Beuret, L., Bille, K., Loubat, A., Hofman, V., Hofman, P., Ponzio, G., et al. (2010). Microphthalmia-associated transcription factor controls the DNA damage response and a lineage-specific senescence program in melanomas. Cancer Res. *70*, 3813–3822.

Goding, C.R. (2000). Mitf from neural crest to melanoma: Signal transduction and transcription in the melanocyte lineage. Genes Dev. *14*, 1712–1728.

Goding, C.R. (2011). A picture of Mitf in melanoma immortality. Oncogene *30*, 2304–2306.

Golan, T., Messer, A.R., Amitai-Lange, A., Melamed, Z., Ohana, R., Bell, R.E., Kapitansky, O., Lerman, G., Greenberger, S., Khaled, M., et al. (2015). Interactions of Melanoma Cells with Distal Keratinocytes Trigger Metastasis via Notch Signaling Inhibition of MITF. Mol. Cell *59*, 664–676.

Goldgeier, M.H., Klein, L.E., Klein-Angerer, S., Moellmann, G., and Nordlund, J.J. (1984). The Distribution of Melanocytes in the Leptomeninges of the Human Brain. J. Invest. Dermatol. *82*, 235–238.

Goodall, J., Carreira, S., Denat, L., Kobi, D., Davidson, I., Nuciforo, P., Sturm, R.A., Larue, L., and Goding, C.R. (2008). Brn-2 represses microphthalmia-associated transcription factor expression and marks a distinct subpopulation of microphthalmia-associated transcription factor-negative melanoma cells. Cancer Res. *68*, 7788–7794.

Gordon, V.M., Benz, R., Fujii, K., Leppla, S.H., and Tweten, R.K. (1997). Clostridium septicum alpha-toxin is proteolytically activated by furin. Infect. Immun. *65*, 4130–4134.

Gordon, W.R., Arnett, K.L., and Blacklow, S.C. (2008). The molecular logic of Notch signaling - a structural and biochemical perspective. J. Cell Sci. *121*, 3109–3119.

Gordon, W.R., Vardar-Ulu, D., L'Heureux, S., Ashworth, T., Malecki, M.J., Sanchez-Irizarry, C., McArthur, D.G., Histen, G., Mitchell, J.L., Aster, J.C., et al. (2009). Effects of S1 cleavage on the structure, surface export, and signaling activity of human Notch1 and Notch2. PLoS One *4*, e6613--e6613.

Guillemot, J., Canuel, M., Essalmani, R., Prat, A., and Seidah, N.G. (2013). Implication of the proprotein convertases in iron homeostasis: Proprotein convertase 7 sheds human transferrin receptor 1 and furin activates hepcidin. Hepatology *57*, 2514–2524.

Guillemot, J., Essalmani, R., Hamelin, J., and Seidah, N.G. (2014). Is there a link between proprotein convertase PC7 activity and human lipid homeostasis? FEBS Open Bio *4*, 741–

745.

Guldberg, P., Thor Straten, P., Birck, A., Ahrenkiel, V., Kirkin, A.F., and Zeuthen, J. (1997). Disruption of the MMAC1/PTEN gene by deletion or mutation is a frequent event in malignant melanoma. Cancer Res. *57*, 3660–3663.

Gyamera-Acheampong, C. (2006). Sperm from Mice Genetically Deficient for the PCSK4 Proteinase Exhibit Accelerated Capacitation, Precocious Acrosome Reaction, Reduced Binding to Egg Zona Pellucida, and Impaired Fertilizing Ability. Biol. Reprod. *74*, 666–673.

Gyamera-Acheampong, C., and Mbikay, M. (2009). Proprotein convertase subtilisin/kexin type 4 in mammalian fertility: a review. Hum. Reprod. Update *15*, 237–247.

Haass, N.K., Smalley, K.S.M., Li, L., and Herlyn, M. (2005). Adhesion, migration and communication in melanocytes and melanoma. Pigment Cell Res. *18*, 150–159.

Haflidadóttir, B.S., Bergsteinsdóttir, K., Praetorius, C., and Steingrímsson, E. (2010). miR-148 regulates Mitf in melanoma cells. PLoS One *5*.

Hajdin, K., D'Alessandro, V., Niggli, F.K., Schäfer, B.W., and Bernasconi, M. (2010). Furin targeted drug delivery for treatment of Rhabdomyosarcoma in a mouse model. PLoS One *5*, e10445.

Halbleib, J.M., and Nelson, W.J. (2006). Cadherins in development: cell adhesion, sorting, and tissue morphogenesis. Genes Dev. *20*, 3199–3214.

Hamada, Y., Kadokawa, Y., Okabe, M., Ikawa, M., Coleman, J.R., and Tsujimoto, Y. (1999). Mutation in ankyrin repeats of the mouse Notch2 gene induces early embryonic lethality. Development *126*, 3415–3424.

Hanahan, D., and Weinberg, R.A. (2011). Hallmarks of cancer: The next generation. Cell *144*, 646–674.

Hanč, P., Schulz, O., Fischbach, H., Martin, S.R., Kjær, S., and Reis E Sousa, C. (2016). A pH- and ionic strength-dependent conformational change in the neck region regulates DNGR-1 function in dendritic cells. EMBO J. *35*, 2484–2497.

Hao, L., Ha, J.R., Kuzel, P., Garcia, E., and Persad, S. (2012). Cadherin switch from E- to N-cadherin in melanoma progression is regulated by the PI3K/PTEN pathway through Twist and Snail. Br. J. Dermatol. *166*, 1184–1197.

Harding, C., Heuser, J., and Stahl, P. (1983). Receptor-mediated endocytosis of transferrin and recycling of the transferrin receptor in rat reticulocytes. J. Cell Biol. *97*, 329–339.

Harris, S.L., and Levine, A.J. (2005). The p53 pathway: positive and negative feedback loops. Oncogene *24*, 2899–2908.

Hartman, M.L., and Czyz, M. (2015). MITF in melanoma: Mechanisms behind its expression

and activity. Cell. Mol. Life Sci. *72*, 1249–1260.

Hartmann, D., de Strooper, B., Serneels, L., Craessaerts, K., Herreman, A., Annaert, W., Umans, L., Lübke, T., Lena Illert, A., von Figura, K., et al. (2002). The disintegrin/metalloprotease ADAM 10 is essential for Notch signalling but not for alpha-secretase activity in fibroblasts. Hum. Mol. Genet. *11*, 2615–2624.

Hatsuzawa, K., Murakami, K., and Nakayama, K. (1992). Molecular and enzymatic properties of furin, a Kex2-like endoprotease involved in precursor cleavage at Arg-X-Lys/Arg-Arg sites. J Biochem *111*, 296–301.

Healy, E., Rehman, I., Angus, B., and Rees, J.L. (1995). Loss of heterozygosity in sporadic primary cutaneous melanoma. Genes Chromosom. Cancer 152–156.

Hedger, M.P., Winnall, W.R., Phillips, D.J., and de Kretser, D.M. (2011). The Regulation and Functions of Activin and Follistatin in Inflammation and Immunity.

Heldin, C.-H. (2013). Targeting the PDGF signaling pathway in tumor treatment. Cell Commun. Signal. *11*, 97.

Hemesath, T.J., Price, E.R., Takemoto, C., Badalian, T., and Fisher, D.E. (1998). MAP kinase links the transcription factor Microphthalmia to c-Kit signalling in melanocytes. Nature *391*, 298–301.

Henderson, S.T., Gao, D., Lambie, E.J., and Kimble, J. (1994). lag-2 may encode a signaling ligand for the GLP-1 and LIN-12 receptors of C. elegans. Development *120*, 2913–2924.

Heng, S., Stephens, A.N., Jobling, T.W., and Nie, G. (2016a). Total PC activity is increased in uterine lavage of post-menopausal endometrial but not ovarian cancer patients. J. Cancer *7*, 1812–1814.

Heng, S., Stephens, A.N., Jobling, T.W., and Nie, G. (2016b). Measuring PC activity in endocervical swab may provide a simple and non-invasive method to detect endometrial cancer in post-menopausal women. Oncotarget *7*.

Henrich, S., Lindberg, I., Bode, W., and Than, M.E. (2005). Proprotein convertase models based on the crystal structures of furin and kexin: Explanation of their specificity. J. Mol. Biol. *345*, 211–227.

Herbst, R.A., Weiss, J., Ehnis, A., Cavenee, W.K., and Arden, K.C. (1994). Loss of heterozygosity for 10q22-10qter in malignant melanoma progression. Cancer Res. *54*, 3111–3114.

Hertwig, P. (1942). Neue Mutationen und Koppelungsgruppen bei der Hausmaus. Z. Indukt. Abstamm. Vererbungsl. *80*, 220–246.

Hinde, E., Digman, M.A., Welch, C., Hahn, K.M., and Gratton, E. (2012). Biosensor Förster

resonance energy transfer detection by the phasor approach to fluorescence lifetime imaging microscopy. Microsc. Res. Tech. *75*, 271–281.

Hingorani, S.R., Jacobetz, M.A., Robertson, G.P., Herlyn, M., and Tuveson, D.A. (2003). Suppression of BRAFV599E in human melanoma abrogates transformation. Cancer Res. *63*, 5198–5202.

Hirohashi, S. (1998). Inactivation of the E-cadherin-mediated cell adhesion system in human cancers. Am J Pathol *153*, 333–339.

Hobson, J.P., Liu, S., Rønø, B., Leppla, S.H., and Bugge, T.H. (2006). Imaging specific cell-surface proteolytic activity in single living cells. Nat. Methods *3*, 259–261.

Hodgkinson, C.A., Moore, K.J., Nakayama, A., Steingrímsson, E., Copeland, N.G., Jenkins, N.A., and Arnheiter, H. (1993). Mutations at the mouse microphthalmia locus are associated with defects in a gene encoding a novel basic-helix-loop-helix-zipper protein. Cell *74*, 395–404.

Hoeben, A., Landuyt, B., Highley, M.S., Wildiers, H., Van Oosterom, A.T., and De Bruijn, E.A. (2004). Vascular Endothelial Growth Factor and Angiogenesis. Pharmacol. Rev. *56*, 549–580.

Hoeflich, K.P., Gray, D.C., Eby, M.T., Tien, J.Y., Wong, L., Bower, J., Gogineni, A., Zha, J., Cole, M.J., Stern, H.M., et al. (2006). Oncogenic BRAF is required for tumor growth and maintenance in melanoma models. Cancer Res. *66*, 999–1006.

Hoek, K.S., and Goding, C.R. (2010). Cancer stem cells versus phenotype-switching in melanoma. Pigment Cell Melanoma Res. *23*, 746–759.

Hoek, K., Rimm, D.L., Williams, K.R., Zhao, H., Ariyan, S., Liu, A., Kluger, H.M., Berger, A.J., Cheng, E., Trombetta, E.S., et al. (2004). Expression profiling reveals novel pathways in the transformation of melanocytes to melanomas. Cancer Res. *64*, 5270–5282.

Hoek, K.S., Schlegel, N.C., Brafford, P., Sucker, A., Ugurel, S., Kumar, R., Weber, B.L., Nathanson, K.L., Phillips, D.J., Herlyn, M., et al. (2006). Metastatic potential of melanomas defined by specific gene expression profiles with no BRAF signature. Pigment Cell Res. *19*, 290–302.

Hoek, K.S., Eichhoff, O.M., Schlegel, N.C., Döbbeling, U., Kobert, N., Schaerer, L., Hemmi, S., and Dummer, R. (2008a). In vivo switching of human melanoma cells between proliferative and invasive states. Cancer Res. *68*, 650–656.

Hoek, K.S., Schlegel, N.C., Eichhoff, O.M., Widmer, D.S., Praetorius, C., Einarsson, S.O., Valgeirsdottir, S., Bergsteinsdottir, K., Schepsky, A., Dummer, R., et al. (2008b). Novel MITF targets identified using a two-step DNA microarray strategy. Pigment Cell Melanoma Res. *21*, 665–676.

References

Hofbauer, G.F.L., Kamarashev, J., Geertsen, R., Böni, R., and Dummer, R. (1998). Melan A/MART-1 immunoreactivity in formalin-fixed paraffin-embedded primary and metastatic melanoma: frequency and distribution. J. Cutan. Pathol. *25*, 204–209.

Huang, Y.H., Lin, K.H., Liao, C.H., Lai, M.W., Tseng, Y.H., and Yeh, C.T. (2012). Furin overexpression suppresses tumor growth and predicts a better postoperative disease-free survival in hepatocellular carcinoma. PLoS One *7*.

Huber, W.E., Price, E.R., Widlund, H.R., Du, J., Davis, I.J., Wegner, M., and Fisher, D.E. (2003). A tissue-restricted cAMP transcriptional response: SOX10 modulates α-melanocyte-stimulating hormone-triggered expression of microphthalmia-associated transcription factor in melanocytes. J. Biol. Chem. *278*, 45224–45230.

Hughes, M.J., Lingrel, J.B., Krakowsky, J.M., and Anderson, K.P. (1993). A helix-loop-helix transcription factor-like gene is located at the mi locus. J. Biol. Chem. *268*, 20687–20690.

Huylebroeck, D., Vannimmen, K., Waheed, A., Vonfigura, K., Marmenout, A., Fransen, L., Dewaele, P., Jaspar, J.M., Franchimont, P., Stunneberg, H., et al. (1990). Expression and processing of the Activin-A erythroid differentiation factor precursor-a member of the transforming growth factor-beta superfamily. Mol Endocrinol *4*, 1153–1165.

Hwang, J.R., and Lindberg, I. (2001). Inactivation of the 7B2 inhibitory CT peptide depends on a functional furin cleavage site. J. Neurochem. *79*, 437–444.

Hwang, E.M., Kim, S.K., Sohn, J.H., Lee, J.Y., Kim, Y., Kim, Y.S., and Mook-Jung, I. (2006). Furin is an endogenous regulator of α-secretase associated APP processing. Biochem. Biophys. Res. Commun. *349*, 654–659.

Imamura, H., Huynh Nhat, K.P., Togawa, H., Saito, K., Iino, R., Kato-Yamada, Y., Nagai, T., and Noji, H. (2009). Visualization of ATP levels inside single living cells with fluorescence resonance energy transfer-based genetically encoded indicators. Proc. Natl. Acad. Sci. *106*, 15651–15656.

Jaaks, P., and Bernasconi, M. (2017). The proprotein convertase furin in tumour progression. Int. J. Cancer *141*, 654–663.

Jaaks, P., D'Alessandro, V., Grob, N., Büel, S., Hajdin, K., Schäfer, B.W., and Bernasconi, M. (2016a). The proprotein convertase furin contributes to rhabdomyosarcoma malignancy by promoting vascularization, migration and invasion. PLoS One *11*, e0161396.

Jaaks, P., Meier, G., Alijaj, N., Brack, E., Bode, P., Koscielniak, E., Wachtel, M., Schäfer, B.W., Bernasconi, M., Jaaks, P., et al. (2016b). The proprotein convertase furin is required to maintain viability of alveolar rhabdomyosarcoma cells. Oncotarget *7*, 76743–76755.

Jares-Erijman, E.A., and Jovin, T.M. (2003). FRET imaging. Nat. Biotechnol. *21*, 1387–1395.

Jean, F., Stella, K., Thomas, L., Liu, G., Xiang, Y., Reason, A.J., and Thomas, G. (1998). alpha1-Antitrypsin Portland, a bioengineered serpin highly selective for furin: Application as an antipathogenic agent. Proc. Natl. Acad. Sci. *95*, 7293–7298.

Jiao, G.-S., Cregar, L., Wang, J., Millis, S.Z., Tang, C., O'Malley, S., Johnson, A.T., Sareth, S., Larson, J., and Thomas, G. (2006). Synthetic small molecule furin inhibitors derived from 2,5-dideoxystreptamine. Proc. Natl. Acad. Sci. U. S. A. *103*, 19707–19712.

Jin, S., and White, E. (2007). Role of autophagy in cancer: management of metabolic stress. Autophagy *3*, 28–31.

Johnsson, A.K.E., Dai, Y., Nobis, M., Baker, M.J., McGhee, E.J., Walker, S., Schwarz, J.P., Kadir, S., Morton, J.P., Myant, K.B., et al. (2014). The Rac-FRET Mouse Reveals Tight Spatiotemporal Control of Rac Activity in Primary Cells and Tissues. Cell Rep. *6*, 1153–1164.

Joukov, V., Sorsa, T., Kumar, V., Jeltsch, M., Claesson-Welsh, L., Cao, Y., Saksela, O., Kalkkinen, N., and Alitalo, K. (1997). Proteolytic processing regulates receptor specificity and activity of VEGF-C. EMBO J. *16*, 3898–3911.

Julius, D., Brake, A., Blair, L., Kunisawa, R., and Thorner, J. (1984). Isolation of the putative structural gene for the lysine-arginine-cleaving endopeptidase required for processing of yeast prepro-alpha-factor. Cell *37*, 1075–1089.

Kacprzak, M.M., Peinado, J.E., Than, M.E., Appel, J., Henrich, S., Lipkind, G., Houghten, R.A., Bode, W., and Lindberg, I. (2004). Inhibition of furin by polyarginine-containing peptides: Nanomolar inhibition by nona-D-arginine. J. Biol. Chem. *279*, 36788–36794.

Kaidbey, K.H., Agin, P.P., Sayre, R.M., and Kligman, A.M. (1979). Photoprotection by melanin—a comparison of black and Caucasian skin. J. Am. Acad. Dermatol. *1*, 249–260.

Kaleko, M., Rutter, W.J., and Miller, A.D. (1990). Overexpression of the human insulinlike growth factor I receptor promotes ligand-dependent neoplastic transformation. Mol. Cell. Biol. *10*, 464–473.

Kamb, A., Gruis, N.A., Weaver-Feldhaus, J., Liu, Q., Harshman, K., Tavtigian, S. V, Stockert, E., Day, R.S., Johnson, B.E., and Skolnick, M.H. (1994). A cell cycle regulator potentially involved in genesis of many tumor types. Science *264*, 436–440.

Kamioka, Y., Sumiyama, K., Mizuno, R., Sakai, Y., Hirata, E., Kiyokawa, E., and Matsuda, M. (2012). Live Imaging of Protein Kinase Activities in Transgenic Mice Expressing FRET Biosensors. Cell Struct. Funct. *37*, 65–73.

Keller, P., Toomre, D., Díaz, E., White, J., and Simons, K. (2001). Multicolour imaging of post-Golgi sorting and trafficking in live cells. Nat. Cell Biol. *3*, 140–149.

Khatib, A.M., Siegfried, G., Prat, A., Luis, J., Chrétien, M., Metrakos, P., and Seidah, N.G.

(2001). Inhibition of proprotein convertases is associated with loss of growth and tumorigenicity of HT-29 human colon carcinoma cells: Importance of insulin-like growth factor-1 (IGF-1) receptor processing in IGF-1-mediated functions. J. Biol. Chem. *276*, 30686–30693.

Kidd, S., and Lieber, T. (2002). Furin cleavage is not a requirement for Drosophila Notch function. Mech. Dev. *115*, 41–51.

Kiefer, M.C., Tucker, J.E., Joh, R., Landsberg, K.E., Saltman, D., and Barr, P.J. (1991). Identification of a second human subtilisin-like protease gene in the fes/fps region of chromosome 15. DNA Cell Biol. *10*, 757–769.

Klein-Szanto, A.J., and Bassi, D.E. (2017). Proprotein convertase inhibition: Paralyzing the cell's master switches. Biochem. Pharmacol. *140*, 8–15.

Klimpel, K.R., Molloy, S.S., Thomas, G., and Leppla, S.H. (1992). Anthrax toxin protective antigen is activated by a cell surface protease with the sequence specificity and catalytic properties of furin. Proc. Natl. Acad. Sci. *89*, 10277–10281.

Komatsu, N., Aoki, K., Yamada, M., Yukinaga, H., Fujita, Y., Kamioka, Y., and Matsuda, M. (2011). Development of an optimized backbone of FRET biosensors for kinases and GTPases. Mol. Biol. Cell *22*, 4647–4656.

Kominami, K., Nagai, T., Sawasaki, T., Tsujimura, Y., Yashima, K., Sunaga, Y., Tsuchimochi, M., Nishimura, J., Chiba, K., Nakabayashi, J., et al. (2012). In Vivo Imaging of Hierarchical Spatiotemporal Activation of Caspase-8 during Apoptosis. PLoS One *7*.

Kopan, R., and Ilagan, M.X.G. (2009). The Canonical Notch Signaling Pathway: Unfolding the Activation Mechanism. Cell *137*, 216–233.

Krebs, L.T., Xue, Y., Norton, C.R., Shutter, J.R., Maguire, M., Sundberg, J.P., Gallahan, D., Closson, V., Kitajewski, J., Callahan, R., et al. (2000). Notch signaling is essential for vascular morphogenesis in mice. Genes Dev. *14*, 1343–1352.

Krebs, L.T., Xue, Y., Norton, C.R., Sundberg, J.P., Beatus, P., Lendahl, U., Joutel, A., and Gridley, T. (2003). Characterization of Notch3-Deficient Mice: Normal Embryonic Development and Absence of Genetic Interactions with a Notch1 Mutation. Genesis *37*, 139–143.

Krepler, C., Xiao, M., Samanta, M., Vultur, A., Chen, H.-Y., Brafford, P., Reyes-Uribe, P.I., Halloran, M., Chen, T., He, X., et al. (2015). Targeting Notch enhances the efficacy of ERK inhibitors in BRAF-V600E melanoma. Oncotarget *7*, 71211–71222.

Kubota, Y., Takubo, K., Shimizu, T., Ohno, H., Kishi, K., Shibuya, M., Saya, H., and Suda, T. (2009). M-CSF inhibition selectively targets pathological angiogenesis and lymphangiogenesis. J. Exp. Med. *206*, 1089–1102.

Kudo-Saito, C., Shirako, H., Takeuchi, T., and Kawakami, Y. (2009). Cancer Metastasis Is

Accelerated through Immunosuppression during Snail-Induced EMT of Cancer Cells. Cancer Cell *15*, 195–206.

Kumano, K., Masuda, S., Sata, M., Saito, T., Lee, S.Y., Sakata-Yanagimoto, M., Tomita, T., Iwatsubo, T., Natsugari, H., Kurokawa, M., et al. (2008). Both Notch1 and Notch2 contribute to the regulation of melanocyte homeostasis. Pigment Cell Melanoma Res. *21*, 70–78.

Kumar, V., Behera, R., Lohite, K., Karnik, S., and Kundu, G.C. (2010). p38 kinase is crucial for osteopontin-induced furin expression that supports cervical cancer progression. Cancer Res. *70*, 10381–10391.

Kuphal, S., Bauer, R., and Bosserhoff, A.-K. (2005). Integrin signaling in malignant melanoma. Cancer Metastasis Rev. *24*, 195–222.

Kusakabe, M., Cheong, P.L., Nikfar, R., McLennan, I.S., and Koishi, K. (2008). The structure of the TGF-β latency associated peptide region determines the ability of the proprotein convertase furin to cleave TGF-βs. J. Cell. Biochem. *103*, 311–320.

Lade-Keller, J., Riber-Hansen, R., Guldberg, P., Schmidt, H., Hamilton-Dutoit, S.J., and Steiniche, T. (2013). E- to N-cadherin switch in melanoma is associated with decreased expression of phosphatase and tensin homolog and cancer progression. Br. J. Dermatol. *169*, 618–628.

Ladinsky, M.S., and Howell, K.E. (1993). An electron microscopic study of TGN38/41 dynamics. J. Cell Sci. Suppl. *17*, 41–47.

Lalou, C., Scamuffa, N., Mourah, S., Plassa, F., Podgorniak, M.P., Soufir, N., Dumaz, N., Calvo, F., Basset-Seguin, N., and Khatib, A.M. (2010). Inhibition of the proprotein convertases represses the invasiveness of human primary melanoma cells with altered p53, CDKN2A and N-Ras genes. PLoS One *5*, e9992.

Lapierre, M., Siegfried, G., Scamuffa, N., Bontemps, Y., Calvo, F., Seidah, N.G., and Khatib, A.M. (2007). Opposing function of the proprotein convertases furin and PACE4 on breast cancer cells' malignant phenotypes: Role of tissue inhibitors of metalloproteinase-1. Cancer Res. *67*, 9030–9034.

Lázár-Molnár, E., Hegyesi, H., Tóth, S., and Falus, A. (2000). Autocrine and paracrine regulation by cytokines and growth factors in melanoma. Cytokine *12*, 547–554.

Lee, M., Ryu, C.H., Chang, H.W., Kim, G.C., Kim, S.W., and Kim, S.Y. (2016). Radiotherapy-associated Furin Expression and Tumor Invasiveness in Recurrent Laryngeal Cancer. Anticancer Res. *36*, 5117–5126.

Lehmann, M., Rigot, V., Seidah, N.G., Marvaldi, J., and Lissitzky, J.C. (1996). Lack of integrin alpha-chain endoproteolytic cleavage in furin-deficient human colon adenocarcinoma cells LoVo. Biochem. J. *317 (Pt 3*, 803–809.

Lehmann, M., André, F., Bellan, C., Remacle-Bonnet, M., Garrouste, F., Parat, F., Lissitsky, J.C., Marvaldi, J., and Pommier, G. (1998). Deficient processing and activity of type I insulin-like growth factor receptor in the furin-deficient LoVo-C5 cells. Endocrinology *139*, 3763–3771.

Leonhardt, R.M., Fiegl, D., Rufer, E., Karger, A., Bettin, B., and Knittler, M.R. (2010). Post-Endoplasmic Reticulum Rescue of Unstable MHC Class I Requires Proprotein Convertase PC7. J. Immunol. *184*, 2985–2998.

Leonhardt, R.M., Vigneron, N., Rahner, C., and Cresswell, P. (2011). Proprotein convertases process Pmel17 during secretion. J. Biol. Chem. *286*, 9321–9337.

Levesque, C., Fugère, M., Kwiatkowska, A., Couture, F., Desjardins, R., Routhier, S., Moussette, P., Prahl, A., Lammek, B., Appel, J.R., et al. (2012). The multi-leu peptide inhibitor discriminates between PACE4 and furin and exhibits antiproliferative effects on prostate cancer cells. J. Med. Chem. *55*, 10501–10511.

Levy, C., Khaled, M., and Fisher, D.E. (2006). MITF: master regulator of melanocyte development and melanoma oncogene. Trends Mol. Med. *12*, 406–414.

Levy, C., Khaled, M., Iliopoulos, D., Janas, M.M., Schubert, S., Pinner, S., Chen, P.H., Li, S., Fletcher, A.L., Yokoyama, S., et al. (2010). Intronic miR-211 Assumes the Tumor Suppressive Function of Its Host Gene in Melanoma. Mol. Cell *40*, 841–849.

Lewis, M.J., and Pelham, H.R. (1990). A human homologue of the yeast HDEL receptor. Nature *348*, 162–163.

Li, M., Chen, X., Ye, Q.Z., Vogt, A., and Yin, X.M. (2012). A high-throughput FRET-based assay for determination of Atg4 activity. Autophagy *8*, 401–412.

Lidke, D.S., Nagy, P., Barisas, B.G., Heintzmann, R., Post, J.N., Lidke, K. a, Clayton, a H. a, Arndt-Jovin, D.J., and Jovin, T.M. (2003). Imaging molecular interactions in cells by dynamic and static fluorescence anisotropy (rFLIM and emFRET). Biochem. Soc. Trans. *31*, 1020–1027.

Lin, A.W., Barradas, M., Stone, J.C., Van Aelst, L., Serrano, M., and Lowe, S.W. (1998). Premature senescence involving p53 and p16 is activated in response to constitutive MEK/MAPK mitogenic signaling. Genes Dev. *12*, 3008–3019.

Lissitzky, J.C., Luis, J., Munzer, J.S., Benjannet, S., Parat, F., Chrétien, M., Marvaldi, J., and Seidah, N.G. (2000). Endoproteolytic processing of integrin pro-alpha subunits involves the redundant function of furin and proprotein convertase (PC) 5A, but not paired basic amino acid converting enzyme (PACE) 4, PC5B or PC7. Biochem. J. *346 Pt 1*, 133–138.

Liu, B., Li, G., Wang, X., and Liu, Y. (2014a). A furin inhibitor downregulates osteosarcoma cell migration by downregulating the expression levels of MT1-MMP via the Wnt signaling pathway. Oncol. Lett. *7*, 1033–1038.

References

Liu, J., Fukunaga-Kalabis, M., Li, L., and Herlyn, M. (2014b). Developmental pathways activated in melanocytes and melanoma. Arch. Biochem. Biophys. *563*, 13–21.

Liu, Y., Ye, F., Li, Q., Tamiya, S., Darling, D.S., Kaplan, H.J., and Dean, D.C. (2009). Zeb1 represses Mitf and regulates pigment synthesis, cell proliferation, and epithelial morphology. Investig. Ophthalmol. Vis. Sci. *50*, 5080–5088.

Liu, Z.J., Xiao, M., Balint, K., Smalley, K.S.M., Brafford, P., Qiu, R., Pinnix, C.C., Li, X., and Herlyn, M. (2006). Notch1 signaling promotes primary melanoma progression by activating mitogen-activated protein kinase/phosphatidylinositol 3-kinase-Akt pathways and up-regulating N-cadherin expression. Cancer Res. *66*, 4182–4190.

Loercher, A.E., Tank, E.M.H., Delston, R.B., and Harbour, J.W. (2005). MITF links differentiation with cell cycle arrest in melanocytes by transcriptional activation of INK4A. J. Cell Biol. *168*, 35–40.

Logeat, F., Bessia, C., Brou, C., LeBail, O., Jarriault, S., Seidah, N.G., and Israël, A. (1998). The Notch1 receptor is cleaved constitutively by a furin-like convertase. Proc. Natl. Acad. Sci. U. S. A. *95*, 8108–8112.

Long, J.Z., and Cravatt, B.F. (2011). The metabolic serine hydrolases and their functions in mammalian physiology and disease. Chem. Rev. *111*, 6022–6063.

Long, G. V., Menzies, A.M., Nagrial, A.M., Haydu, L.E., Hamilton, A.L., Mann, G.J., Hughes, T.M., Thompson, J.F., Scolyer, R.A., and Kefford, R.F. (2011). Prognostic and clinicopathologic associations of oncogenic BRAF in metastatic melanoma. J. Clin. Oncol. *29*, 1239–1246.

Longuespée, R., Couture, F., Levesque, C., Kwiatkowska, A., Desjardins, R., Gagnon, S., Vergara, D., Maffia, M., Fournier, I., Salzet, M., et al. (2014). Implications of proprotein convertases in ovarian cancer cell proliferation and tumor progression: Insights for pace4 as a therapeutic target. Transl. Oncol. *7*, 410–419.

Van De Loo, J.W.H.P., Creemers, J.W.M., Bright, N.A., Young, B.D., Roebroek, A.J.M., and Van De Ven, W.J.M. (1997). Biosynthesis, distinct post-translational modifications, and functional characterization of lymphoma proprotein convertase. J. Biol. Chem. *272*, 27116–27123.

Loomans, H.A., Andl, C.D., Andl, C.D., Andl, C.D., Andl, C.D., and Andl, C.D. (2014). Intertwining of activin a and TGFβ signaling: Dual roles in cancer progression and cancer cell invasion. Cancers (Basel). *7*, 70–91.

López-Otín, C., and Overall, C.M. (2002). Protease degradomics: A new challenge for proteomics. Nat. Rev. Mol. Cell Biol. *3*, 509–519.

Lopez-Perez, E., Seidah, N.G., and Checler, F. (1999). Proprotein convertase activity

contributes to the processing of the Alzheimer's beta-amyloid precursor protein in human cells: evidence for a role of the prohormone convertase PC7 in the constitutive alpha-secretase pathway. J Neurochem *73*, 2056–2062.

Lopez-Perez, E., Zhang, Y., Frank, S.J., Creemers, J., Seidah, N., and Checler, F. (2001). Constitutive alpha-secretase cleavage of the beta-amyloid precursor protein in the furin-deficient LoVo cell line: Involvement of the pro-hormone convertase 7 and the disintegrin metalloprotease ADAM10. J. Neurochem. *76*, 1532–1539.

López de Cicco, R., Bassi, D.E., Page, R., and Klein-Szanto, A.J. (2002). Furin expression in squamous cell carcinomas of the oral cavity and other sites evaluated by tissue microarray technology. Acta Odontológica Latinoam. AOL *15*, 29–37.

Lorigan, J.G., Wallace, S., and Mavligit, G.M. (1991). The prevalence and location of metastases from ocular melanoma: Imaging study in 110 patients. Am. J. Roentgenol. *157*, 1279–1281.

Louagie, E., Taylor, N. a, Flamez, D., Roebroek, A.J.M., Bright, N. a, Meulemans, S., Quintens, R., Herrera, P.L., Schuit, F., Van de Ven, W.J.M., et al. (2008). Role of furin in granular acidification in the endocrine pancreas: identification of the V-ATPase subunit Ac45 as a candidate substrate. Proc. Natl. Acad. Sci. U. S. A. *105*, 12319–12324.

Luo, C., Tetteh, P.W., Merz, P.R., Dickes, E., Abukiwan, A., Hotz-Wagenblatt, A., Holland-Cunz, S., Sinnberg, T., Schittek, B., Schadendorf, D., et al. (2013). miR-137 Inhibits the Invasion of Melanoma Cells through Downregulation of Multiple Oncogenic Target Genes. J. Invest. Dermatol. *133*, 768–775.

Lusson, J., Vieau, D., Hamelin, J., Day, R., Chrétien, M., and Seidah, N.G. (1993). cDNA structure of the mouse and rat subtilisin/kexin-like PC5: a candidate proprotein convertase expressed in endocrine and nonendocrine cells. Proc. Natl. Acad. Sci. U. S. A. *90*, 6691–6695.

Luzio, J.P., Brake, B., Banting, G., Howell, K.E., Braghetta, P., and Stanley, K.K. (1990). Identification, sequencing and expression of an integral membrane protein of the trans-Golgi network (TGN38). Biochem. J. *270*, 97–102.

Ma, Y.-C., Fan, W.-J., Rao, S.-M., Gao, L., Bei, Z.-Y., and Xu, S.-T. (2014). Effect of Furin inhibitor on lung adenocarcinoma cell growth and metastasis. Cancer Cell Int. *14*, 43.

Machen, T.E., Leigh, M.J., Taylor, C., Kimura, T., Asano, S., and Moore, H.-P.H. (2003). pH of TGN and recycling endosomes of H+/K+-ATPase-transfected HEK-293 cells: implications for pH regulation in the secretory pathway. AJP Cell Physiol. *285*, C205–C214.

Maehama, T., and Dixon, J.E. (1999). PTEN: A tumour suppressor that functions as a phospholipid phosphatase. Trends Cell Biol. *9*, 125–128.

Malide, D., Seidah, N.G., Chrétien, M., and Bendayan, M. (1995). Electron microscopic

immunocytochemical evidence for the involvement of the convertases PC1 and PC2 in the processing of proinsulin in pancreatic beta-cells. J. Histochem. Cytochem. *43*, 11–19.

Malkani, N., and Schmid, J.A. (2011). Some secrets of fluorescent proteins: Distinct bleaching in various mounting fluids and photoactivation of cyan fluorescent proteins at YFP-excitation. PLoS One *6*, e18586.

Mallet, W.G., and Maxfield, F.R. (1999). Chimeric forms of furin and TGN38 are transported from the plasma membrane to the trans-Golgi network via distinct endosomal pathways. J. Cell Biol. *146*, 345–359.

Mansky, K.C., Sankar, U., Han, J., and Ostrowski, M.C. (2002). Microphthalmia transcription factor is a target of the p38 MAPK pathway in response to receptor activator of NF-κB ligand signaling. J. Biol. Chem. *277*, 11077–11083.

Maquoi, E., Noël, A., Frankenne, F., Angliker, H., Murphy, G., and Foidart, J.M. (1998). Inhibition of matrix metalloproteinase 2 maturation and HT1080 invasiveness by a synthetic furin inhibitor. FEBS Lett. *424*, 262–266.

Maret, D., Gruzglin, E., Sadr, M.S., Siu, V., Shan, W., Koch, A.W., Seidah, N.G., Del Maestro, R.F., and Colman, D.R. (2010). Surface expression of precursor N-cadherin promotes tumor cell invasion. Neoplasia *12*, 1066–1080.

Maret, D., Sadr, E.S., Colman, D.R., Del Maestro, R.F., and Seidah, N.G. (2012). Opposite Roles of Furin and PC5A in N-cadherin Processing. Neoplasia *14*, 880–892, IN1–IN3.

Markwardt, M.L., Kremers, G.J., Kraft, C.A., Ray, K., Cranfill, P.J.C., Wilson, K.A., Day, R.N., Wachter, R.M., Davidson, M.W., and Rizzo, M.A. (2011). An improved cerulean fluorescent protein with enhanced brightness and reduced reversible photoswitching. PLoS One *6*.

Marschner, K., Kollmann, K., Schweizer, M., Braulke, T., and Pohl, S. (2011). A Key Enzyme in the Biogenesis of Lysosomes Is a Protease That Regulates Cholesterol Metabolism. Science (80-.). *333*, 87–90.

Mason, A.J., Farnworth, P.G., and Sullivan, J. (1996). Characterization and determination of the biological activities of noncleavable high molecular weight forms of inhibin A and activin A. Mol. Endocrinol. *10*, 1055–1065.

Massagué, J. (2008). TGFβ in Cancer. Cell *134*, 215–230.

Massi, D., Tarantini, F., Franchi, A., Paglierani, M., Di Serio, C., Pellerito, S., Leoncini, G., Cirino, G., Geppetti, P., and Santucci, M. (2006). Evidence for differential expression of Notch receptors and their ligands in melanocytic nevi and cutaneous malignant melanoma. Mod. Pathol. *19*, 246–254.

Maxwell, K.N., and Breslow, J.L. (2004). Adenoviral-mediated expression of Pcsk9 in mice

results in a low-density lipoprotein receptor knockout phenotype. Proc. Natl. Acad. Sci. *101*, 7100–7105.

Maxwell, K.N., Fisher, E.A., and Breslow, J.L. (2005). Overexpression of PCSK9 accelerates the degradation of the LDLR in a post-endoplasmic reticulum compartment. Proc. Natl. Acad. Sci. U. S. A. *102*, 2069–2074.

Mayer, G., Hamelin, J., Asselin, M.C., Pasquato, A., Marcinkiewicz, E., Tang, M., Tabibzadeh, S., and Seidah, N.G. (2008). The regulated cell surface zymogen activation of the proprotein convertase PC5A directs the processing of its secretory substrates. J. Biol. Chem. *283*, 2373–2384.

Mbikay, M., Tadros, H., Ishida, N., Lerner, C.P., De Lamirande, E., Chen, A., El-Alfy, M., Clermont, Y., Seidah, N.G., Chrétien, M., et al. (1997a). Impaired fertility in mice deficient for the testicular germ-cell protease PC4. Proc. Natl. Acad. Sci. U. S. A. *94*, 6842–6846.

Mbikay, M., Sirois, F., Yao, J., Seidah, N.G., and Chrétien, M. (1997b). Comparative analysis of expression of the proprotein convertases furin, PACE4, PC1 and PC2 in human lung tumours. Br. J. Cancer *75*, 1509–1514.

McColl, B.K., Paavonen, K., Karnezis, T., Harris, N.C., Davydova, N., Rothacker, J., Nice, E.C., Harder, K.W., Roufail, S., Hibbs, M.L., et al. (2007). Proprotein convertases promote processing of VEGF-D, a critical step for binding the angiogenic receptor VEGFR-2. FASEB J. *21*, 1088–1098.

McMahon, S., Grondin, F., McDonald, P.P., Richard, D.E., and Dubois, C.M. (2005). Hypoxia-enhanced expression of the proprotein convertase furin is mediated by hypoxia-inducible factor-1: Impact on the bioactivation of proproteins. J. Biol. Chem. *280*, 6561–6569.

McNutt, M.C., Lagace, T. a, and Horton, J.D. (2007). Catalytic activity is not required for secreted PCSK9 to reduce low density lipoprotein receptors in HepG2 cells. J. Biol. Chem. *282*, 20799–20803.

Meerabux, J., Yaspo, M.L., Roebroek, A.J., Van De Ven, W.J.M., Lister, T.A., and Young, B.D. (1996). A new member of the proprotein convertase gene family (LPC) is located at a chromosome translocation breakpoint in lymphomas. Cancer Res. *56*, 448–451.

Mercapide, J., De Cicco, R.L., Bassi, D.E., Castresana, J.S., Thomas, G., and Klein-Szanto, A.J.P. (2002). Inhibition of furin-mediated processing results in suppression of astrocytoma cell growth and invasiveness. Clin. Cancer Res. *8*, 1740–1746.

Mesnard, D., and Constam, D.B. (2010). Imaging proprotein convertase activities and their regulation in the implanting mouse blastocyst. J. Cell Biol. *191*, 129–139.

Mesnard, D., Donnison, M., Fuerer, C., Pfeffer, P.L., and Constam, D.B. (2011). The microenvironment patterns the pluripotent mouse epiblast through paracrine furin and Pace4

proteolytic activities. Genes Dev. *25*, 1871–1880.

Mi, L.-Z., Brown, C.T., Gao, Y., Tian, Y., Le, V.Q., Walz, T., and Springer, T.A. (2015). Structure of bone morphogenetic protein 9 procomplex. Proc. Natl. Acad. Sci. 201501303.

Miller, A.J., Levy, C., Davis, I.J., Razin, E., and Fisher, D.E. (2005). Sumoylation of MITF and its related family members TFE3 and TFEB. J. Biol. Chem. *280*, 146–155.

Millington, M., Grindlay, G.J., Altenbach, K., Neely, R.K., Kolch, W., Benčina, M., Read, N.D., Jones, A.C., Dryden, D.T.F., and Magennis, S.W. (2007). High-precision FLIM-FRET in fixed and living cells reveals heterogeneity in a simple CFP-YFP fusion protein. Biophys. Chem. *127*, 155–164.

Miura, H., Matsuda, M., and Aoki, K. (2014). Development of a FRET Biosensor with High Specificity for Akt. Cell Struct. Funct. *39*, 9–20.

Miyawaki, a, Llopis, J., Heim, R., McCaffery, J.M., Adams, J. a, Ikura, M., and Tsien, R.Y. (1997). Fluorescent indicators for Ca2+ based on green fluorescent proteins and calmodulin. Nature *388*, 882–887.

Mizutani, T., Kondo, T., Darmanin, S., Tsuda, M., Tanaka, S., Tobiume, M., Asaka, M., and Ohba, Y. (2010). A novel FRET-based biosensor for the measurement of BCR-ABL activity and its response to drugs in living cells. Clin. Cancer Res. *16*, 3964–3975.

Molloy, S.S., Thomas, L., Vanslyke, J.K., Stenberg1, P.E., and Thomas2, G. (1994). Intracellular trafficking and activation of the furin proprotein convertase: localization to the TGN and recycling from the cell surface. EMBO J. *13*, 18–33.

Molloy, S.S., Thomas, L., Kamibayashi, C., Mumby, M.C., and Thomas, G. (1998). Regulation of endosome sorting by a specific PP2A isoform. J. Cell Biol. *142*, 1399–1411.

Molloy, S.S., Anderson, E.D., Jean, F., and Thomas, G. (1999). Bi-cycling the furin pathway: From TGN localization to pathogen activation and embryogenesis. Trends Cell Biol. *9*, 28–35.

Monahan, K.B., Rozenberg, G.I., Krishnamurthy, J., Johnson, S.M., Liu, W., Bradford, M.K., Horner, J., Depinho, R. a, and Sharpless, N.E. (2010). Somatic p16(INK4a) loss accelerates melanomagenesis. Oncogene *29*, 5809–5817.

Moriyama, M., Osawa, M., Mak, S.S., Ohtsuka, T., Yamamoto, N., Han, H., Delmas, V., Kageyama, R., Beermann, F., Larue, L., et al. (2006). Notch signaling via Hes1 transcription factor maintains survival of melanoblasts and melanocyte stem cells. J. Cell Biol. *173*, 333–339.

Mort, R.L., Jackson, I.J., and Patton, E.E. (2015). The melanocyte lineage in development and disease. Development *142*, 1387–1387.

Munzer, J.S., Basak, A., Zhong, M., Mamarbachi, A., Hamelin, J., Savaria, D., Lazure, C.,

Hendy, G.N., Benjannet, S., Chretien, M., et al. (1997). In vitro characterization of the novel proprotein convertase PC7. J Biol Chem *272*, 19672–19681.

Murakami, H., and Arnheiter, H. (2005). Sumoylation modulates transcriptional activity of MITF in a promoter-specific manner. Pigment Cell Res. *18*, 265–277.

Murdoch, C., Muthana, M., Coffelt, S.B., and Lewis, C.E. (2008). The role of myeloid cells in the promotion of tumour angiogenesis. Nat. Rev. Cancer *8*, 618–631.

Nagy, J.A., Chang, S.-H., Dvorak, A.M., and Dvorak, H.F. (2009). Why are tumour blood vessels abnormal and why is it important to know? Br. J. Cancer *100*, 865–869.

Nagy, J.A., Chang, S.H., Shih, S.C., Dvorak, A.M., and Dvorak, H.F. (2010). Heterogeneity of the tumor vasculature. Semin. Thromb. Hemost. *36*, 321–331.

Nakagawa, T., Murakami, K., and Nakayama, K. (1993). Identification of an isoform with an extremely large Cys-rich region of PC6, a Kex2-like processing endoprotease. FEBS Lett. *327*, 165–171.

Nakajima, T., Konda, Y., Kanai, M., Izumi, Y., Kanda, N., Nanakin, A., Kitazawa, S., and Chiba, T. (2002). Prohormone convertase furin has a role in gastric cancer cell proliferation with parathyroid hormone-related peptide in a reciprocal manner. Dig. Dis. Sci. *47*, 2729–2737.

Nakayama, K. (1997). Furin: a mammalian subtilisin/Kex2p-like endoprotease involved in processing of a wide variety of precursor proteins. Biochem. J. *327 (Pt 3*, 625–635.

Nassoury, N., Blasiole, D.A., Tebon Oler, A., Benjannet, S., Hamelin, J., Poupon, V., McPherson, P.S., Attie, A.D., Prat, A., and Seidah, N.G. (2007). The cellular trafficking of the secretory proprotein convertase PCSK9 and its dependence on the LDLR. Traffic *8*, 718–732.

Nejjari, M., Berthet, V., Rigot, V., Laforest, S., Jacquier, M.-F., Seidah, N.G., Remy, L., Bruyneel, E., Scoazec, J.-Y., Marvaldi, J., et al. (2004). Inhibition of proprotein convertases enhances cell migration and metastases development of human colon carcinoma cells in a rat model. Am. J. Pathol. *164*, 1925–1933.

Nelsen, S.M., and Christian, J.L. (2009). Site-specific cleavage of BMP4 by furin, PC6, and PC7. J. Biol. Chem. *284*, 27157–27166.

Nemunaitis, J., Barve, M., Orr, D., Kuhn, J., Magee, M., Lamont, J., Bedell, C., Wallraven, G., Pappen, B.O., Roth, A., et al. (2014). Summary of bi-shRNA [furin] /GM-CSF Augmented Autologous Tumor Cell Immunotherapy (FANG[TM]) in Advanced Cancer of the Liver. Oncology *87*, 21–29.

Nicholson, K.M., and Anderson, N.G. (2002). The protein kinase B/Akt signalling pathway in human malignancy. Cell. Signal. *14*, 381–395.

Nicolas, M., Wolfer, A., Raj, K., Kummer, J.A., Mill, P., van Noort, M., Hui, C., Clevers, H.,

Dotto, G.P., and Radtke, F. (2003). Notch1 functions as a tumor suppressor in mouse skin. Nat. Genet. *33*, 416–421.

Nobis, M., McGhee, E.J., Morton, J.P., Schwarz, J.P., Karim, S.A., Quinn, J., Edward, M., Campbell, A.D., McGarry, L.C., Evans, T.R.J., et al. (2013). Intravital FLIM-FRET imaging reveals dasatinib-induced spatial control of Src in pancreatic cancer. Cancer Res. *73*, 4674–4686.

Nobori, T., Miura, K., Wu, D.J., Lois, A., Takabayashi, K., and Carson, D.A. (1994). Deletions of the cyclin-dependent kinase-4 inhibitor gene in multiple human cancers. Nature *368*, 753–756.

Nour, N., Basak, A., Chrétien, M., and Seidah, N.G. (2003). Structure-function analysis of the prosegment of the proprotein convertase PC5A. J. Biol. Chem. *278*, 2886–2895.

Nour, N., Mayer, G., Mort, J.S., Salvas, A., Mbikay, M., Morrison, C.J., Overall, C.M., and Seidah, N.G. (2005). The Cysteine-rich Domain of the Secreted Proprotein Convertases PC5A and PACE4 Functions as a Cell Surface Anchor and Interacts with Tissue Inhibitors of Metalloproteinases □ D. Mol. Biol. Cell *16*, 5215–5226.

Nowell, C.S., and Radtke, F. (2017). Notch as a tumour suppressor. Nat. Rev. Cancer *17*, 145–159.

Oexle, K., Ried, J.S., Hicks, A.A., Tanaka, T., Hayward, C., Bruegel, M., Gögele, M., Lichtner, P., Müller-Myhsok, B., Döring, A., et al. (2011). Novel association to the proprotein convertase PCSK7 gene locus revealed by analysing soluble transferrin receptor (sTfR) levels. Hum. Mol. Genet. *20*, 1042–1047.

Oh, J., Barve, M., Matthews, C.M., Koon, E.C., Heffernan, T.P., Fine, B., Grosen, E., Bergman, M.K., Fleming, E.L., DeMars, L.R., et al. (2016). Phase II study of Vigil® DNA engineered immunotherapy as maintenance in advanced stage ovarian cancer. Gynecol. Oncol. *143*, 504–510.

Olenych, S.G., Claxton, N.S., Ottenberg, G.K., and Davidson, M.W. (2007). The Fluorescent Protein Color Palette. In Current Protocols in Cell Biology, p.

Omholt, K., Platz, A., Kanter, L., Ringborg, U., and Hansson, J. (2003). NRAS and BRAF Mutations Arise Early during Melanoma Pathogenesis and Are Preserved throughout Tumor Progression. Clin. Cancer Res. *9*, 6483–6488.

Ortega, S., Malumbres, M., and Barbacid, M. (2002). Cyclin D-dependent kinases, INK4 inhibitors and cancer. Biochim. Biophys. Acta - Rev. Cancer *1602*, 73–87.

Ouyang, M., Lu, S., Li, X.-Y., Xu, J., Seong, J., Giepmans, B.N.G., Shyy, J.Y.-J., Weiss, S.J., and Wang, Y. (2008). Visualization of polarized membrane type 1 matrix metalloproteinase activity in live cells by fluorescence resonance energy transfer imaging. J. Biol. Chem. *283*,

17740–17748.

Ozawa, M., and Kemler, R. (1990). Correct proteolytic cleavage is required for the cell adhesive function of uvomorulin. J. Cell Biol. *111*, 1645–1650.

Page, R.E., Klein-Szanto, A.J.P., Litwin, S., Nicolas, E., Al-Jumaily, R., Alexander, P., Godwin, A.K., Ross, E.A., Schilder, R.J., and Bassi, D.E. (2007). Increased expression of the pro-protein convertase furin predicts decreased survival in ovarian cancer. Cell. Oncol. *29*, 289–299.

Page-McCaw, A., Ewald, A.J., and Werb, Z. (2007). Matrix metalloproteinases and the regulation of tissue remodelling. Nat. Rev. Mol. Cell Biol. *8*, 221–233.

Paquet, L., Bergeron, F., Boudreault, A., Seidah, N.G., Chrétien, M., Mbikay, M., and Lazure, C. (1994). The neuroendocrine precursor 7B2 is a sulfated protein proteolytically processed by a ubiquitous furin-like convertase. J. Biol. Chem. *269*, 19279–19285.

Park, S.W., Moon, Y.-A., and Horton, J.D. (2004). Post-transcriptional regulation of low density lipoprotein receptor protein by proprotein convertase subtilisin/kexin type 9a in mouse liver. J. Biol. Chem. *279*, 50630–50638.

Parmiter, A.H., Balaban, G., Clark, W.H., and Nowell, P.C. (1988). Possible involvement of the chromosome region 10q24-q26 in early stages of melanocytic neoplasia. Cancer Genet. Cytogenet. *30*, 313–317.

Pasquato, A., Pullikotil, P., Asselin, M.C., Vacatello, M., Paolillo, L., Ghezzo, F., Basso, F., Di Bello, C., Dettin, M., and Seidah, N.G. (2006). The proprotein convertase SKI-1/S1P: In vitro analysis of Lassa virus glycoprotein-derived substrates and ex vivo validation of irreversible peptide inhibitors. J. Biol. Chem. *281*, 23471–23481.

Paster, W., Paar, C., Eckerstorfer, P., Jakober, A., Drbal, K., Schutz, G.J., Sonnleitner, A., and Stockinger, H. (2009). Genetically Encoded Forster Resonance Energy Transfer Sensors for the Conformation of the Src Family Kinase Lck. J. Immunol. *182*, 2160–2167.

Paulino, C., and Kühlbrandt, W. (2014). pH- and sodium-induced changes in a sodium/proton antiporter. Elife *3*, e01412.

Pei, D., and Weiss, S.J. (1995). Furin-dependent intracellular activation of the human stromelysin-3 zymogen. Nature *375*, 244–247.

Perl, A.-K., Wilgenbus, P., Dahl, U., Semb, H., and Christofori, G. (1998). A causal role for E-cadherin in the transition from adenoma to carcinoma. Nature *392*, 190–193.

Peschon, J.J. (1998). An Essential Role for Ectodomain Shedding in Mammalian Development. Science (80-.). *282*, 1281–1284.

Pesu, M., Watford, W.T., Wei, L., Xu, L., Fuss, I., Strober, W., Andersson, J., Shevach, E.M.,

Quezado, M., Bouladoux, N., et al. (2008). T-cell-expressed proprotein convertase furin is essential for maintenance of peripheral immune tolerance. Nature *455*, 246–250.

Pierrat, M.J., Marsaud, V., Mauviel, A., and Javelaud, D. (2012). Expression of microphthalmia-associated transcription factor (MITF), which is critical for melanoma progression, is inhibited by both transcription factor GLI2 and transforming growth factor-β. J. Biol. Chem. *287*, 17996–18004.

Pietras, K., Pahler, J., Bergers, G., and Hanahan, D. (2008). Functions of paracrine PDGF signaling in the proangiogenic tumor stroma revealed by pharmacological targeting. PLoS Med. *5*, 0123–0138.

Pinner, S., Jordan, P., Sharrock, K., Bazley, L., Collinson, L., Marais, R., Bonvin, E., Goding, C., and Sahai, E. (2009). Intravital Imaging Reveals Transient Changes in Pigment Production and Brn2 Expression during Metastatic Melanoma Dissemination and Brn2 Expression during Metastatic Melanoma Dissemination. Cancer Res. *69*, 7969–7977.

Pinnix, C.C., and Herlyn, M. (2007). The many faces of Notch signaling in skin-derived cells. Pigment Cell Res. *20*, 458–465.

Pinnix, C.C., Lee, J.T., Liu, Z.J., McDaid, R., Balint, K., Beverly, L.J., Brafford, P.A., Xiao, M., Himes, B., Zabierowski, S.E., et al. (2009). Active Notch1 confers a transformed phenotype to primary human melanocytes. Cancer Res. *69*, 5312–5320.

Pomerantz, J., Schreiber-Agus, N., Liégeois, N.J., Silverman, A., Alland, L., Chin, L., Potes, J., Chen, K., Orlow, I., Lee, H.W., et al. (1998). The Ink4a tumor suppressor gene product, p19(Arf), interacts with MDM2 and neutralizes MDM2's inhibition of p53. Cell *92*, 713–723.

Posthaus, H., Dubois, C.M., Laprise, M.H., Grondin, F., Suter, M.M., and Müller, E. (1998). Proprotein cleavage of E-cadherin by furin in baculovirus over-expression system: Potential role of other convertases in mammalian cells. FEBS Lett. *438*, 306–310.

Postina, R., Schroeder, A., Dewachter, I., Bohl, J., Schmitt, U., Kojro, E., Prinzen, C., Endres, K., Hiemke, C., Blessing, M., et al. (2004). A disintegrin-metalloproteinase prevents amyloid plaque formation and hippocampal defects in an Alzheimer disease mouse model. J. Clin. Invest. *113*, 1456–1464.

Price, E.R., Horstmann, M.A., Wells, A.G., Weilbaecher, K.N., Takemoto, C.M., Landis, M.W., and Fisher, D.E. (1998). Alpha-Melanocyte-stimulating Hormone Signaling Regulates Expression of microphthalmia, a Gene Deficient in Waardenburg Syndrome. J. Biol. Chem. *273*, 33042–33047.

Proweller, A., Tu, L., Lepore, J.J., Cheng, L., Lu, M.M., Seykora, J., Millar, S.E., Pear, W.S., and Parmacek, M.S. (2006). Impaired notch signaling promotes De novo squamous cell carcinoma formation. Cancer Res. *66*, 7438–7444.

Pullikotil, P., Benjannet, S., Mayne, J., and Seidah, N.G. (2007). The proprotein convertase SKI-1/S1P: Alternate translation and subcellular localization. J. Biol. Chem. *282*, 27402–27413.

Qin, J.-Z., Stennett, L., Bacon, P., Bodner, B., Hendrix, M.J.C., Seftor, R.E.B., Seftor, E. a, Margaryan, N. V, Pollock, P.M., Curtis, A., et al. (2004). p53-independent NOXA induction overcomes apoptotic resistance of malignant melanomas. Mol. Cancer Ther. *3*, 895–902.

Qiu, H., Tang, X., Ma, J., Shaverdashvili, K., Zhang, K., and Bedogni, B. (2015). Notch1 Autoactivation via Transcriptional Regulation of Furin, Which Sustains Notch1 Signaling by Processing Notch1-Activating Proteases ADAM10 and Membrane Type 1 Matrix Metalloproteinase. Mol. Cell. Biol. *35*, 3622–3632.

Radtke, F., and Raj, K. (2003). The role of Notch in tumorigenesis: oncogene or tumour suppressor? Nat. Rev. Cancer *3*, 756–767.

Rajendran, L., Honsho, M., Zahn, T.R., Keller, P., Geiger, K.D., Verkade, P., and Simons, K. (2006). Alzheimer's disease beta-amyloid peptides are released in association with exosomes. Proc. Natl. Acad. Sci. *103*, 11172–11177.

Rajendran, L., Schneider, A., Schlechtingen, G., Weidlich, S., Ries, J., Braxmeier, T., Schwille, P., Schulz, J.B., Schroeder, C., Simons, M., et al. (2008). Efficient inhibition of the Alzheimer's disease beta-secretase by membrane targeting. Science (80-.). *320*, 520–523.

Rajendran, L., Knölker, H.-J., and Simons, K. (2010). Subcellular targeting strategies for drug design and delivery. Nat. Rev. Drug Discov. *9*, 29–42.

Ran, F.A., Hsu, P.D., Wright, J., Agarwala, V., Scott, D.A., and Zhang, F. (2013). Genome engineering using the CRISPR-Cas9 system. Nat. Protoc. *8*, 2281–2308.

Randriamampita, C., Mouchacca, P., Malissen, B., Marguet, D., Trautmann, A., and Lellouch, A.C. (2008). A novel ZAP-70 dependent FRET based biosensor reveals kinase activity at both the immunological synapse and the antisynapse. PLoS One *3*.

Rao, D.D., Maples, P.B., Senzer, N., Kumar, P., Wang, Z., Pappen, B.O., Yu, Y., Haddock, C., Jay, C., Phadke, a P., et al. (2010). Enhanced target gene knockdown by a bifunctional shRNA: a novel approach of RNA interference. Cancer Gene Ther. *17*, 780–791.

Raposo, G., and Marks, M.S. (2007). Melanosomes — dark organelles enlighten endosomal membrane transport. Nat. Rev. Mol. Cell Biol. *8*, 786–797.

Rashid, S., Curtis, D.E., Garuti, R., Anderson, N.N., Bashmakov, Y., Ho, Y.K., Hammer, R.E., Moon, Y.-A., and Horton, J.D. (2005). Decreased plasma cholesterol and hypersensitivity to statins in mice lacking Pcsk9. Proc. Natl. Acad. Sci. U. S. A. *102*, 5374–5379.

Rawlings, N.D., and Barrett, A.J. (1999). MEROPS: The peptidase database. Nucleic Acids

Res. *27*, 325–331.

Raza, A., Franklin, M.J., and Dudek, A.Z. (2010). Pericytes and vessel maturation during tumor angiogenesis and metastasis. Am. J. Hematol. *85*, 593–598.

Remacle, A.G., Shiryaev, S.A., Oh, E.S., Cieplak, P., Srinivasan, A., Wei, G., Liddington, R.C., Ratnikov, B.I., Parent, A., Desjardins, R., et al. (2008). Substrate cleavage analysis of furin and related proprotein convertases: A comparative study. J. Biol. Chem. *283*, 20897–20906.

Rizzo, M.A., Springer, G.H., Granada, B., and Piston, D.W. (2004). An improved cyan fluorescent protein variant useful for FRET. Nat. Biotechnol. *22*, 445–449.

Rizzo, M. a, Springer, G., Segawa, K., Zipfel, W.R., and Piston, D.W. (2006). Optimization of pairings and detection conditions for measurement of FRET between cyan and yellow fluorescent proteins. Microsc. Microanal. *12*, 238–254.

Roebroek, A.J., Umans, L., Pauli, I.G., Robertson, E.J., van Leuven, F., Van de Ven, W.J., and Constam, D.B. (1998). Failure of ventral closure and axial rotation in embryos lacking the proprotein convertase Furin. Development *125*, 4863–4876.

Roebroek, A.J.M., Taylor, N.A., Louagie, E., Pauli, I., Smeijers, L., Snellinx, A., Lauwers, A., Van De Ven, W.J.M., Hartmann, D., and Creemers, J.W.M. (2004). Limited redundancy of the proprotein convertase furin in mouse liver. J. Biol. Chem. *279*, 53442–53450.

Roebroek, a J., Schalken, J. a, Leunissen, J. a, Onnekink, C., Bloemers, H.P., and Van de Ven, W.J. (1986). Evolutionary conserved close linkage of the c-fes/fps proto-oncogene and genetic sequences encoding a receptor-like protein. EMBO J. *5*, 2197–2202.

Rounseville, M.P., and Davis, T.P. Prohormone convertase and autocrine growth factor mRNAs are coexpressed in small cell lung carcinoma.

Rousselet, E., Benjannet, S., Hamelin, J., Canuel, M., and Seidah, N.G. (2011a). The proprotein convertase PC7: Unique zymogen activation and trafficking pathways. J. Biol. Chem. *286*, 2728–2738.

Rousselet, E., Benjannet, S., Marcinkiewicz, E., Asselin, M.C., Lazure, C., and Seidah, N.G. (2011b). Proprotein convertase PC7 enhances the activation of the EGF receptor pathway through processing of the EGF precursor. J. Biol. Chem. *286*, 9185–9195.

Van Roy, F., and Berx, G. (2008). The cell-cell adhesion molecule E-cadherin. Cell. Mol. Life Sci. *65*, 3756–3788.

Saito, H., Yasumoto, K.I., Takeda, K., Takahashi, K., Fukuzaki, A., Orikasa, S., and Shibahara, S. (2002). Melanocyte-specific microphthalmia-associated transcription factor isoform activates its own gene promoter through physical interaction with lymphoid-enhancing factor 1. J. Biol. Chem. *277*, 28787–28794.

Salonikidis, P.S., Niebert, M., Ullrich, T., Bao, G., Zeug, A., and Richter, D.W. (2011). An ion-insensitive cAMP biosensor for long term quantitative ratiometric fluorescence resonance energy transfer (FRET) measurements under variable physiological conditions. J. Biol. Chem. *286*, 23419–23431.

Salti, G.I., Manougian, T., Farolan, M., Shilkaitis, A., Majumdar, D., and Das Gupta, T.K. (2000). Micropthalmia transcription factor: A new prognostic marker in intermediate-thickness cutaneous malignant melanoma. Cancer Res. *60*, 5012–5016.

San Martín, A., Ceballo, S., Ruminot, I., Lerchundi, R., Frommer, W.B., and Barros, L.F. (2013). A Genetically Encoded FRET Lactate Sensor and Its Use To Detect the Warburg Effect in Single Cancer Cells. PLoS One *8*.

Sanchez-Duffhues, G., Fotsis, T., and Dijke, P. Ten (2015). Signal transduction: Gain of activin turns muscle into bone. Curr. Biol. *25*, R1136–R1138.

Sánchez-Tilló, E., Liu, Y., De Barrios, O., Siles, L., Fanlo, L., Cuatrecasas, M., Darling, D.S., Dean, D.C., Castells, A., and Postigo, A. (2012). EMT-activating transcription factors in cancer: Beyond EMT and tumor invasiveness. Cell. Mol. Life Sci. *69*, 3429–3456.

Santavicca, M., Noel, A., Angliker, H., Stoll, I., Segain, J.P., Anglard, P., Chretien, M., Seidah, N., and Basset, P. (1996). Characterization of Structural Determinants and Molecular Mechanisms Involved in Pro-Stromelysin-3 Activation by 4- Aminophenylmercuric Acetate and Furin-Type Convertases. Biochem. J. *Vol 315*, 953–958.

Sarac, M.S., Cameron, A., and Lindberg, I. (2002). The furin inhibitor hexa-D-arginine blocks the activation of Pseudomonas aeruginosa exotoxin a in vivo. Infect. Immun. *70*, 7136–7139.

Saxena, M.T., Schroeter, E.H., Mumm, J.S., and Kopan, R. (2001). Murine Notch Homologs (N1-4) Undergo Presenilin-dependent Proteolysis. J. Biol. Chem. *276*, 40268–40273.

Scamuffa, N., Calvo, F., Chrétien, M., Seidah, N.G., and Khatib, A.-M. (2006). Proprotein convertases: lessons from knockouts. FASEB J. *20*, 1954–1963.

Scamuffa, N., Siegfried, G., Bontemps, Y., Ma, L., Basak, A., Cherel, G., Calvo, F., Seidah, N.G., and Khatib, A.M. (2008). Selective inhibition of proprotein convertases represses the metastatic potential of human colorectal tumor cells. J. Clin. Invest. *118*, 352–363.

Scamuffa, N., Sfaxi, F., Ma, J., Lalou, C., Seidah, N., Calvo, F., and Khatib, A.M. (2014). Prodomain of the proprotein convertase subtilisin/kexin Furin (ppfurin) protects from tumor progression and metastasis. Carcinogenesis *35*, 528–536.

Schäfer, W., Stroh, A., Berghöfer, S., Seiler, J., Vey, M., Kruse, M.L., Kern, H.F., Klenk, H.D., and Garten, W. (1995). Two independent targeting signals in the cytoplasmic domain determine trans-Golgi network localization and endosomal trafficking of the proprotein convertase furin. EMBO J. *14*, 2424–2435.

References

Schalken, J.A., Roebroek, A.J.M., Oomen, P.P.C.A., Wagenaar, S.S., Debruyne, F.M.J., Bloemers, H.P.J., and Van De Ven, W.J.M. (1987). fur Gene expression as a discriminating marker for small cell and nonsmall cell lung carcinomas. J. Clin. Invest. *80*, 1545–1549.

Schlierf, B., Fey, G.H., Hauber, J., Hocke, G.M., and Rosorius, O. (2000). Rab11b is essential for recycling of transferrin to the plasma membrane. Exp Cell Res *259*, 257–265.

Schmid, J.A., and Neumeier, H. (2005). Evolutions in science triggered by green fluorescent protein (GFP). ChemBioChem *6*, 1149–1156.

Schmoranzer, J., and Simon, S.M. (2003). Role of Microtubules in Fusion of Post-Golgi Vesicles to the Plasma Membrane. Mol. Biol. Cell *14*, 1558–1569.

Schouwey, K., and Beermann, F. (2008). The Notch pathway: Hair graying and pigment cell homeostasis. Histol. Histopathol. *23*, 609–616.

Schouwey, K., Delmas, V., Larue, L., Zimber-Strobl, U., Strobl, L.J., Radtke, F., and Beermann, F. (2007). Notch1 and Notch2 receptors influence progressive hair graying in a dose-dependent manner. Dev. Dyn. *236*, 282–289.

Schouwey, K., Larue, L., Radtke, F., Delmas, V., and Beermann, F. (2010a). Transgenic expression of Notch in melanocytes demonstrates RBP-Jκ-dependent signaling. Pigment Cell Melanoma Res. *23*, 134–136.

Schouwey, K., Larue, L., Radtke, F., Delmas, V., and Beermann, F. (2010b). Transgenic expression of Notch in melanocytes demonstrates RBP-Jκ-dependent signaling. Pigment Cell Melanoma Res. *23*, 134–136.

Segura, M.F., Hanniford, D., Menendez, S., Reavie, L., Zou, X., Alvarez-Diaz, S., Zakrzewski, J., Blochin, E., Rose, A., Bogunovic, D., et al. (2009). Aberrant miR-182 expression promotes melanoma metastasis by repressing FOXO3 and microphthalmia-associated transcription factor. Proc. Natl. Acad. Sci. *106*, 1814–1819.

Seidah, N.G. (2011). The proprotein convertases, 20 years later. Methods Mol. Biol. *768*, 23–57.

Seidah, N.G., and Chretien, M. (1999). Proprotein and prohormone convertases: A family of subtilases generating diverse bioactive polypeptides. Brain Res. *848*, 45–62.

Seidah, N.G., and Prat, A. (2012). The biology and therapeutic targeting of the proprotein convertases. Nat. Rev. Drug Discov. *11*, 367–383.

Seidah, N.G., Gaspar, L., Mion, P., Marcinkiewicz, M., Mbikay, M., and Chrétien, M. (1990). cDNA sequence of two distinct pituitary proteins homologous to Kex2 and furin gene products: tissue-specific mRNAs encoding candidates for pro-hormone processing proteinases. DNA Cell Biol. *9*, 789.

Seidah, N.G., Day, R., Hamelin, J., Gaspar, A., Collard, M.W., and Chrétien, M. (1992). Testicular expression of PC4 in the rat: molecular diversity of a novel germ cell-specific Kex2/subtilisin-like proprotein convertase. Mol. Endocrinol. *6*, 1559–1570.

Seidah, N.G., Chrétien, M., and Day, R. (1994). The family of subtilisin/kexin like pro-protein and pro-hormone convertases: Divergent or shared functions. Biochimie *76*, 197–209.

Seidah, N.G., Hamelin, J., Mamarbachi, M., Dong, W., Tardos, H., Mbikay, M., Chretien, M., and Day, R. (1996). cDNA structure, tissue distribution, and chromosomal localization of rat PC7, a novel mammalian proprotein convertase closest to yeast kexin-like proteinases. Proc. Natl. Acad. Sci. U. S. A. *93*, 3388–3393.

Seidah, N.G., Day, R., Marcinkiewicz, M., and Chrétien, M. (1998). Precursor convertases: An evolutionary ancient, cell-specific, combinatorial mechanism yielding diverse bioactive peptides and proteins. In Annals of the New York Academy of Sciences, pp. 9–24.

Seidah, N.G., Mowla, S.J., Hamelin, J., Mamarbachi, A.M., Benjannet, S., Touré, B.B., Basak, A., Munzer, J.S., Marcinkiewicz, J., Zhong, M., et al. (1999a). Mammalian subtilisin/kexin isozyme SKI-1: A widely expressed proprotein convertase with a unique cleavage specificity and cellular localization. Proc. Natl. Acad. Sci. U. S. A. *96*, 1321–1326.

Seidah, N.G., Benjannet, S., Hamelin, J., Mamarbachi, a M., Basak, a, Marcinkiewicz, J., Mbikay, M., Chrétien, M., and Marcinkiewicz, M. (1999b). The subtilisin/kexin family of precursor convertases. Emphasis on PC1, PC2/7B2, POMC and the novel enzyme SKI-1. Ann. N. Y. Acad. Sci. *885*, 57–74.

Seidah, N.G., Benjannet, S., Wickham, L., Marcinkiewicz, J., Jasmin, S.B., Stifani, S., Basak, A., Prat, A., and Chretien, M. (2003). The secretory proprotein convertase neural apoptosis-regulated convertase 1 (NARC-1): Liver regeneration and neuronal differentiation. Proc. Natl. Acad. Sci. *100*, 928–933.

Seidah, N.G., Khatib, A.M., and Prat, A. (2006). The proprotein convertases and their implication in sterol and/or lipid metabolism. In Biological Chemistry, pp. 871–877.

Seidah, N.G., Mayer, G., Zaid, A., Rousselet, E., Nassoury, N., Poirier, S., Essalmani, R., and Prat, A. (2008). The activation and physiological functions of the proprotein convertases. Int. J. Biochem. Cell Biol. *40*, 1111–1125.

Seiter, S., Monsurro, V., Nielsen, M.B., Wang, E., Provenzano, M., Wunderlich, J.R., Rosenberg, S.A., and Marincola, F.M. (2002). Frequency of MART-1/MelanA and gp100/PMel17-specific T cells in tumor metastases and cultured tumor-infiltrating lymphocytes. J Immunother *25*, 252–263.

Seitz, A., Terjung, S., Zimmermann, T., and Pepperkok, R. (2012). Quantifying the influence of yellow fluorescent protein photoconversion on acceptor photobleaching–based

fluorescence resonance energy transfer measurements. J. Biomed. Opt. *17*, 11010.

Semb, H., and Christofori, G. (1998). The tumor-suppressor function of E-cadherin. Am. J. Hum. Genet. *63*, 1588–1593.

Senzer, N., Barve, M., Kuhn, J., Melnyk, A., Beitsch, P., Lazar, M., Lifshitz, S., Magee, M., Oh, J., Mill, S.W., et al. (2012). Phase I Trial of "bi-shRNAifurin/GMCSF DNA/Autologous Tumor Cell" Vaccine (FANG) in Advanced Cancer. Mol. Ther. *20*, 679–686.

Seong, J., Tajik, A., Sun, J., Guan, J.-L., Humphries, M.J., Craig, S.E., Shekaran, A., Garcia, A.J., Lu, S., Lin, M.Z., et al. (2013). Distinct biophysical mechanisms of focal adhesion kinase mechanoactivation by different extracellular matrix proteins. Proc. Natl. Acad. Sci. *110*, 19372–19377.

Serrano, M., Hannon, G.J., and Beach, D. (1993). A new regulatory motif in cell-cycle control causing specific inhibition of cyclin D/CDK4. Nature *366*, 704–707.

Shain, A.H., and Bastian, B.C. (2016). From melanocytes to melanomas. Nat. Rev. Cancer *16*, 345–358.

Shao, H., Cai, L., Grichnik, J.M., Livingstone, A.S., Velazquez, O.C., and Liu, Z.-J. (2011). Activation of Notch1 signaling in stromal fibroblasts inhibits melanoma growth by upregulating WISP-1. Oncogene *30*, 4316–4326.

Sharpless, N., and Chin, L. (2003). The INK4a/ARF locus and melanoma. Oncogene *22*, 3092–3098.

Shi, M., Zhu, J., Wang, R., Chen, X., Mi, L., Walz, T., and Springer, T.A. (2011). Latent TGF-β structure and activation. Nature *474*, 343–349.

Shimomura, O. (2009). Discovery of green fluorescent protein (GFP) (Nobel Lecture). Angew. Chem. Int. Ed. Engl. *48*, 5590–5602.

Shrestha, D., Jenei, A., Nagy, P., Vereb, G., and Szöllősi, J. (2015). Understanding FRET as a research tool for cellular studies. Int. J. Mol. Sci. *16*, 6718–6756.

Siegfried, G., Basak, A., Cromlish, J.A., Benjannet, S., Marcinkiewicz, J., Chrétien, M., Seidah, N.G., and Khatib, A.M. (2003). The secretory proprotein convertases furin, PC5, and PC7 activate VEGF-C to induce tumorigenesis. J. Clin. Invest. *111*, 1723–1732.

Siegfried, G., Basak, A., Prichett-Pejic, W., Scamuffa, N., Ma, L., Benjannet, S., Veinot, J.P., Calvo, F., Seidah, N., and Khatib, A.-M. (2005). Regulation of the stepwise proteolytic cleavage and secretion of PDGF-B by the proprotein convertases. Oncogene *24*, 6925–6935.

Siezen, R.J., and Leunissen, J.A. (1997). Subtilases: the superfamily of subtilisin-like serine proteases. Protein Sci. *6*, 501–523.

Simmen, T., Höning, S., Icking, A., Tikkanen, R., and Hunziker, W. (2002). AP-4 binds

basolateral signals and participates in basolateral sorting in epithelial MDCK cells. Nat. Cell Biol. *4*, 154–159.

Singh, H., Heng, S., Nicholls, P.K., Li, Y., Tai, L.T., Jobling, T., Salamonsen, L.A., and Nie, G. (2012). Proprotein convertases in post-menopausal endometrial cancer: Distinctive regulation and non-invasive diagnosis. Biochem. Biophys. Res. Commun. *419*, 809–814.

Smeekens, S.P., Avruch, a S., LaMendola, J., Chan, S.J., and Steiner, D.F. (1991). Identification of a cDNA encoding a second putative prohormone convertase related to PC2 in AtT20 cells and islets of Langerhans. Proc. Natl. Acad. Sci. U. S. A. *88*, 340–344.

Smeekens, S.P., Montag, A.G., Thomas, G., Albiges-Rizo, C., Carroll, R., Benig, M., Phillips, L.A., Martin, S., Ohagi, S., Gardner, P., et al. (1992). Proinsulin processing by the subtilisin-related proprotein convertases furin, PC2, and PC3. Proc. Natl. Acad. Sci. U. S. A. *89*, 8822–8826.

Smyth, M.J., Teng, M.W.L., Swann, J., Kyparissoudis, K., Godfrey, D.I., and Hayakawa, Y. (2006). CD4+CD25+ T regulatory cells suppress NK cell-mediated immunotherapy of cancer. J. Immunol. *176*, 1582–1587.

de Snoo, F.A., Kroon, M.W., Bergman, W., ter Huurne, J.A.C., Houwing-Duistermaat, J.J., van Mourik, L., Snels, D.G.C.T.M., Breuning, M.H., Willemze, R., Frants, R.R., et al. (2007). From sporadic atypical nevi to familial melanoma: Risk analysis for melanoma in sporadic atypical nevus patients. J. Am. Acad. Dermatol. *56*, 748–752.

Srour, N., Lebel, A., McMahon, S., Fournier, I., Fugère, M., Day, R., and Dubois, C.M. (2003). TACE/ADAM-17 maturation and activation of sheddase activity require proprotein convertase activity. FEBS Lett. *554*, 275–283.

Stacker, S.A., Stenvers, K., Caesar, C., Vitali, A., Domagala, T., Nice, E., Roufail, S., Simpson, R.J., Moritz, R., Karpanen, T., et al. (1999). Biosynthesis of vascular endothelial growth factor-D involves proteolytic processing which generates non-covalent homodimers. J. Biol. Chem. *274*, 32127–32136.

Stawowy, P., and Fleck, E. (2005). Proprotein convertases furin and PC5: Targeting atherosclerosis and restenosis at multiple levels. J. Mol. Med. *83*, 865–875.

Stawowy, P., Meyborg, H., Stibenz, D., Stawowy, N.B.P., Roser, M., Thanabalasingam, U., Veinot, J.P., Chrétien, M., Seidah, N.G., Fleck, E., et al. (2005). Furin-like proprotein convertases are central regulators of the membrane type matrix metalloproteinase-pro-matrix metalloproteinase-2 proteolytic cascade in atherosclerosis. Circulation *111*, 2820–2827.

Stockli, J. (2004). The Palmitoyltransferase of the Cation-dependent Mannose 6-Phosphate Receptor Cycles between the Plasma Membrane and Endosomes. Mol. Biol. Cell *15*, 2617–2626.

Stossel, T.P., Condeelis, J., Cooley, L., Hartwig, J.H., Noegel, a, Schleicher, M., and Shapiro, S.S. (2001). Filamins as integrators of cell mechanics and signalling. Nat. Rev. Mol. Cell Biol. *2*, 138–145.

Stott, F.J., Bates, S., James, M.C., McConnell, B.B., Starborg, M., Brookes, S., Palmero, I., Ryan, K., Hara, E., Vousden, K.H., et al. (1998). The alternative product from the human CDKN2A locus, p14(ARF), participates in a regulatory feedback loop with p53 and MDM2. EMBO J. *17*, 5001–5014.

Sugino, K., Nakamura, T., Takio, K., Miyamoto, K., Hasegawa, Y., Igarashi, M., Titani, K., and Sugino, H. (1992). Purification and characterization of high molecular weight forms of inhibin from bovine follicular fluid. Endocrinology *130*, 789–796.

Sun, X., Essalmani, R., Seidah, N.G., and Prat, A. (2009). The proprotein convertase PC5/6 is protective against intestinal tumorigenesis: in vivo mouse model. Mol. Cancer *8*, 73.

Susan-Resiga, D., Essalmani, R., Hamelin, J., Asselin, M.C., Benjannet, S., Chamberland, A., Day, R., Szumska, D., Constam, D., Bhattacharya, S., et al. (2011). Furin is the major processing enzyme of the cardiac-specific growth factor bone morphogenetic protein 10. J. Biol. Chem. *286*, 22785–22794.

Suzuki, I., Cone, R.D., Im, S., Nordlund, J., and Abdel-Malek, Z.A. (1996). Binding of melanotropic hormones to the melanocortin receptor MC1R on human melanocytes stimulates proliferation and melanogenesis. Endocrinology *137*, 1627–1633.

Szabà, G., Pine, P.S., Weaver, J.L., Kasari, M., and Aszalos, A. (1992). Epitope mapping by photobleaching fluorescence resonance energy transfer measurements using a laser scanning microscope system. Biophys. J. *61*, 661–670.

Tachibana, M. (1999). Sound needs sound melanocytes to be heard. Pigment Cell Res. *12*, 344–354.

Takahashi, N., Sawada, W., Noguchi, J., Watanabe, S., Ucar, H., Hayashi-Takagi, A., Yagishita, S., Ohno, M., Tokumaru, H., and Kasai, H. (2015). Two-photon fluorescence lifetime imaging of primed SNARE complexes in presynaptic terminals and β cells. Nat. Commun. *6*, 8531.

Takahashi, S., Nakagawa, T., Kasai, K., Banno, T., Duguay, S.J., Van de Ven, W.J.M., Murakami, K., and Nakayama, K. (1995a). A second mutant allele of furin in the processing-incompetent cell line, LoVo. Evidence for involvement of the homo B domain in autocatalytic activation. J. Biol. Chem. *270*, 26565–26569.

Takahashi, S., Nakagawa, T., Banno, T., Watanabe, T., Murakami, K., and Nakayama, K. (1995b). Localization of furin to the trans-Golgi network and recycling from the cell surface involves Ser and Tyr residues within the cytoplasmic domain. J. Biol. Chem. *270*, 28397–

28401.

Takemoto, K., Nagai, T., Miyawaki, A., and Miura, M. (2003). Spatio-temporal activation of caspase revealed by indicator that is insensitive to environmental effects. J. Cell Biol. *160*, 235–243.

Tamura, K., Shan, W.S., Hendrickson, W.A., Colman, D.R., and Shapiro, L. (1998). Structure-function analysis of cell adhesion by neural (N-) cadherin. Neuron *20*, 1153–1163.

Tatari, M.N., De Craene, B., Soen, B., Taminau, J., Vermassen, P., Goossens, S., Haigh, K., Cazzola, S., Lambert, J., Huylebroeck, D., et al. (2014). ZEB2-transgene expression in the epidermis compromises the integrity of the epidermal barrier through the repression of different tight junction proteins. Cell. Mol. Life Sci. *71*, 3599–3609.

Taylor, N.A., Van De Ven, W.J.M., and Creemers, J.W.M. (2003). Curbing activation: proprotein convertases in homeostasis and pathology. FASEB J. *17*, 1215–1227.

van Tetering, G., and Vooijs, M. (2011). Proteolytic cleavage of Notch: "HIT and RUN". Curr. Mol. Med. *11*, 255–269.

Teuchert, M., Schäfer, W., Berghöfer, S., Hoflack, B., Klenk, H.D., and Garten, W. (1999a). Sorting of furin at the trans-Golgi network: Interaction of the cytoplasmic tail sorting signals with AP-1 Golgi-specific assembly proteins. J. Biol. Chem. *274*, 8199–8207.

Teuchert, M., Berghöfer, S., Klenk, H.D., and Garten, W. (1999b). Recycling of furin from the plasma membrane. Functional importance of the cytoplasmic tail sorting signals and interaction with the AP-2 adaptor medium chain subunit. J. Biol. Chem. *274*, 36781–36789.

Thacker, C., and Rose, A.M. (2000). A look at the Caenorhabditis elegans Kex2/Subtilisin-like proprotein convertase family. BioEssays *22*, 545–553.

Theos, A.C., Truschel, S.T., Raposo, G., and Marks, M.S. (2005). The Silver locus product Pmel17/gp100/Silv/ME20: Controversial in name and in function. Pigment Cell Res. *18*, 322–336.

Thomas, G. (2002). Furin at the cutting edge: From protein traffic to embryogenesis and disease. Nat. Rev. Mol. Cell Biol. *3*, 753–766.

Thurber, A.E., Douglas, G., Sturm, E.C., Zabierowski, S.E., Smit, D.J., Ramakrishnan, S.N., Hacker, E., Leonard, J.H., Herlyn, M., and Sturm, R.A. (2011). Inverse expression states of the BRN2 and MITF transcription factors in melanoma spheres and tumour xenografts regulate the NOTCH pathway. Oncogene *30*, 3036–3048.

Tian, S., Huajun, W., and Wu, J. (2012). Computational prediction of furin cleavage sites by a hybrid method and understanding mechanism underlying diseases. Sci. Rep. *2*, 261.

Tolcher, A.W., Messersmith, W.A., Mikulski, S.M., Papadopoulos, K.P., Kwak, E.L., Gibbon,

D.G., Patnaik, A., Falchook, G.S., Dasari, A., Shapiro, G.I., et al. (2012). Phase I study of RO4929097, a gamma secretase inhibitor of notch signaling, in patients with refractory metastatic or locally advanced solid tumors. J. Clin. Oncol. *30*, 2348–2353.

Tooze, S.A. (1998). Biogenesis of secretory granules in the trans-Golgi network of neuroendocrine and endocrine cells. Biochim. Biophys. Acta - Mol. Cell Res. *1404*, 231–244.

Tsuji, A., Hashimoto, E., Ikoma, T., Taniguchi, T., Mori, K., Nagahama, M., and Matsuda, Y. (1999). Inactivation of proprotein convertase, PACE4, by alpha1-antitrypsin Portland (alpha1-PDX), a blocker of proteolytic activation of bone morphogenetic protein during embryogenesis: evidence that PACE4 is able to form an SDS-stable acyl intermediate with alpha1-PDX. J. Biochem. *126*, 591–603.

Tsuji, A., Sakurai, K., Kiyokage, E., Yamazaki, T., Koide, S., Toida, K., Ishimura, K., and Matsuda, Y. (2003). Secretory proprotein convertases PACE4 and PC6A are heparin-binding proteins which are localized in the extracellular matrix: Potential role of PACE4 in the activation of proproteins in the extracellular matrix. Biochim. Biophys. Acta - Proteins Proteomics *1645*, 95–104.

Tsuneoka, M., Nakayama, K., Hatsuzawa, K., Komada, M., Kitamura, N., and Mekada, E. (1993). Evidence for involvement of furin in cleavage and activation of diphtheria toxin. J. Biol. Chem. *268*, 26461–26465.

Turpeinen, H., Kukkurainen, S., Pulkkinen, K., Kauppila, T., Ojala, K., Hytönen, V.P., and Pesu, M. (2011). Identification of proprotein convertase substrates using genome-wide expression correlation analysis. BMC Genomics *12*, 618.

Turpeinen, H., Oksanen, A., Kivinen, V., Kukkurainen, S., Uusimäki, A., Rämet, M., Parikka, M., Hytönen, V.P., Nykter, M., and Pesu, M. (2013). Proprotein Convertase Subtilisin/Kexin Type 7 (PCSK7) Is Essential for the Zebrafish Development and Bioavailability of Transforming Growth Factor β1a (TGFβ1a). J. Biol. Chem. *288*, 36610–36623.

Tyas, L., Brophy, V.A., Pope, A., Rivett, A.J., and Tavaré, J.M. (2000). Rapid caspase-3 activation during apoptosis revealed using fluorescence-resonance energy transfer. EMBO Rep. *1*, 266–270.

Tzimas, G.N., Chevet, E., Jenna, S., Nguyên, D.T., Khatib, A.M., Marcus, V., Zhang, Y., Chrétien, M., Seidah, N., and Metrakos, P. (2005). Abnormal expression and processing of the proprotein convertases PC1 and PC2 in human colorectal liver metastases. BMC Cancer *5*, 149.

Valentin, G. (2005). Photoconversion of YFP into a CFP-like species during acceptor photobleaching FRET expe时ments. Nat. Methods *2*, 801.

Valverde, P., Healy, E., Jackson, I., Rees, J.L., and Thody, A.J. (1995). Variants of the

melanocyte–stimulating hormone receptor gene are associated with red hair and fair skin in humans. Nat. Genet. *11*, 328–330.

Vandame, P., Spriet, C., Trinel, D., Gelaude, A., Caillau, K., Bompard, C., Biondi, E., and Bodart, J.F. (2014). The spatio-temporal dynamics of PKA activity profile during mitosis and its correlation to chromosome segregation. Cell Cycle *13*, 3232–3240.

Vassar, R. (1999). Beta-Secretase Cleavage of Alzheimer's Amyloid Precursor Protein by the Transmembrane Aspartic Protease BACE. Science (80-.). *286*, 735–741.

Vassar, R. (2002). Beta-secretase (BACE) as a drug target for Alzheimer's disease. Adv. Drug Deliv. Rev. *54*, 1589–1602.

van de Ven, W.J.M., Voorberg, J., Fontijn, R., Pannekoek, H., van den Ouweland, A.M.W., van Duijnhoven, H.L.P., Roebroek, A.J.M., and Siezen, R.J. (1990). Furin is a subtilisin-like proprotein processing enzyme in higher eukaryotes. Mol. Biol. Rep. *14*, 265–275.

Verastegui, C., Bille, K., Ortonne, J.P., and Ballotti, R. (2000). Regulation of the microphthalmia-associated transcription factor gene by the Waardenburg syndrome type 4 gene, SOX10. J. Biol. Chem. *275*, 30757–30760.

Vereb, G., Nagy, P., and Szöllosi, J. (2011). Flow cytometric FRET analysis of protein interaction. Methods Mol. Biol. *699*, 371–392.

Vevea, J.D., Alessi Wolken, D.M., Swayne, T.C., White, A.B., and Pon, L.A. (2013). Ratiometric Biosensors that Measure Mitochondrial Redox State and ATP in Living Yeast Cells. J. Vis. Exp.

Vezenkov, L., Honson, N.S., Kumar, N.S., Bosc, D., Kovacic, S., Nguyen, T.G., Pfeifer, T.A., and Young, R.N. (2015). Development of fluorescent peptide substrates and assays for the key autophagy-initiating cysteine protease enzyme, ATG4B. Bioorganic Med. Chem. *23*, 3237–3247.

Villanueva, J., and Herlyn, M. (2008). Melanoma and the tumor microenvironment. Curr. Oncol. Rep. *10*, 439–446.

Villeneuve, P., Feliciangeli, S., Croissandeau, G., Seidah, N.G., Mbikay, M., Kitabgi, P., and Beaudet, A. (2002). Altered processing of the neurotensin/neuromedin N precursor in PC2 knock down mice: A biochemical and immunohistochemical study. J. Neurochem. *82*, 783–793.

Viros, A., Fridlyand, J., Bauer, J., Lasithiotakis, K., Garbe, C., Pinkel, D., and Bastian, B.C. (2008). Improving melanoma classification by integrating genetic and morphologic features. PLoS Med. *5*, 0941–0952.

Vischer, U.M., and Wagner, D.D. (1994). von Willebrand factor proteolytic processing and

multimerization precede the formation of Weibel-Palade bodies. Blood *83*, 3536–3544.

Vleminckx, K., Vakaet, L., Mareel, M., Fiers, W., and Van Roy, F. (1991). Genetic manipulation of E-cadherin expression by epithelial tumor cells reveals an invasion suppressor role. Cell *66*, 107–119.

Volchkov, V.E., Feldmann, H., Volchkova, V.A., and Klenk, H.D. (1998). Processing of the Ebola virus glycoprotein by the proprotein convertase furin. Proc. Natl. Acad. Sci. U. S. A. *95*, 5762–5767.

Walker, G.J., Flores, J.F., Glendening, J.M., Lin, A., Markl, I.D.C., and Fountain, J.W. (1998). Virtually 100% of melanoma cell lines harbor alterations at the DNA level within CDKN2A, CDKN2B, or one of their downstream targets. Genes Chromosom. Cancer *22*, 157–163.

Wallrabe, H., and Periasamy, A. (2005). Imaging protein molecules using FRET and FLIM microscopy. Curr. Opin. Biotechnol. *16*, 19–27.

Wan, L., Molloy, S.S., Thomas, L., Liu, G., Xiang, Y., Rybak, S.L., and Thomas, G. (1998). PACS-1 defines a novel gene family of cytosolic sorting proteins required for trans-Golgi network localization. Cell *94*, 205–216.

Wang, Y., Botvinick, E.L., Zhao, Y., Berns, M.W., Usami, S., Tsien, R.Y., and Chien, S. (2005). Visualizing the mechanical activation of Src. Nature *434*, 1040–1045.

Watanabe, K., Nagaoka, T., Lee, J.M., Bianco, C., Gonzales, M., Castro, N.P., Rangel, M.C., Sakamoto, K., Sun, Y., Callahan, R., et al. (2009). Enhancement of Notch receptor maturation and signaling sensitivity by Cripto-1. J. Cell Biol. *187*, 343–353.

Watnick, R.S. (2012). The role of the tumor microenvironment in regulating angiogenesis. Cold Spring Harb. Perspect. Med. *2*, a006676.

Weatherhead, S.C., Haniffa, M., and Lawrence, C.M. (2007). Melanomas arising from naevi and de novo melanomas - Does origin matter? Br. J. Dermatol. *156*, 72–76.

Weiss, A., and Attisano, L. (2013). The TGFbeta superfamily signaling pathway. Wiley Interdiscip. Rev. Dev. Biol. *2*, 47–63.

Welsh, C.F., Roovers, K., Villanueva, J., Liu, Y., Schwartz, M. a, and Assoian, R.K. (2001). Timing of cyclin D1 expression within G1 phase is controlled by Rho. Nat. Cell Biol. *3*, 950–957.

Westphal, C.H., Muller, L., Zhou, a, Zhu, X., Bonner-Weir, S., Schambelan, M., Steiner, D.F., Lindberg, I., and Leder, P. (1999). The neuroendocrine protein 7B2 is required for peptide hormone processing in vivo and provides a novel mechanism for pituitary Cushing's disease. Cell *96*, 689–700.

Wetsel, W.C., Rodriguiz, R.M., Guillemot, J., Rousselet, E., Essalmani, R., Kim, I.H., Bryant,

J.C., Marcinkiewicz, J., Desjardins, R., Day, R., et al. (2013). Disruption of the expression of the proprotein convertase PC7 reduces BDNF production and affects learning and memory in mice. Proc. Natl. Acad. Sci. *110*, 17362–17367.

Wheelock, M.J., Shintani, Y., Maeda, M., Fukumoto, Y., and Johnson, K.R. (2008). Cadherin switching. J. Cell Sci. *121*, 727–735.

Wick, W., Wild-Bode, C., Frank, B., and Weller, M. (2004). BCL-2-induced glioma cell invasiveness depends on furin-like proteases. J. Neurochem. *91*, 1275–1283.

Widmer, D.S., Cheng, P.F., Eichhoff, O.M., Belloni, B.C., Zipser, M.C., Schlegel, N.C., Javelaud, D., Mauviel, A., Dummer, R., and Hoek, K.S. (2012). Systematic classification of melanoma cells by phenotype-specific gene expression mapping. Pigment Cell Melanoma Res. *25*, 343–353.

Willson, J.A., Muir, C.A., Evered, C.L., Cepeda, M.A., and Damjanovski, S. (2017). Stable expression of α1-antitrypsin Portland in MDA-MB-231 cells increased MT1-MMP and MMP-9 levels, but reduced tumour progression. J. Cell Commun. Signal.

Wong, G., and Pawelek, J. (1973). Control of phenotypic expression of cultured melanoma cells by melanocyte stimulating hormones. Nat. New Biol. *241*, 213–215.

Wong, E., Maretzky, T., Peleg, Y., Blobel, C.P., and Sagi, I. (2015). The functional maturation of a disintegrin and metalloproteinase (ADAM) 9, 10, and 17 requires processing at a newly identified proprotein convertase (PC) cleavage site. J. Biol. Chem. *290*, 12135–12146.

Wouters, S., Leruth, M., Decroly, E., Vandenbranden, M., Creemers, J.W., van de Loo, J.W., Ruysschaert, J.M., Courtoy, P.J., and S Wouters E Decroly, M Vandenbranden, J W Creemers, J W van de Loo, J M Ruysschaert, and P J Courtoy, M.L. (1998). Furin and proprotein convertase 7 (PC7)/lymphoma PC endogenously expressed in rat liver can be resolved into distinct post-Golgi compartments. Biochem J. *336*, 311–316.

Wu, H., Goel, V., and Haluska, F.G. (2003). PTEN signaling pathways in melanoma. Oncogene *22*, 3113–3122.

Wu, X., Simone, J., Hewgill, D., Siegel, R., Lipsky, P.E., and He, L. (2006). Measurement of two caspase activities simultaneously in living cells by a novel dual FRET fluorescent indicator probe. Cytom. Part A *69*, 477–486.

Xia, Z., and Liu, Y. (2001). Reliable and global measurement of fluorescence resonance energy transfer using fluorescence microscopes. Biophys.J. *81*, 2395–2402.

Xiang, Y., Molloy, S.S., Thomas, L., and Thomas, G. (2000). The PC6B cytoplasmic domain contains two acidic clusters that direct sorting to distinct trans-Golgi network/endosomal compartments. Mol. Biol. Cell *11*, 1257–1273.

Xie, Z., Nair, U., and Klionsky, D.J. (2008). Atg8 Controls Phagophore Expansion during Autophagosome Formation. Mol. Biol. Cell *19*, 3290–3298.

Xu, X., Gerard, A.L., Huang, B.C., Anderson, D.C., Payan, D.G., and Luo, Y. (1998). Detection of programmed cell death using fluorescence energy transfer. Nucleic Acids Res *26*, 2034–2035.

Yajima, I., and Larue, L. (2008). The location of heart melanocytes is specified and the level of pigmentation in the heart may correlate with coat color. Pigment Cell Melanoma Res. *21*, 471–476.

Yajima, I., Sato, S., Kimura, T., Yasumoto, K.I., Shibahara, S., Goding, C.R., and Yamamoto, H. (1999). An L1 element intronic insertion in the black-eyed white (Mitf(mi-bw)) gene: The loss of a single Mitf isoform responsible for the pigmentary defect and inner ear deafness. Hum. Mol. Genet. *8*, 1431–1441.

Yamashiro, D.J., and Maxfield, F.R. (1987). Kinetics of endosome acidification in mutant and wild-type Chinese hamster ovary cells. J. Cell Biol. *105*, 2713–2721.

Yan, D., da Dong, X., Chen, X., Yao, S., Wang, L., Wang, J., Wang, C., Hu, D.N., Qu, J., and Tu, L.L. (2012). Role of microRNA-182 in posterior uveal melanoma: Regulation of tumor development through MITF, BCL2 and cyclin D2. PLoS One *7*.

Yana, I., and Weiss, S.J. (2000). Regulation of membrane type-1 matrix metalloproteinase activation by proprotein convertases. Mol. Biol. Cell *11*, 2387–2401.

Yang, J., and Weinberg, R.A. (2008). Epithelial-Mesenchymal Transition: At the Crossroads of Development and Tumor Metastasis. Dev. Cell *14*, 818–829.

Yang, G., Li, Y., Nishimura, E.K., Xin, H., Zhou, A., Guo, Y., Dong, L., Denning, M.F., Nickoloff, B.J., and Cui, R. (2008). Inhibition of PAX3 by TGF-β Modulates Melanocyte Viability. Mol. Cell *32*, 554–563.

Yashiro-Ohtani, Y., He, Y., Ohtani, T., Jones, M.E., Shestova, O., Xu, L., Fang, T.C., Chiang, M.Y., Intlekofer, A.M., Blacklow, S.C., et al. (2009). Pre-TCR signaling inactivates Notch1 transcription by antagonizing E2A. Genes Dev. *23*, 1665–1676.

Yasumoto, K., Yokoyama, K., Shibata, K., Tomita, Y., and Shibahara, S. (1994). Microphthalmia-associated transcription factor as a regulator for melanocyte-specific transcription of the human tyrosinase gene. Mol. Cell. Biol. *14*, 8058–8070.

Yavuzer, U., Keenan, E., Lowings, P., Vachtenheim, J., Currie, G., and Goding, C.R. (1995). The Microphthalmia gene product interacts with the retinoblastoma protein in vitro and is a target for deregulation of melanocyte-specific transcription. Oncogene *10*, 123–134.

Yoshimura, A., and Muto, G. (2011). TGF-β function in immune suppression. Curr. Top.

Microbiol. Immunol. *350*, 127–147.

Zaid, A., Roubtsova, A., Essalmani, R., Marcinkiewicz, J., Chamberland, A., Hamelin, J., Tremblay, M., Jacques, H., Jin, W., Davignon, J., et al. (2008). Proprotein convertase subtilisin/kexin type 9 (PCSK9): Hepatocyte-specific low-density lipoprotein receptor degradation and critical role in mouse liver regeneration. Hepatology *48*, 646–654.

Zhong, M., Benjannet, S., Lazure, C., Munzer, S., and Seidah, N.G. (1996). Functional analysis of human PACE4-A and PACE4-C isoforms: Identification of a new PACE4-CS isoform. FEBS Lett. *396*, 31–36.

Zhong, M., Munzer, J.S., Basak, A., Benjannet, S., Mowla, S.J., Decroly, E., Chrétien, M., and Seidah, N.G. (1999). The prosegments of furin and PC7 as potent inhibitors of proprotein convertases. In vitro and ex vivo assessment of their efficacy and selectivity. J. Biol. Chem. *274*, 33913–33920.

Zhou, A., Martin, S., Lipkind, G., LaMendola, J., and Steiner, D.F. (1998). Regulatory roles of the P domain of the subtilisin-like prohormone convertases. J. Biol. Chem. *273*, 11107–11114.

Zhu, J., Declercq, J., Roucourt, B., Ghassabeh, G.H., Meulemans, S., Kinne, J., David, G., Vermorken, A.J.M., Van de Ven, W.J.M., Lindberg, I., et al. (2012). Generation and characterization of non-competitive furin-inhibiting nanobodies. Biochem. J. *448*, 73–82.

Zhu, X., Rouille, Y., Lamango, N.S., Steiner, D.F., and Lindberg, I. (1996). Internal cleavage of the inhibitory 7B2 carboxyl-terminal peptide by PC2: a potential mechanism for its inactivation. Proc. Natl. Acad. Sci. U. S. A. *93*, 4919–4924.

Zhu, X., Orci, L., Carroll, R., Norrbom, C., Ravazzola, M., and Steiner, D.F. (2002). Severe block in processing of proinsulin to insulin accompanied by elevation of des-64,65 proinsulin intermediates in islets of mice lacking prohormone convertase 1/3. Proc. Natl. Acad. Sci. U. S. A. *99*, 10299–10304.

Zumsteg, A., and Christofori, G. (2009). Corrupt policemen: inflammatory cells promote tumor angiogenesis. Curr. Opin. Oncol. *21*, 60–70.

Avenue de Tivoli 70

CH-1007 Lausanne

E-Mail: pginefra85@gmail.com

Date of birth: 24th of May 1985

Italian

CURRICULUM VITAE
PIERPAOLO GINEFRA

EDUCATION

2013 – 2017 (exp)	PhD in Molecular Biology, EPF Lausanne (CH)
	Topic: Imaging Porprotein Convertases activities in melanoma model
2012	M.S. in Management of Biomedical Devices (PROBIOMED), equivalent of second level university degree, "LUISS Business School", Rome, Italy
2008 – 2010	MSc in Biotechnology and Molecular Medicine, University Aldo Moro of Bari(IT)
	Master thesis at Campus IFOM-IEO Milan (IT)
	Topic Cloning and Characterization of "Tumor Suppressor Genes" in Drosophila melanogaster
2005 – 2008	BSc in Healthcare and Pharmaceutical Biotechnology, University Aldo Moro of Bari (IT)
2004	High School Diploma from Secondary School (specializing in scientific studies) "E. Fermi", Bari (IT)

WORK EXPERIENCE

2010 – 2011	Fellow at Campus IFOM-IEO (Milan, Italy) in the laboratory of Prof. T. Vaccari

Responsibilities:

- Project title: "Characterization of syb and usnp, two potential tumor suppressor genes"
- Characterization of SNARE function in epithelial formation in *Drosophila Melanogaster*. (Morelli E, Ginefra P *et al*, Autophagy 2014)

PUBLICATIONS

Multiple functions of the SNARE protein Snap29 in autophagy, endocytic, and exocytic trafficking during epithelial formation in Drosophila

Elena Morelli,1 **Pierpaolo Ginefra**,1 Valeria Mastrodonato,1 Galina V Beznoussenko,1 Tor Erik Rusten,2 David Bilder,3 Harald Stenmark,2 Alexandre A Mironov,1 and Thomas Vaccari1,

1IFOM - The FIRC Institute of Molecular Oncology; Milan, Italy

2Centre for Cancer Biomedicine; Oslo University Hospital; Oslo, Norway

3Department of Molecular and Cell Biology; University of California; Berkeley, CA USA

Autophagy. 2014 Dec; 10(12): 2251–2268.

CONFERENCE ATTENDENCE

"**5th Faculty & Staff Retreat of the Lausanne Cancer Research Community**", Lausanne, Switzerland, November 8th/9th 2016. Oral presentation

"**ISREC-SCCL Symposium 2016: horizon of Cancer Biology and Therapy**", Lausanne, Switzerland,September 7th/10th 2016.Poster presentation

 Gordon Conference **" Proteolytic Enzymes & Their Inhibitors"** Lucca , Italy. June 26th/July 1st 2016. Poster presentation.

 "**4th Faculty & Staff Retreat of the Lausanne Cancer Research Community**", Lausanne, Switzerland, November 10th/11th 2016. Poster presentation

LANGUAGE SKILLS

Italian	Mother tongue
English	Good knowledge written and spoken
French	Fair knowledge written and spoken